UNIVERSITY OF NOVA GORICA
GRADUATE SCHOOL

ROLE OF TDP-43 AGGREGATION IN NEURODEGENERATION: A *DROSOPHILA MELANOGASTER* DISEASE MODEL AND INNOVATIVE THERAPEUTIC APPROACHES

DISSERTATION

Lucía Cragnaz

Mentor: Dr. Marco Baralle

Nova Gorica, 2016

UNIVERZA V NOVI GORICI
FAKULTETA ZA PODIPLOMSKI ŠTUDIJ

VLOGA KOPIČENJA TDP-43 PRI NEVRODEGENERACIJI:
***DROSOPHILA MELANOGASTER* KOT MODEL BOLEZNI IN**
INOVATIVNI TERAPEVTSKI PRISTOPI

DISERTACIJA

Lucía Cragnaz

Mentor: Dr. Marco Baralle

Nova Gorica, 2016

Table of Contents

List of Figures

List of Tables

Abstract

TDP-43 inclusions are important histopathological features of various neurodegenerative disorders, including Amyotrophic Lateral Sclerosis. However, the relation of these inclusions with the pathogenesis of the disease is still unclear. Various hypotheses have been proposed. For instance, it was suggested that the inclusions are (1) primary toxic species, (2) part of the normal cellular protective response to toxic intermediates and (3) responsible for the nuclear depletion of TDP-43. Understanding the relationship between TDP-43 aggregation and neurodegeneration is crucial for the eventual management of the disease.

TDP-43 is a protein that has a marked tendency to unfold and become insoluble. In particular, its C-terminal end has a so-called "prion-like domain", a sequence rich in Glutamine (Q) and Asparagine (N) that is involved in both the interactions with other proteins and the self-aggregation process. A cellular model of aggregation has been previously developed by our group, using the TDP-43 Q/N rich amino acid sequence repeated 12 times (12xQ/N) fused to EGFP reporter. The EGFP-12xQ/N cellular inclusions are capable of sequestering wild type TDP-43 both in non-neuronal and neuronal cells.

In this study we went further with ALS modeling, creating a *Drosophila* model with EGFP-12xQ/N-induced aggregates. We show here that *Drosophila melanogaster* TDP-43 ortholog (TBPH) overexpression in *Drosophila* eye using GMR-Gal4 driver, is neurotoxic and causes necrosis and loss of function of the eye. More important, the neurotoxicity of TBPH can be abolished by its incorporation to the insoluble aggregates induced by EGFP-12xQ/N. This data indicates that aggregation is not toxic *per se* and instead has a protective role, modulating the functional TBPH available in the tissue.

Notwithstanding the fact that aggregation is protective in presence of an excess of TBPH, we wanted to further understand the role of the aggregates in an environment where just the endogenous TBPH is present. For this purpose, we induced EGFP-12xQ/N transgene constitutively in CNS using ELAV-Gal4 driver. The flies were born and went through the larval stage without differing from control flies in any significant feature of their

phenotype. However, during aging the locomotion ability and survival rate of EGFP-12xQ/N flies were impaired. Interestingly, the climbing deficit was correlated with a physiological reduction in the endogenous TBPH levels. Thus, the aggregation, when coupled with low TDP-43 levels generates phenotypic consequences in our *Drosophila* model, probably due to a TDP-43 loss of function.

In sum, these data suggest that although the aggregates may be a result of neuroprotection in a context where TBPH is in excess, at a certain stage they become responsible for the pathology, likely due to the TBPH loss of function. If we consider that TDP-43/TBPH inclusions act as a sink for the newly formed soluble TDP-43/TBPH, the modulation of these inclusions could be used as a potential therapeutic approach, as this would restore the normal levels of TDP-43/TBPH and its function. Consequently, in the last part of the study we were interested to understand if the clearance of TDP-43/TBPH aggregates could be an effective strategy to treat ALS, by recovering TDP-43/TBPH function. For this purpose, using the previously established cell-based TDP-43 aggregation models we analyzed aggregate clearance after treatment with several FDA approved drugs. Three of these drugs were found to significantly reduce aggregation through the proteasome pathway. Furthermore, one of the drugs (nortriptyline) was shown to rescue EGFP-12xQ/N dependent locomotor dysfunction in the *Drosophila* model. Altogether these data indicate that the clearance of TDP-43 aggregates may be a novel therapeutic strategy for ALS treatment.

Povzetek

Vključki proteinov TDP-43 so pomembne histopatološke značilnosti različnih nevrodegenerativnih bolezni, vključno z amiotrofično lateralno sklerozo (ALS), kljub temu pa je njihova povezava s temi boleznimi še vedno nejasna. Postavljene so bile mnoge hipoteze. Med drugim je bilo predlagano, da so tovrstni vključki (1) primarne toksične strukture, (2) del običajnega celičnega obrambnega odziva proti toksičnim intermediatom in (3) so odgovorni za odsotnost TDP-43 v jedrih celic. Razumevanje odnosa med kopičenjem TDP-43 v citoplazmi in nevrodegeneracijo je ključnega pomena za morebitno vodenje bolezni.

TDP-43 je protein z izrazito težnjo po porušenju strukture in pojavu netopnosti. Njegov C-terminalni konec ima tako imenovano "prionu podobno domeno", ki je zaporedje bogato z glutaminom (Q) in asparaginom (N) in je vpleteno v interakcije z drugimi proteini in procesom kopičenja. Naša skupina je predhodno razvila model celične agregacije z uporabo TDP-43 Q/N bogatega aminokislinskega zaporedja, ki se ponovi 12-krat (12xQ/N) in je priključeno na EGFP reporter. EGFP-12xQ/N celični vključki so sposobni sekvestriranja TDP-43 v ne-nevronskih in nevronskih celicah.

Za proučevanje ALS smo v tej študiji ustvarili model vinske mušice z kopičenjem TDP-43, ki v temelji na EGFP-12xQ/N vključkih. Pokazali smo, da je povečano izražanje TBPH v očeh vinske mušice z GMR-Gal4 nevrotoksično ter povzroči nekrozo in izgubo funkcije očesa. Še pomembneje, nevrotoksičnost TBPH je lahko odpravljena z vključitvijo le-tega v netopne agregate. Ti podatki kažejo, da kopičenje ni nevarno samo po sebi in ima namesto tega zaščitno vlogo, in sicer s spreminjanjem prisotnosti delujočega TBPH v tkivu.

Ne glede na dejstvo, da ima kopičenje zaščitno vlogo v prisotnosti prebitka TBPH, smo želeli bolje razumeti vlogo vključkov v okolju, kjer je prisoten samo endogeni TBPH. Za ta namen smo konstitutivno izrazili EGFP-12xQ/N v CŽS z uporabo ELAV-Gal4. Vinske mušice so se rodile brez fenotipskih sprememb. Kasneje so se kljub temu pojavile nepravilnosti v gibalnosti ter krajše preživetje EGFP-12xQ/N mušic. Zanimivo je, da so bile pomanjkljivosti v plezanju v korelaciji s fiziološkim znižanjem nivoja endogenega TBPH.

Kopičenje z združenimi znižanimi vrednostmi TDP-43 tako povzroči spremembe v fenotipu vinskih mušic, po vsej verjetnosti zaradi izgube funkcije TDP-43.

Ti podatki kažejo, da so vključki kljub možnim nevroprotektivnim lastnostim kadar je TBPH v prebitku, še vedno vzrok patoloških stanj, kot je npr. izguba funkcije TBPH. Če upoštevamo, da TDP-43/TBPH vključki delujejo kot vaba za topne TDP-43/TBPH, se bi spreminjanje teh vključkov lahko uporabilo kot potencialni terapevtski pristop, saj bi s tem povrnili normalno raven TDP-43/TBPH in njegovo funkcijo. Zato smo v zadnjem delu študije raziskovali ali je uničenje TDP-43/TBPH agregatov lahko učinkovita strategija za zdravljenje ALS zaradi povrnitve funkcije TDP-43/TBPH. Za ta namen smo uporabili predhodno pripravljene celične modele kopičenja TDP-43, ki smo jih tretirali z FDA-potrjenimi zdravili. Tri od teh zdravil so bistveno zmanjšale kopičenje. Poleg tega je eno od zdravil (nortriptilin) povzročilo povrnitev gibalnih sposobnosti na modelu vinske mušice. V študiji smo torej pokazali, da je uničenje TDP-43 agregatov lahko nova terapevtska strategija za zdravljenje ALS.

KLJUČNE BESEDE: TDP-43/TBPH, vključki, *Drosophila melanogaster*, ALS.

List of Abbreviations

AD Alzheimer's disease

ALS Amyotrophic Lateral Sclerosis

ASO Antisense oligonucleotides

Atg Autophagy-related gene

CFTR9 Cystic Fibrosis Trans-membrane Regulator

CK casein kinase

CNS Central Nervous System

CP Core particle

CTF C-terminal fragments

DMEM Dulbbeco's Modified Eagle Medium

fALS Familial Amyotrophic Lateral Sclerosis

FDA Food and Drug Administration

FUS/TLS Sarcoma/translocated in liposarcoma

GOF Gain of function

GWAS Genome-wide association studies

HD Huntington's disease

HIV Human Immunodeficiency Virus

hnRNP Heterogeneous nuclear ribonucleoprotein

LC3 Light chain 3

LOF Loss of function

NES Nuclear export signal

NLS Nuclear localization signal

NMJ Neuromuscular Junction

NTF N-terminal fragments

mTOR Mammalian Target of Rapamycin

OPTN Optimeurin

PD Parkinson's disease

PFN1 Profilin 1

POLDIP3 Polymerase delta interacting protein

PrP Protease-resistant prion protein

RAN Repeat-associated non-ATG-dependent

RP Regulatory particle

RRM RNA recognition motifs

sALS Sporadic Amyotrophic Lateral Sclerosis

SDS-PAGE Sodium Dodecyl Sulfate Polyacrylamide Gel Electrophoresis

SOD1 Superoxide dismutase-1

SQSTM1 Sequestrosome 1

TBPH *Drosophila melanogaster* TDP-43 ortholog

TCA Tricyclic antidepressant

TDP-43 TAR-Binding Protein 43

TDPBR TDP-43 binding region

UAS Upstream activating sequence

UBQLN2 Ubiquilin 2

UPS Ubiquitin-proteasome system

UTR Untranslated Region

VCP Valosin-containing protein

Introduction

1. Neurodegenerative disorders

Neurodegeneration is a widely used term to refer to all the diseases that primarily affect neurons in the human brain, such as Alzheimer's disease, Amyotrophic Lateral Sclerosis, Huntington's disease and Parkinson's disease. Approximately 35 years ago little was known about the causes of the neurodegeneration (Prusiner, 2001). Nowadays, however, it is increasingly recognized that these diseases share a common feature, that is the abnormal production, processing and removal of proteins in neurons. These alterations result in the accumulation of one or more neuronal proteins triggering cell death and neuronal loss (Soto, 2003). Even though these diseases are characterized by the accumulation of insoluble aggregates, of normally soluble proteins in the central nervous system, there are striking phenotypic differences among them. This diversity is due to: (a) distinct temporal and regional patterns of deposition of aggregates, (b) varying cellular hosts or extracellular location of the aggregates, and (c) different protein constituents of the aggregates (**Table 1**) (Skovronsky et al., 2006).

Disease	Location	Aggregated protein
Alzheimer´s disease	Extracellular	Amyloid-β
	Intracytoplasmic	Tau
	Intracytoplasmic	α-synuclein
Amyotrophic lateral sclerosis	Intracytoplasmic	Superoxide dismutase-1 (SOD-1)
	Intracytoplasmic	TAR-Binding Protein 43 (TDP-43)
	Intracytoplasmic	Sarcoma/translocated in liposarcoma (FUS/TLS)
Frontotemporal Dementia	Intracytoplasmic	Tau
	Intracytoplasmic	TAR-Binding Protein 43 (TDP-43)
	Intracytoplasmic	Sarcoma/translocated in liposarcoma (FUS/TLS)
Cortical basal degeneration	Intracytoplasmic	Tau
Dementia with Lewy bodies	Intracytoplasmic	α-synuclein
Huntington disease	Intranuclear	Hungtintin
Multiple system atrophy	Intracytoplasmic	α-synuclein
Parkinson´s disease	Intracytoplasmic	α-synuclein
Pick´s disease	Intracytoplasmic	Tau
Prion diseases	Extracellular	Protease-resistant prion protein (PrP)
Spinocerebellar ataxia	Intranuclear	Ataxin

Table 1. Common neurodegenerative diseases characterized by deposition of aggregated proteins.

Moreover, the patient's innate and variable response to the protein aggregates may in turn alter the cascade of events leading to a particular temporal and regional pattern of neuronal dysfunction and death, which manifests as a specific clinical syndrome. For example, intracytoplasmic aggregates of α-synuclein could trigger dementia in Alzheimer's disease or movement disorder in Parkinson's disease (Skovronsky et al., 2006).

As neurodegenerative diseases are age-related pathologies, and as the average life expectancy of many populations extends into the eighth decade, the prevalence of most of these diseases is dramatically increased. For instance, for Alzheimer's disease, which is the most prevalent of these disorders (affecting approximately 15 million people worldwide), the number of affected individuals in the United States is expected to reach 13.2 million by the year 2050 (Forman et al., 2004).

Even though the protein inclusions in the brain are the main histopatological hallmarks of neurodegeneration, the relation of these inclusions with the pathology of the disease is still unclear. Several lines of research indicate that the inclusion bodies are the main cause of toxicity, but other studies indicate that they might be part of the cellular protective response to toxic intermediates (Ross & Poirier, 2005).

Protein aggregation could be a result of a mutation in the disease-related protein, or could be an sporadic event which could be originated by environmental stress or aging (Ross & Poirier, 2005).

1.1. Amyotrophic Lateral Sclerosis

1.1.1. General Overview

Amyotrophic Lateral Sclerosis (ALS), colloquially known as Lou Gehrig's disease, is a rapidly progressive, invariably fatal neurodegenerative disease that affects motor neurons in the primary motor cortex, brainstem and spinal cord (Shaw et al., 2001). The disease was first documented in 1869 by the French neurologist Jean-Martin Charcot (Charcot, 1869).

"A-myo-trophic" comes from the Greek language. "A" means no, "myo" refers to muscle, and "trophic" means nutriment ("No muscle nutriment").

When the muscle has no nourishment it atrophies, loosing the capacity of contracting. The term "Lateral Sclerosis" indicates the hardening of the anterior and lateral corticospinal tracts, due to degeneration of motor neurons in these areas (Rowland & Shneider, 2001).

Early symptoms of ALS include muscle weakness, specially involving the arms, legs, speech and swallowing or breathing as a result of dysfunction of both upper and lower motor neurons. All these symptoms aggravate with the progression of the disease, and during the final stage the muscle action is lost and the patients become totally paralyzed. Finally, the patients commonly die because of respiratory failure due to denervation of the respiratory muscles (**Figure 1**).
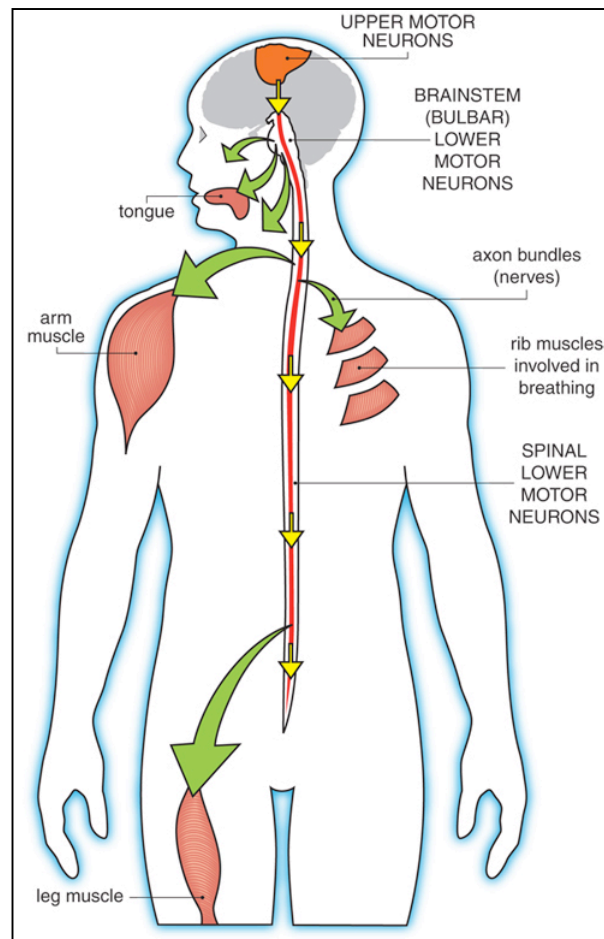
Figure 1. ALS mechanism.

Upper motor neurons send signals to lower motor neurons, which send signals to muscles. In ALS patients the neuromuscular junction is degenerated as a consequence of upper and lower motor neuronal dysfunction. Adapted from MD's ALS Division Publication.

Most people develop ALS between 55 and 65 years old (Haverkamp et al., 1995). The life expectancy of a patient is approximately 2 to 5 years from the onset of the disease (Rowland, 1998). The disease has an estimated incidence (frequency of new cases per year) of approximately 2/100,000 people, and a prevalence (proportion of affected individuals in the population) of 6/100,000 individuals (Boillée et al., 2006).

Despite the fact that ALS is the most common neuromuscular disease, and that it was discovered almost 150 years ago, the absence of specific biomarkers (with the exception of identified mutations in specific genes, that account for approximately 10% of all ALS cases) makes its diagnosis extremely difficult. In this respect, signs suggestive of combined upper and lower motor neuron impairment, that cannot be explained by any other disease process (evident on electrophysiological, imaging, cerebrospinal fluid or serological studies), together with progression compatible with a neurodegenerative process, are invariably suggestive of ALS (Silani et al., 2011). In order to have some common criteria in diagnosing and classifying patients, the World Federation of Neurology has developed "El Escorial" (Brooks, 1994) and the revised "El Escorial revisited" (Brooks et al., 2000) protocols. According to these protocols patients can be classified into four categories: "Clinically definite", "Clinically probable", "Clinically probable - Laboratory supported" and "Clinically possible". This classification helps the diagnosis of the patients and is useful for therapeutic trials and research purpose.

The majority of ALS cases (90-95%) are sporadic (sALS), while 5-10% of the cases present a family history (fALS), due to inherited genetic mutations (Pasinelli & Brown, 2006). Even though these two variants have different etiology, they are indistinguishably from a symptomatic point of view, suggesting a common pathogenesis. Despite the heterogeneity of ALS, a consistent pathological feature at the molecular level is the presence of ubiquitin-positive cytoplasmic inclusions in the degenerating neurons of ALS patients (Leigh et al., 1991). In 2006, a breakthrough study by Neumann and colleagues identified the TAR DNA binding protein-43 (TDP-43) as the major component in these protein inclusions (Neumann et al., 2006). Nowadays, it is broadly recognized that TDP-43 inclusions are present in almost all ALS

cases regardless *TARDBP* mutations (see section 3.1 for more detail). However, the cause underlying the motor neuron degeneration is still unclear, and as the clinical course of the disease is highly variable, it has been proposed that multiple factors account for the disease mechanism (Bruijn et al., 2004). Several processes have been suggested to cause the selective degeneration of motor neurons, such as oxidative stress (Yim et al., 1996), mitochondrial dysfunction (Cozzolino et al., 2012), defective protein degradation (Otomo et al., 2012) that causes abnormal protein aggregation (Watanabe et al., 2001), glutamate excitotoxicity (Van Damme et al., 2005), impaired axonal transport (Shaw, 2005), microglial activation (Ince et al., 1996), and RNA processing defects (Lagier-Tourenne et al., 2010). The relative importance of these different pathways may well vary in different subgroups of patients, and a very important task of the scientist and clinicians is to further delineate these subcategories, in order to find new therapeutic strategies for each disease process.

1.1.2. ALS Genetics

1.1.2.1. Familial ALS

Only 5-10% of ALS cases show familial inheritance. Unraveling the molecular basis by which these mutant gene products cause disease may shed light on the pathological mechanism underlying the common sporadic form of ALS (Pasinelli & Brown, 2006).

Mutations in 9 genes account for the etiology of two-thirds (68%) of fALS cases. The remaining one-third is still unknown. Among the identified genes, Cu/Zn superoxide dismutase 1 (*SOD1*) (Rosen et al., 1993), TAR-Binding Protein 43 (*TARDBP*) (Kabashi et al., 2008b; Sreedharan et al., 2008), Sarcoma/translocated in liposarcoma (*FUS/TLS*) (Kwiatkowski et al., 2009; Vance et al., 2009) and *C9ORF72* (Dejesus-Hernandez et al., 2012; Renton et al., 2012) account for over the 50% of fALS cases (**Figure 2, Table 2**). Mutations in Optineurin (*OPTN*), Valosin-containing protein (*VCP*), Ubiquilin 2 (*UBQLN2*), Sequestosome 1 (*SQSTM1*) and Profilin 1 (*PFN1*) are known to cause the other 18% of the cases.
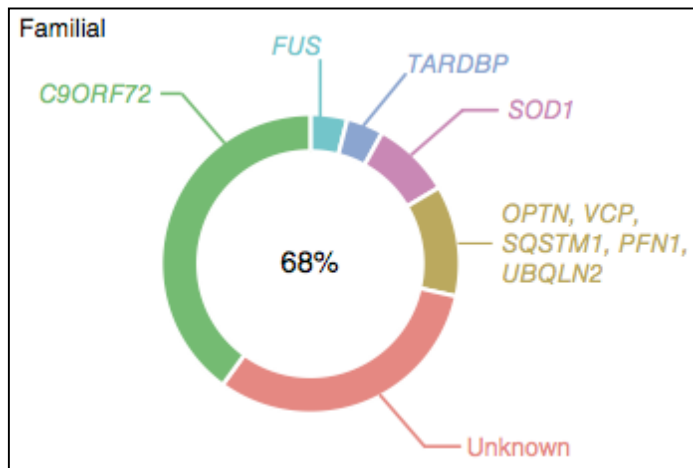
Figure 2. Proportion of ALS explained by each gene known to carry mutations in fALS.
Adapted from Renton et al., 2014.

Gene	Location	Inheritance	Percentage explained fALS	Putative protein function
TARDBP	1p36	AD	4	RNA metabolism
SQSTM1	5q35	AD	1	Ubiquitination; autophagy
C9ORF72	9p21	AD	40	DENN protein
VCP	9p13	AD	1	Proteasome; vesicle trafficking
OPTN	10p13	AR/AD	<1	Vesicle trafficking
FUS/TLS	16p11	AD/AR	4	RNA metabolism
PFN1	17p13	AD	<1	Cytoskeletal dynamics
SOD1	21q22	AD/AR	12	Superoxide metabolism
UBQLN2	Xp11	XD	<1	Proteasome

Table 2. Genes known to carry ALS-causing mutations in fALS.

AD: Autosomal Dominant, AR: Autosomal Recessive, XD: X-linked Dominant. Adapted from Renton et al., 2014.

The genetic defects found in these subtypes of ALS could be associated to the mechanisms underlying the pathogenesis of the disease, taking into account the putative protein function of each mutated gene.

Finally, mutations in several other genes have been reported as rare causes of ALS or ALS-like syndromes (**Table 3**).

Gene	Location	Inheritance	Putative protein function
DCTN1	2p13	AD	Axonal transport
ALS2	2q33	AR	Vesicle trafficking
CHMP2B	3p11	AD	Vesicle trafficking
FIG4	6q21	AD/AR	Vesicle trafficking
HNRNPA2B1	7p15	AD	RNA metabolism
ELP3	8p21	Undefined	RNA metabolism
SETX	9q34	AD	RNA metabolism
HNRNPA1	12q13	AD	RNA metabolism
ATXN2	12q24	Undefined	Endocytosis; RNA translation
ANG	14q11	AD	Angiogenesis
SPG11	15q14	AR	DNA damage repair
VAPB	20q13	AD	Vesicle trafficking
NEFH	22q12	AD	Axonal transport

Table 3. Other genes implicated in the fALS-pathogenesis.

AD: Autosomal Dominant, AR: Autosomal Recessive. Adapted from Renton et al., 2014.

1.1.2.2. Sporadic ALS

The cause of sALS is currently unknown. In 2002 the first *de novo* mutation in a sALS patient was identified, demonstrating that at least a portion of sporadic cases is due to spontaneous mutation (Alexander et al., 2002). Since then, a small percentage of these cases (11%) has been linked to mutations in specific genes (**Figure 3, Table 4**) (Renton et al., 2014).
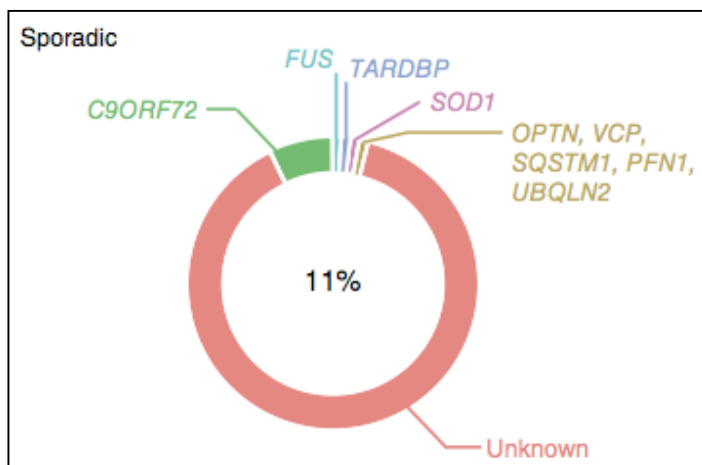
Figure 3. Proportion of ALS explained by each gene known to carry mutations in sALS.
Adapted from Renton et al., 2014.

Gene	Location	Percentage explained sALS	Putative protein function
TARDBP	1p36	1	RNA metabolism
SQSTM1	5q35	<1	Ubiquitination; autophagy
C9ORF72	9p21	7	DENN protein
VCP	9p13	1	Proteasome; vesicle trafficking
OPTN	10p13	<1	Vesicle trafficking
FUS/TLS	16p11	1	RNA metabolism
PFN1	17p13	<1	Cytoskeletal dynamics
SOD1	21q22	1-2	Superoxide metabolism
UBQLN2	Xp11	<1	Proteasome

Table 4. Genes known to carry ALS-causing mutations in sALS. Adapted from Renton et al., 2014.

Despite the evidence for a role of genetics, no common genetic variants have been unequivocally linked to sALS (Schymick et al., 2007), and the majority of sALS cases (90%) have still no evident genetic component. Regarding this, lots of efforts are being done to find genetic variants underlying sALS using genome-wide association studies (GWAS) (Renton et al., 2014). The GWAS have the objective of identifying genetic variants associated with an increased or decreased risk for developing ALS. In this way, publicly available genotype data from sALS patients and controls is being generated since 2007 (Schymick et al., 2007). However, in order to avoid false-positive findings, GWAS studies require several thousand case and control samples to have sufficient power to identify risk loci. Given the advanced genetics technology, it is expected that the number of genes implicated in ALS will continue to increase.

1.1.2.3. ALS-related genes

As already mentioned, among the ALS-related genes, mutations in four of them (*SOD1*, *TARDBP*, *FUS/TLS* and *C9ORF72*) account for over the 50% of fALS and 10% of sALS cases. In this section, a deeper overview will be given for these four genes.

1.1.2.3.1. *SOD1*

SOD1 is a ubiquitously expressed 153-amino acid polypeptide with a stabilizing zinc ion and a catalytic copper ion in each subunit. It forms an homodimer tightly packed and held together by strong hydrophobic interactions between the β-strands, making the dimer extremely stable (Andersen, 2006). SOD1 is responsible of converting the toxic superoxide anion, a by-product of oxidative phosphorylation in the mitochondrion, to innocuous hydrogen peroxide (Mccord & Fridovich, 1969). The disproportionation of superoxide is a two-step oxidation-reduction reaction that involves the cycling of the copper atom in SOD1 from Cu^{2+} to Cu^{+} and back to Cu^{2+} (Franco et al., 2013).

SOD1 localizes in the intermembrane space of the mitochondria and in the nucleus (Liu et al., 2004). It is found ubiquitously in almost all organisms above the evolutionary chain from bacteria and the amino acid sequence is also evolutionarily conserved, suggesting that SOD1 plays a crucial function in cellular homeostasis. Approximately the 0.5% of the total protein content in the human brain is SOD1 (Andersen, 2006).

The first ALS-associated *SOD1* mutation was discovered more than 20 years ago (Rosen et al., 1993). It was identified based on linkage analyses in autosomal dominant fALS pedigrees, which mapped to chromosome 21q22.1 (Chen et al., 2013). *SOD1* was the first gene known to be associated with ALS. Nowadays, we know that mutations in *SOD1* gene account for a remarkable percentage of fALS (approximately 12%). Furthermore, mutations in *SOD1* gene are infrequently found in sALS (around 1%) (Renton et al., 2014).

To date, more than 100 mutations have been described, spanning the 5 exons of *SOD1* gene, although no mutagenesis hotspot has being identified. The majority of these mutations are missense, although a small percentage of nonsense mutations, insertions and deletions have been also reported (Chen et al., 2013). How these *SOD1* mutations cause ALS is still controversial. A subset of these pathogenic mutations affects SOD1 activity, while others do not affect the catalytic activity of the protein (Hayward et al., 2002). Since its discovery as ALS associated gene, many animal models have been developed to assess this topic. Initial hypotheses favored a

reduced SOD1 function and consequent toxic free radical accumulation. However, animal models showed that the disease is not a consequence of the SOD1 loss of function, as knockout animals do no develop ALS symptoms (Reaume et al., 1996). Instead, it seems that gain of a new toxic function, possibly related to an increase tendency of mutant SOD1 molecules to aggregate in motor neurons, results in disease (Bruijn et al., 1998). Based on this data, the first-in-man trial of gene therapy, using antisense oligonucleotides (ASOs) against SOD1 mRNA, has been done to lower the levels of the protein (Miller et al., 2013). The aim of this study was to assess tolerability and safety of the molecule. In the future, evaluation of specific binding of ASOs to the target mRNA, and its ability to decrease the SOD1 mRNA level through the nuclear RNase H activation will be undertaken.

1.1.2.3.2. *TARDBP*

The TAR DNA-binding protein (TDP-43) is a highly conserved, 43-KDa, heterogeneous nuclear ribonucleoprotein (hnRNP) (Krecic & Swanson, 1999). It is ubiquitously expressed, and was initially described as a transcription factor (Ou et al., 1995). However, its roles have rapidly expanded, among others, to splicing regulation, mRNA stability (including its own), microRNA processing, mRNA transport and translation (Buratti & Baralle, 2012).

TARDBP gene, is located in chromosome 1p36.22 and contains six exons (Kabashi et al., 2008b). TDP-43 protein (**Figure 4**) contains two fully functional RNA recognition motifs (RRM) with distinct RNA/DNA binding characteristics. It has been reported that the protein can bind a minimum number of six UG (or TG) single-stranded dinucleotide stretches, and its binding affinity increases with the number of repeats (Ayala et al., 2005; Buratti & Baralle, 2001). However, more recently, several cross-linking and immunoprecipitation-sequencing analyses have indicated that TDP-43 can specifically bind loosely conserved UG/GU-rich repeats interspersed by other nucleotides (Bhardwaj et al., 2013). In particular, the highly conserved phenylalanine residues in the first RRM region play a key role in nucleic acid recognition (Buratti & Baralle, 2001). The protein contains a bipartite classic

nuclear localization signal (NLS) at the N-terminus (Winton et al., 2008) and a nuclear export signal (NES) within the RRM2. These sequences allow the protein to shuttle between the nucleus and the cytoplasm (Ayala et al., 2008), although the majority of TDP-43 appears to be nuclear in most cells at steady state. The remaining portion of the protein is composed by the C-terminal region, that contains a glycine-rich motif (Ayala et al., 2008). It was early observed that within the glycine-rich C-terminal tail, the TDP-43 contains a Q/N rich region that is involved in protein-protein interaction (D'Ambrogio et al., 2009).
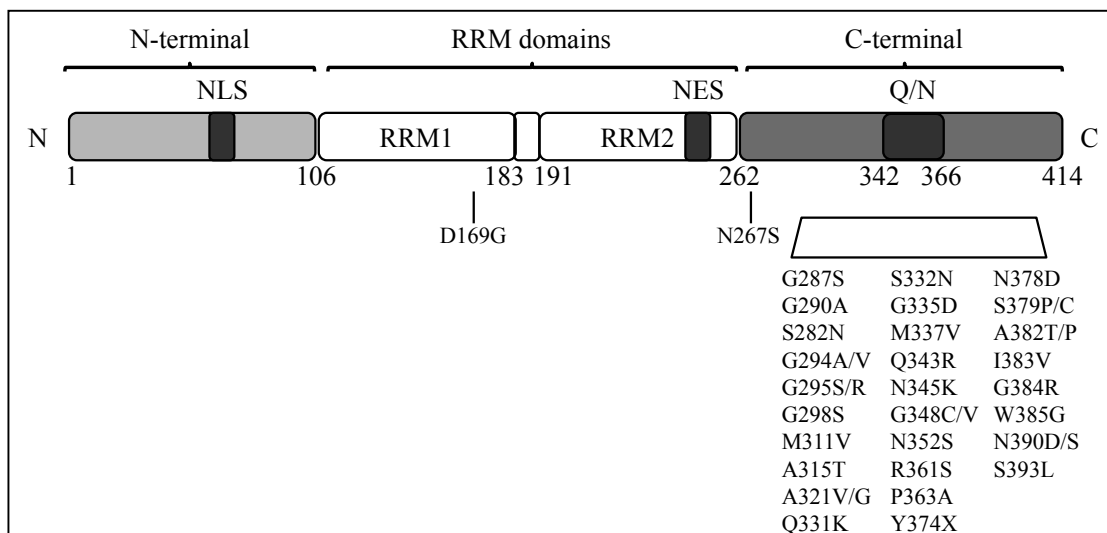
Figure 4. Schematic representation of TDP-43 protein basic architecture.
The protein is divided into N-terminal, RNA binding and C-terminal regions. Regions of special interest: NLS, NES, Q/N rich region. ALS-related mutations are shown.

Mutations in *TARDBP* gene were first reported in fALS and sALS cases in 2008 (Kabashi et al., 2008b; Sreedharan et al., 2008). Since then, more than 40 mutations have been identified (**Figure 4**) with an incidence of 4% in fALS and 1% in sALS (Renton et al., 2014). These pathogenic variants are mostly located in the C-terminal region of TDP-43 (Chen et al., 2013). This region is involved in the binding of TDP-43 with other hnRNPs and splicing (Ayala et al., 2008; D'Ambrogio et al., 2009), and in the self-aggregation (Budini et al., 2012a). On this respect, it was shown by Johnson et al. in 2009 that TDP-43 is an aggregation-prone protein, and that ALS-associated mutations increase

this aggregation (Johnson et al., 2009). More detailed overview of TDP-43 and its aggregation capacity will be given later (see sections 2 and 3).

1.1.2.3.3. *FUS/TLS*

Shortly after the identification of *TARDBP* as an ALS-related gene, mutations in the *FUS/TLS* gene have been reported (Kwiatkowski et al., 2009; Vance et al., 2009). *FUS/TLS* also encodes for an RNA/DNA binding protein, and its discovery had a great impact in the field, due to its high homology with TDP-43, which reinforced the importance of abnormal RNA metabolism in motor neuron degeneration (Renton et al., 2014).

FUS/TLS is a 526 amino acid protein encoded by 15 exons (Aman et al., 1996), and is located in chromosome 16p11.2 (Chen et al., 2013). It is characterized by an N-terminal domain enriched in glutamine, glycine, serine and tyrosine residues (QGSY region), a glycine-rich region, an RRM, multiple arginine/glycine/glycine (RGG) repeats and a C-terminal zinc finger motif (Lagier-Tourenne et al., 2010) (**Figure 5**). The protein harbors a NLS within the C-terminal tail (Dormann & Haass, 2011), and a NES signal in the RRM. This makes FUS/TLS mainly a nuclear protein, with lower accumulations in the cytoplasm of most cell types (Andersson et al., 2008).
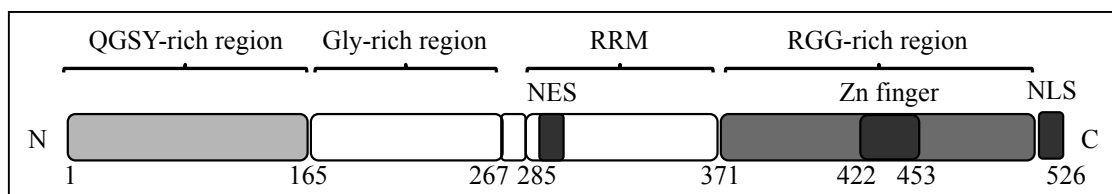
Figure 5. Schematic representation of FUS/TLS protein structure.
The protein is divided into: QGSY-rich, Gly-rich, RNA binding and RGG-rich regions. Regions of special interest: NLS, NES, Zinc finger rich region.

Similar to TDP-43, mutations in FUS/TLS cluster in its C-terminal part and account for 1% sALS and 4% fALS cases.

The precise roles of FUS/TLS are not fully elucidated. It was originally discovered as part of fusion oncogenes in human cancers (Crozat et al., 1993; Rabbitts et al., 1993). Later, it was described as a regulator of

transcription, pre-mRNA splicing and mRNA transport (Lagier-Tourenne & Cleveland, 2009). Although there is no evidence that TDP-43 and FUS/TLS act together, they both belong to the hnRNP family, and they could have roles in RNA processing such as coupling the transcription with splicing. In fact, many reports strongly implicate FUS/TLS and TDP-43 in neurodegeneration through errors in multiple steps of RNA processing (Lagier-Tourenne et al., 2010).

1.1.2.3.4. *C9ORF72*

The latest gene associated with ALS has been recently discovered. It has been reported that a massive hexanucleotide repeat expansion on *C9ORF72* is the cause of chromosome 9p21-linked ALS (Dejesus-Hernandez et al., 2012; Renton et al., 2012). This was a tremendous breakthrough as it was the first time that a large repeat expansion was associated with ALS. Taking into consideration that in other neurodegenerative disorders repeat expansions are known to cause RNA metabolism disorders, this pathway is increasingly gaining importance.

The pathogenic expansion is found in approximately 40% of fALS and around 7% of apparently sALS cases (Renton et al., 2014), representing the most common genetic cause of ALS.

The function of the C9ORF72 protein is unknown, and there is still no consensus about the mechanism by which the expansions in *C9ORF72* cause disease, but initial observations point to either a loss of function of the endogenous *C9ORF72* gene, and/or a toxic gain of function of the expanded RNA. The toxic gain of function may be mediated either by sequestration of RNA-binding proteins into RNA foci or by production of aberrant polypeptides through repeat-associated non-ATG-dependent (RAN) translation (Mori et al., 2013). RAN translation showed that expansion mutations can express homopolymeric expansion proteins in all three reading frames without an AUG start codon (Zu et al., 2010).

However, it was recently demonstrated that TDP-43 cytoplasmic aggregation is a dominant feature of ALS spinal cord pathology irrespective of *C9ORF72* mutation status (Gomez-Deza et al., 2015).

2. TDP-43 in physiological conditions

2.1. TDP-43 functions

TDP-43 was first described as a protein that binds to the regulatory TAR element of Human Immunodeficiency Virus (HIV) type 1, which is critical for the activation of gene expression by the transactivator protein Tat (Ou et al., 1995). It was demonstrated that TDP-43 is capable, in this way, of suppressing HIV-1 transcription and gene expression. However, this concept was revisited in 2014 by Nehls and coworkers, and they argued against a role of TDP-43 in repressing HIV-1 infection in human immune cells (Nehls et al., 2014).

TDP-43 was then described in 2001, as an RNA-binding protein, capable of binding to UG repeats near the 3' splice site of human *cystic fibrosis trans membrane regulator* (*CFTR*) exon 9 (Buratti et al., 2001), and since then it has been shown to be involved in several roles of RNA metabolism, including transcription, splicing, RNA transport, RNA stability and turnover, and in particular alternative splicing (Buratti & Baralle, 2012). On this respect, when localized near the 3' or 5' splice sites of several exons, TDP-43 binding to UG-repeats can silence splicing, as in the case of *CFTR* exon 9 (Buratti et al., 2001), or it can enhance splicing, as in the case of *polymerase delta interacting protein/S6 kinase 1 Aly/REF-like target* (*POLDIP3/SKAR*) (Fiesel et al., 2012).

2.2. Regulation of *POLDIP3* exon 3 alternative splicing by TDP-43

POLDIP3 is a protein that interacts with DNA polymerase II and functions by recruiting S6K1 protein to the exon junction complex, regulating translation and cell growth. In particular, it has been reported to enhance mammalian target of rapamycin (mTOR) S6K1-mediated translation efficiency of mRNA, which is implicated in cell proliferation and growth (Ma et al., 2008).

POLDIP3 has two variants, variant-1 which includes exon 3, and variant-2, which lacks exon 3. When TDP-43 is present there is more variant-1 than variant-2. However, it was demonstrated by two groups independently that

when TDP-43 is silenced in cells, *POLDIP3* variant-1 decreases and variant-2 increases (**Figure 6**) (Fiesel et al., 2012; Shiga et al., 2012). The RNA binding ability of TDP-43 is necessary for *POLDIP3* exon 3 inclusion. In physiological conditions, when TDP-43 is present, it recognizes the consensus sequence $(GAGU)_3(GA)_8(UG)_3$ in the intronic region downstream *POLDIP3* exon 3. In particular, the RRM1, but not the RRM2 is necessary, as mutations in Phe147 and Phe149 in RRM1 abolish exon 3 inclusion, but mutations in Phe194, Phe229 and Phe231 in RRM2 do not.
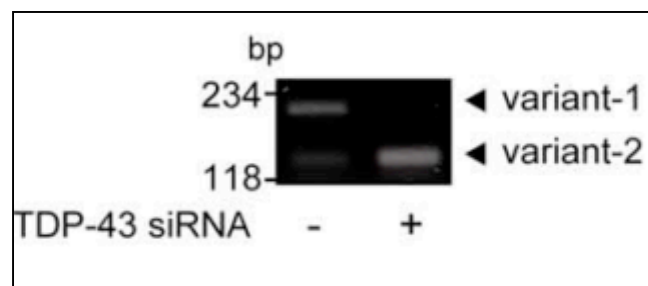
Figure 6. *POLDIP3* alternative splicing is regulated by TDP-43.
Representative gel of RT-PCR products from control cells, and cells treated with TDP-43 siRNA, using *POLDIP3* specific primers spanning exon 3. Adapted from Shiga et al., 2012.

Furthermore, Shiga and co-workers found an increment of *POLDIP3* variant-2 mRNA in motor cortex, spinal cord and spinal motor neurons from ALS-patients (Shiga et al., 2012). This result was further corroborated recently by Yang and collaborators, confirming that TDP-43 functions are altered in human ALS, and that TDP-43 loss of function may be responsible for the pathogenesis (Yang et al., 2014).

Little is known about the functionality of the two different *POLDIP3* isoforms, but it was suggested that variant-2 activates S6K1 more efficiently than variant-1 (Fiesel et al., 2012). In fact, it was shown that in absence of TDP-43 the cell size increases, due to the presence of variant-2 that is more active than variant-1.

2.3. TDP-43 autoregulation

To ensure cellular viability, the levels of TDP-43 must be tightly regulated. Interestingly, TDP-43 achieves the control of its own levels, by modulating its mRNA production at post-transcriptional RNA processing level. In fact, it binds to its own transcript and triggers a series of events that lead to degradation of the RNA (Ayala et al., 2011; Avendaño-Vázquez et al., 2012). Baralle and collaborators first described the TDP-43 self-regulation process in 2011 when they realized that upon overexpression of exogenous TDP-43, the endogenous TDP-43 levels decrease (Ayala et al., 2011). TDP-43 cellular levels are maintained through a negative-feedback loop guaranteed by the binding of TDP-43 protein to its own 3'UTR, in a specific region known as TDP-43 binding region (TDPBR). In particular, there is the activation of a normally silent intron (intron 7) that is located within the 3'UTR. Splicing of this intron results in the usage of an alternative poly-adenylation site (polyA2), that leads to mRNA instability, nuclear retention and degradation (Bembich et al., 2013). The RRM1 and the C-terminal domains are necessary for the autoregulatory mechanism, as mutations in Phe147 and Phe149 in RRM1 and deletion of residues 321-366 abolish autoregulation (Ayala et al., 2011).

Regarding the disease process, where the pathological aggregates may act as a cytoplasmic "sink" for the cellular TDP-43, a lower nuclear TDP-43 level could trigger higher TDP-43 production (Bembich et al., 2013).

3. TDP-43 in Amyotrophic Lateral Sclerosis

3.1. Protein inclusions in ALS

Despite the heterogeneity of ALS, this disease, as other neurodegenerative diseases, is characterized by the presence of inclusions in the patient's affected motor neurons (Leigh et al., 1991; Lowe, 1994). Although it was recognized in 1991 that ubiquitin-positive inclusions are frequent in motor neurons of ALS patients on autopsy (Leigh et al., 1991), its importance and composition remained a mystery for almost two decades. It was in 2006 that TAR-DNA binding protein 43 was identified as the major

protein constituent of ALS patients inclusions (Arai et al., 2006; Neumann et al., 2006). This breakthrough supports the idea that protein aggregation is crucial in ALS pathology.

Shortly after this revolutionary discovery, mutations in *TARDBP* gene were identified as a cause of ALS (Kabashi et al., 2008b; Sreedharan et al., 2008). However, it is important to notice that *TARDBP* gene mutations represent just 1% of sALS cases and 4% of fALS cases (Renton et al., 2014), while TDP-43 is found aggregated in the 97% of all ALS cases (Ling et al. 2013). This means that TDP-43 protein aggregates regardless *TARDBP* mutations, making the understanding of the aggregation process more difficult.

Besides TDP-43, other proteins are found to be aggregated to a lesser extent in ALS patients' motor neurons. Based on the identity of the main protein component aggregated, the disease is classified in: ALS-TDP-43 (97%), ALS-SOD1 (2%) and ALS-FUS (1%) (**Figure 7**) (Ling et al. 2013).
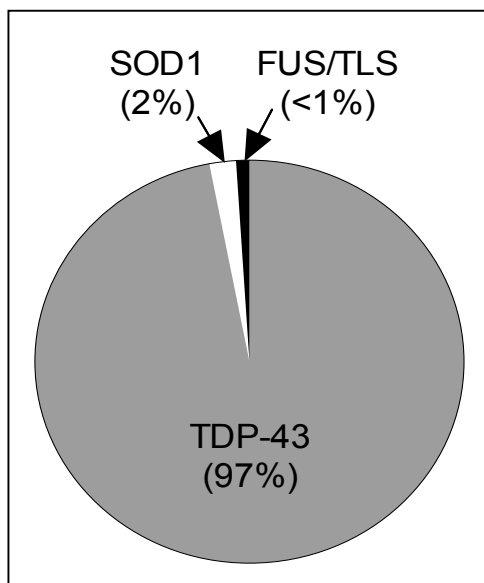
Figure 7. Pathological protein inclusions identified in ALS patients.

As already mentioned, TDP-43 pathology can be found in postmortem tissue of the majority of ALS cases, with the exception of patients with SOD1-ALS, which are positive for ubiquitin neuronal inclusions but negative for TDP-43 and FUS/TLS (Mackenzie et al., 2007). In fact, the pathology of ALS-SOD1 is recognized to be distinct of the other types of ALS, and thus ALS-SOD1 patients should be treated differently (Renton et al., 2014).

Pathological TDP-43 inclusions can be found in the nucleus and cytoplasm of neurons and glia cells, with abnormal ubiquitination (Arai et al., 2006; Neumann et al., 2006). Furthermore the protein is cleaved in C-terminal fragments of 18-26 KDa and 35 KDa, which are hyperphosphorylated and ubiquitinated (Hasegawa et al., 2008; Inukai et al., 2008; Neumann et al., 2006).

From a structural point of view, it is not so clear if the TDP-43 inclusions are amyloid-like structures or not. They are formed by infrequent straight filaments 10-20 nm in diameter and generally described as disordered amorphous aggregates unlike the amyloid fibrils that characterize protein accumulations in other neurodegenerative diseases such as AD or PD (Kwong et al., 2007; Neumann et al., 2007b). However, recent studies have shown that Thioflavin-S positive inclusions are found in the spinal cord of a subset of ALS cases (Bigio et al., 2013; Robinson et al., 2012), and Thioflavin-S fluoresces when bound to amyloid fibrils (Westermark et al., 1999). However, the same study showed that TDP-43 outside the spinal cord, lack this chemical property of amyloid, suggesting that TDP-43 inclusions have heterogeneous properties (Robinson et al., 2012).

Despite their initial discovery in ALS and Frontotemporal Dementia with ubiquitin positive inclusions, TDP-43 inclusions are present in many other neurodegenerative disorders, such as, Alzheimer's disease, Parkinson's disease, Lewy body disease, which leads to the new disease category called TDP-43 proteinopathies (Geser et al., 2009). The histology in all these cases is the same, which consists in the presence of glial and neuronal TDP-43 cytoplasmic inclusions, with partially or totally clearance of the nuclear TDP-43 (Baloh, 2011). Moreover, it was recently described that these types of inclusions are also present in the brain of approximately 30-40% cognitively normal individuals over 65 years old (Geser et al., 2010; Uchino et al., 2015), reflecting the fact that TDP-43 is an aggregate-prone protein (Johnson et al., 2009), and that there may be additional features that make aggregation pathological.

The role of the TDP-43 inclusions in proteinopathies is a topic of great debate in the field. Many hypotheses have been proposed. It was suggested that the inclusions are (1) primary toxic species, (2) part of the normal cellular

protective response to toxic intermediates and (3) responsible for the nuclear depletion of TDP-43. Regarding the first hypothesis, TDP-43 aggregation could exert toxic effects via sequestration of multiple binding partners or even interactomes essential for neuronal proper function (Blokhuis et al., 2013).

The second hypothesis is based on the evidence that inclusion bodies might represent an end-stage manifestation of a multistep aggregation process. In this respect, early events before the formation of the inclusion bodies might cause toxicity, and thus the insolubilization of toxic intermediates might preserve the cell (Ross & Poirier, 2005). Importantly, several studies suggests that pre-fibrillar species of neurodegenerative disease proteins may be more detrimental than fibrillar ones (Ludolph & Brettschneider, 2015).

The last hypothesis, is based on the observation that in ALS patients cytoplasmic aggregation is accompanied by nuclear clearing of the protein, suggesting that the loss of function of the protein could be responsible for the neuronal dysfunction (Baloh, 2011). Finally, it is possible that more than one of these mechanisms co-exist and contribute to the pathogenesis of the disease.

Understanding the relationship between TDP-43 aggregation and neurodegeneration is crucial, as we need to consider ways to modulate the inclusions formation as a potential therapeutic approach for ALS.

3.2. Prion-like properties of TDP-43

Seeding reactions were initially observed in prion disease with the PrP^{Sc} protein and occur when distinct misfolded conformation of a protein recruit native monomers to induce a conformational misfolding on to the native protein. This leads to protein aggregation and propagation (Smethurst et al., 2015). The seeding activity is also a notable feature of TDP-43 inclusions. Although it has not been shown *in vivo*, the seeding reaction has been found to occur in neuronal SH-SY5Y cells that have been transduced with TDP-43 aggregated material prepared from diseased brains (Nonaka et al., 2013). In this study, the authors demonstrated, furthermore, the cell-to-cell propagation of TDP-43 inclusions. In another study, the insoluble fraction from cells

harboring TDP-43 aggregates was shown to be able to trigger intracellular TDP-43 aggregation when transduced in non-neuronal HEK293 cells (Furukawa et al., 2011). Altogether these results suggest that insoluble TDP-43 has prion-like properties.

The fact that TDP-43 can be propagated from cell to cell implies the necessity to cross membrane barriers. The notion that TDP-43 could be released from neurons is supported by the presence of this protein in human cerebrospinal fluid (Kasai et al., 2009).

Regarding the histopathological characteristics, Braak and collaborators observed that initial lesions found in ALS patients are spread from the frontal neocortex (where they originate) to the corticofugal axonal pathways, from where they can spread to other brain regions (Braak et al., 2014).

It should be noticed that prion-like proteins are different from prions as prions are by definition infectious and cause major epidemics (Sikorska & Liberski, 2012). Misfolded variants of prion-like proteins can spread when transduced into cells, but they cannot be termed prions because they are neither infectious nor zoonoses in the way prion diseases are (Ludolph & Brettschneider, 2015).

In conclusion, the onset and progression of TDP-43 proteinopathy may be, in part, due to the propagation of TDP-43 aggregates between neuronal cells. If this is the case, suppressing the seeding reaction and propagation of aggregated TDP-43 may be a new therapeutic strategy for ALS.

3.3.   Pathological post-translational modifications

In addition to the already mentioned abnormal distribution and aggregation of TDP-43 in disease, the molecular signature of pathogenic TDP-43 includes ubiquitination, phosphorylation and proteolytic cleavage that results in accumulation of 35 and 25 KDa C-terminal fragments (CTF), in addition to other minor CTFs. Although the associated N-terminal fragments (NTF) of TDP-43 are degraded quickly, the CTFs form aggregates that can also sequester full-length TDP-43. N-terminal analysis of CTFs obtained from brain autopsies of patients has resulted in the identification of three cleavage sites, Arg208, Asp219 and Asp247 (Igaz et al., 2009; Nonaka et al., 2009).

However, the sizes of the resulting CTFs are less than the expected ones, which suggests that probably TDP-43 is cleaved at different positions. Recent work of Kawaharas' lab demonstrated that CTF25 is comprised of two fragments of TDP-43, which are cleaved after Asp174 and Asp169 (situated in RRM1) by caspase-4. CTF35 is generated independently, by cleavage after Asp89 (situated within the NLS) (Li et al., 2015).

In physiological conditions, it is unclear if TDP-43 is phosphorylated in the brain. However, phosphorylation mainly of Ser409/410 is a typical signature of TDP-43 pathology. *In vitro* phosphorylation experiments demonstrated that by incubation of TDP-43 with casein kinase (CK) 1 or CK 2 the pS409/410 epitope is generated, and that this phosphorylation at these sites increases TDP-43 oligomerization (Hasegawa et al., 2008). However, the significance of hyperphosphorylation is still controversial. Contrasting evidence show that it could be both protective and toxic. On one hand, Zhang and collaborators demonstrated that phosphorylation enhances accumulation of TDP-43 in insoluble aggregate, as it becomes resistant to proteasomal degradation (Zhang et al., 2010). On the other hand, Pang-hsien Tu's lab showed that hyperphosphorylation reduces TDP-43 aggregation, as a defense mechanism (Li et al., 2011). They proposed that phosphorylation occurs after aggregation, and that once formed, the phosphorylated aggregates can be degraded via proteasome.

Ubiquitination is another pathological signature in TDP-43 pathology. The presence of ubiquitinated aggregates is an indirect evidence of a failure in the degradation of defective proteins, physiologically performed by the proteasome or autophagy systems (a more detailed discussion on autophagy and proteasome alterations in ALS will be given later). Parkin is an E3 ligase that was found to be regulated by TDP-43. Moreover, Parkin ubiquitinates TDP-43 in residues K48 and K63, facilitating its cytosolic accumulation (Hebron et al., 2013).

3.4. ALS-TDP-43 models

Since the discovery of TDP-43 as the major component of inclusions found in ALS patients, many cellular and animal models have been

developed in order to elucidate the role of this protein and, in particular, of its aggregates, in the pathogenesis of the disease. Furthermore, these models are useful to identify effective treatments for this fatal disease.

As already mentioned, a key question regarding the role of TDP-43 is whether it causes neurotoxicity by a gain of function (GOF) or a loss of function (LOF) mechanism. Both hypotheses have been analyzed using different cellular and animal models. To do so, gain-of-function models and loss-of-function models, by gene overexpression and by gene knockout or knockdown respectively, have been generated. Cells in culture, yeast, *Mus musculus*, *Rattus norvegicus*, *Caenorhabditis elegans, Danio rerio* and *Drosophila melanogaster* models have been developed. However, to date, model systems that faithfully reproduce the human pathology have not been generated, thus a definite answer to the question regarding the role of TDP-43 in the pathology of ALS has remained elusive. Nevertheless, all these findings agree in the fact that a fine-tuning of the TDP-43 expression level is extremely important for the neuronal cell viability. Thus, the distinct possibility of combined effects; in which gain of toxic properties and loss of normal TDP-43 functions act together, needs to be considered.

3.4.1. Non-mammalian ALS-TDP-43 animal models

Non-mammalian animal models of TDP-43 proteinopathy are common and convenient for understanding the molecular basis of the pathology. *C. elegans*, *D. rerio* and *D. melanogaster* are the organisms of choice due to the simple nervous systems. Many studies have been conducted in this field and the main models generated are summarized in **Table 5** (GOF) and **Table 6** (LOF). As shown in the tables below, most of these models resemble some of the features found in patients, such as inclusions, ubiquitination, loss of nuclear TDP-43, etc. However, there is no model that recapitulates all the signs observed in patients' affected neurons.

35

Species	Transgene	Expression site	TDP-43 inclusions	Ubiquitin and TDP-43 inclusions	Loss of nuclear TDP-43	Truncated TDP-43	Phosphorylated TDP-43	Neuro-degeneration	Ref.
C. elegans	TDP-1	Ubiquitous	NA	NA	X	NA	NA	O	(1)
	WT-hTDP-43	Ubiquitous	NA	X	X	NA	NA	O	
	WT-hTDP-43	Ubiquitous	O	O	X	O	X	O	(2)
	A315T-hTDP-43	Ubiquitous	O	O	X	O	O	O	
	G290A- hTDP-43	Ubiquitous	O	NA	X	O	O	O	
	M337V- hTDP-43	Ubiquitous	O	NA	X	O	O	O	
D. rerio	WT-hTDP-43	Ubiquitous	NA	NA	NA	NA	NA	X	(3)
	A315T-hTDP-43	Ubiquitous	NA	NA	NA	NA	NA	O	
	G348C-hTDP-43	Ubiquitous	NA	NA	NA	NA	NA	O	
	A382T-hTDP-43	Ubiquitous	NA	NA	NA	NA	NA	O	
D. melanogaster	WT-hTDP-43-RFP	Eye	O	X	NA	NA	NA	O	(4)
	WT-hTDP-43-RFP	Mushroom body	NA	NA	NA	NA	NA	O	
	WT-hTDP-43-RFP	Motor neuron	O	X	NA	NA	NA	O	
	WT-hTDP-43	Eye	NA	NA	NA	NA	NA	O	(5)
	WT-hTDP-43	Motor neuron	O (rare)	NA	NA	NA	NA	O	
	WT-hTDP-43	Eye	NA	NA	NA	O	NA	O	(6)
	NES-mut-hTDP-43	Eye	NA	NA	NA	O	NA	X	
	NLS-mut-hTDP-43	Eye	NA	NA	NA	O	NA	O	
	M337V-hTDP-43	Eye	NA	NA	NA	O	NA	O	
	WT-hTDP-43	Pan neuronal or motor neuron	NA	NA	X	NA	NA	O	(7)
	A315T-hTDP-43	Pan neuronal or motor neuron	NA	NA	X	NA	NA	O	
	CTF-hTDP-43	Pan neuronal or motor neuron	NA	NA	O	NA	NA	X	
	FFLL-hTDP-43	Pan neuronal or motor neuron	NA	NA	X	NA	NA	X	
	WT-hTDP-43	Eye or pan neuronal	X	NA	X	O	O	O	(8)
	NES-mut-hTDP-43	Eye or pan neuronal	O	NA	X	O	O	X	
	NLS-mut-TDP-43	Eye or pan neuronal	X	NA	O	O	O	O	
	WT-hTDP-43	Eye or motor neuron	O	NA	NA	NA	NA	O	(9)
	A315T-hTDP-43	Eye or motor neuron	O	NA	NA	NA	NA	O	
	dTDP-43	Mushroom body or motor neuron	O	NA	NA	NA	NA	O	(10)
	WT-dTDP-43	Pan neuronal, upper motor neuron or eye	X (eye)	X (eye)	X (eye)	NA	NA	O	(11)

Table 5. Non-mammalian ALS models generated by wild type or mutant TDP-43 over-expression.

NA: not analyzed. O: yes. X: no. hTDP-43: human TDP-43. TDP-1: *C. elegans* homolog of hTDP-43. dTDP-43: *D. melanogaster* homolog of hTDP-43.

References: (1) Ash et al., 2010; (2) Liachko et al., 2011; (3) Kabashi et al., 2010; (4) Li et al., 2010; (5) Hanson et al., 2010; (6) Ritson et al., 2010; (7) Voigt et al., 2010; (8) Miguel et al., 2011; (9) Estes et al., 2011; (10) Lin et al., 2011; (11) Diaper et al., 2013.

Species	Line	Deletion	Deletion site	Embryonic lethality	Loss of nuclear TDP-43	Neuro-degeneration	Ref.
C. elegans	*ok803*	Deletion mutant that removes 2 RRMs and the NES of TDP-1	Ubiquitous	X	O	O	(1,2)
	ok781	Deletion mutant that removes 2 RRMs and the NES of TDP-1	Ubiquitous	X	NA	O	(1)
D. rerio	Tardbp[fh301]	Single point mutations introduces a premature stop codon (Y220X)	Ubiquitous	X	NA	O	(3)
	TDP-43 AMO	AMO complementary to *tardbp* generates gene knockdown	Ubiquitous	X	NA	O	(4)
	tardbp^{-/-} and *tardb1p^{-/-}*	Genome editing with zinc finger nucleases, which target *tardbp* and *tardbp1*	Ubiquitous	X	NA	O	(5)
D. melanogaster	*tbph[Δ23]*, *tbph[Δ142]*	Imprecise mobilization of TBPH transposon by transposase	Ubiquitous	X	NA	O	(6)
	TBPH-null	Imprecise P-element mobilization	Ubiquitous	O	NA	NA	(7)
	dTDP[ex26]	Imprecise P-element mobilization	Ubiquitous	X	O	O	(8)
	TBPH[DD100], TBPH[DD96]	Imprecise P-element mobilization	Ubiquitous	X	NA	O	(9)

Table 6. Non-mammalian ALS models generated by TDP-43 knockout or knockdown.

NA: not analyzed. O: yes. X: no. AMO: antisense morpholino oligonucleotide. hTDP-43: human TDP-43. TDP-1: *C. elegans* homolog of hTDP-43. Tardbp1: *D. rerio* Tardbp-like protein. dTDP-43: *D. melanogaster* homolog of hTDP-43. References: (1) Zhang et al., 2012; (2) Vaccaro et al., 2012; (3) Hewamadduma et al., 2013; (4) Kabashi et al., 2010; (5) Schmid et al., 2013; (6) Feiguin et al., 2009; (7) Fiesel et al., 2010; (8) Lin et al., 2011; (9) Diaper et al., 2013.

3.4.2. Mammalian ALS-TDP-43 animal models

Mammalian models have also been generated to study TDP-43 proteinopathy. In particular, mouse models have been widely used to understand the pathology of ALS. In order to evaluate the effect of TDP-43 overexpression, different promoters have been used. Each promoter triggers different expression patterns and leads to different phenotypes. The use of the human endogenous promoter may be a better choice than viral promoters, as it mimics the ubiquitous and moderate TDP-43 expression level occurring in the human context. Wild type and mutant TDP-43 (A315T or G348C) overexpression under the control of human endogenous promoter triggers an ALS like phenotype, including cytosolic ubiquitinated aggregates, motor dysfunction and age-related phenotypic defects (Swarup et al., 2011).

On the other hand, the pathological mechanism resulting from a TDP-43 loss of function has also been addressed using mouse modeling. In this case, the lack of TDP-43 was shown to be embryonic lethal (Wu et al., 2010). However, the targeted depletion of TDP-43 in the spinal cord motor neurons of mice induces progressive motor dysfunction and muscle atrophy, as in ALS (Wu et al., 2012).

3.4.3. Novel cellular ALS-TDP-43 models

Besides the animal models, several attempts were done to mimic the TDP-43 aggregation in cells in culture. Such models are valuable to investigate the impact of aggregation on the cellular metabolism, as well as to evaluate new therapeutic strategies to overcome aggregation.

It was early observed that the TDP-43 C-terminal tail contains a Q/N rich region that is involved in the protein-protein interactions (D'Ambrogio et al., 2009). Moreover, it was showed that expression of C-terminal fragments of TDP-43 is sufficient to generate cytoplasmic aggregates (Igaz et al., 2009). The importance of the Q/N rich region within the C-terminal tail of TDP-43 in the self-aggregation process was also confirmed by Fuentealba et al. (Fuentealba et al., 2010). Moreover, as already stated the majority of the mutations that have been found in ALS patients, are localized in the C-

terminal tail (Chen et al., 2013), and the aggregation tendency is enhanced by these ALS-linked TDP-43 mutations (Budini et al., 2012b; Johnson et al., 2009). In addition, the protein is cleaved, generating C-terminal fragments that are associated with cellular toxicity and/or increased TDP-43 mislocalization (Zhang et al., 2009). Based on these findings, and with the aim of looking for methodologies that could model the disease, our laboratory developed a cellular model of aggregation using a 30 amino acid TDP-43 C-terminal peptide to promote TDP-43 aggregation (Budini et al., 2012a; Budini et al., 2012b) (**Figure 8**).
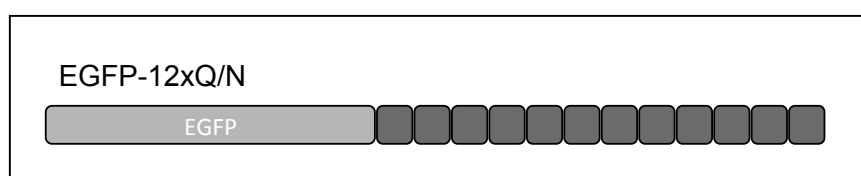
Figure 8. Schematic representation of the EGFP-12xQ/N construct.

The introduction of tandem repeats of TDP-43 Q/N rich amino acid sequence 331-369 (12xQ/N) linked to EGFP reporter is able to trigger the formation of predominantly cytoplasmic aggregates, capable of sequestering either exogenous or endogenous full-length TDP-43, recapitulating some of the features of the inclusions present in patients, such as ubiquitination and phosphorylation (**Figure 9**).
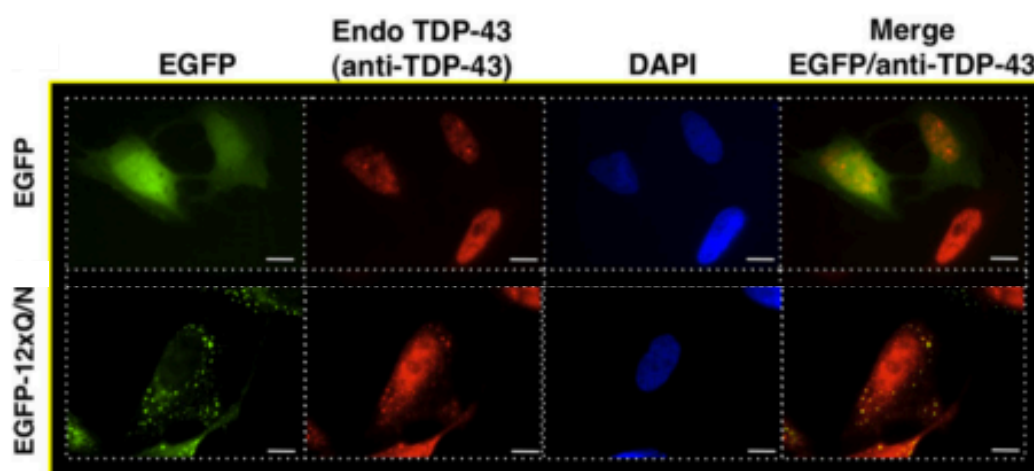
Figure 9. Immunoflorescence of U2OS cells transfected with EGFP or EGFP-12xQ/N constructs.

EGFP-12xQ/N forms aggregates, which co-localizes with endogenous TDP-43. Adapted from Budini et. al, 2012a.

However, there was no detectable splicing function deterioration in the presence of these TDP-43 aggregates induced by EGFP-12xQ/N, suggesting that they were not efficient enough in trapping endogenous TDP-43 to cause a loss of function in the short interval measured in a cell system. In fact, it can be seen in **Figure 9** that there is still TDP-43 present in the nuclei of EGFP-12xQ/N expressing cells.

In order to generate a model that could accomplish the nuclear loss of function of TDP-43 that is characteristic of ALS, a new variant of the previous model was generated. This new model is based on the TDP-43 molecule itself linked to the tandem repeats 12xQ/N (TDP-12xQ/N) (**Figure 10**).
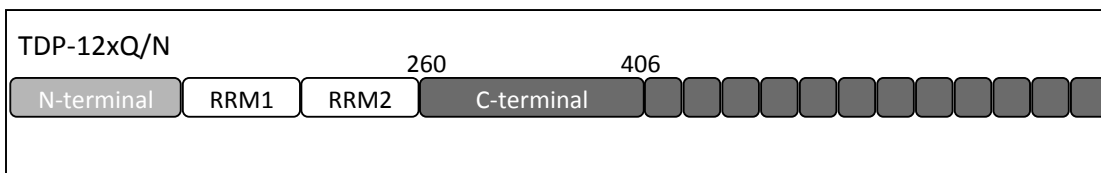
Figure 10. **Schematic representation of the TDP-12xQ/N construct.**

The TDP-12xQ/N model was shown to induce TDP-43 aggregation that was accompanied by TDP-43 nuclear depletion (**Figure 11**) and consequent alteration of its splicing function (Budini et al., 2014) (**Figure 12**).
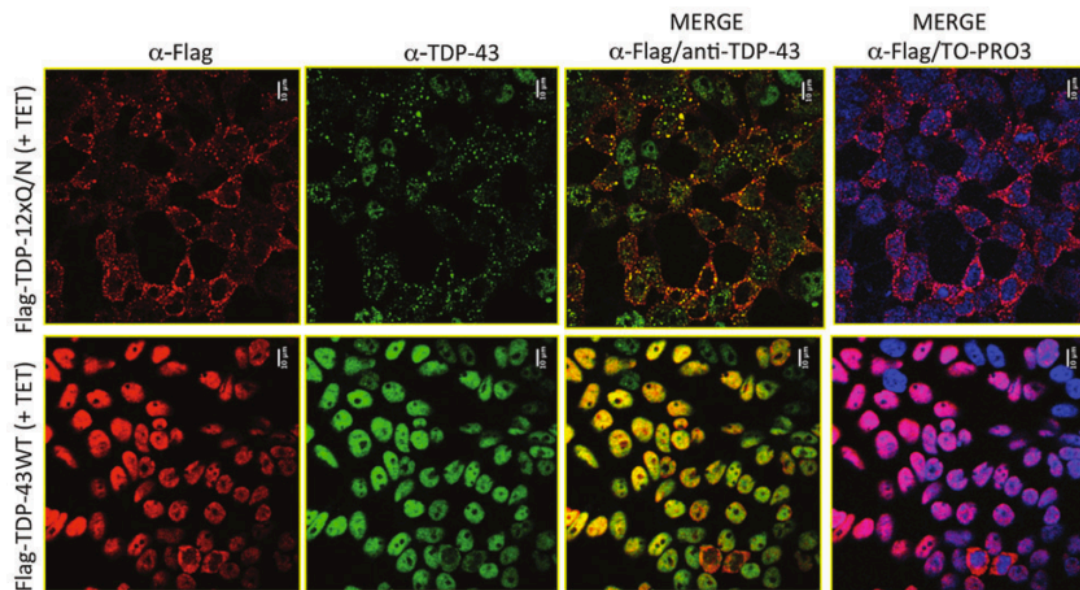
Figure 11. Immunoflorescence of TDP-12xQ/N HEK293 stable cells.
Adapted from Budini et. al, 2014.
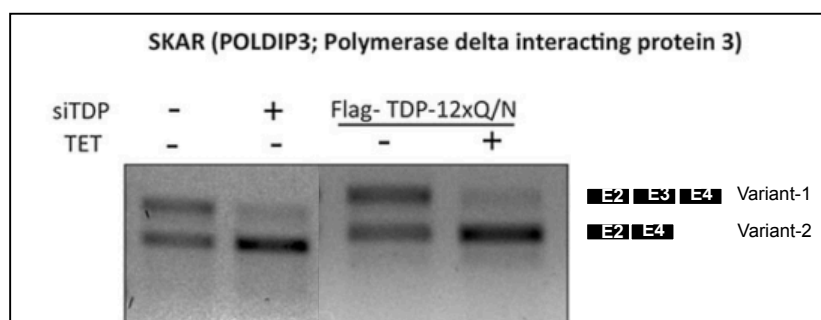
Figure 12. *POLDIP3* alternative splicing is affected in cells expressing TDP-12xQ/N.
Representative gel of RT-PCR products from control cells, cells treated with TDP-43 siRNA, and cells expressing TDP-12xQ/N construct (upon Tetracyclin induction), using *POLDIP3* specific primers spanning exon 3. Adapted from Budini et al, 2014.

Therefore, our cell-based models of ALS could be useful tools for the identification of active agents capable of reducing TDP-43 inclusions. With such approach we can gain some new therapeutic strategies/effectors, which hopefully could have a broad therapeutic potential in human TDP-43 proteinopathies.

In addition, generating an animal model based on this 12xQ/N construct would extend these studies looking at *in vivo* phenotype. On this way we hope to gain more knowledge about the impact of the aggregation on the cellular metabolism *in vivo*.

3.5. Autophagy and proteasome alterations in ALS

The biological activity of a protein is defined by its unique three-dimensional structure, and maintaining this structure during its lifetime is a delicate process. Misfolded proteins expose hydrophobic patches that are normally buried internally in the native folded state. Such hydrophobic regions are prone to trigger aggregation of other proteins, compromising their functionality (Dobson, 2003). It is estimated that approximately 30% of newly synthetized proteins are incorrectly folded (Schubert et al., 2000), but under normal conditions, the protein quality control is able to maintain the cellular homeostasis by preventing accumulation of aggregation-prone misfolded proteins (Hwang, 2011).

The first line of defense against protein misfolding and aggregation are the molecular chaperones, such as heat shock proteins (Hartl et al., 2011). In normal conditions, the misfolded proteins may be refolded to recover their normal conformation. In order to achieve this, the chaperones bind to the unfolded stretches present in the proteins and keep them in a folding-competent state while preventing aggregation. In addition, molecular chaperones, such as Hsp70, Hsp104 and Hsp40 help to disassemble intracellular protein aggregates and to accelerate the refolding of the insoluble molecules into soluble, native species (Glover & Lindquist, 1998; Parsell et al., 1994). In the case the misfolded proteins cannot be refolded they are directed to degradation.

In eukaryotic cells, there are two main systems that carry out proteolysis; one is the ubiquitin-proteasome system (UPS) and the other the lysosome-autophagy pathway. Proteolysis plays a paramount role in protein turnover, which maintains the quality of the cellular proteins by degrading the unnecessary or defective ones. Thus, proteins within the cells exist in a dynamic state, a balance between synthesis and degradation (Tanaka & Matsuda, 2014).

The proteasome, in collaboration with the ubiquitin system, is responsible for the basal protein turnover in the cell, as well as for the selective elimination of abnormal, short-lived or in-excess proteins (Jariel-Encontre et al., 2008). The proteasome is a sophisticated 2.5-MDa complex comprising a catalytic core particle (CP) and one or two terminal regulatory particles (RP) (Coux et al., 1996) (**Figure 13**).
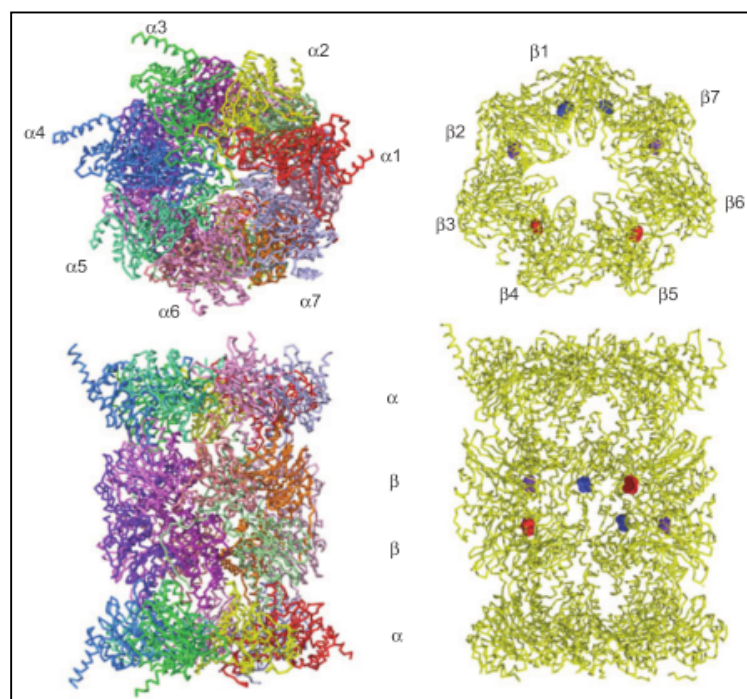
Figure 13. Crystal structure of the bovine proteasome CP.

Top view of the α-rings (top left) and side view (bottom left). Top view of the β rings (top right) and cutaway representation of the CP (bottom right). Active residues of β_1, β_2 and β_5 appear in blue, green and red, respectively. Adapted from Tanaka et al., 2012.

The CP forms a barrel-shaped particle of approximately 730 KDa consisting of four heptameric rings (two outer α rings and two inner β rings), which are made up of seven structurally related, but not identical, α and β subunits, positioned in a $\alpha_{1-7}\beta_{1-7}\beta_{1-7}\alpha_{1-7}$ orientation. The β_1, β_2 and β_5 subunits are associated with caspase-like hydrolyzing, trypsin-like and chymotrypsin-like activities, respectively, that cleave peptide bonds at post-acidic, basic or hydrophobic amino-acid residues, respectively (**Figure 13, right**). The crystal structures of the CP reveal that the center of the α-ring is almost completely closed, preventing the proteins from entering the cavity where the active sites are located (Groll et al., 1997) (**Figure 13, left**). Thus, a substrate is able to access the active sites only after passing through a narrow opening in the closed gate at the center of the α-ring.

Targeted proteins must become conjugated to a polyubiquitin chain to be recognized by the proteasome. Ubiquitination is a highly ordered process, in which an ubiquitin-activating enzyme (E1) first activates and transfers

ubiquitin to an ubiquitin-conjugating enzyme (E2) that then acts in concert with an E3 ligase to transfer ubiquitin to a lysine residue on the target protein. A chain of at least four ubiquitins is required for substrate recognition by the proteasome complex. The regulatory particle of the proteasome is the subunit that serves to recognize polyubiquitylated substrates. Furthermore, after trapping ubiquitinated proteins, the RP recycles ubiquitin molecules by detaching them from the protein. Finally, the RP unfolds and translocates the target protein into the interior of the CP for proteolysis (**Figure 14**).
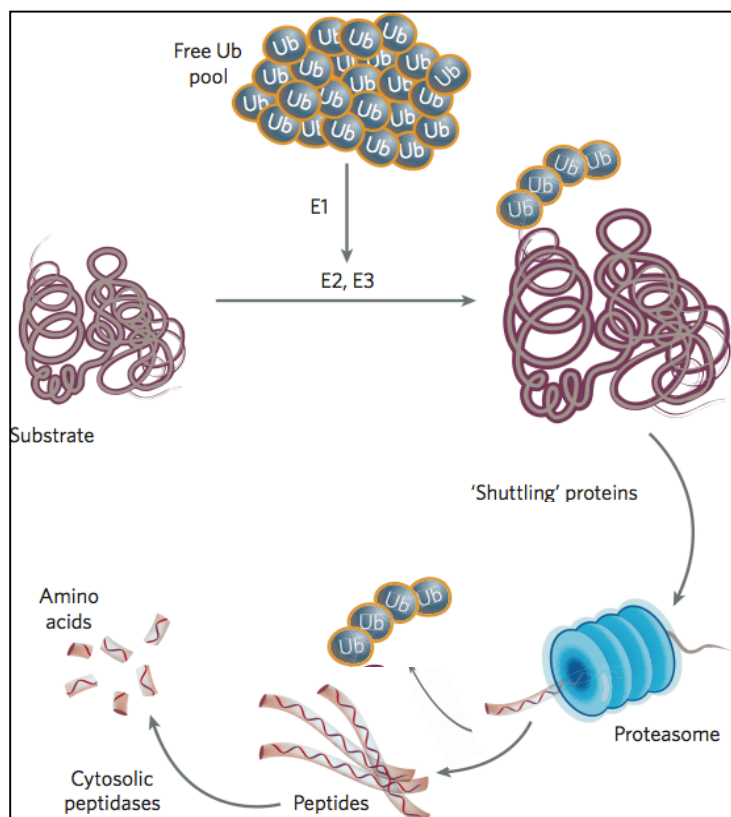
Figure 14. Schematic representation of the ubiquitin-proteasome system.
For proteasomal degradation, most proteins must be first covalently modified with ubiquitin. This process is orchestrated by three enzymes (E1, E2 and E3). Ubiquitinated proteins are then transported to the proteasome where they are degraded and the ubiquitin molecules recycled. Adapted from Rubinsztein, 2006.

On the other hand, autophagy is a degradative-recycling system, coupled with the lysosome, which contains hydrolytic enzymes for all the macromolecules, such as proteins, lipids, carbohydrates and nucleic acids. The major autophagic pathway is called macroautophagy, hereafter referred

to as autophagy. Autophagy uses specialized, cytosolic, double-membrane structures that engulf substrates to form autophagic vesicles termed autophagosomes. Autophagosomes are formed in the cytoplasm and are then trafficked along microtubules in a dynein-dependent manner towards the microtubule-organizing center, where they rapidly fuse to lysosomes, forming autolysosomes, after which their content, is degraded by a variety of lysosomal digestive hydrolases (He & Klionsky, 2010; Nakatogawa et al., 2009). Although, autophagy was initially thought to be a non-selective degradation system, it was demonstrated to work in tandem with ubiquitin, also contributing to the selective degradation of proteins (Johansen & Lamark, 2011; Kraft et al., 2010; Yao, 2010).

Autophagy is activated upon nutrient and bioenergetic stresses (Cherra & Chu, 2008). The principal role of this type of autophagy is to supply nutrients to cells during energetic crisis. In addition, there is a basal autophagy that is constitutively active at low levels, even under nutrient-rich conditions, and is involved in the global turnover of cellular components in order to maintain cellular homeostasis (Tanaka & Matsuda, 2014). Autophagy is also in charge of the clearance of disease proteins, long-lived proteins, protein complexes, microbes, or damaged organelles such as mitochondria (Bursch & Ellinger, 2005).

Misfolded proteins should be tagged with ubiquitin in order to bind the adaptor protein p62. On the other hand, the cytosolic form of LC3 (LC3-I) is conjugated to phosphatidylethanolamine to form LC3-II, which is recruited to autophagosomal membranes (Tanida et al., 2008). Additionally to its ubiquitin-binding domain, p62 has an LC3 interacting region, by which it can also bind LC3-II that is conjugated with the lipids in the double membrane of the forming autophagosomes (Bjørkøy et al., 2005). This allows the cargo to be included in the forming autophagosomes, which subsequently fuses with the lysosome for hydrolytic degradation (Tyedmers et al., 2010). p62 itself is degraded via autophagy, and is often used as a marker of autophagy induction. Moreover, HDAC6 controls the fusion of the autophagosomes with the lysosome by recruiting the actin-remodeling machinery that is involved in this process (Lee et al., 2010) (**Figure 15**).
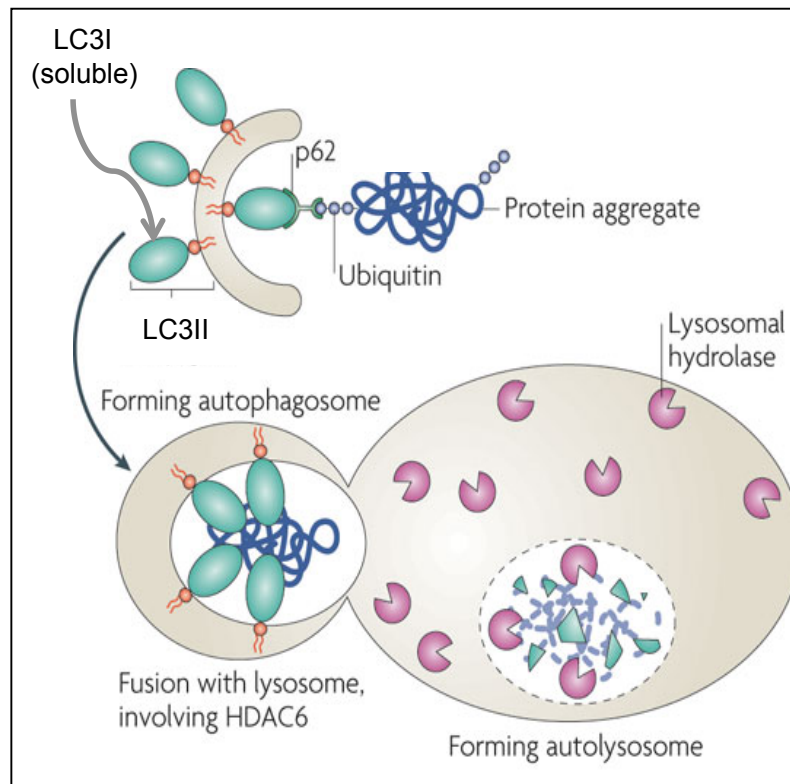
Figure 15. Model of the autophagic degradation of protein aggregates.
Ubiquitination of the protein aggregates is the signal that triggers the degradation of the protein aggregate. Main players include LC3, p62 and HDAC6. Adapted from Tyedmers et al., 2010.

Different conditions, such as metabolic or environmental stress or aging, increase the production of misfolded proteins and thus challenge the capacity of the cellular protein quality control system (Haigis & Yankner, 2010). It has also been suggested that during aging, the cells lose their ability to efficiently deal with misfolded proteins as the capacity of the proteasome and autophagy pathways declines. Protein aggregation seems to result from exhaustion of the cell´s quality control system, when generation of misfolded proteins exceeds the refolding or the degradative capacity of the cell. Furthermore, reduced activity of these two pathways is known to be associated with neurodegenerative diseases (Anglade et al., 1997; Cataldo et al, 1996; Kegel et al., 2000; Keller et al, 2000; Keller et al., 2001; McNaught & Jenner, 2001). It is possible that this situation leads to excessive accumulation and aggregation of proteins, which in turn causes

46

neuronal dysfunction and neurotoxicity, ultimately leading to neurodegeneration.

The crucial role of the autophagy pathway in the clearance of aggregate-prone proteins was first determined by a deductive approach using a brain-specific autophagy-ablated mouse model (Komatsu et al., 2006). In this study, Komatsu et al. reported that loss of Atg7 (autophagy-related gene 7), a gene essential for autophagy, leads to neurodegeneration, reflected by the behavioral defects, reduction in coordinated movements and decrease lifespan. Moreover, polyubiquitinated proteins accumulated in autophagy-deficient neurons forming inclusion bodies that increased in size and number with aging. Additionally, two years later, it was reported for the first time, that specifically 26S proteasomal dysfunction in a mouse model is sufficient to trigger neurodegeneration (Bedford et al., 2008). In this study, the authors inactivated the PSMC1 that is an essential subunit of the proteasome 26S, which in turn impaired ubiquitin-mediated protein degradation, which led to protein aggregation and signs of neurodegeneration. Taken together these observations indicate that the correct functioning of the cell's quality control system is crucial to avoid protein aggregation and neurodegeneration.

Particularly for ALS, proteasome impairment has been demonstrated in patients' samples. Kabashi et al. demonstrated in 2012 a reduction in proteasome activity in the spinal cord of ALS affected individuals, that was accompanied by a loss of substantial amount of proteasomes in motor neurons (Kabashi et al., 2012). Similar results were obtained by the same group using a transgenic animal model (Kabashi et al., 2004; Kabashi et al., 2008a). On the other hand, accumulation of autophagosomes was observed in the spinal cord of ALS affected patients, indicating autophagic dysfunction in ALS (Sasaki, 2011).

Finally, it was demonstrated that inhibition of UPS or autophagy dramatically increases TDP-43 aggregation, suggesting that this important protein can be degraded by both degradative systems (Wang et al., 2010). This observation was further confirmed by a study that shows that soluble TDP-43 is degraded primary by the UPS, whereas the clearance of its aggregates is mediated by autophagy (Scotter et al., 2014).

3.6. ALS treatment

As previously mentioned, several processes have been proposed to cause the selective dysfunction of motor neurons seen in ALS. One of these hypotheses considers that glutamate, the primary excitatory neurotransmitter in the central nervous system, accumulates to toxic concentrations at synapses, causing neuronal death. Several therapeutic approaches have been focused on targeting this glutamate related toxicity. In fact, the only FDA approved drug for ALS treatment is an inhibitor of the glutamate release, riluzole. Riluzole was approved for ALS treatment in 1995 (Bensimon et al., 1994), and since then, it remains the only treatment for this pathology. However, riluzole prolongs the median survival by about two or three months in patients with ALS (Miller et al., 2007).

Nowadays, there are a large number of drug candidates to treat ALS under investigation. Among them, Arimoclomol is currently in Phase III clinical trial for ALS-SOD1 treatment ("Phase II/III Randomized, Placebo-controlled Trial of Arimoclomol in SOD1 Positive Familial Amyotrophic Lateral Sclerosis - ClinicalTrials.gov," n.d.). It was shown that this drug is capable of activating molecular chaperones, and in particular it induces the heat shock response, acting on the Hsp70 (Brown, 2007; Kalmar et al., 2013; Kieran et al., 2004). Furthermore, also for ALS-SOD1 treatment but not yet in clinical trial, androgens, such as Dihydrotestosterone, have been proposed to increase muscle size and strength. In addition to the anabolic effects on muscle, androgens were shown to be neuroprotective, promoting neuronal survival and neurite outgrowth in motor neurons of the spinal cord (Yoo & Ko, 2012).

3.6.1. ALS treatment through autophagy or proteasome induction

Several studies suggest that activation of autophagy or proteasome may be protective in some neurodegenerative diseases by enhancing the removal of pathological protein aggregates. Autophagy induction was first evaluated in 2005 in a study where cultured cells, that expressed a polyglutamine mutant protein, known to cause Huntington's disease, were treated with rapamycin. Rapamycin activates autophagy by inhibiting mTOR, one of the

natural inhibitors of autophagy. Upon rapamycin treatment the clearance of aggregate-prone proteins was increased (Slow et al., 2005). Similar results were also obtained in another study with cells expressing α-synuclein (Webb et al., 2003), and in flies that expressed mutant aggregate-prone Tau (Berger et al., 2006). This effect of rapamycin in aggregate clearance was further confirmed by the treatment of a mouse model of Huntington's disease with a rapamycin analogue. In this case, not only the aggregate formation was decreased, but animals improved performance in four different behavioral tests (Ravikumar et al., 2004). Despite these promising results, mTOR inhibition was proved to have many side effects, as it is centrally involved in the regulation of cell growth and metabolism.

Current efforts are focused on finding compounds that can trigger autophagy clearance independently of mTOR. For example, it was shown that lithium treatment promotes aggregate clearance through autophagy induction, in cell and *Drosophila* models, independently of mTOR (Sarkar et al., 2005, 2008; Williams et al., 2008). Moreover, it was recently shown that ALS patients treated with lithium for 15 month survived, while 30% of control patients receiving riluzole died (Fornai et al., 2008a; Fornai et al., 2008b). Lithium is commonly used as a mood-stabilizing agent, but it was also shown to be neuroprotective (Chuang, 2004; Rowe & Chuang, 2004). However, follow-up studies showed no benefit from lithium dosing using a standard fALS mice model (Gill et al., 2009).

Overall, chemical inducers of autophagy are thought to offer a great potential for future studies in proteinopathies treatment.

In contrast to the development of autophagy inducers, drugs that can activate or enhance proteasome activity are rare and not well studied. Overexpression of PA28, a 20S proteasome activator, was shown to enhance the survival of HD neuronal model cells (Seo et al., 2007). This beneficial effect of PA28 overexpression on the HD cell model suggests that proteasome activation might be a useful target for drug development for proteinopathies treatment.

3.6.2. Tricyclic compounds and possible role in protein aggregate clearance

The tricyclic drugs are composed by a three-ring nucleus, which can be substituted on the central ring with a side-chain substituent. They were first used as antihistamines with sedative properties, and later as antipsychotics. They include an important group of tricyclic antidepressants (TCAs), which have been used for over 50 years (Pilkington et al., 2006). TCAs have been identified as inhibitors of mitochondrial permeability transition, which is one of the key factors in the damage to neurons. The increased permeability of the mitochondrial membrane to molecules smaller than 1,500 Da causes the depolarization of the mitochondria and, as a consequence, the electrochemical gradient, which is necessary for the ATP production, is lost. The common involvement of mitochondria in cell death pathways suggests that heterocyclic compounds might be considered as potential candidates to treat individuals suffering from neurodegenerative diseases that involve neuron loss in the central nervous system (Stavrovskaya et al., 2004). As part of the possible neuroprotective effect, there is evidence that support that these compounds could induce the protein aggregate clearance. Regarding this, Tsvetkov and collaborators demonstrated that some tricyclic compounds (nortriptyline, promethazine, thioridazine and chlorpromazine, among others) induce a protective autophagy response in striatal neurons. Moreover, the neuroprotective effect of nortriptyline was further established in a primary striatal culture model of HD. In this study the authors generalized that structurally related tricyclic compounds have similar actions in autophagy induction (Tsvetkov et al., 2010). Furthermore, in a United States Patent Application Publication the authors confirmed that tricyclic compounds could be used to treat protein aggregation diseases. It was suggested the use of a first active medicament (fluphenazine or thioridazine, among others) to prevent aggregation and a second active medicament (clomipramine or nortriptyline, among others) to disaggregate previously formed inclusions (Wilson & Standley, 2011).

From the list of the FDA approved tricyclic drugs, and because of the reasons stated so far, we have selected eight compounds for this study as shown in **Table 7**.

These drugs appear to offer several advantages as potential ALS therapeutic agents. First, they are clinically approved by the FDA, suggesting potential rapid movement into clinical trials. Second, they are able to cross the blood brain barrier and to act as neuroprotective agents. Third, they are safe for long-term use in humans, with only minor side effects.
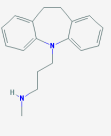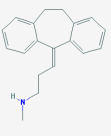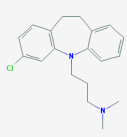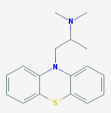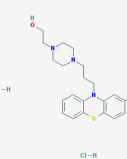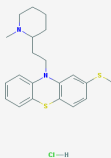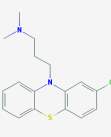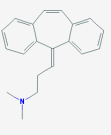
Compound	Drug class	Structure
Desipramine	Antidepressant	
Nortriptyline	Antidepressant	
Clomipramine	Antidepressant	
Promethazine	Antihistaminic	
Flufenazine	Antihistaminic	
Thioridazine	Antipsychotic	
Chlorpomazine	Antipsychotic	
Cyclobenzaprine	Muscle relaxant	

Table 7. Tricyclic compounds used in this study.
The structures were adapted from NCBI PubChem Data Bank.

4. *Drosophila melanogaster* as a model system

4.1. General Overview

Drosophila melanogaster has emerged as a powerful model to study human neurodegenerative diseases during the last decade. Several characteristics make *Drosophila* the organism of choice. Among them, the short generation time (approximately 10 days) and short life span (around 60 to 80 days). In particular these features make *Drosophila* amenable to study age-related disorders. In addition, approximately 75% of human genes known to be associated with disease have a *Drosophila* ortholog (Reiter et al., 2001). For each disease, specific neuronal regions begin to degenerate late in life. In order to study this, several methods are available to express genes in a spatially and temporally restricted manner. Moreover, synaptic activity can be measured in *Drosophila* using electrophysiological and imaging techniques from the neuromuscular junction and adult central nervous system, making this organism particularly amenable to study neurodegenerative diseases, such as ALS.

Drosophila melanogaster is also known as the fruit fly, as it usually accumulate around spoiled fruit. As other members of the *Drosophila* genus, it has a segmented body, composed by head, thorax and abdomen. The six legs and the two wings are attached to the thorax. *Drosophila* has also two antennae and one pair of red eyes on its head.

Flies have 4 pairs of chromosomes, usually represented as lines for the arms and circles for the centromeres. The X and the fourth chromosomes have major left arms and tiny right arms. The size of the X, 2L, 2R, 3L and 3R are roughly comparable, whereas chromosome 4 is only about one-fifth as large (**Figure 16**).
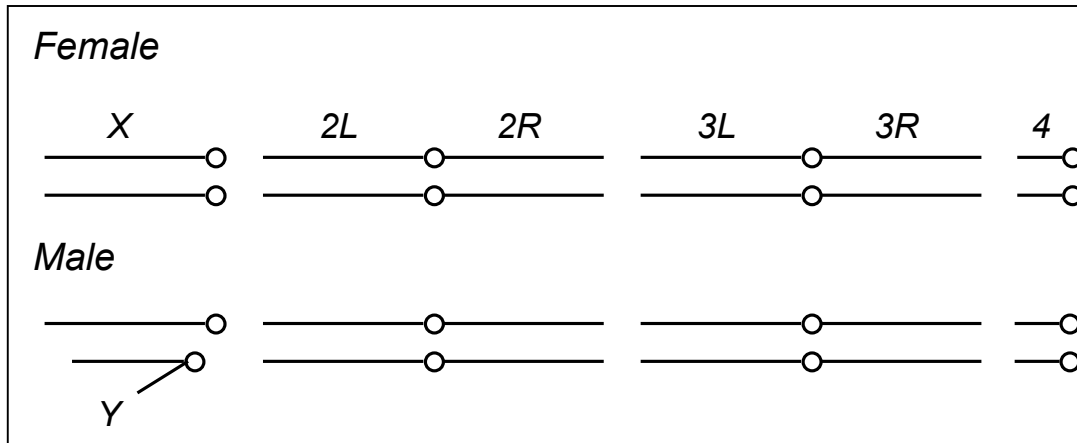
Figure 16. Schematic representation of flies' chromosomes.

Flies have 4 pair of chromosomes. In this figure arms are represented as lines and centromeres as circles.

The sex determination in *Drosophila* is based on the ratio of X chromosomes to autosomal set. In males, one X with two autosomal sets gives a ratio of 0.5, whereas the ratio is 1 in females. The Y chromosome is not required for most aspects of male development, only for proper sperm motility. One important feature of fly genetics is the total absence of recombination in males. On the other hand, recombination in females is completely normal.

Males are smaller and have darker and more rounded abdomens compared to females. Furthermore, the males have black sex combs on their first pair of legs that are important for male mating success (**Figure 17**).
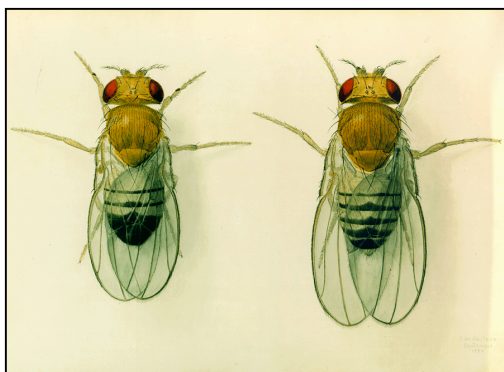
Figure 17. Schematic representation of the adult external dorsal aspect of *Drosophila*.

Males (left) and females (right) are phenotypically different. Adapted from St. Pierre et al., 2014.

Drosophila melanogaster has a rapid development, but it varies with the temperature. As other insects, the *Drosophila melanogaster*'s life cycle consists of four stages: egg, larva, pupa and adult (**Figure 18**). In optimal conditions (25°C with 60% humidity) it will take approximately 10 days to complete the life cycle. After mating, the females deposit the eggs in the food. Embryogenesis occurs within the egg, and around 24 hours later the first instar larvae hatches. Immediately after hatching the larvae start to feed themselves, molting 1 day, 2 days and 4 days after hatching, known as the first, second and third instar larval stages. During the growth period that lasts in total 4 to 5 days the larva increases approximately 200-fold weight. After 2 days the third instar larva molts one more time to form an immobile pupa. Metamorphosis takes place in the pupal case, lasting 4 to 5 days. After metamorphosis, the newly born fly breaks the pupal case to emerge. Immediately after birth, the fly has the wings still closed and a clear body pigmentation. The wings are completely opened 3 hours after birth, at the same time that the body acquires the normal brownish pigmentation.
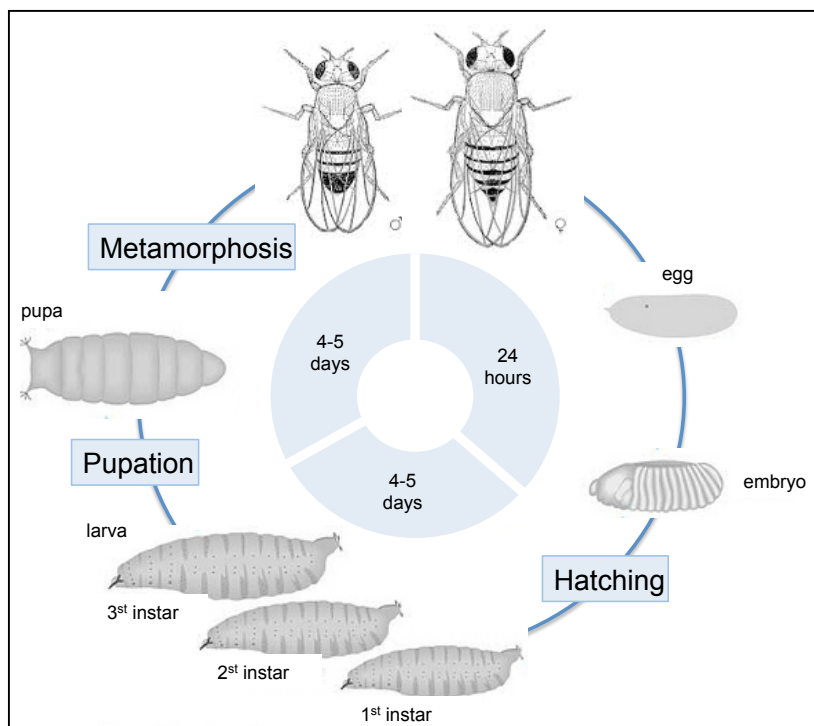
Figure 18. Schematic representation of *Drosophila melanogaster*'s life cycle.
The cycle lasts approximately 10 days and includes four stages: egg, larva, pupa and adult.

4.2. UAS/Gal4 System

Currently, almost all *Drosophila* models of neurodegenerative diseases have been developed using the Gal4/UAS system (Brand & Perrimon, 1993), which allows the tissue-specific expression of the transgene of interest. In this system, the transgene of interest is placed under an upstream activating sequence (UAS) that consists of Gal4-binding sites. In the absence of Gal4, the transgene will be transcriptionally repressed. When flies that carry the transgene are crossed with flies that express Gal4 in a specific tissue (also known as "driver" flies), the transgene will be activated in the offspring specifically in this tissue (**Figure 19**). A wide array of "driver" flies has been generated. The Gal4 is placed under a specific cell or tissue specific promoter, and this is of particular interest for the study of neurodegenerative diseases, where specific neuronal regions are compromised in patients' brain.
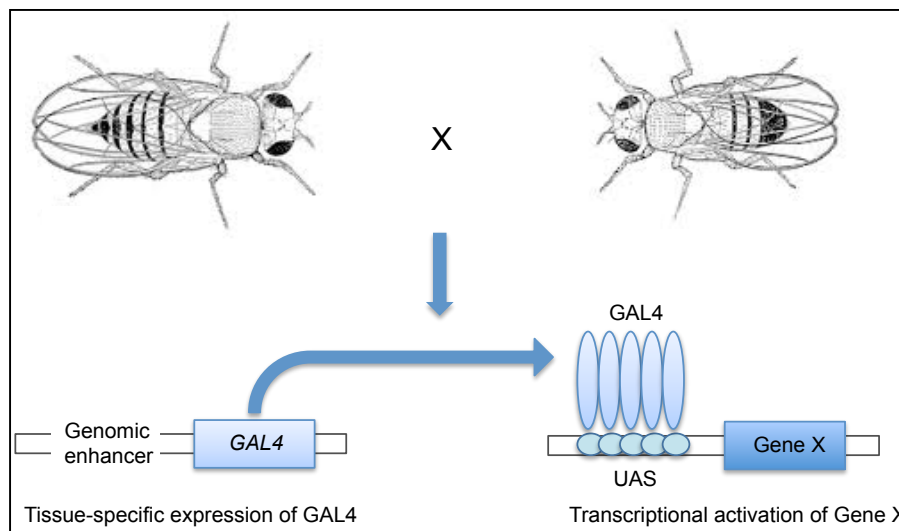
Figure 19. Directed gene expression in *Drosophila melanogaster*.

4.3. Markers and Balancer

Marker mutations are the key to deciphering genotypes. A vast array of mutations affecting eye color, eye shape, wing shape, wing vein morphology, bristle color, bristle shape, and cuticle pigmentation (this are the main categories) serve to tag the various chromosome arms. They may be used to mark the chromosomes that need to be followed or lost during a cross.

Balancer chromosomes are multiple inverted chromosomes, which cannot undergo exchange with their normal homolog during the homolog recombination process. Balancer chromosomes also carry marker mutations, in order to facilitate the synthesis of defined genotypes by segregation analysis.

Many balancers exist for the X, 2 and 3 chromosomes. There is no need of balancer of the fourth because there is no exchange on that chromosome. The most effective balancers are those, which suppress the exchange all along the chromosome.

4.4. Nomenclature

- The genotype of a chromosome is indicated only if there is a variant on it. The order is always X/Y, 2, 3 and 4.
- Semicolons are used to separate chromosomes.
- Commas are used to indicate rearrangements on a particular chromosome.
- A chromosomal genotype is written in one line if the stock is homozygous. Heterozygosis is indicated by a two-line genotype, each line corresponding to one of the homologs present.
- Anything that is not shown, or that indicated with "+" is presumed to be wild type.

4.5. TBPH: *Drosophila melanogaster* TDP-43 ortholog

TDP-43 protein is highly conserved through species. In particular, the human and *Drosophila melanogaster* proteins show striking similarities in their nucleic acid binding domains (75% of identity). Moreover the *Drosophila* TDP-43 is able to replace the function of the human protein both *in vitro* and *in vivo* (Ayala et al., 2005; Feiguin et al., 2009). The striking conservation between the human and *Drosophila* proteins suggests that TDP-43 has an important role in RNA metabolism.

The *Drosophila* protein, TBPH, is coded by the homonymous gene, which is located in the second chromosome. There are six annotated transcripts,

encoded by 5-6 exons, generated by alternative splicing (**Figure 20**). Importantly, TBPH C-terminal tail contains also Q/N stretches, as the human protein.
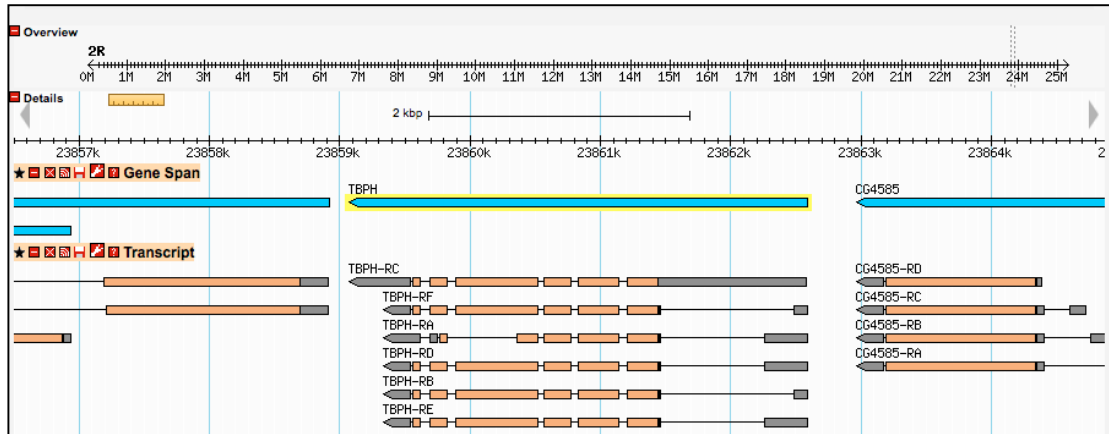
Figure 20. TBPH chromosomal location, and representation of its transcripts.
Adapted from FlyBase.

Research aims

Neurodegenerative diseases typically involve deposits of inclusion bodies formed by abnormal aggregated proteins. TDP-43 is the main protein aggregated in ALS patients' motor neurons, suggesting that these protein aggregates could be toxic. However, several lines of research indicate that inclusion bodies may represent the end-stage manifestation of an aggregation process, which could be part of the cellular protective response to toxic intermediates. Furthermore, in patients' brain the cytoplasmic TDP-43 aggregates are accompanied by the nuclear clearance of the protein, suggesting that the inclusions could be responsible for the entrapment of the protein in the cytoplasm, with the consequent nuclear loss of function of TDP-43.

Although the ubiquitous presence of TDP-43 inclusions in ALS and other TDP-43 proteinopathies suggests they are central to pathophysiology, there is still no universal agreement about the role they play.

The aim of this study was to characterize the role of TDP-43 aggregates in order to better understand their connection to the disease. Moreover, it was of interest to evaluate the functional consequences that the degradation of the aggregates could have *in vitro* and *in vivo*.

In order to achieve these objectives, the following specific aims were defined:

1. To create a *Drosophila* model that reproduces the alterations identified in patients suffering from ALS.
2. To determine if the TDP-43 inclusions are toxic by themselves or are a protective cellular response.
3. To use two already created and well-defined cellular TDP-43 aggregation models to perform a screening of compounds capable of triggering the degradation of the aggregates.
4. To study the functional consequences of the aggregate clearance, both in the cellular and fly models.

Materials and Methods

1. General reagents and protocols

1.1. Bacterial cultures

Escherichia coli K12 strain DH5α was used to perform transformation with all the plasmids of interest. Bacterial colonies were maintained at 4°C on Luria-Bertani (LB) agar plates with the desired antibiotic. When necessary, bacteria were grown overnight in liquid LB medium. In this case the antibiotic was added directly to the medium at a final concentration of 100 μg/ml.

1.2. Preparation of bacterial competent cells

Bacterial competent cells were prepared following standard procedures. Briefly, *E. coli* K12 strain DH5α was grown overnight in 10 ml liquid LB at 37°C (pre-inoculum). The day after, the pre-inoculum was transferred to a 300 ml fresh liquid LB, and cells were grown at 37°C for about 4-5 hours until OD_{600} was 0.3-0.4.

Cell growth was stopped by putting the cells on ice and then centrifuged at 4°C for 10 minutes at 0,1 x g. The pellet was resuspended in 30 ml of cold TSS solution (10% (w/v) PEG, 5% (v/v) DMSO, 35 mM $MgCl_2$, pH 6.5 in LB medium). Finally, cells were aliquoted and rapidly frozen in liquid nitrogen and stored at -80°C.

1.3. Bacterial transformation

Transformation was performed using 10 μl of ligation reaction, or 20 ng of DNA plasmids. DNA was incubated with 60 μl of competent cells on ice for 20 minutes and then the heat shock was performed by transferring the vial to 42°C for 2 minutes. Another incubation on ice was performed for 5 minutes and finally the bacteria were allow to recover at 37°C for 30 minutes. Cells were then plated on LB agarose plates containing the proper antibiotic and incubated for about 12 hours at 37°C.

1.4. Small-scale preparation of plasmid DNA from bacterial cultures

In order to extract DNA plasmids from bacterial cultures, a single colony was inoculated and grown in 6 ml of Terrific Broth (TB) medium overnight at 37°C. The Wizard plus SV miniprep DNA purification system from Promega (Promega # A1330) was used according to the manufacturer's instructions.

1.5. Plasmidic DNA digestion

DNA digestion was performed using the corresponding digestion buffer specifically created by the same company for each restriction enzyme. In general, the digestion was performed with 100-500 ng of DNA in a final volume of 50 µl containing 5 units of the restriction enzyme of interest. 2-3 hours incubation was performed at the optimal temperature indicated by the manufacturer.

1.6. DNA ligation

To perform DNA ligation the T4 ligase (Roche # 11635379001) was used. This enzyme is able to adjoin double stranded DNA fragments having compatible sticky or blunt ends. The reaction was performed with 20 ng of digested vector and 5-10 fold molar excess of the digested insert in a total volume of 20 µl, containing 1X ligase buffer and 1 unit of T4 DNA ligase. The reaction was incubated for 4-10 hours at room temperature.

1.7. Agarose gel electrophoresis of DNA

Size fractionation of DNA samples was performed through electrophoresis in agarose gel 1-2% (w/v) prepared in TBE 1X (220 mM Tris; 180 mM Borate; 5 mM EDTA; pH 8.3). The samples of interest were loaded in gels containing ethidium bromide (0.5 µg/µl), at 80 mA in TBE 1X running buffer. DNA was visualized by UV trans illuminator machine and the result was photographed using a digital camera.

1.8. DNA sequencing

Sequence analysis was performed by sending 2 µg of plasmid DNA preparation to Macrogen Company.

2. An ALS *Drosophila* model

2.1. Generation of transgenic fly lines

2.1.1. Generation of constructs

In order to generate the transgenic flies used in this work, the constructs were cloned in pUASTattB and pKS69.

pUASTattB is highly used in the field as it allows site specific insertion of the transgene of interest in the *Drosophila* genome. The plasmid (**Figure 21**) is 8.4 Kb long (Gene Bank accession number EF362409). It contains the *white* gene (coding for the red color of the eye) as a genetic marker, a region with 5 UAS binding sites upstream of the hsp70 promoter, loxP sequences, a multiple cloning site, the sequence attB and ampicillin resistance. The attB site allows the integration of the transgene in the attP landing platform in the fly genome, taking advantage of the phage ΦC31 integrase system (Bischof et al., 2007). EGFP-12xQ/N and EGFP constructs were cloned in pUASTattB, and specific inserted in *Drosophila*'s third chromosome.
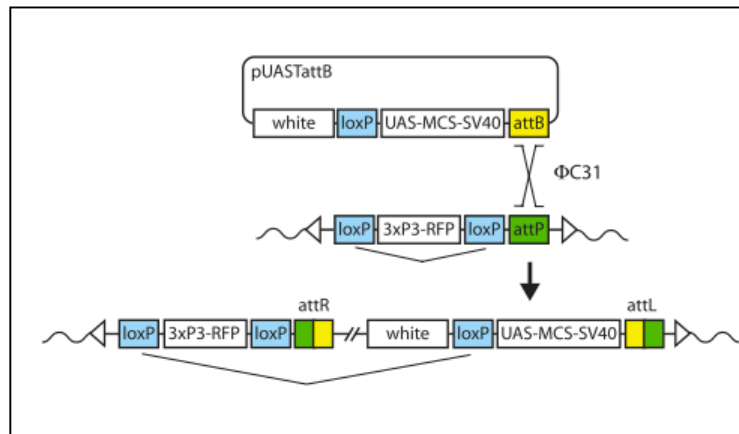
Figure 21. Schematic representation of pUASTattB vector and its integration mechanism into attP landing sites.

pUASTattB contains a 285-bp attB fragment, the white^{+} selectable marker, a UAS-MCS-SV40 cassette (Brand & Perrimon, 1993), and a single loxP site. The ΦC31 integrase mediates recombination between attB and attP sites, resulting in the integration of pUASTattB into the landing site, thereby creating the two hybrid sites attL and attR, which are refractory to the ΦC31 integrase. Adapted from Bischof et al. 2007.

pKS69 plasmid (**Figure 22**) is 13 Kb long and is derived from a modification of a plasmid pP{CaSpeR-lacZ}. It presents sequences of the P element that mediates recombination of the gene of interest into the genome of the fruit fly. As pUASTattB, pKS69 contains the *white* gene as a genetic marker that allows the identification of the recombinant (red eye). It contains 10 tandemly arrayed optimized Gal4 binding sites (the UAS sequences) followed by the hsp70 promoter, a poly linker containing 2 unique restriction sites (EcoRI and XbaI), the SV40 terminator site with the poly adenilation site and ampicillin resistance. This plasmid has been used for the integration of TBPH, its truncated form TBPHΔC (1-332) and human Tau cDNA (4N2R isoform) constructs.
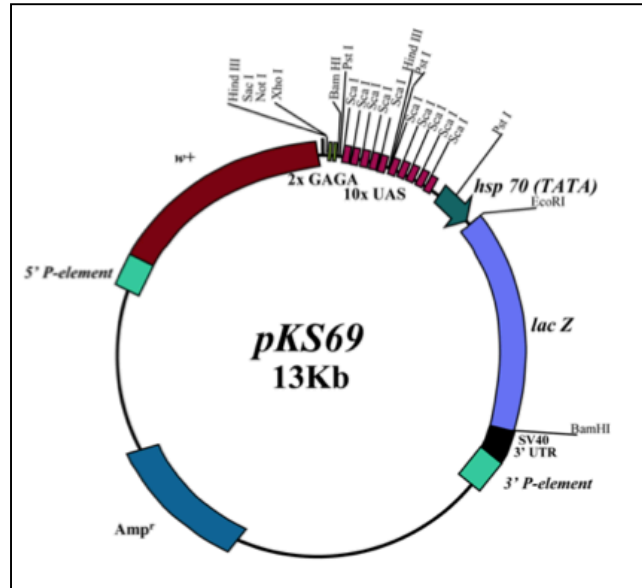
Figure 22. Schematic representation of pKS69 vector.

It contains the *white* gene as a genetic marker (w+), 10 tandem arrayed optimized Gal4 binding sites (UAS), the hsp70 TATA box and transcriptional start, a poly linker containing multiple restriction sites and the SV40 terminator site with the polyadenylation site. The vector presents also ampicillin resistance.

2.1.2. S2 cells transfection

The S2 cells derive from primary culture of late stage (20-24 hours) *Drosophila melanogaster* embryos (Schneider, 1972). They form semi-adherent monolayer when grown in culture flasks at room temperature, without CO_2. Insect Express medium (Lonza # BE12-730F) supplemented with 10% (v/v) heat-inactivated fetal bovine serum and 1X antibiotic-antimycotic (Sigma # A5955) was used to maintain the cells in culture.

Before sending the constructs to Best Gene Company for the generation of the transgenic flies, the expression level and the potential toxicity of the exogenous protein were tested in S2 cells.

Transfection was performed using Effectene transfection reagent kit (Qiagen # 301425), a non-liposomal lipid reagent for DNA transfection. S2 cells were plated at a concentration of $3x10^6$ cells/ml with 4 ml of complete Insect Express medium. The transfection reaction was prepared as follows: 4 µl of DNA plasmid containing the construct of interest (final concentration 0.25 ug/ul), 1 µg of plasmid harboring Gal4 factor and 8 µl of Enhancer were

added to the Condensation buffer up to a total volume of 150 μl and incubated at room temperature for 5 minutes. 25 μl of Effectene reagent was subsequently added to the mixture, mixed by vortexing and incubated at room temperature for 10 minutes to allow formation of the transfection complex. Then, the transfection complex was added to 1 ml of medium and finally it was transferred to the dish containing the cells. The cells were incubated at 25°C for at least 48 hours in order to obtain the expression of the recombinant protein.

2.1.3. Transgenic flies

Endogenous TBPH, its truncated form TBPHΔC (1-332) and human Tau cDNA (4N2R isoform) were Flag tagged and cloned in pKS69. EGFP-12xQ/N (12 repetitions of the TDP-43 331-369 sequence) and EGFP constructs were cloned in the pUASTattB vector (Bischof et al., 2007). All the constructs have been sequenced and subsequently used to create transgenic flies by standard embryo injections (Best Gene Inc.). While random insertions in yellow-white stain have been chosen for TBPH, TBPHΔC and human Tau, a specific insertion using strain 24486 was chosen for EGFP-12xQ/N and EGFP. All transgenic flies have been subsequently balanced on the required chromosome.

2.2. *Drosophila* technics

2.2.1. *Drosophila* stocks handling

W1118, Oregon-R, GMR-Gal4, ELAV-Gal4 and D42-Gal4 were obtained from Bloomington *Drosophila* Stock Center at Indiana University (http://flystocks.bio.indiana.edu/). Additional stocks were kindly provided by colleagues or were generated as part of this study.

Flies were fed on standard cornmeal (2,9% (w/v)), sugar (4,2% (w/v)), yeast (6,3% (w/v)) fly food and maintained in a humidified incubator at 25°C with a 12 hours-12 hours light-dark cycle. Experimental crosses were performed at 25°C or 29°C with the same conditions of humidity and light-dark cycle as stock flies.

2.2.2. *Drosophila* anaesthetization

To allow the identification of the sex and genotype, the flies were anaesthetized on a pad with CO_2 gas. The constant gas flow provided, allows the immediate and continuous anaesthetization.

2.2.3. *Drosophila* crossing technics

Experimental crosses were established by adding males to virgin females. Females with less than 8 hours old reject countership and, therefore, are considered virgins. On this basis, all adults from a vial were removed and after 7-8 hours the newly eclosed females were harvested. They were kept for up to one week in order to collect a considerable number to proceed with the crosses. Virgin females were then combined with males in a fresh tube and stored at 25°C or 29°C for up to 7 days. The parental flies were then removed to allow the collection of the progeny.

2.2.4. Balancing of transgenic flies to avoid loss of the transgene

Transgene insertion could be in any of the fly's chromosomes: X, II or III. Transgenes inserted on the fourth chromosome are very rare as this chromosome is very small and it is essentially formed by heterochromatin. Transgenic flies obtained from Best Gene Company were directly crossed with the specific balancer on the second or third chromosome to avoid loss of the transgene. To do so, an individual male carrying the transgene (which contains the *white* gene coding for the red color of the eye, marked as w+) is crossed with a balancer female. If the insertion lays on the second chromosome the male is crossed with a Pin/Cyo balancer female (carrying the dominant morphological marker curly wings). To create the final stock one male and one female carrying both, the transgene (marked with w+) and the CyO balancer are crossed again. From the F2 progeny only the flies with the CyO balancer are kept to produce the stock (**Figure 23**).
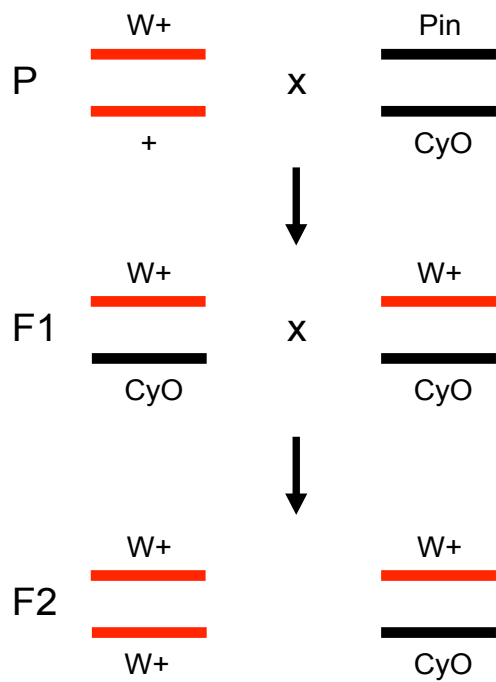
Figure 23. Schematic representation of the crosses with the second chromosome balancer Pin/CyO.

If the insertion has been made in the third chromosome, Apc/TM3,Sb female balancer flies are used (carrying the dominant morphological marker stubble hairs), following the same procedure already explained for the second chromosome (**Figure 24**).
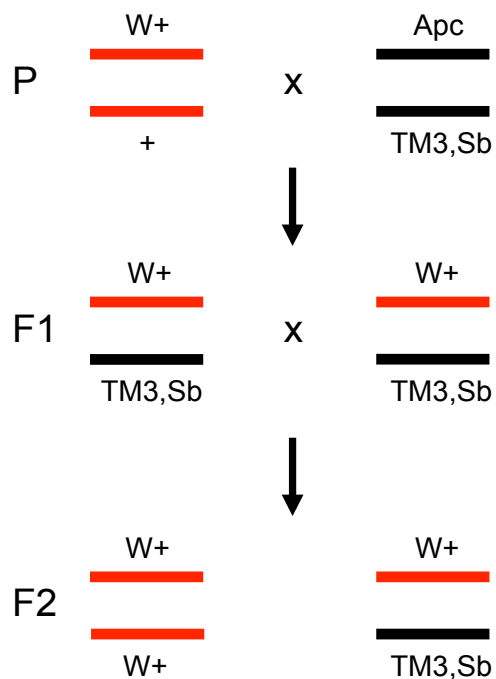
Figure 24. Schematic representation of the crosses with the third chromosome balancer Apc/TM3,Sb.

EGFP-12xQ/N and EGFP transgenic lines were balanced on the third chromosome, whereas TBPH, TBPHΔC and human Tau were balanced on the second chromosome.

2.2.5. Nortriptyline feeding procedure

Flies were harvest for 1 or 2 days and placed in instant food (Formula 4-24, Carolina Biologicals # 173200) containing different concentrations of nortriptyline (33 mM, 12 mM and 7 mM). 7 mM was chosen for the rest of the experiments, as this concentration presented no detrimental effects on the survival rate of the flies. To prepare the food, 8 grams of instant food were mixed with 25 ml nortriptyline 7 mM dissolved in water. The food was displaced in tubes and after 5 minutes the flies were introduced. Control flies were grown in food dissolved in water. The tubes were changed every 2 days, and finally climbing assay was performed after 7 days of treatment.

2.3.   *Drosophila* phenotypic analysis

2.3.1. Light microscopy of fly eyes

Eye phenotypes of 1 day-old flies were analyzed with stereomicroscope (Leica MZ75) and photographed with camera (Leica DFC420C).

For the quantitative analysis of the induced eye phenotypes we defined arbitrarily 3 categories: (1) normal eye, (2) loss of pigmentation and small regions of necrosis, (3) loss of pigmentation and massive regions of necrosis. At least 50 1 day-old flies were analyzed for each genotype.

2.3.2. Phototaxis assay

Drosophila has long been known to be phototactically positive in adult and negative in larval stages (Gong, 2012). The altered behavior could reflect a deficit in motor output, light reception or the processing of the visual information (Rahman et al., 2012). Phototaxis assay was performed in a Y-maze with one arm exposed to violet light (peak wavelength 400 nm) and the other arm completely in the dark. Flies from each genotype were

independently introduced into the stem of the Y-maze, and had the choice between violet light and the dark. After 30 seconds the number of flies that moved towards the illuminated chamber was determined. In each test 50 flies were analyzed. At least 100 (1 day-old) flies of each genotype were tested. The number of phototactic flies was converted into % value, and the mean % value (±SEM) was calculated. One-way ANOVA followed by Bonferroni's multiple comparison was used to compare measures among 4 groups. The significance between the variables was shown based on the p-value obtained (ns indicates $p > 0.05$, *indicates $p < 0.05$, **indicates $p < 0.01$, ***indicates $p < 0.001$ and ****indicates $p < 0.0001$).

2.3.3. Climbing assay

The negative geotaxis (movement against gravity) is an innate characteristic of *Drosophila* (Benzer, 1967). Moreover, the flies are naturally attracted to light stimulus (phototaxis). Thus, flies were transferred without anesthesia to a 50 ml glass-cylinder, tapped to the bottom of the tube, with a distal lamp to provide the stimulus, and their subsequent climbing activity was quantified as number of flies that reach the top of the tube in 15 seconds. This behavior is stable during the first three weeks of adult life, but progressively declines with age. Therefore, the climbing ability was measured at 3, 7 and 14 days of fly's life.

At least 100 flies of each genotype were tested. In each set of experiments 20 flies (1:1 male:female ratio) were introduced in the cylinder and tested in triplicate. The number of top climbing flies was converted into % value, and the mean % value (±SEM) was calculated for at least 5 experiments. One-way ANOVA followed by Bonferroni's multiple comparison was used to compare measures among 4 groups. Unpaired t-test analysis was used to compare measures between 2 groups. The significance between the variables was shown based on the p-value obtained (ns indicates $p > 0.05$, *indicates $p < 0.05$, **indicates $p < 0.01$, ***indicates $p < 0.001$ and ****indicates $p < 0.0001$).

2.3.4. Life span

Adult flies were collected for 2 days and transferred to tubes with food. Each tube contained 20 flies in a proportion 1:1 male:female ratio. The lifespan trials were conducted in humidity and temperature controlled conditions. Every third day, flies were transferred, without anesthetization to a fresh tube and deaths were scored. Survival rate was plotted as percentage of survival flies against day. Approximately 100 flies were tested of each genotype. Long rank test was performed to compare survival distribution between genotypes. The significance between the variables was shown based on the p-value obtained (ns indicates $p > 0.05$, *indicates $p < 0.05$, **indicates $p < 0.01$, ***indicates $p < 0.001$ and ****indicates $p < 0.0001$).

2.3.5. Larval movement

Drosophila larvae show natural peristaltic movements, characterized by a wave, which starts at one end of the larvae, passes through all the body, and ends in the mouth. This muscle contraction allows the anterior movement. In physiological conditions, the movement is interrupted by pausing, turning and head swinging (Rodriguez Moncalvo and Campos, 2009). During each wave the larval hook makes an anchor point in advance. Evaluation of peristaltic waves has been done testing the movement of third instar larvae.

Wandering third instar larvae were selected, washed and transferred to a Petri dish with a layer of 0,7% (w/v) agarose. After a period of adaptation, the peristaltic waves within 2 minutes were counted. At least 20 larvae from each genotype were counted, and the mean was calculated. One-way ANOVA followed by Bonferroni's multiple comparison was used to compare measures among 4 groups. Unpaired t-test analysis was used to compare measures between 2 groups. The significance between the variables was shown based on the p-value obtained (ns indicates $p > 0.05$, *indicates $p < 0.05$, **indicates $p < 0.01$, ***indicates $p < 0.001$ and ****indicates $p < 0.0001$). Values are presented as a mean and error bars indicate standard error means (SEM).

2.4. Biochemical technics

2.4.1. Protein extraction

Transfected S2 cells were transferred to 1.5 ml tubes and collected by centrifugation at 16,000 x g and resuspended in 100 µl of Lysis Buffer (50 mM Tris-HCl pH 7.6, 750 mM NaCl, 1% (v/v) Triton X-100 and protease inhibitors (Roche Diagnostic # 11836170001)).

Regarding flies, total proteins were extracted from the head. Whole flies were frozen in liquid nitrogen and then vortexed to separate the head from the body. *Drosophila* heads were homogenized in lysis buffer (8-10 µl/head) (10 mM Tris-HCl, pH 7,4, 150 mM NaCl, 5 mM EDTA, 5 mM EGTA, 10% (v/v) Glycerol, 50 mM NaF, 5 mM DTT, 4 M Urea, and protease inhibitors (Roche Diagnostic # 11836170001)).

Material in lysis buffer was homogenized manually with pestles for 2 minutes, followed by centrifugation at 0.5 x g for 5 minutes at 4°C. Supernatants were collected, used and/or stored at -80°C.

Larval brains were dissected in Phosphate Buffer with 0,1% (v/v) Tween 20 (PBT) and collected in Loading Buffer (0.1 M Tris-HCl pH 6.8, 30% (v/v) glycerol, 8% (w/v) SDS, 9.8% (v/v) β-mercaptoethanol and 0.1% (w/v) bromophenol blue), and homogenized.

Mouse whole brains were homogenized with mechanical agitator (ForLab, Bergamo, Italy) in RIPA buffer (150 mM NaCl, 1% (v/v) NP-40, 0,5% (w/v) DOC, 0,1% (w/v) SDS, 50mM Tris HCl, pH8, 2X protease inhibitors (Roche Diagnostic # 11836170001)).

2.4.2. SDS-PAGE

Sodium dodecyl sulfate polyacrylamide gel electrophoresis (SDS-PAGE) is a widely used method to separate proteins according to their sizes. Protein samples were diluted in Laemmli buffer (0.1 M Tris-HCl pH 6.8, 30% (v/v) glycerol, 8% (w/v) SDS, 9.8% (v/v) β-mercaptoethanol and 0.1% (w/v) bromophenol blue), and boiled at 95°C for 5 minutes. Gels were prepared as detailed in **Table 8**.

Components	Resolving gel	Stacking gel
Acrylamide-BIS	8% or 10% (v/v)	5% (v/v)
Tris-HCl pH 8.8	0.37 M	-
Tris-HCl pH 6.8	-	0.125 M
Ammonium persulphate	0.1% (w/v)	0.1% (w/v)
SDS	0.1% (w/v)	0.1% (w/v)
TEMED	0.02% (v/v)	0.02% (v/v)

Table 8. SDS gel preparation.

The amperage applied for the running was 25mA in 2X running buffer, prepared from a 10X stock (**Table 9**).

Reagent	Quantity
Tris (Invitrogen # 15504-020)	30,3 gr
Glycine (Sigma # 33226)	144 gr
SDS (BDH # 301754L)	5 gr

Table 9. 10X running buffer preparation.

2.4.3. *Drosophila* Immunoblotting

Proteins were separated by 8% SDS-PAGE, transferred to nitrocellulose membranes (Whatman # NBA083C) and probed with primary antibodies: mouse anti-GFP (1:2,000, Roche # 11814460001), rabbit anti-TBPH (1:1,500, home-made), mouse anti-synapsin (1:4,000, Hybridoma Bank # 3C11) and mouse anti-tubulin (1:4,000, Calbiochem # CP06). The membranes were incubated with the secondary antibodies: HRP-labeled anti-mouse (1:1,000, Thermo Scientific # 32430) or HRP-labeled anti-rabbit (1:1,000, Thermo Scientific # 32460). Finally, protein detection was assessed with Femto Super Signal substrate (Thermo Scientific # 34095).

Protein bands were quantified using NIH ImageJ. The intensity of the band of interest was normalized with tubulin. The respective histogram for each western blot shows the relative expression of at least 3 independent experiments.

Unpaired t-test analysis was used to compare measures between 2 groups. The significance between the variables was shown based on the p-value obtained (ns indicates p>0.05, *indicates p<0.05, **indicates p<0.01, ***indicates p<0.001 and ****indicates p<0.0001). Values are presented as a mean and error bars indicate standard deviation (SD).

2.4.4. Mouse brain Immunoblotting

Total protein extracts were separated by 10% SDS-PAGE, transferred to nitrocellulose membranes (Whatman # NBA083C) and probed with primary antibodies: rabbit anti-TDP-43 (1:1,000, Proteintech # 10782-2-AP), rabbit anti-synapsin I (1:1,000, Abcam # ab18814), rabbit anti GAPDH (1:1,000, Santa Cruz # sc-25778). The membranes were incubated with the secondary antibodies: HRP-labeled anti-rabbit (1:1,000, Thermo Scientific # 32460). Finally, protein detection was assessed with ECL Western Blotting Substrate (Thermo Scientific # 32106). Protein bands were quantified using NIH ImageJ. The intensity of the band of interest was normalized with GAPDH. The histogram for the western blot shows the relative expression of at least 3 independent experiments.

2.4.5. Solubility test

24 adult fly heads were dissected and homogenized in 192 µl of RIPA buffer (50 mM Tris-HCl, pH 8, 150 mM NaCl, 2 mM EDTA, 1% (v/v) Nonidet-P40, 0.1% (w/v) SDS, 1% (w/v) Na-deoxycholate and a cocktail of protease inhibitors (Roche Diagnostic # 11836170001)). The samples were incubated under agitation for 1 h at 4°C and then centrifuged at 1,000 x g for 10 minutes at 4°C. An aliquot was taken at this point as the input, and after a further centrifugation step at 100,000 x g for 30 minutes at 4°C, the supernatant was collected as the soluble fraction. The remaining pellet was re-extracted in 60 µl of urea buffer (9 M urea, 50 mM Tris-HCl, pH 8, 1% (w/v) CHAPS and a cocktail of protease inhibitors (Roche # 04693159001)) and spun down to remove any precipitate, while the 9 M urea soluble material was collected as the insoluble fraction. Proteins were separated by

8% SDS-PAGE. The different samples were loaded in a proportion 1:1:1 for the input, soluble and insoluble fractions. Proteins were electro-blotted to a nitrocellulose membrane (Whatman # NBA083C) and probed with the following primary antibodies: rabbit anti-TBPH (1:3,000, home-made), mouse anti-GFP (1:2,000, Roche # 11814460001) and mouse anti-tubulin (1:4,000, Calbiochem # CP06). The membranes were incubated with the secondary antibodies: HRP-labeled anti-mouse (1:1,000, Thermo Scientific # 32430) or HRP-labeled anti-rabbit (1:1,000, Thermo Scientific # 32460). Finally, protein detection was assessed with Femto Super Signal substrate (Thermo Scientific # 34095).

2.4.6. RNA extraction from adult flies

Whole flies were frozen in liquid nitrogen and then vortexed to separate the head from the body. The heads were collected in TRIzol reagent (Invitrogen # 15596-026) (30 µl/head) and squeezed with a pestle for 2 minutes. After centrifugation at 12,000 x g for 15 minutes at 4°C to remove debris, the supernatant was recovered and 120 µl of chloroform / 1ml of TRIzol were added. Samples were mixed, incubated 15 minutes at room temperature and centrifuged at 12,000 x g at 4°C for 15 minutes. The aqueous phase was recovered and 500 µl of isopropanol / 1ml of TRIzol were added. The samples were again centrifuged at 12,000 x g at 4°C for 8 minutes. The RNA pellet was finally washed with 1 ml ethanol and spinned down at 7,500 x g at 4°C for 5 minutes. RNA was dissolved in 50 µl of RNase free water, and quantified with Nanodrop equipment.

2.4.7. RNA extraction from mouse

Regarding mouse brain total RNA, the same protocol as for *Drosophila* was performed with the exception that the whole brain was homogenized in TRIzol using a mechanical agitator (ForLab, Bergamo, Italy) prior to RNA extraction.

2.4.8. cDNA synthesis

1µg of total RNA was treated with DNAse (Promega RQ1 # M610A) (**Table 10**). The mixture was incubated at 37°C for 30 minutes and then DNAse stop solution was added and incubated at 65°C for 10 minutes to inactivate the DNAse enzyme.

Component	Volume
RNA (1µg)	1-8 µl
10X buffer	1 µl
DNAse enzyme	1 µl
H_2O	Up to 10 µl

Table 10. DNAse treatment.

The RNA was subsequently retrotranscribed with Superscript III (Invitrogen # 18080-044) as indicated in **Table 11** and **Table 12**.

MIX 1	Volume
RNA	8 µl
OligodT (50 mM)	1 µl
dNTPs (10 mM)	1 µl

Table 11. Reverse transcription reaction 1.

The mixture 1 was incubated at 65°C for 5 minutes and then immediately was placed on ice for at least 2 minutes.

MIX 2	Volume
10X RT buffer	2 µl
MgCl$_2$ (25 mM)	4 µl
DTT (0.1 M)	2 µl
RNase OUT	1 µl
Superscript III	1 µl

Table 12. Reverse transcription reaction 2.

The mixture 2 was added to the mixture 1 and incubated at 50°C for 50 minutes to allow cDNA synthesis. The reaction was stopped by putting the sample at 85°C for 5 minutes to inactivate the enzyme.

2.4.9. Real-time PCR

RNA samples were used to prepare cDNA samples as explained in section 2.4.8. cDNA was used as template for the real time PCR, in order to asses the expression levels using housekeeping genes. All amplifications were done on CFX96 real-time PCR detection system (Biorad) using SYBR Green technology (Biorad # 720000601). The relative expression levels were calculated according to Livak method (Schmitten & Livak, 2008), using the equation $\Delta CT = CT(target) - CT(normalizer)$ for Ct normalization; and the difference between ΔCT (test) and ΔCT (calibrator) to calculate the expression ratio and compare the expression levels. Statistical significance was calculated using unpaired t-test analysis (indicated as * for $p < 0.05$ and ns for not statistically significant). Values are presented as a mean and error bars indicate standard deviation (SD).

For each plate a melting curve analysis was performed at the end of each run to test the primer specificity.

The specific primers used are listed below.

Drosophila TBPH

forward: 5'-CGGCAAGCCGAGCACGATGAG-3'

reverse: 5'-CGCGGAGTTCGCTCCAACGAG-3'

Mouse TDP-43

forward: 5'-GCAGTCCAGAAAACA-3'

reverse: 5'-CACCATCGCCCATCTA-3'

Rpl-11 (as fly housekeeping gene)

forward: 5'-CCATCGGTATCTATGGTCTGGA-3'

reverse: 5'-CATCGTATTTCTGCTGGAACCA-3'

GAPDH (as mouse housekeeping gene)

forward: 5'- AGGTCGGTGTGAACGG-3'

reverse: 5'- AGTCATACTGGAACAT-3'

2.5. Immunohistochemistry studies

2.5.1. S2 cells immunohistochemistry

S2 cells were plated into a 6-well plate, containing, in each well, a cover glass that was previously sterilized. After transfection (see section 2.1.2) the cells were washed with 3 ml of PBS 1X (NaCl 137 mM, KCl 2.7 mM, Na_2HPO_4 10 mM, KH_2PO_4 1.8 mM pH 7.4) and fixed with 3.7% (v/v) paraformaldehyde for 40 minutes at room temperature. After fixing, three 5-minutes washes were performed with PBS 1X. Subsequently, the plate was placed on ice and 2 ml of PBS with 0.3% (v/v) Triton X-100 were added for 5 minutes. This step was done in order to permeabilize the cells, and after it, a washing step (three 5-minutes washes with PBS 1X) was performed to remove the permeabilization solution. The cells were then blocked for 20 minutes at room temperature with 2% (w/v) of BSA prepared in PBS 1X. Then, the slides were incubated in a humidified chamber with the primary antibodies: mouse anti-FlagM5 (1:200, Sigma # F4042), rabbit anti-GFP (1:250, Life technologies # A11122). After 1-hour incubation at room temperature, three 5-minutes washes with PBS 1X were performed and the secondary antibodies (Alexa 555 anti-mouse (1:500, Invitrogen # A21422), Alexa 488 anti-rabbit (1:500, Invitrogen # A11008)) were added and incubated for 1 hour at room temperature in a humidified chamber. Finally the slides were rinsed with PBS 1X for 5 minutes. For the mounting, the slide was placed up side down on a cover slip with a small drop of mounting

medium (Slow fade gold antifade reagent, Life technologies # S36936), and sealed with nail polish. The samples were imaged under a confocal laser-scanning microscope (LSM 510 META; Carl Zeiss, Inc). Images were acquired by using 63X oil immersion objective and 2X zoom. Image processing was done with ImageJ software.

2.5.2. Larval brain dissection

Larval brain dissection was performed according to the protocol published by Wu and Lou (Wu & Luo, 2006). Wandering third instar were taken from the culture tube and quickly washed in water and transferred on a glass slide in a drop of PBT buffer (Phosphate Buffer supplemented with 0.3% (v/v) Triton X100). *Drosophila* larval brain is composed by two eye discs, two optic lobes, the ventral ganglia and the imaginal discs (**Figure 25**).
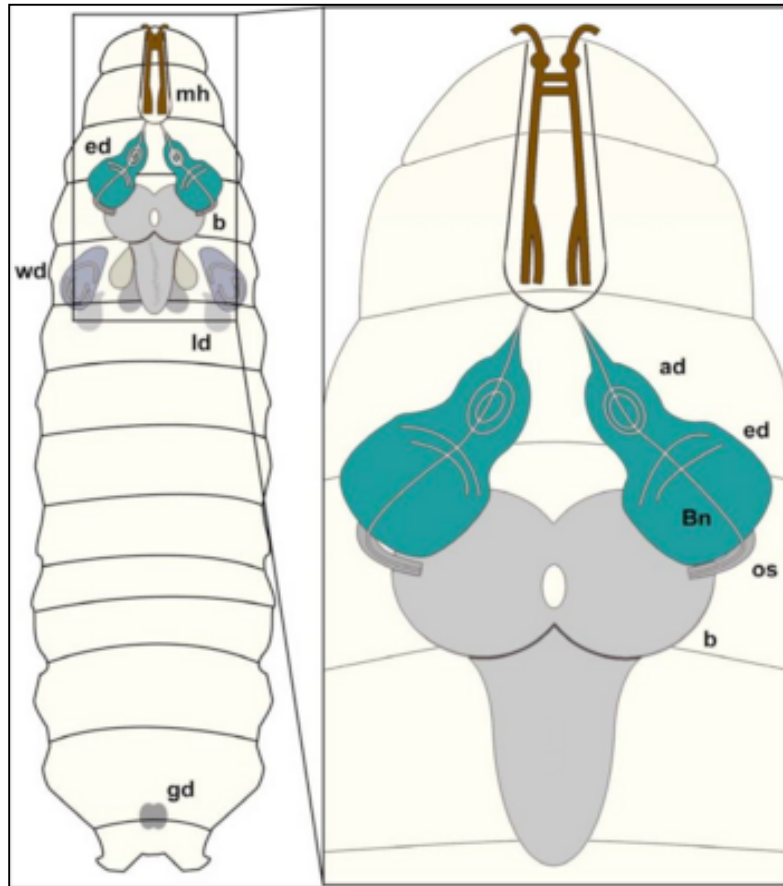
Figure 25. Schematic representation of the *Drosophila* larvae brain.
It is composed by two eye discs, two optic lobe and a central ventral ganglia, and imaginal eye discs. Abbreviations: brain hemispheres (b), eye imaginal discs (ed), wing discs (wd), leg discs (ld), mouth hooks (mh) and gonads (gd). Magnification: Schematic view of brain hemispheres (b), eye imaginal discs (ed) as well as antennal discs (ad). The eye imaginal disc will form the adult compound eye whereas the antennal disc will develop into the antenna, the adult olfactory organ. The optic stalk (os) connects the brain hemispheres with the eye imaginal discs, whereas Bolwig nerve (Bn) constitutes the link of the larval brain to the larval photoreceptors.

The brains were removed under the stereoscope, using special forceps, and were placed into a 0.5 ml-tube containing cold 4% (v/v) paraformaldehyde kept on ice. After all brains were collected (usually 20 for each genotype) the immunostaining was performed as explain in section 2.5.5.

2.5.3. Eye disc dissection

The eye disc dissection was performed in the same way as for the whole larval brain. After immunostaining (see section 2.5.5), the eye disc were separated from the rest of the brain and mounted on a glass slide to be afterwards analyzed with the confocal microscope.

2.5.4. Adult brain dissection

Unlike most other larval organs, the CNS persists into the adult stage. Most motor neurons and large interneurons of the insect adult nervous system are of embryonic origin. To this set of embryonically born neurons, a large number of neurons are added during larval and early pupal stages.

The *Drosophila* adult brain is composed by the central brain, which is localized in the head, and the ventral ganglion that prolongs into the thorax (**Figure 26**).
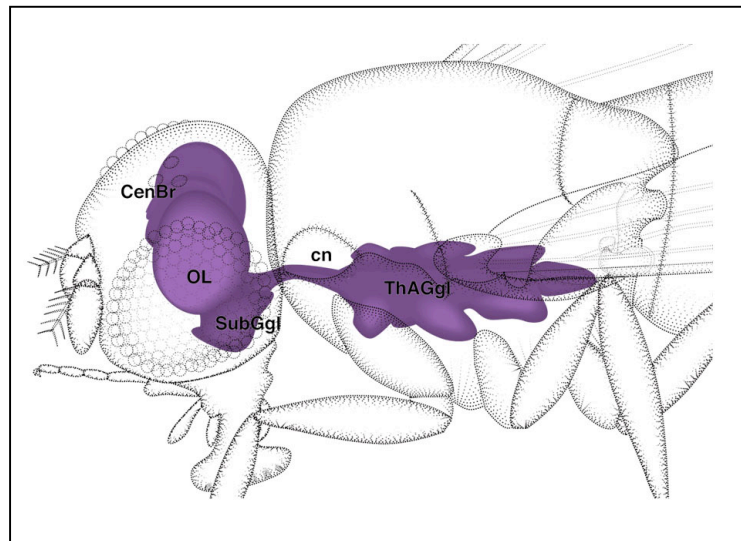
Figure 26. Schematic representation of the *Drosophila* adult brain.
It is composed by the central brain (CenBr) and the thoracic ventral ganglia (ThAGgl). Abbreviations: (OL) optic lobes, (SubGgl) subesophageal ganglion, (cn) and cervical connective.

In order to obtain the adult central brain the *Drosophila* head was separated, under the stereoscope, from the rest of the body using a scalpel.

Once the head was obtained it was placed on a glass slide in a drop of PBT buffer (Phosphate Buffer supplemented with 0.3% (v/v) Triton X100). The mouth hook was removed, and the resulting whole was used as a entering point to eliminate all the tissue that covers the brain, with the help of special forceps. The brains were placed into a 0.5 ml-tube containing cold 4% (v/v) paraformaldehyde and kept on ice. After all brains were collected (usually 20 for each genotype) the immunostaining was performed as explain in section 2.5.5.

In order to obtain the adult ventral ganglia the flies were pinned at both ends with minute pins (Austerlic Insect Pins, 0.1 mm diameter, Fine Science Tools, Germany) and the thorax walls were carefully opened at the dorsal side using special scissors (Fine Science Tools, Germany). The thoracic walls were pinned out and the ventral ganglion was removed carefully, and placed into a 0.5 ml-tube containing cold 4% (v/v) paraformaldehyde and kept on ice. After all ventral ganglia were collected (usually 20 for each genotype) the immunostaining was performed as explain in section 2.5.5.

2.5.5. *Drosophila* larvae and adult brains immunostaining

Immunostaining was performed according to standard protocols (Wu & Luo, 2006). *Drosophila* larvae and adult brains were dissected as already explained and fixed in ice-cold 4% (v/v) paraformaldehyde (Alfa Aesar # 30525-89-4) for 20 minutes, washed in Phosphate Buffer with 0,1% (v/v) Tween 20 (PBT) and blocked with 5% (v/v) Normal Goat Serum (NGS, Chemicon # S26-100 ML) 30 minutes at room temperature. The samples were incubated with primary antibodies: rabbit anti-TBPH (1:300, home-made), mouse anti-FlagM5 (1:200, Sigma # F4042), rabbit anti-GFP (1:250, Life technologies # A11122) and rat anti-ELAV (1:300, Hydridoma bank # 7E8A10) over night at 4˚C with agitation. After primary antibodies incubation four 5-minutes washes with PBT were performed, followed by incubation with fluorescent conjugated secondary antibodies Alexa 555 anti-mouse (1:500, Invitrogen # A21422), Alexa 555 anti-rabbit (1:500, Invitrogen # A21428), Alexa 488 anti-rabbit (1:500, Invitrogen # A11008) and Alexa 647 anti-rat (1:500, Invitrogen # A21472) for 2 h at room temperature. The excess of

secondary antibody was removed by four 5-minutes washes with PBT were performed. All primary and secondary antibodies were diluted in PBT-5% (v/v) NGS. Slow fade gold antifade reagent (Life technologies # S36936) was used as mounting medium. The samples were imaged under a confocal laser-scanning microscope (LSM 510 META; Carl Zeiss, Inc). Images were acquired by using 63X oil immersion objective and 2X zoom. Image processing was done with ImageJ software. All images were displayed as a single section of 0.5 µm.

2.5.6. Adult neuromuscular junction dissection and immunostaining

Neuromuscular junctions were performed from adult *Drosophila* abdomen. We focused our attention on A2 and A3 abdominal muscles, and in particular on the ventral NMJ (**Figure 27**).
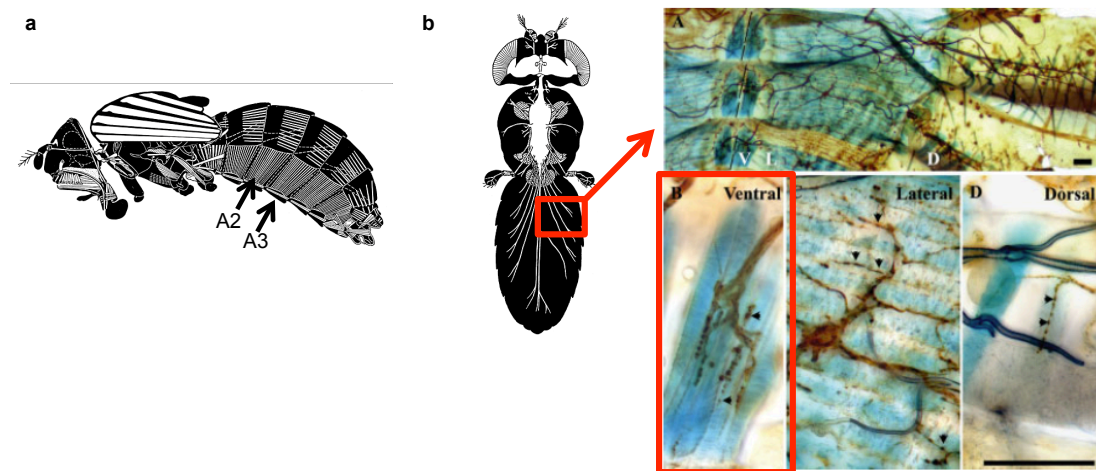
Figure 27. Schematic representation of the *Drosophila* adult abdominal neuromuscular junction.

(a) Abdominal segmentation of adult *Drosophila.* Arrows point to abdominal muscles A2 and A3. **(b)** Upper panel: Abdominal muscles (blue) visualized in a dissected preparation of a 2 days-old female fly. Innervation of the muscles is visualized with anti-HRP (brown). The three main abdominal muscle sets are arranged in a ventral, dorsal and lateral fashion. Bottom panel: Neuromuscular junction of ventral, dorsal and lateral abdominal muscles at a higher magnification. Adapted from Hebbar et al., 2006.

Drosophila head was separated, under the stereoscope, from the rest of the body using a scalpel. The body without head was placed on a Sylgard

dish in a drop of Ringer's solution (116 mM NaCl; 2.9 mM KCl; 1.8 mM CaCl2; 5.0 mM HEPES, pH 7.2) for dissection, and pinned at both ends (in the thorax and the abdomen end) with minute pins (Austerlic Insect Pins, 0.1 mm diameter, Fine Science Tools, Germany). The abdominal walls were carefully opened at the dorsal side using special scissors (Fine Science Tools, Germany). The muscle walls were pinned out and the internal organs were removed and carefully washed with dissection solution. The structure was fixed on the plate for 40 minutes with cold 4% (v/v) paraformaldehyde. After fixing was completed, the tissue was recovered in a 0.5-ml tube containing TBST buffer (Tris-buffered saline supplemented with 0.1% (v/v) Triton X100). To remove the excess of fixing solution, three 5-minutes washes were performed in this buffer under agitation. Subsequently, the sample was blocked with 5% (v/v) Normal Goat Serum (NGS, Chemicon # S26-100 ML) for 30 minutes at room temperature under agitation. After blocking, the samples were incubated with the primary antibody rabbit anti-HRP (1:100, Jackson ImmunoResearch # 323-005-021) over night at 4°C with agitation. Anti-HRP antibody is used to label neuronal membranes because it is capable of interacting with a number of glycoproteins that are present in the synapse. As a consequence it is useful for calculating the NMJ area. After primary antibody incubation four 5-minutes washes with TBST were performed, followed by incubation with fluorescent conjugated secondary Alexa 488 anti-rabbit (1:500, Invitrogen # A11008) for 2 h at room temperature. The excess of secondary antibody was removed by four 5-minutes washes with TBST were performed. The primary and secondary antibodies were diluted in TBST-5% (v/v) NGS. Slow fade gold antifade reagent (Life technologies # S36936) was used as mounting medium. After mounting, the slide was sealed with nail polish. The samples were imaged under a confocal laser-scanning microscope (LSM 510 META; Carl Zeiss, Inc). Images were acquired by using 63X oil immersion objective and 2X zoom. Image processing was done with ImageJ software.

3. Innovative therapeutic approaches to treat TDP-43-ALS

3.1. Cell culture

Two different HEK293 cell lines were used in this study (EGFP-12xQ/N and TDP-12xQ/N). These cell lines were previously developed in the lab using the Flp-In System (Invitrogen # K6010-01) and the T-Rex-293 cells (Invitrogen # R710-07). Both cell lines were cultured in Dulbecco's Mem with Glutamax I (Dulbecco's modified Eagle's medium with glutamine, sodium pyruvate, pyridoxine and glucose) supplemented with 10% (v/v) heat-inactivated fetal bovine serum (FBS) and 1X antibiotic-antimycotic (Sigma # A5955). 100 μg/ml of Hygromycin B (Invitrogen # 10687-010) was used to select the stably integrated transgene, and 10 μg/ml Blasticidin S (Sigma # 15205) was used to select the T-Rex-293 plasmid containing the tetracycline repressor (pcDNA6/TR). The expression of the gene of interest is controlled by the CMV promoter into which 2 copies of the tet operator 2 ($TetO_2$) sequence have been inserted in tandem. Insertion of these $TetO_2$ sequences into the CMV promoter confers regulation by tetracycline to the promoter. For the induction of the transgenic proteins 1 μg/ml of tetracycline (Sigma # 87128) was added.

For cell seeding, dishes containing confluent monolayer of cells were washed with PBS 1X, treated with 3 ml of PBS/EDTA/trypsin solution (PBS containing 0.04% (w/v) EDTA and 0.1% (w/v) trypsin) at 37°C for 30 seconds in order to dislodge the cells. Then, trypsin was deactivated by adding complete DMEM, and the cells were collected and pelleted by centrifugation for 5 minutes at 0,1 x g at room temperature. The cellular pellet was resuspended in 10 ml of DMEM and cells were counted with the Neubauer chamber.

3.2. Clearance assay

The clearance assay was performed with both cell lines independently. For EGFP-12xQ/N cell line, 100,000 cells/well were seeded in a 6-well plate, and induced for 24 hours. For the TDP-12xQ/N cell line, 30.000 cells/well were seeded in a 6-well plate, and induced for 72 hours. After induction, cells

were washed twice with PBS 1X in order to get rid of the tetracycline. Fresh DMEM without antibiotic-antimycotic was added to the plates, and the different drugs at different concentration were added (nortriptyline, desipramine, promethazine, clomipramine, fluphenazine, chlorpromazine, thioridazine and cyclobenzaprine). Drugs were incubated for 24 hours and then fresh medium with drugs was added again for other 24 hours. Control cells were also induced for 24 hours and then tetracycline was also washed out. Finally, these cells were kept for 48 hours with normal DMEM without any additive (also in this case the medium was replaced with fresh medium after 24 hours).

After the incubation time was finished, the cells were collected and pelleted at 0,1 x g for 5 minutes at room temperature. Finally, protein and RNA were extracted as explained in sections 3.3 and 3.7.

3.3.   Protein extraction

For cellular protein analysis, cells with and without drug treatment were harvested and lysate with Lysis buffer (15 mM Hepes pH=7.5, 250 mM NaCl, 0.5% (v/v) NP-40, 10% (v/v) Glycerol and protease inhibitors (Roche Diagnostic # 11836170001)). Cells were sonicated for 10 minutes at the highest potency. Then, the solution was centrifuged at 700 x g for 10 minutes at 4°C. Pellet was discarded and the total cell lysate was quantified by Bradford assay using Biorad reagent (Biorad # 500-0006). 20-30 µg were loaded in SDS-PAGE.

3.4.   SDS-PAGE

Sodium dodecyl sulfate polyacrylamide gel electrophoresis (SDS-PAGE) is a widely used method to separate proteins according to their sizes. Protein samples were diluted in Laemmli buffer with 8 M urea (0.1 M Tris-HCl pH 6.8, 30% (v/v) glycerol, 8% (w/v) SDS, 9.8% (v/v) β-mercaptoethanol and 0.1% (w/v) bromophenol blue), and boiled at 95°C for 5 minutes. 8% or 15% gels were prepared as detailed in section 2.4.2.

The amperage applied for the running was 25mA in 2X running buffer, prepared from a 10X stock (**Table 9**).

3.5. Immunoblotting

Proteins were separated by 8 or 15% SDS-PAGE, transferred to nitrocellulose membranes (Whatman # NBA083C) and probed with primary antibodies: rabbit anti-GFP (1:1,000, Santa Cruz #), rabbit anti-LC3B (1:1,000, Sigma # L7543), guinea pig anti-p62 (1:1,000, Progen # GP62-C), mouse anti-Flag (1:1,000, Sigma # F1804) and mouse anti-tubulin (1:4,000, Calbiochem # CP06). The membranes were incubated with the secondary antibodies: HRP-labeled anti-mouse (1:1,000, Thermo Scientific # 32430), HRP-labeled anti-guinea pig (1:10,000, Jackson ImmunoResearch #706-035-148) or HRP-labeled anti-rabbit (1:1,000, Thermo Scientific # 32460). Finally, protein detection was assessed with ECL Western Blotting Substrate (Thermo Scientific # 34106).

Protein bands were quantified using NIH ImageJ. The intensity of the band of interest was normalized with tubulin. The respective histogram for each western blot shows the relative expression of at least 3 independent experiments.

Unpaired t-test analysis was used to compare measures between 2 groups. The significance between the variables was shown based on the p-value obtained (ns indicates $p > 0.05$, *indicates $p < 0.05$, **indicates $p < 0.01$, ***indicates $p < 0.001$ and ****indicates $p < 0.0001$). Values are presented as a mean and error bars indicate standard deviation (SD).

3.6. Inhibitors experiment

After EGFP-12xQ/N induction, tetracycline was washed out and 1 hour before the addition of the compound of interest (5 µM thioridazine, 10 µM nortriptyline or 10 µM chlorpromazine) the proteasomal or autophagy inhibitors were added to the culture medium.

For the proteasome blockage 5 µM lactacystin (Adipogen # AG-CN2-0104) was used. Lactacystin binds certain catalytic subunits of the core

particle of the proteasome, and inhibits the three best-characterized peptidase activities, two irreversibly. This small molecule is currently the only compound known to inhibit the proteasome specifically without inhibiting any other protease; also and very important, it does not inhibit lysosomal protein degradation in the cell (Fenteany and Schreiber, 1998).

For the autophagy blockage 30 mM of NH_4Cl (Merck # 101145) was used. NH_4Cl is a lysosomotropic agent, meaning that it accumulates in lysosome. By doing so, the drug is able to change the pH of the organelle, neutralizing its low pH, and in this way, it will inhibit autophagosome maturation and stalls the pathway.

After 48 hours of incubation with the drugs and inhibitors, cells were collected and proteins were extracted. SDS-PAGE followed by immunoblotting was performed with anti-GFP and anti-tubulin antibodies.

3.7. RNA extraction

To perform RNA extraction, cultured cells were washed once with PBS 1X and then harvested by centrifugation at room temperature at 0,1 x g for 5 minutes. The cellular pellet was resuspended in 500 µl of TRIzol reagent (Invitrogen # 15596-026). RNA extraction was performed by adding 100 µl chloroform to each sample and after 15 minutes of incubation at room temperature, samples were centrifuged for other 15 minutes at 13,4 x g at 4°C. The upper phase, containing the RNA was transferred into a new tube and RNA was precipitated by adding an equal volume of isopropanol. After 10 minutes of incubation at room temperature, the samples were centrifuged again for 10 minutes at 13,4 x g at 4°C. Finally, RNA pellet was washed with 70% (v/v) ethanol and resuspended in water.

3.8. cDNA synthesis

The cDNA synthesis was performed with 1µg of total RNA. To start with, RNA was treated with DNAse (Promega RQ1 # M610A) (**Table 13**). The mixture was incubated at 37°C for 30 minutes and then DNAse stop solution

was added and incubated at 65°C for 10 minutes to inactivate the DNAse enzyme.

Component	Volume
RNA (1µg)	1-8 µl
10X buffer	1 µl
DNAse enzyme	1 µl
H$_2$O	Up to 10 µl

Table 13. DNAse treatment.

The RNA was subsequently retrotranscribed with Moloney murine leukemia virus reverse transcriptase (Invitrogen # M1701) using random primers at a final concentration of 2.5 mM (Pharmacia # 27-2166-01). RNA denaturation was carried out at 70°C for 3 minutes. After denaturation, the following reagents (**Table 14**) were added and incubated for 1 hours at 37°C.

MIX	Volume
5X RT buffer	6 µl
DTT (0.1 M)	3 µl
dNTPs (5 mM)	3 µl
M-MVL RT	0.5 µl
H$_2$O	2.5 µl

Table 14. Reverse transcription reaction with M-MVL RT.

3.9. RT-PCR and splicing assay

For *POLDIP3* splicing assay, HEK293 TDP-12xQ/N cells were induced and treated with the drugs for 48 hours as already described for the clearance assay. The cells were harvested and RNA was extracted as previously described. After retrotrascription with M-MLV Reverse Transcriptase (Invitrogen # M1701), total cDNA was analyzed by PCR using the following primers: *POLDIP3* exon 3 forward: 5'gcttaatgccagaccgggagttgga3' and *POLDIP3* exon 3 reverse: 5' tcatcttcatccaggtcatataaatt3'. PCR was performed using DNA Polymerase

(Biolabs # M0273L) with the following settings: 95°C for 5 minutes, 95°C for 30 seconds, 50°C for 30 seconds, 72°C for 1 minute, 72°C for 7 minutes, repeated 35 times from step 2 to 5. All PCR products were analyzed on 2% (w/v) agarose gels with ethidium bromide (Sigma # E1510).

Results

1. An ALS *Drosophila* model

Despite the fact that ALS was characterized for the first time in 1869 (Charcot, 1869), it was not until 1991 that it was recognized that ubiquitin-positive inclusions present in patients' motor neurons are a major hallmark of the disease (Leigh et al., 1991). However, the composition of these inclusions remained unknown until 2006 when it was discovered by two groups in parallel, that TDP-43 is the main protein aggregated in patients' brain (Arai et al., 2006; Neumann et al., 2006). After this revolutionary discovery a new era in ALS-research started. Before 2006, very little was known about TDP-43 function and even less about its aggregation and dysfunction.

Notwithstanding the tremendous efforts and progress that have been done in order to understand ALS pathology, there is still no consensus about how the TDP-43 inclusions are related to the disease mechanism. Animal models constitute great tools that help our understanding of the disease process. Many models have been created up to now, and from all of them new conclusions and notions have arisen. Still, there are many open questions that researchers need to address, as for example, which is the role of TDP-43 aggregation in ALS pathology. With the objective of shedding some light on this topic, in this study we created a novel *in vivo* model of TDP-43 aggregation that is able to mimic some of the major aspects of TDP-43-ALS. For this purpose we took advantage of *Drosophila melanogaster* as a model system. *Drosophila* is an excellent candidate to model neurodegenerative diseases in general because it is easy to handle and manipulate genetically. Furthermore, biologically, the architecture of the fly nervous system resembles that of mammals, with areas that separate specialized functions such as vision, olfaction, learning and memory. In addition, and very important, approximately 75% of human genes known to be associated with diseases have a *Drosophila* ortholog.

1.1. Creation of EGFP-12xQ/N transgenic *Drosophila* lines

TDP-43 is increasingly being recognized as a prion-like protein. One of the characteristics that make this protein fit this classification is its seeding capacity. The prion-like behavior was first documented in 2011 by Furukawa and collaborators (Furukawa et al., 2011). Several algorithms have identified prion-like domains in the TDP-43 protein sequence (King et al., 2013). This domains possess properties similar to those found in yeast prions that in response to stress can recruit the native protein into an inactive aggregate (Cushman et al., 2010). A distinctive and portable prion domain enriched in asparagine, glutamine, tyrosine and glycine residues unifies the majority of yeast prion proteins (King et al., 2013). As in yeast, human TDP-43 presents a glycine-asparagine (Q/N) rich region within its C-terminal domain. A structural characterization of this region demonstrated that this segment is normally in a disordered conformation, but it can form β–sheet strands spontaneously over time (Mompeán et al., 2014).

Based on this information, a cellular model of TDP-43 aggregation was previously developed in our laboratory, based on repeated segments of the Q/N rich region. Twelve repetition of the 331-369 sequence (Q/N) were cloned downstream an EGFP reporter. The 12xQ/N construct was shown to be capable of interacting with wild type TDP-43 inducing its aggregation both in non-neuronal and neuronal cells (Budini et al., 2012a).

To determine whether similar interactions occur *in vivo*, and to further model ALS pathology, we created transgenic *Drosophila melanogaster* lines encoding the 12 repetitions of the 331-369 sequence of TDP-43 tagged with EGFP (EGFP-12xQ/N), under the control of the upstream activating sequence (UAS) (Brand & Perrimon, 1993). The EGFP-12xQ/N construct was cloned into pUASTattB vector and sequenced. Once the sequencing analysis was done, we decided to analyze the correct expression of the protein EGFP-12xQ/N before proceeding with the creation of the transgenic fly. For this purpose, we performed transient transfections in S2 insect cells with pUAST-EGFP-12xQ/N, pUAST-EGFP and pUAST-EGFP-TBPH. A plasmid containing Gal4 was co-transfected in each case in order to activate the gene expression that is under the control of the UAS sequence. The S2 cells derive from primary culture of late stage (20-24 hours) *Drosophila*

melanogaster embryos (Schneider, 1972). Usually, it is a normal practice in the *Drosophila* field to test the expression level and the potential toxicity of the exogenous protein in S2 cells before sending the constructs to Best Gene Company for the generation of the transgenic flies. After transfection time was completed, the cellular proteins were extracted and separated with SDS-PAGE. Subsequently, a western blot with anti-GFP antibody was performed. As it can be seen in **Figure 28a** all three vectors pUAST-EGFP-12xQ/N, pUAST-EGFP and pUAST-EGFP-TBPH drive the expression of the protein of interest when Gal4 is present (lanes 1 to 3). In each case a single band with the predicted molecular weight can be observed (75.7 KDa for EGFP-12xQ/N, 32.7 KDa for EGFP and 90.7 KDa for EGFP-TBPH). On the contrary, and as an example, pUAST-EGFP-12xQ/N was also transfected alone, obtaining no protein expression as expected (lane 4).

Furthermore, it was of our interest to analyze the cellular distribution of the transgenic proteins. For this reason we proceeded again with a transient transfection in S2 cells followed by immunofluorescence. pUAST-EGFP-12xQ/N or pUAS-EGFP were co-transfected with pUAST-TBPH in the presence of Gal4. The transgenic proteins were then analyzed by microscopy using specific anti-GFP and anti-Flag antibodies. The immunofluorescence analysis revealed that EGFP-12xQ/N construct aggregates, and that it is able to trap TBPH. On the contrary, with EGFP construct, the protein is diffusively distributed in the nucleus and cytoplasm, without evident aggregate formation (**Figure 28b**).
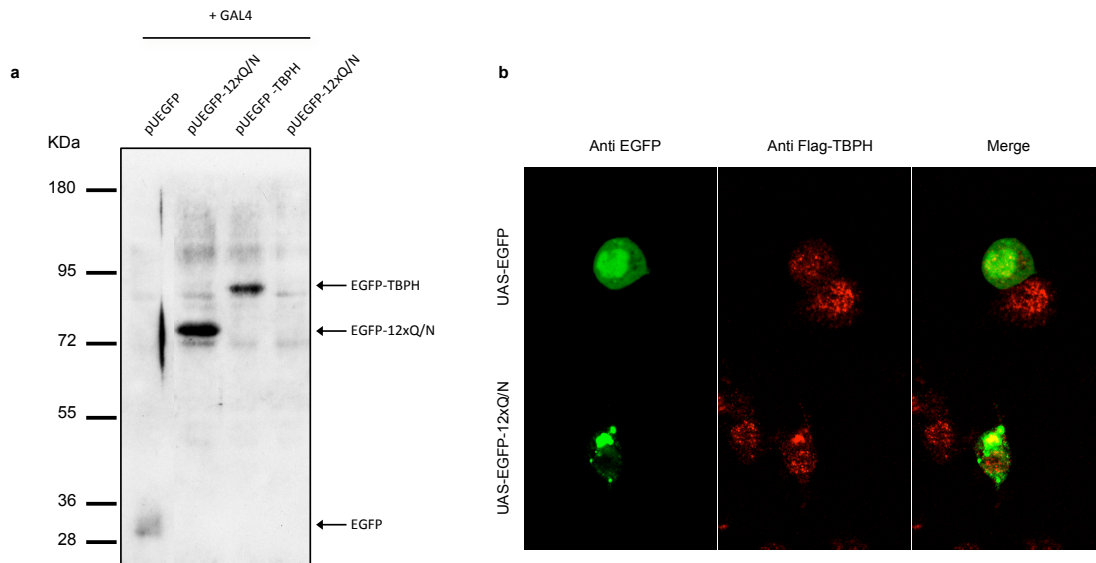
Figure 28. EGFP-12xQ/N is correctly expressed in S2 cells.
(a) Western blot of proteins obtained from S2 cells transfected with pUAST-EGFP (lane 1), pUAST-EGFP-12xQ/N (lane 2 and 4) and pUAST-EGFP-TBPH (lane 3) respectively. Gal4 was used as inducer (lanes 1 to 3). Total proteins were extracted using RIPA buffer and then separated by 8 % SDS-PAGE, followed by western blotting with anti-GFP. **(b)** Confocal images of S2 cells co-transfected with pUAST-EGFP-TBPH and pUAST-EGFP or pUAST-EGFP-TBPH and pUASTEGFP-12xQ/N, stained for EGFP (green) and Flag-TBPH (red).

After confirming the correct expression of the EGFP-12xQ/N construct and that the protein is not toxic for cells, transgenic *Drosophila* lines were generated by site-specific insertion (Best Gene Inc.). Five independent transgenic lines were obtained by microinjection in the posterior pole of *Drosophila* embryos. The first approach was to confirm the correct expression of EGFP-12xQ/N transgene in all the lines that were sent by the company. In order to do this, all the lines UAS-EGFP-12xQ/N were independently crossed with GMR-Gal4 driver flies, to drive the expression of EGFP-12xQ/N specifically in the eye-tissue (Li et al. 2012). After crossing the flies and obtaining the progeny, we analyzed if the transgenic protein was present in the *Drosophila* adult heads. For this purpose, we extracted the proteins from the adult heads and resolved the extracts on SDS-PAGE. After this, the protein levels of each single line were assessed by western blot using a specific polyclonal antibody anti-GFP that recognizes the EGFP-12xQ/N construct. As shown in **Figure 29**, all lines expressed comparable levels of EGFP-12xQ/N protein that can be observed as a band of around 75

KDa. These results confirmed the correct expression of the protein in the transgenic flies, and as all the lines were expressing the construct at comparable levels, we arbitrarily chose to use number 3 for the rest of the experiments.
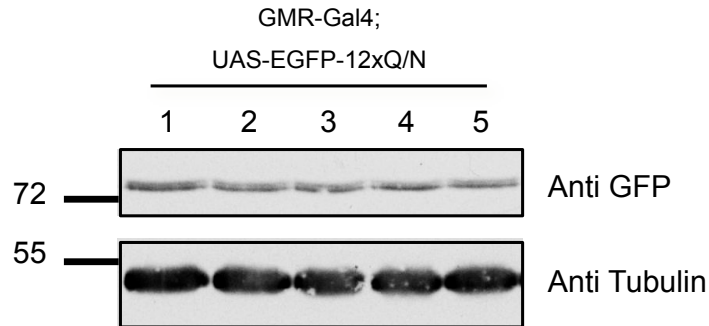
Figure 29. *Drosophila* **EGFP-12xQ/N transgenic lines.**
Immunoblot of proteins obtained from adult fly heads of 5 different UAS-EGFP-12xQ/N transgenic lines, after crossing them with GMR-Gal4 driver flies. Total proteins were extracted using RIPA buffer and then separated by 8 % SDS-PAGE, followed by western blotting with anti-GFP. Tubulin served as loading control. Line number 3 has been chosen arbitrarily for the rest of the experiments.

1.2. EGFP-12xQ/N expression forms insoluble aggregates in retinal cells with no consequence for the eye structure

Once we had obtained a transgenic fly that correctly expresses EGFP-12xQ/N, we wanted to determine whether this protein was able to aggregate in neurons. For this purpose, we again performed crosses between UAS-EGFP-12xQ/N transgenic flies and GMR-Gal4 driver flies. We use UAS-EGFP transgenic line as a control. After the correct selection of the progeny, total proteins were extracted from adult heads and a fractionation experiment was performed, in order to see the solubility pattern of the transgenic proteins. The fractionated proteins were separated by SDS-PAGE and afterwards western blot with anti-GFP antibody was performed. **Figure 30a** shows a representative western blot of the fractionated proteins obtained from GMR-Gal4;UAS-EGFP-12xQ/N and GMR-Gal4;UAS-EGFP adult fly heads. Three fractions were loaded into the gel, the input, the soluble and the insoluble fractions, respectively. In the case of GMR-Gal4;UAS-EGFP-

12xQ/N, the transgenic protein was found mainly in the insoluble fraction, and a little amount of it, was also present in the soluble fraction. On the contrary, EGFP alone, when expressed under GMR-Gal4 driver, was found to be mainly soluble. From this result we can conclude that EGFP-12xQ/N aggregates in *Drosophila* as it does in cells. Our following step consisted in analyzing if this aggregates could have any detrimental effect on the tissue. In order to do this, EGFP-12xQ/N was expressed in *Drosophila* eye again and the effect that the expression of this protein could have in the morphology of the eye was evaluated. As a control we expressed EGFP protein without the 12xQ/N tail. Despite the formation of the aggregates in the eye upon EGFP-12xQ/N expression, we could not observe any modification of the external structure of the eye, suggesting that the aggregates, *per se*, are not neurotoxic. Moreover, EGFP expression alone did not trigger any modification either **(Figure 30b)**.
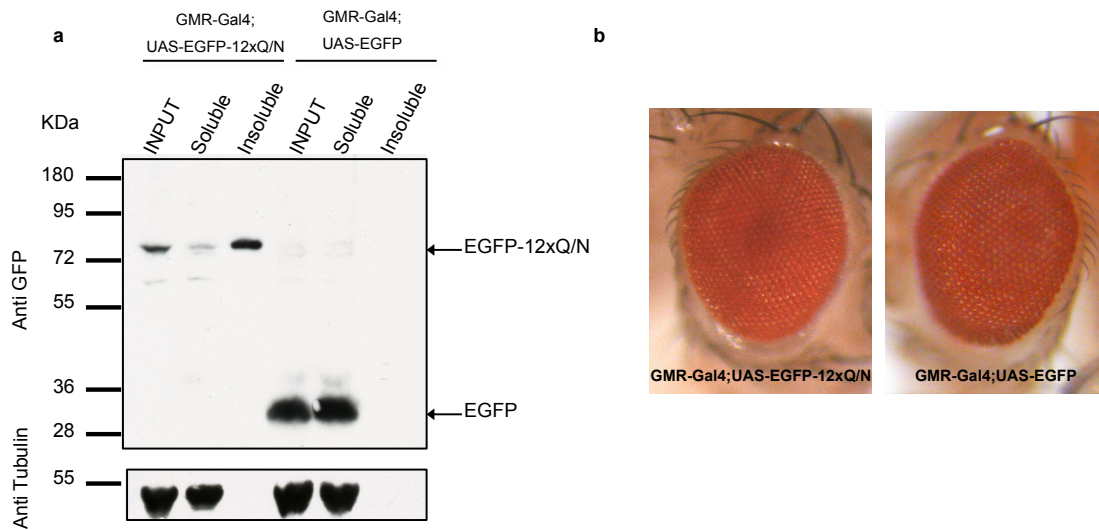
Figure 30. EGFP-12xQ/N expression forms insoluble aggregates in *Drosophila* eye, without affecting its structure.

(a) Western blot of fractionated proteins obtained from GMR-Gal4;UAS-EGFP-12xQ/N and GMR-Gal4;UAS-EGFP adult fly heads. Total proteins were extracted using RIPA buffer and then separated into soluble and insoluble fractions by centrifugation. The fractions were separated by 8 % SDS-PAGE, followed by western blotting with anti-GFP. EGFP-12xQ/N is mainly an insoluble protein, whereas EGFP alone is found only in the soluble fraction. Tubulin served as loading control. **(b)** External eye phenotype of flies GMR-Gal4;UAS-EGFP-12xQ/N and GMR-Gal4;UAS-EGFP, the external eye phenotype of both flies is completely normal.

1.3. EGFP-12xQ/N expression rescues TBPH-induced neurodegeneration

As already explained, the role that the TDP-43 aggregates play in the pathology of the disease is not clear. In particular, it is not known if these inclusions are primary toxic species or part of the normal cellular protective response to other toxic protein species. With the objective of clarifying this topic, we first overexpressed TBPH in eye-tissue with GMR-Gal4 driver. It was already reported by others that the overexpression of the human TDP-43 in the *Drosophila* eye, induces a remarkable degeneration of the eye surface, characterized by the formation of necrotic patches and loss of eye pigmentation (Li et al., 2010; Miguel et al., 2011). Interestingly, the same phenotypic consequence is seen by light microscopy of the fly eyes after expressing the *Drosophila* ortholog of TDP-43 (TBPH) under the control of

GMR-Gal4 driver **(compare Figures 31a and 31b)**. TBPH expression induces a strong degeneration of the surface of the eye, which is characterized by necrotic areas with different degrees of severity and loss of the normal pigmentation. We next wanted to analyze what happens when the aggregate-inducer EGFP-12xQ/N is expressed in the presence of excess of TBPH. For this reason, we co-expressed both transgenes in the *Drosophila* eye. Surprisingly, the strong neurodegeneration induced by the excess of TBPH was completely reverted by the co-expression of TBPH together with EGFP-12xQ/N, as can be appreciated in **Figure 31c**, in which the external surface of the eye is comparable to the wild type. At this point, we supposed that the recovery of the eye external surface was most probably due to the sequestration of the protein within the EGFP-12xQ/N aggregates that would modulate the excess of soluble TBPH.

In order to confirm that the recovery of the degeneration is dependent on 12xQ/N and not a non-specific effect triggered by EGFP expression, we co-expressed EGFP alone and TBPH, and demonstrated that the retinal degeneration induced by TBPH expression was not prevented **(Figure 31d)**.

A quantitative analysis of the phenotypes is presented in **Figure 31e**. The classification was done by defining 3 arbitrary categories. The fly eyes were examined by light microscopy and after careful analyses they were classified: (1) was given to the eyes that presented no difference with wild type eyes. (2) was assigned in the case in which the eyes presented loss of pigmentation and small regions of necrosis, and finally, eyes with loss of pigmentation and massive regions of necrosis were classified as (3). At least 50 flies per genotype were analyzed**.** From this classification we can easily observe that the co-expression of EGFP-12xQ/N with TBPH completely recovers the normal structure of the eye, as all the flies are classified as (1). On the contrary, the overexpression of TBPH or the co-expression of TBPH and EGFP in the eye give rise to phenotypes that can be classified as (2) (57% and 55% respectively) or (3) (43% and 45% respectively) but in none of the cases as (1).
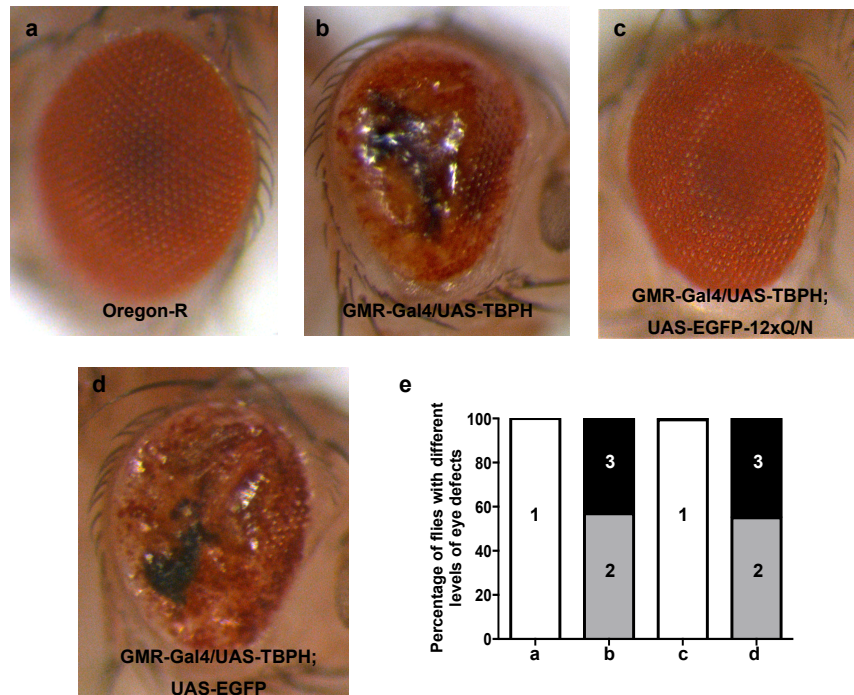
Figure 31. EGFP-12xQ/N expression rescues TBPH-induced neurodegeneration.
External eye phenotype of flies **(a)** Oregon-R, **(b)** GMR-Gal4/UAS-TBPH, **(c)** GMR-Gal4/UAS-TBPH;UAS-EGFP-12xQ/N, **(d)** GMR-Gal4/UAS-TBPH;UAS-EGFP. Expression of TBPH induces degeneration in *Drosophila* eye **(b)**. The co-expression of EGFP-12xQ/N rescues the eye degeneration **(c)**, whereas the co-expression of EGFP alone does not change the phenotype induced by TBPH expression **(d)**. **(e)** Quantification of eye defects in Oregon-R, GMR-Gal4/UAS-TBPH, GMR-Gal4/UAS-TBPH;UAS-EGFP-12xQ/N, GMR-Gal4/UAS-TBPH;UAS-EGFP flies. We defined arbitrarily 3 categories: (1) normal eye, (2) loss of pigmentation and small regions of necrosis, (3) loss of pigmentation and massive regions of necrosis.

1.4.   The TBPH C-terminal amino acids are essential for the interaction with the EGFP-12xQ/N aggregates

As already mentioned in the Introduction (see section 3.4.3), it was previously demonstrated *in vitro* that the C-terminal tail of human TDP-43 is the protein domain required for the protein-protein interaction (Budini et al., 2012a). In order to demonstrate that this region is also implicated in the TBPH-EGFP-12xQ/N interaction *in vivo,* TBPH lacking the C-terminal tail (TBPHΔC) was expressed under GMR-Gal4 driver. The expression of this TBPH variant also induced a remarkable phenotype in the eye, characterized by rough degeneration of the surface and extensive depigmentation of the

retina **(Figure 32a)**. Although this phenotype was milder compared to the expression of the TBPH full-length protein, we did not observe any improvement of the phenotype co-expressing TBPHΔC and EGFP-12xQ/N (in both cases, 100% of the eyes were classified as (2)) **(compare Figures 32a and 32b)**. This result confirms that the C-terminal tail of TBPH is responsible for the protein-protein interaction, and that this interaction is required to prevent the TBPH-mediated retinal degeneration by EGFP-12xQ/N.
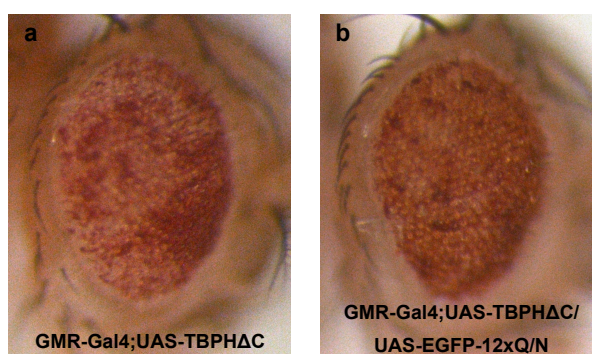
Figure 32. TBPH C-terminal tail is essential for the interaction with EGFP-12xQ/N aggregates.
External eye phenotype of flies **(a)** GMR-Gal4;UAS-TBPHΔC, **(b)** GMR-Gal4;UAS-TBPHΔC/UAS-EGFP-12xQ/N. The expression of TBPHΔC also induces degeneration in *Drosophila* eye **(a)**. The co-expression of EGFP-12xQ/N does not rescue this degeneration **(b)**.

Furthermore, it was of interest to determine if the effect seen with EGFP-12xQ/N was specific for the neurodegeneration induced by TBPH overexpression, or if it was a general effect that could rescue the degeneration derived from other proteinopathy-causing proteins. For this purpose, we used Tau protein, whose expression in *Drosophila* eye caused degeneration of the retinal tissue **(Figure 33a)**. As shown in **Figure 33b** EGFP-12xQ/N is not able to prevent the Tau-induced phenotype (in both cases, 100% of the eyes were classified as (2)), confirming that the effect that EGFP-12xQ/N has on TBPH solubility is specific for this protein.
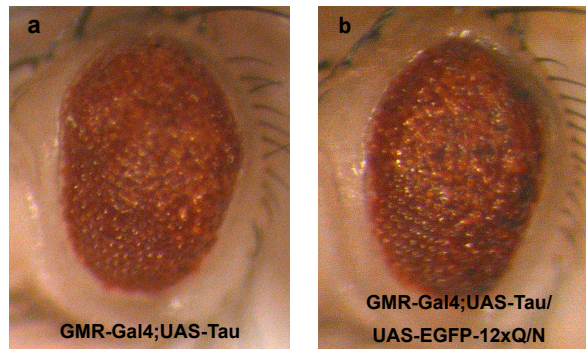
Figure 33. EGFP-12xQ/N is not able to rescue Tau-induced neurodegeneration.
External eye phenotype of flies **(a)** GMR-Gal4;UAS-Tau, **(b)** GMR-Gal4;UAS-Tau/UAS-EGFP-12xQ/N. The expression of Tau also induces degeneration in *Drosophila* eye **(a)**, and the co-expression of EGFP-12xQ/N does not rescue this degeneration **(b)**.

1.5. EGFP-12xQ/N expression promotes TBPH aggregation in retinal cells

Taking into account that the phenotype induced by TDP-43 overexpression has been shown to be dose-dependent (Estes et al., 2011); one possible explanation of the recovery of the TBPH-induced phenotype by EGFP-12xQ/N could be that EGFP-12xQ/N expression is somehow down-regulating the TBPH expression. Therefore, and in order to further investigate the mechanism by which EGFP-12xQ/N expression suppresses the TBPH-induced eye phenotype, the total TBPH levels were evaluated. Total protein were extracted from GMR-Gal4/UAS-TBPH;UAS-EGFP-12xQ/N and GMR-Gal4/UAS-TBPH;UAS-EGFP *Drosophila* adult heads, and separated by SDS-PAGE. Finally, the TBPH levels were assessed by western blot using an anti-TBPH antibody. **Figure 34** shows a representative blot and an ImageJ quantification of TBPH levels, in which total TBPH levels were normalized using tubulin as housekeeping. Comparable levels of the TBPH (58 KDa) were found when co-expressing it with EGFP-12xQ/N or EGFP alone. In this way, it can be ruled out that the rescue is due to simple down-regulation of transgene expression.
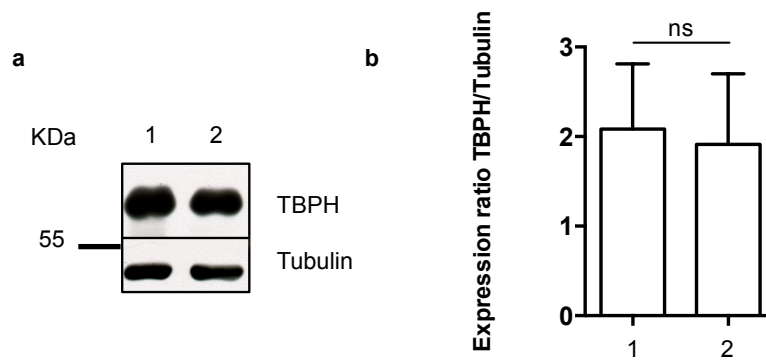
Figure 34. Total content of endogenous TBPH is not altered in EGFP-12xQ/N expressing flies.
(a) Quantification of TBPH level on total protein extracts prepared from adult fly heads GMR-Gal4/UAS-TBPH;UAS-EGFP-12xQ/N (lane 1) and GMR-Gal4/UAS-TBPH;UAS-EGFP (lane 2). A representative western blot is shown. Tubulin was used as loading control. **(b)** Image J quantification of TBPH was performed from two independent experiments. ns indicates $p>0.05$ (not significant) calculated by unpaired t-test. Error bars indicate SD.

More likely, the recovery of the phenotype could be related to a different functionality of the protein most probably due to its physical status (solubility). To explore this possibility, we quantified the degree of TBPH solubility by performing a biochemical fractionation of the *Drosophila* adult head proteins extracted from flies expressing either TBPH in combination with EGFP or EGFP-12xQ/N. Three fractions were loaded in the SDS-PAGE, the input, the soluble and the insoluble fractions respectively, followed by western blot with anti-TBPH antibody. **Figure 35** shows a representative western blot of the fractionated proteins obtained from GMR-Gal4/UAS-TBPH;UAS-EGFP-12xQ/N and GMR-Gal4/UAS-TBPH;UAS-EGFP adult fly heads. TBPH protein (58 KDa) shifts from the soluble fraction in GMR-Gal4/UAS-TBPH;UAS-EGFP flies to the insoluble fraction in GMR-Gal4/UAS-TBPH;UAS-EGFP-12xQ/N flies, confirming the capability of EGFP-12xQ/N to induce the aggregation of TBPH.
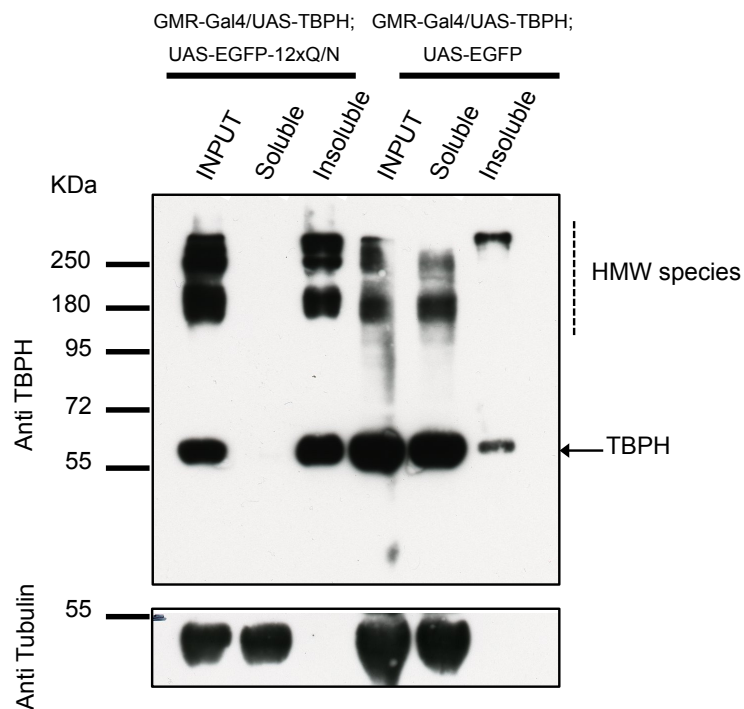
Figure 35. EGFP-12xQ/N promotes TBPH aggregation in retinal cells.

Western blot of fractionated proteins obtained from GMR-Gal4/UAS-TBPH;UAS-EGFP-12xQ/N and GMR-Gal4/UAS-TBPH;UAS-EGFP adult fly heads. Total proteins were extracted using RIPA buffer and then separated into soluble and insoluble fractions by centrifugation. The fractions were separated by 8 % SDS-PAGE, followed by western blotting with anti-TBPH. Co-expression of EGFP-12xQ/N and TBPH leads to formation of insoluble protein aggregates. In contrast, TBPH remains mainly soluble when co-expressing it with EGFP. Tubulin served as loading control.

1.6. EGFP-12xQ/N and TBPH co-localize in the *Drosophila* eye discs

To further confirm the sequestration of TBPH within the EGFP-12xQ/N aggregates we analyzed the localization of both proteins in the retinal cells. Immunohistochemistry of the third instar larvae eye discs was performed in order to examine the cellular distribution of the proteins, in GMR-Gal4/UAS-TBPH;UAS-EGFP and GMR-Gal4/UAS-TBPH;UAS-EGFP-12xQ/N transgenic lines. The larvae eye discs are the structures that will give rise to the adult eyes. These structures are characterized by the nucleation of big amount of neurons (photoreceptors). **Figure 36a** shows the distribution of the proteins of interest in the eye disc of larvae expressing TBPH and EGFP, where it can be seen that both proteins are homogeneously distributed. On

the contrary, TBPH was found aggregated and co-localizing with the EGFP-12xQ/N aggregates in the larvae eye discs when both proteins were co-expressed under GMR-Gal4 driver **(Figure 36b)**. Furthermore, we confirmed that in larvae co-expressing TBPH without its C-terminal tail and EGFP-12xQ/N the co-localization of the two proteins was abrogated **(Figure 36c)**.
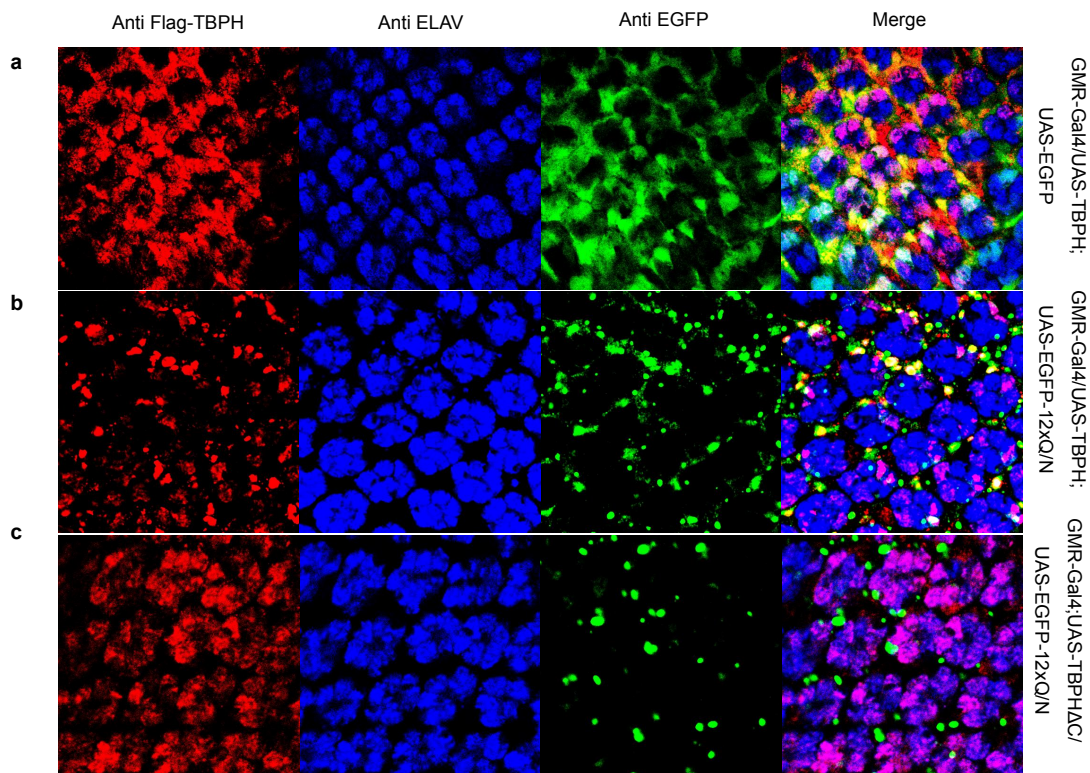
Figure 36. EGFP-12xQ/N and TBPH co-localize in *Drosophila* eye discs.
Confocal images of third instar larvae eye disc co-expressing TBPH and EGFP **(a)**, TBPH and EGFP-12xQ/N **(b)**, TBPHΔC and EGFP-12xQ/N **(c)**. Samples were stained for Flag-TBPH (red), EGFP (green) and ELAV (blue). All the figures correspond to a single confocal section.

From these results, it can be concluded that the degeneration caused by high levels of TBPH *in vivo* can be modulated by its aggregation, which titrates the excess of the active TBPH.

1.7. EGFP-12xQ/N expression restores eye functionality in TBPH expressing flies

To determine whether the suppression of TBPH toxicity by EGFP-12xQ/N has a functional consequence for the eye, phototaxis assay was performed with 1 day-old flies from the different genotypes.

Drosophila has long been known to be phototactically positive in adult and negative in larval stages (Gong, 2012). The altered behavior could reflect a deficit in motor output, light reception or the processing of the visual information (Rahman et al., 2012). To analyze further the phenotypical consequence of EGFP-12xQ/N expression, phototaxis assay was performed in a Y-maze with one arm exposed to violet light (peak wavelength 400 nm) and the other arm completely in the dark. As expected, flies overexpressing TBPH under GMR-Gal4 driver had defective vision as they were not attracted to the light source, and this was consistent with the degeneration of the eye structure that they presented. On the contrary, flies co-expressing TBPH and the aggregate inducer EGFP-12xQ/N were attracted to the light source to the same extent that wild type flies. In this case, the vision restoration was consistent with the recovery of the eye morphology. Furthermore, in control flies co-expressing EGFP and TBPH the vision deficit was not recovered (**Figure 37a**).

To confirm that the phototactic deficit was not due to a motor impairment, climbing test of all genotypes was performed. This test is based on the negative geotaxis (movement against gravity) that is an innate characteristic of *Drosophila* (Benzer, 1967). Furthermore, as already stated the flies are naturally attracted to light stimulus (phototaxis). Thus, flies were transferred without anesthesia to a 50 ml glass-cylinder, tapped to the bottom of the tube, with a distal lamp to provide the stimulus, and their subsequent climbing activity was quantified as number of flies that reach the top of the tube in 15 seconds. **Figure 37b** shows the percentage of flies that reached the top of the cylinder within 15 seconds. As it can be appreciated the ability to climb of flies from each genotype was similar to wild type flies, indicating that the phototactic deficit of GMR-Gal4/UAS-TBPH and GMR-Gal4/UAS-TBPH;UAS-EGFP flies was not due to a defective climbing ability.
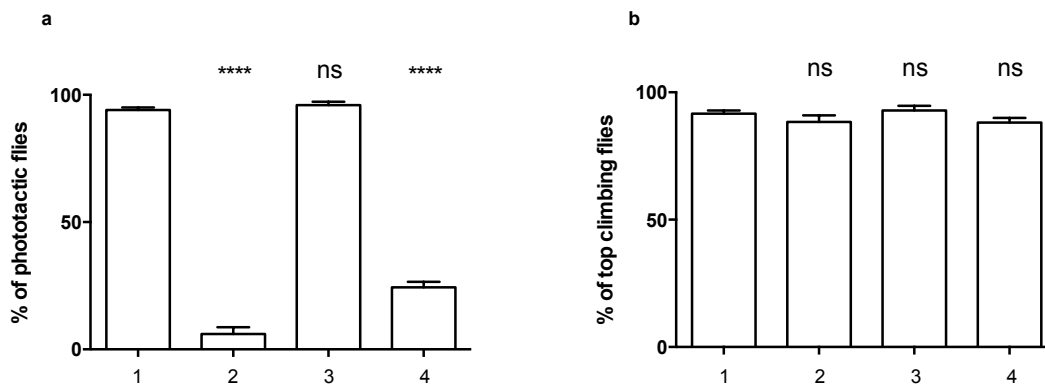
Figure 37. EGFP-12xQ/N expression restores eye functionality in TBPH expressing flies.

(a) Phototaxis assay of 1-day old flies of different genotypes indicated as follows: (1) Oregon-R (2) GMR-Gal4/UAS-TBPH (3) GMR-Gal4/UAS-TBPH;UAS-EGFP-12xQ/N (4) GMR-Gal4/UAS-TBPH;UAS-EGFP. Flies expressing TBPH are not attracted to the light, whereas flies co-expressing TBPH and EGFP-12xQ/N are attracted in the same proportion as wild type flies. On the contrary, the co-expression of TBPH and EGFP does not restore the vision. **** indicates $p<0.0001$ and ns indicates $p>0.05$ (not significant) calculated by one-way ANOVA followed by Bonferroni's multiple comparison. Error bars indicate SEM. **(b)** Climbing assay of 1-day old flies of different genotypes. The climbing capacity of all the genotypes were comparable to the wild type. ns indicates $p>0.05$ (not significant) calculated by one-way ANOVA followed by Bonferroni's multiple comparison. Error bars indicate SEM.

1.8. The expression of the TBPH aggregate inducer in *Drosophila* CNS does not hamper normal development

Notwithstanding the fact that aggregation is protective in the presence of an excess of TBPH, we wanted to further understand the role of the aggregates in an environment where just the endogenous TBPH is present. In particular, the main goal of this part of the study was to understand if the aggregates could induce an ALS-like phenotype due to a partial TBPH loss of function. To do so, we decided to investigate the effect that expression of the aggregate-inducer EGFP-12xQ/N have in *Drosophila's* central nervous system.

It was already demonstrated by Feiguin and co-workers (Feiguin et al., 2009), that TBPH is not essential for the development of the normal eye structure, as the TBPH null-allele mutants have completely normal eyes. Consequently, we decided to analyze the effect that EGFP-12xQ/N has in

other tissues that do get affected by the absence of TBPH. Moreover, ALS is a motor neuron disease, and it was interesting to see the effect of aggregation in this particular type of cells. For all these reasons we decided to further evaluate our aggregate-inducer system by constitutively expressing EGFP-12xQ/N transgene in CNS using ELAV-Gal4 driver (Yannoni & White, 1999), without TBPH overexpression.

We first confirmed the correct expression of EGFP-12xQ/N in CNS, by crossing the UAS-EGFP-12xQ/N line with ELAV-Gal4 line. UAS-EGFP line was used as control. After selecting the progeny, we checked the transgenic protein expression and its solubility status by immunohistochemistry of the third instar larval brain. **Figure 38** shows that also in CNS EGFP-12xQ/N is correctly expressed and forms aggregates, but EGFP without the 12xQ/N tail does not. In this experiment we stained the tissue also with anti-TBPH antibody, in order to evaluate the possible entrapment of the endogenous protein within the EGFP-12xQ/N aggregates. The co-localization of EGFP-12xQ/N aggregates with the endogenous TBPH was not so evident, suggesting that the entrapment, at least in this developmental stage, is not so efficient. Two different temperatures were used to raise the larvae, 25°C and 29°C. The higher temperature accelerates aging and induces a stronger expression of the transgenic protein, but neither in this condition we could improve sequestration of TBPH by EGFP-12xQ/N.
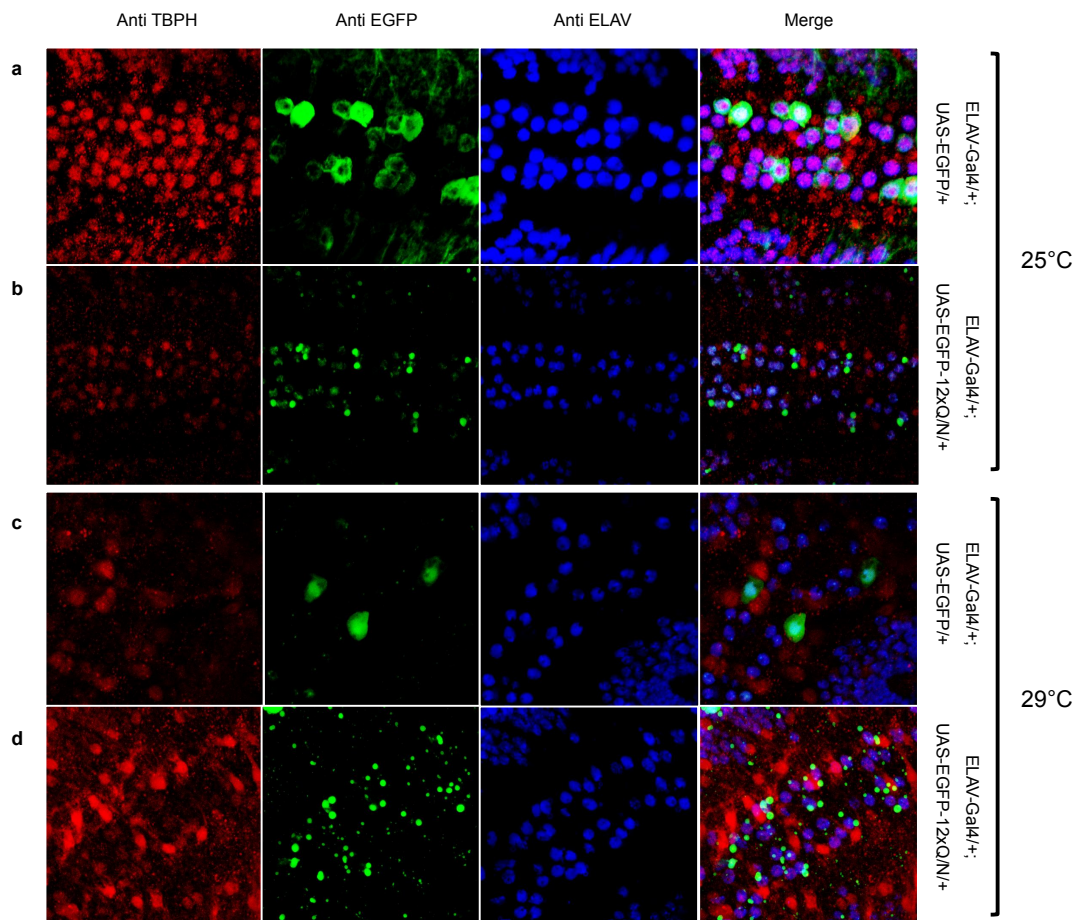
Figure 38. EGFP-12xQ/N is correctly expressed in *Drosophila* larval brain.
Confocal images of larval brain expressing EGFP **(a,c)** or EGFP-12xQ/N **(b,d)** with ELAV-Gal4 diver at 2 different temperatures. Samples were stained for TBPH (red), EGFP (green) and ELAV (blue). All the figures correspond to a single confocal section.

Even though there was no evident co-localization between EGFP-12xQ/N and TBPH, we decided to analyze the larval phenotype. *Drosophila* larvae show natural peristaltic movements, characterized by a wave, which starts at one end of the larvae, passes through all the body, and ends in the mouth. A reduction of the total larval waves could reflect a motor deficit.

The transgenic EGFP-12xQ/N larvae were born and went through the developmental stages without differing from control larvae in their phenotype, as the larval peristaltic waves within 2 minutes, both at 25°C and 29°C, in larvae expressing EGFP-12xQ/N or EGFP alone were similar (**Figure 39**).

106

Larval movement 25°C **Larval movement 29°C**
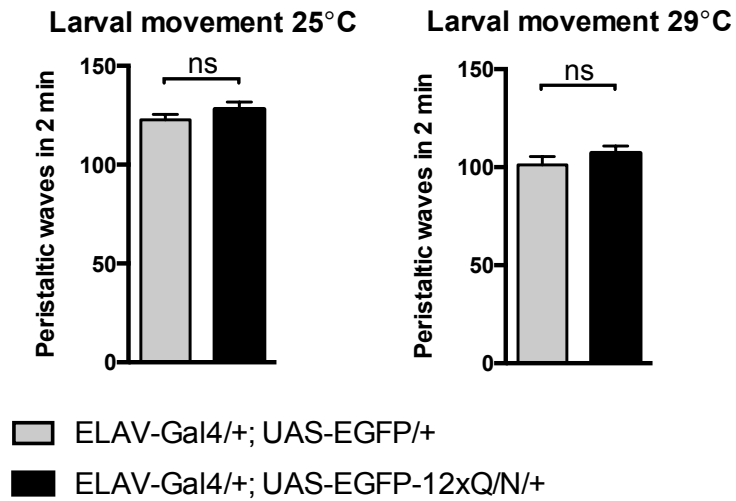
Figure 39. EGFP-12xQ/N expression under ELAV-Gal4 driver does not hamper larval movement.

Quantification of peristaltic waves of third instar larvae, expressing EGFP-12xQ/N or EGFP alone under ELAV-Gal4 driver. More than 20 larvae from each genotype were counted, and the mean was calculated. ns indicates p>0,05 (not significant) calculated by unpaired t-test. Error bars indicate SEM.

To further confirm this result we used the D42-Gal4 driver (Sanyal, 2009) that induces the expression of the protein of interest mainly in motor neurons. Also in this case, EGFP-12xQ/N expression in central nervous system does not affect the larval motility. In **Figure 40** no significant difference can be seen in the peristaltic waves of EGFP-12xQ/N expressing larvae and EGFP control.
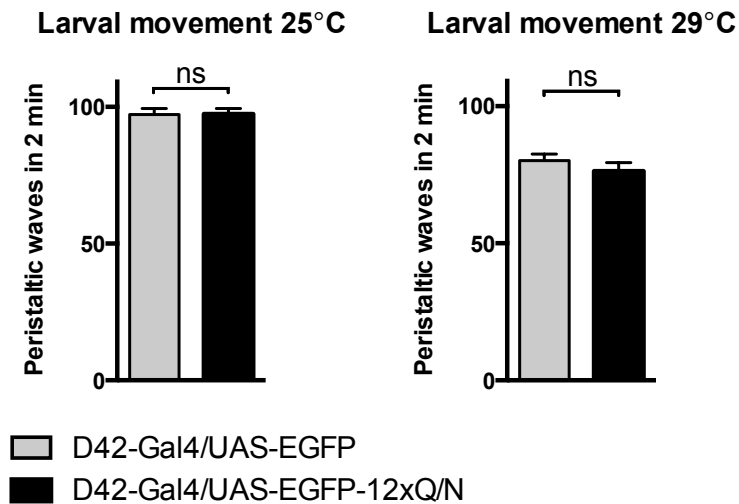
Figure 40. EGFP-12xQ/N expression under D42-Gal4 driver does not hamper larval movement.

Quantification of peristaltic waves of third instar larvae, expressing EGFP-12xQ/N or EGFP alone under D42-Gal4 driver. More than 20 larvae from each genotype were counted, and the mean was calculated. ns indicates p>0,05 (not significant) calculated by unpaired t-test. Error bars indicate SEM.

1.9. EGFP-12xQ/N expression triggers an age-related locomotion defect in *Drosophila*

As there was no larval phenotype, probably due to the little entrapment of endogenous TBPH by the EGFP-12xQ/N aggregates, we decided look at the possible phenotype in adult flies. For this reason, after the pupae stage the adult flies were kept either at 25°C or 29°C. The climbing ability following geotaxis (Benzer, 1967) was assessed at different time-points (day 3, 7 and 14) and the life span was measured.

As shown in **Figure 41**, at 25°C the transgenic flies constitutively producing aggregates showed significant locomotive alterations starting from 14 days of age (60% of top scoring flies compared to control with 80% of top scoring flies). On the other hand, flies kept at 29°C presented a locomotive phenotype earlier in life, that is significant already at day 3 (65% of top scoring flies compared to control with 85% of top scoring flies), consistent with the faster development of flies at this temperature. This decline in the climbing ability indicates that EGFP-12xQ/N expression might initiate a

neurodegenerative process. In agreement with this hypothesis, the expression of EGFP-12xQ/N also induced a strong reduction in the lifespan of this flies compared to control flies expressing EGFP alone. Specifically, EGFP-12xQ/N expressing flies at 25°C and 29°C have a half-life 20% and 40% shorter than the EGFP control, respectively **(Figure 41a and b right panels).**
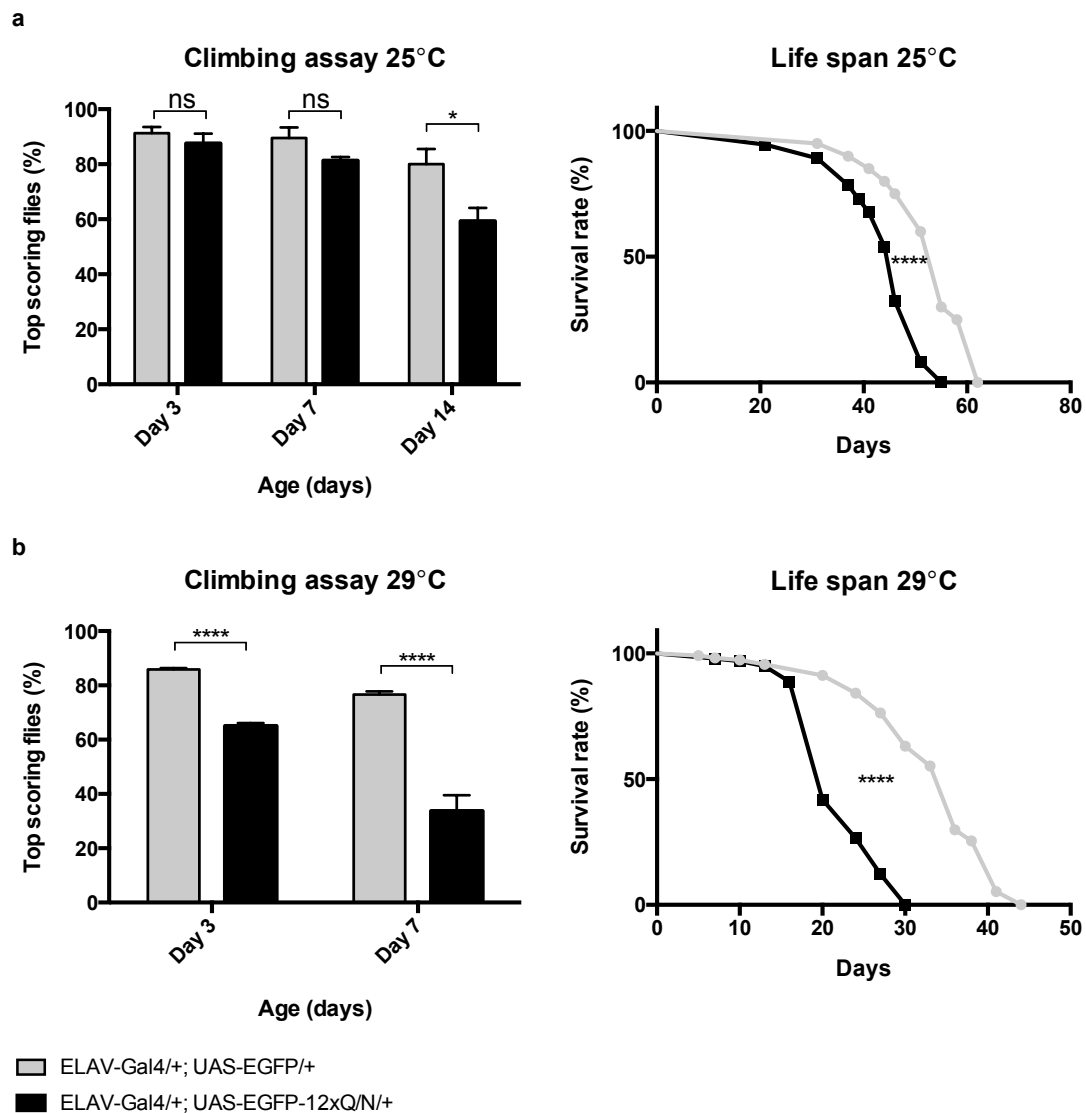
Figure 41. EGFP-12xQ/N expression under ELAV-Gal4 driver triggers an age-related phenotype in *Drosophila* adult flies.

(a) Climbing assay and life span of ELAV-Gal4/+;UAS-EGFP-12xQ/N/+ compared with control flies ELAV-Gal4/+;UAS-EGFP flies at 25°C **(b)** and 29°C. Unpaired t-test analysis was used to compare measures between 2 groups. Long rank test was performed to compare survival distribution between genotypes. ns indicates p>0,05 (not significant), * indicates p<0,05, **** indicates p<0,0001. Error bars indicate SEM.

Moreover, we found that EGFP-12xQ/N expression in a more restricted population of neurons that include motor neurons, by D42-Gal4 driver triggers the same phenotypical defects seen with the neural post-mitotic ELAV-Gal4 driver. **Figure 42** shows a significant difference in the climbing ability and survival rate of D42-Gal4/UAS-EGFP-12xQ/N flies and D42-Gal4/UAS-EGFP control flies, which is age-related. In this case, the defect in

the climbing ability upon EGFP-12xQ/N expression is evident earlier during the fly life if compared with ELAV-Gal4 driver. This effect could be related to the particular sensibility of motor neurons to TBPH aggregation, and to the consequent soluble TBPH levels.
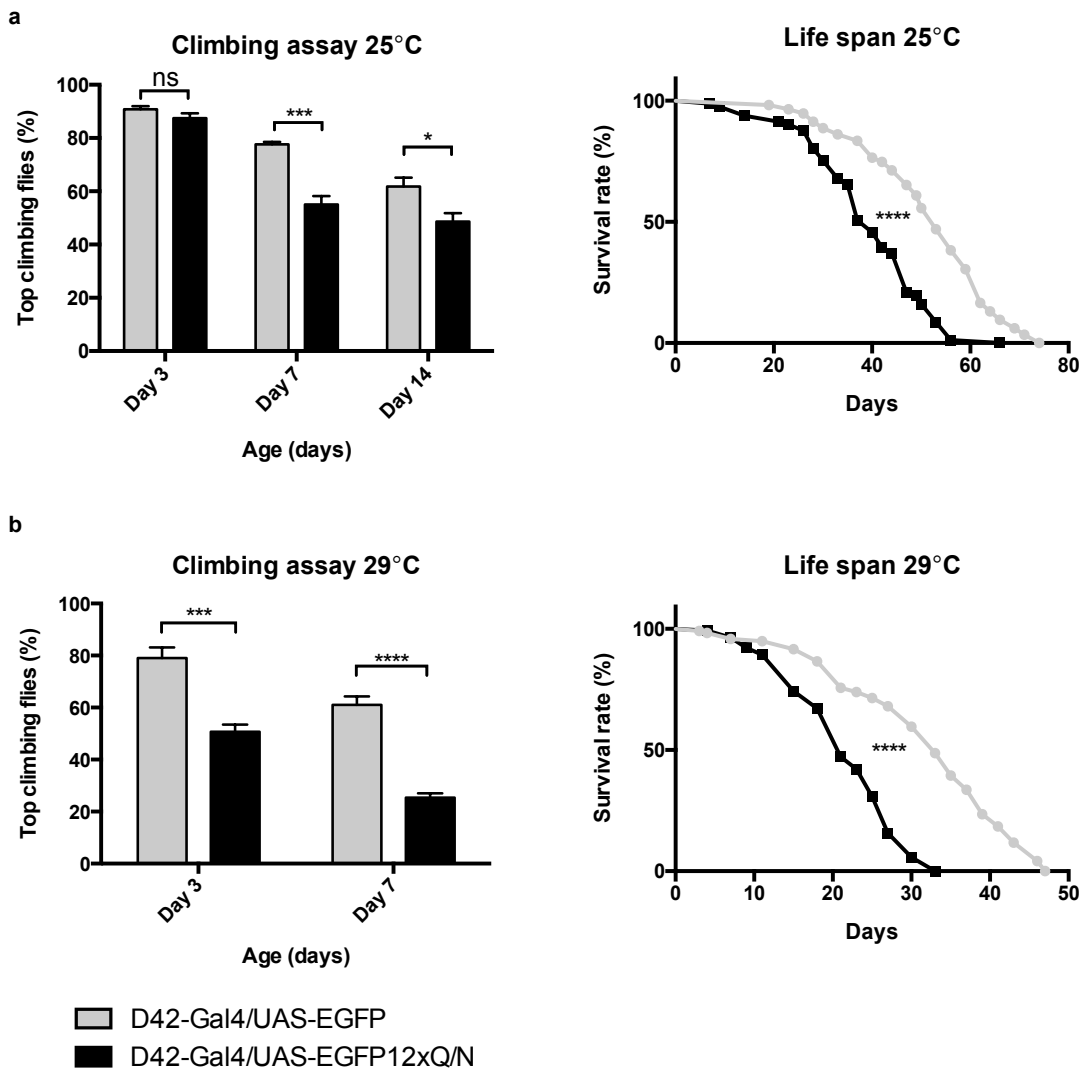
Figure 42. EGFP-12xQ/N expression under D42-Gal4 driver triggers an age-related phenotype in *Drosophila* adult flies.

(a) Climbing assay and life span of D42-Gal4/UAS-EGFP-12xQ/N flies compared with control flies D42-Gal4/UAS-EGFP at 25°C **(b)** and 29°C. Unpaired t-test analysis was used to compare measures between 2 groups. Long rank test was performed to compare survival distribution between genotypes. ns indicates p>0,05 (not significant), * indicates p<0,05, **** indicates p<0,0001. Error bars indicate SEM.

Altogether these experiments demonstrate that the EGFP-12xQ/N expression in CNS produces neurological consequences in locomotive behavior and alterations in life span, suggesting that the entrapment of the endogenous TBPH within the EGFP-12xQ/N aggregates is harmful possibly due to a TBPH loss of function.

1.10. EGFP-12xQ/N also forms aggregates in *Drosophila* adult brain

In order to confirm the correct expression of EGFP-12xQ/N in the adult brain we extracted total proteins of ELAV-Gal4/+;UAS-EGFP-12xQ/N and D42-Gal4/UAS-EGFP-12xQ/N head flies raised at 25°C. The obtained extracts were loaded in SDS-PAGE to allow protein separation and western blot was subsequently performed using an anti-GFP antibody. As it can be seen in **Figure 43** the level of expression of EGFP-12xQ/N (75.7 KDa) with the post-mitotic driver ELAV-Gal4 is higher than with the motor neuron enriched driver D42-Gal4. It should be noted that even though ELAV-Gal4 driver promotes a higher expression of EGFP-12xQ/N than D42-Gal4 driver, the climbing deficit appears earlier in life with D42-Gal4 driver, suggesting that the level of expression is not as important as the subtype of neurons where the protein is expressed.
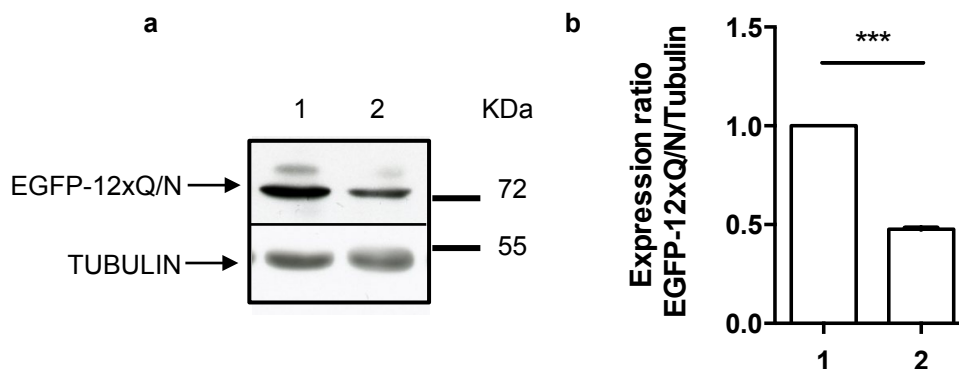
Figure 43. EGFP-12xQ/N level of expression in adult fly heads.

(a) Quantification of EGFP-12xQ/N level on total protein extracts prepared from adult fly heads ELAV-Gal4/+;UAS-EGFP-12xQ/N/+ (lane 1) and D42-Gal4/UAS-EGFP-12xQ/N (lane 2). A representative western blot is shown. Tubulin was used as loading control. **(b)** Image J quantification of EGFP-12xQ/N was performed from two independent experiments. *** indicates $p < 0,001$ calculated by unpaired t-test. Error bars indicate SD.

Moreover, we performed brain immunohistochemistry of 8 days-old D42-Gal4/UAS-EGFP-12xQ/N fly, in order to confirm the presence of EGFP-12xQ/N aggregates and its co-localization with the endogenous TBPH. After dissecting the adult fly brain the staining was performed with anti-GFP, anti-TBPH and anti-ELAV antibodies. The *Drosophila* adult brain is composed by the central brain, which is localized in the head, and the ventral ganglion that prolongs into the thorax (see Material and Methods, section 2.5.4 for further details). As it can be seen in **Figure 44**, both in central brain and ventral ganglia, EGFP-12xQ/N forms inclusions, which co-localize, at least in part, with endogenous TBPH. The extent of the co-localization has not been determined.
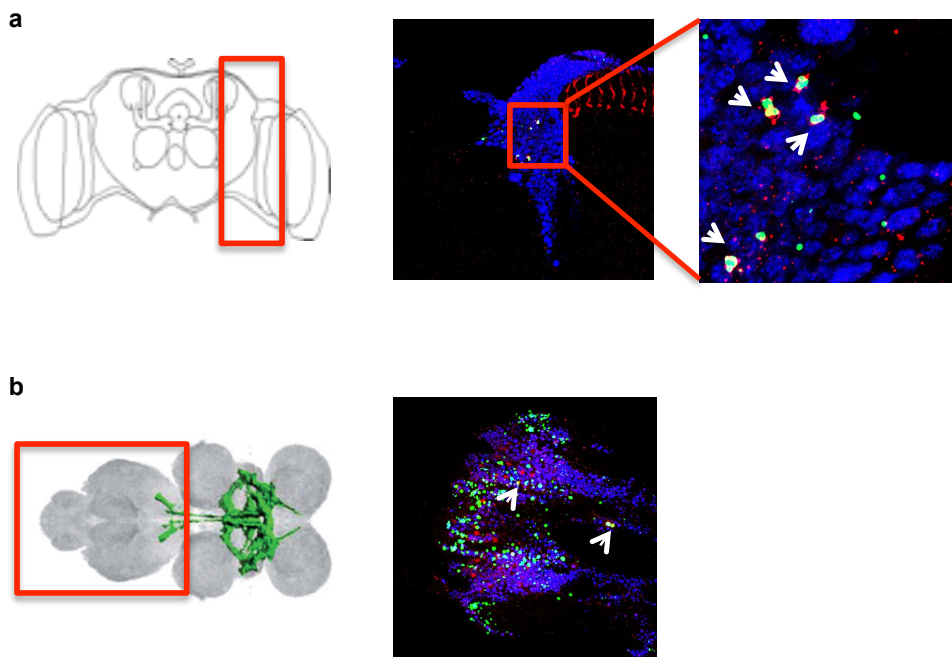
Figure 44. EGFP-12xQ/N co-localized with endogenous TBPH in *Drosophila* adult brain.

Confocal images of adult brain expressing EGFP-12xQ/N with D42-Gal4 driver. Samples were stained for TBPH (red), EGFP (green) and ELAV (blue). All the figures correspond to a single confocal section. Panel **(a)** shows a representative image of the central brain and a magnification. In panel **(b)** the ventral ganglia is shown. The left parts of both panels indicate with red boxes the specific part of the brain that was analyzed in each case. Arrowheads indicate co-localization of TBPH and EGFP-12xQ/N.

1.11. EGFP-12xQ/N expression generates a reduction in the area of *Drosophila* adult NMJ

Nerves from motor neurons project to their target muscles, branch a few times, and form synaptic boutons to innervate the muscle. The neuromuscular junction (NMJ) is formed by the contact between the presynaptic terminal of a motor neuron and the postsynaptic membrane of a muscle fiber. It is in the NMJ that the muscle receives the signals from motor neurons that finally cause muscle contraction. In order to further investigate the locomotive defects seen in adult flies expressing EGFP-12xQ/N, we were interested in analyzing the NMJs of these flies. For this reason, the NMJs of D42-Gal4/UAS-EGFP-12xQ/N and D42-Gal4/UAS-EGFP flies were examined. After dissecting the abdominal muscles, staining with anti-HRP was performed. Anti-HRP antibody is widely used in the field, as it recognizes specifically the presynaptic compartment in *Drosophila* (Jan & Jan, 1982). **Figure 45** shows an example of NMJ architecture of both transgenic flies, and an ImageJ quantification of the area of these NMJs. Transgenic D42-Gal4/UAS-EGFP-12xQ/N animals presented a reduction in the total area, compared to control flies D42-Gal4/UAS-EGFP. This result is consistent with the impairment of the locomotive ability that the EGFP-12xQ/N expressing flies presented.
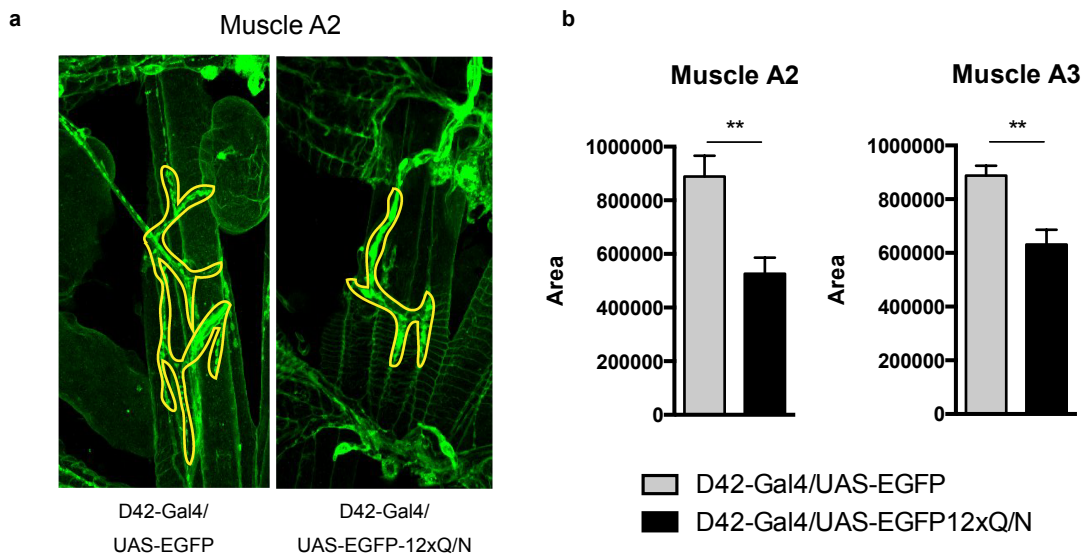
Figure 45. EGFP-12xQ/N expression generates a reduction in the NMJ area.
(a) Confocal images of adult NMJ in abdominal muscle A2 stained with anti-HPP. The yellow line indicates the NMJ limits. **(b)** Quantification of NMJ total area in abdominal muscles A2 and A3. Unpaired t-test analysis was used to compare measures between the 2 groups. ** indicates p<0,001. Error bars indicate SEM.

1.12. The locomotion defect correlates with an age-related decrease in TBPH levels

A peculiarity of the flies was that notwithstanding the constitutive production of EGFP-12xQ/N the resulting aggregates do not generate a phenotypic consequence until adulthood. Based on previous reports that showed that TDP-43 levels decrease with age in laboratory mouse strains (Huang et al., 2010; Liu et al., 2015) we decided to investigate whether this programmed reduction of TDP-43 levels arose early in evolution and can be observed also in non-mammalian species, specifically in *Drosophila*. For this reason we performed protein extraction from adult wild type fly heads at different ages. The protein extracts were separated by SDS-PAGE and analyzed by western blot with anti-TBPH antibody. TBPH levels were quantified using ImageJ software and the relative levels were assessed by normalization with tubulin. **Figure 46a** shows the relative TBPH levels during aging in wild type fly heads at 25°C **(left panel)** and 29°C **(right panel)**. The data shows a two-step drop at day 3 and 7 at 25°C and at day 2 and 3 at

29°C, with a final level of 4-fold less TBPH than in the immediate after pupa stage (8 hours). It should be noted that the two-step drop in TBPH/TDP-43 expression is conserved even in the case of accelerated aging. Most interestingly, the final drop coincides with the time point where the locomotive defect starts to be visible in the transgenic EGFP-12xQ/N fly (indicated with an arrow in **Figure 46a**). At this point, we reasoned that as EGFP-12xQ/N is not so efficient in trapping endogenous TBPH, the trapping starts to generate a visible phenotype only when the TBPH levels are low, as it lowers the amount of functional TBPH below a critical threshold.

In order to confirm previous reports, we also extracted total protein from mouse brain samples and after separation by SDS-PAGE and western blot with anti-TDP-43 antibody we were able to confirm that, also in mouse brain, TDP-43 levels showed an age-related decrease, following a pattern similar to the fly with two major decrease steps **(Figure 46b)**.
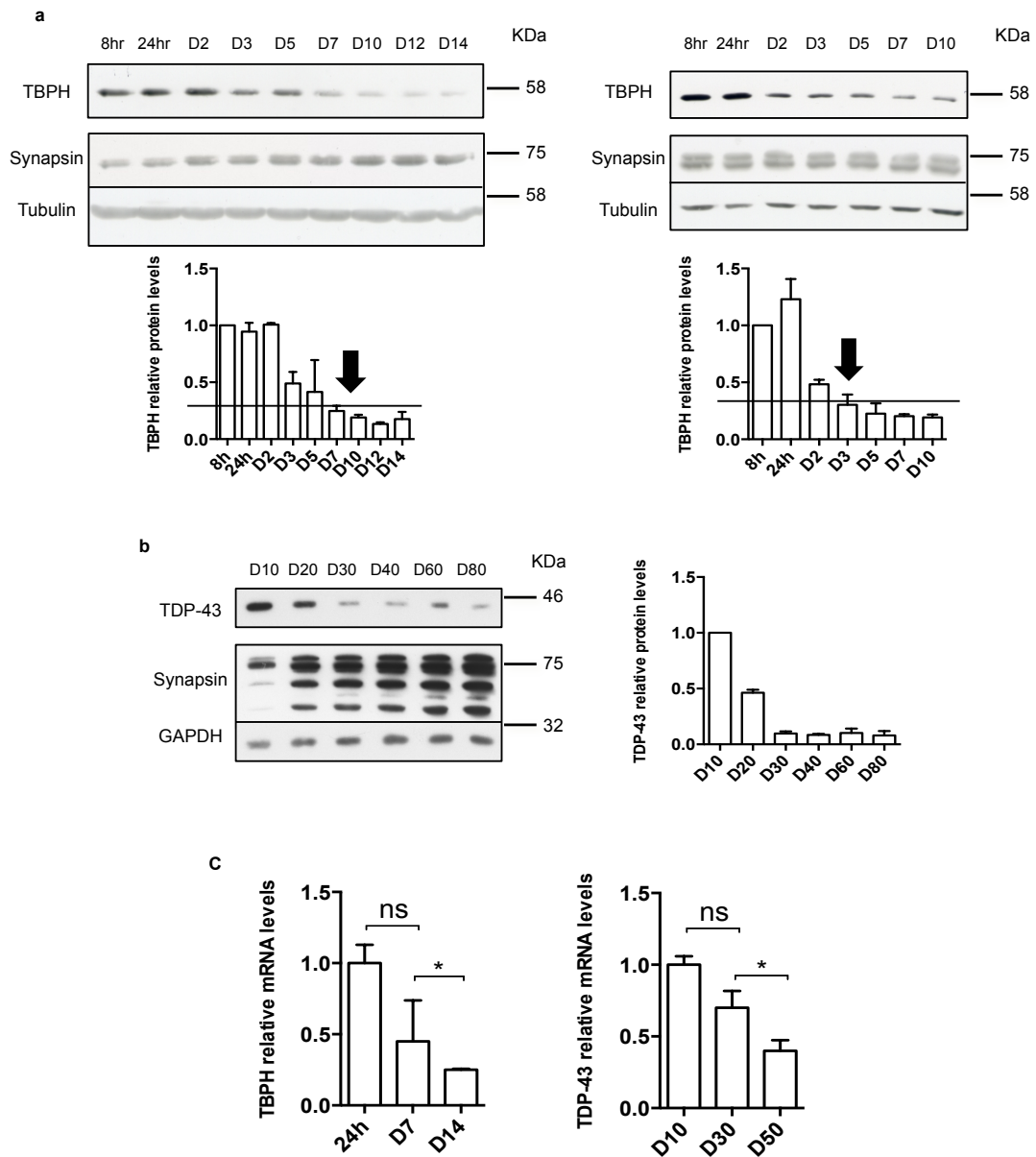
Figure 46. TBPH levels drop physiologically during normal aging of wild type flies.

(a) Western blot analyses showing endogenous TBPH and synapsin levels from adult wild type fly heads aged at 25°C (left panel) and 29°C (right panel). The histograms show the TBPH expression levels normalized with tubulin. D stands for day. The arrow indicates the point where the climbing ability of the flies is significantly reduced (see Figure 2). **(b)** Western blot analyses showing endogenous TDP-43 and synapsin levels from wild type mice during aging. The corresponding histogram shows the relative expression levels of TDP-43 normalized with GADPH. Error bars indicate SEM. **(c)** Real-time PCR quantification of fly TBPH (left panel) and mouse TDP-43 (right panel). The proteins levels were normalized with Rpl-11 or GADPH respectively. Unpaired t-test analysis was used to compare measures between the 2 groups. ns indicates p>0,05 (not significant) and * indicates p<0,05. Error bars indicate SD.

To discard that TBPH/TDP-43 drop was due to an age-related neuronal loss, we compared in fly and mouse the variations of TBPH/TDP-43 levels during aging with the fluctuation in the levels of synapsin, a strictly neuronal protein. Western blot with anti-synapsin antibody showed that both in *Drosophila* and mice, the synapsin levels do not decrease with age as TBPH does (**Figures 46a and b**). This indicates that the reduction of brain TBPH/TDP-43 levels is not due to significant neuronal loss, as in that case a similar decrease in synapsin would have been observed. In addition, we are analyzing relatively young age groups not expected to have any significant neuronal loss. This observation is also consistent with what has been reported to occur in humans (Wickelgren, 1996). Wickelgren and others showed that, on the contrary of what was thought for a long time, the cell death in the brain is not the cause of the cognitive changes in normal aging. Imaging studies have demonstrated that the brain shrinks with age and many people have interpreted that shrinkage as cell loss. But other studies indicate that brain shrinkage might be due almost exclusively to loss of white matter, and not because of neuronal death. In relation to this, we do not see neuronal loss during normal aging in *Drosophila* and mice, measured indirectly by analyzing the synapsin levels.

We further analyzed if the TBPH/TDP-43 drop was occurring at transcriptional or translational level. For this purpose, we extracted total RNA from wild type *Drosophila* heads and wild type mouse brain at different ages and performed real time RT-PCR. In the case of *Drosophila* TBPH mRNA levels were quantified and normalized with the housekeeping gene *Rpl11*. For the mouse, TDP-43 mRNA levels were measured and the normalization was done using *GADPH* as housekeeping gene. We could confirm that the lower protein levels observed in **Figures 46a and b** correspond to lower mRNA levels both in flies and mouse (**Figure 46c**), indicating that there is a pre-translational mechanism for age-programmed reduction of TDP-43/TBPH levels.

Our data strengthens the hypothesis that the decrease in TBPH/TDP-43 levels represents an evolutionary conserved feature characteristic of aging of the organisms.

1.13. Constitutive reduction of TBPH levels from birth anticipates the locomotive defect in EGFP-12xQ/N expressing flies

If the low TBPH levels seen with aging predispose to the locomotion defects observed upon expression of EGFP-12xQ/N, it follows that the sensitivity to the presence of aggregates will be higher in a fly with low TBPH levels from birth and hence the phenotype should arise earlier in life. To test this hypothesis we created a fly that constitutively expresses a siRNA against TBPH in neurons, and crossed this fly with UAS-EGFP-12xQ/N and UAS-EGFP transgenic strains. In order to confirm that endogenous TBPH levels were effectively reduced, we extracted total proteins from third instar larval brain. The brain extracts were resolved in SDS-PAGE followed by western blot anti-TBPH. Tubulin was used as loading control. **Figure 47a** shows a representative western blot and the quantification of the TBPH levels in wild type larvae (W1118) and in larvae expressing TBPH siRNA (ELAV-Gal4,TBPH$^{\Delta23}$/+;TBPH^{RNAi}/EGFP and ELAV-Gal4,TBPH$^{\Delta23}$/+;TBPH^{RNAi}/EGFP-12xQ/N). As it can be seen, these larvae have from birth reduced TBPH levels, comparable to 14 days-old wild type flies, however this level is sufficient for their development.

The following approach was to evaluate the larval movement. As it can be appreciated from **Figure 47b**, there is already a locomotion phenotype at the third instar larval stage at 25°C when EGFP-12xQ/N is co-expressed with the TBPH siRNA, indicating that the phenotypic consequence of the EGFP-12xQ/N aggregates is indeed dependent on endogenous TBPH levels.
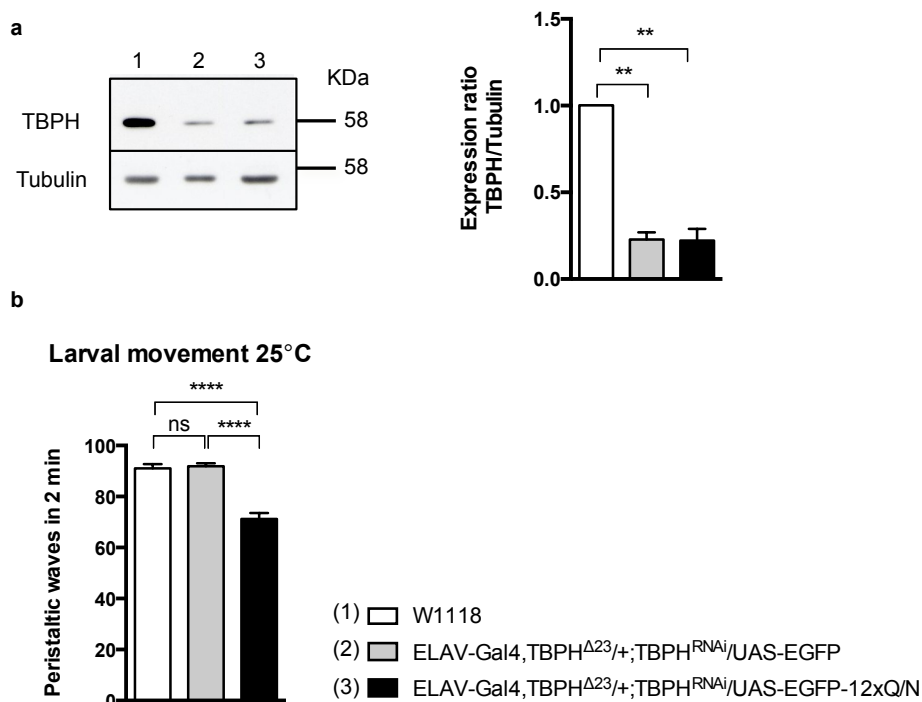
Figure 47. Constitutive reduction of TBPH levels anticipates EGFP-12xQ/N-related phenotype.

(a) Quantification of TBPH level in wild type (W1118) larval brains and larvae expressing TBPH siRNA. The different genotypes are indicated and defined by the color code at the bottom of the figure. The histogram shows the TBPH expression levels normalized with tubulin. One-way ANOVA followed by Bonferroni's multiple comparison was used to compare measures among 3 groups. ** indicates p<0,01. Error bars indicate SD. **(b)** Quantification of peristaltic waves of third instar larvae. One-way ANOVA followed by Bonferroni's multiple comparison was used to compare measures among 3 groups. ns indicates p>0,05 (not significant) and **** indicates p<0,0001. Error bars indicate SEM.

Our data demonstrates the existence of a physiological decrease in TDP-43/TBPH levels with aging in brain tissue, both in wild type mice and flies, showing that it is an evolutionary conserved phenomenon. The maintenance of most functions sustained by TBPH/TDP-43 depends on the cell capacity of producing this protein and its availability in a functional form and in the proper cellular location. Available TDP-43 levels lower than a certain threshold would lead to abnormal function of TDP-43 on targets critical for neuronal structure and function, which might be responsible for the ALS pathologies.

2.   Innovative therapeutic approaches to treat TDP-43-ALS

The data presented so far suggest that, although the aggregates may be a result of neuroprotection when TBPH is in excess, they might be responsible for the pathology when TBPH levels are low, likely due to the loss of nuclear function of TBPH. If we consider that TDP-43/TBPH inclusions act as a sink for the newly formed soluble TDP-43/TBPH, the modulation of these TDP-43/TBPH inclusions could be used as a potential therapeutic approach, as they would restore the normal levels of TDP-43/TBPH and therefore its function.

2.1.   Searching for compounds that can clear TDP-43 aggregates

Proteins that aggregate in neurodegenerative diseases share with prions the molecular properties of nucleation, growth, multiplication and spread. Each of these phenomena presents potential therapeutic targets. For instance, stimulating the removal of aggregates could help to reduce nucleation and growth (Jucker & Walker, 2013). Considering the prion-like properties of TDP-43 (see Introduction section 3.2) it would be interesting to design new therapeutic strategies to interfere with the template-directed replication. It has been shown that this property is a common molecular pathway for the spread of toxic proteins in neurodegenerative diseases affecting the CNS, and thereby offers novel opportunities for therapeutic strategies to disrupt or to delay the cascade of events that underlie the propagation of protein misfolding and transmission of these misfolded proteins (Ludolph & Brettschneider, 2015).

We reasoned that by inducing the cellular proteolysis we could get rid of the aggregates and in this way the newly synthetized TDP-43/TBPH would be free to carry out its nuclear function. In eukaryotic cells, there are two main systems that carry out proteolysis; one is the ubiquitin-proteasome system and the other the lysosome-autophagy pathway.

Using our previously established cell-based TDP-43 aggregation models (see Introduction section 3.4.3) we analyzed aggregate clearance after treatment with several FDA approved drugs. These drugs have already been shown to be neuroprotective, they are able to cross the blood brain barrier

and they are proven to be safe for long-term use in human, with only minor side effects.

In order to assess the potential clearance capacity of each compound, different concentrations of each of them were tested. In order not to be dependent on transfection efficiency and to obtain reliable and reproducible results, a HEK293 stable cell line was generated by introducing only one copy of EGFP-12xQ/N construct into the cellular genome. In this cell line, the transgene expression is blocked by the tetracycline repressor (TetR). Only in the presence of tetracycline the EGFP-12xQ/N expression will be induced.

Using this cell line we performed a clearance assay upon drug treatment (Wang et al., 2010). Briefly, HEK293 EGFP-12xQ/N cell line was inducibly expressed for 24 hours. After EGFP-12xQ/N aggregate formation, tetracycline was washed out, and the treatment with the compounds was performed for 48 hours. As control, we performed the experiment without drugs. This control is necessary as the cells continue to replicate during the 48 hours of treatment, and the cellular clearance system is working, however with the drugs we expect to have an increase of the clearance. In this way, we could determine whether EGFP-12xQ/N inclusions can be degraded when protein expression is arrested, as there is no tetracycline in the medium during the drug treatment. After the incubation time with the compounds was over, the cells were harvested and the total proteins were extracted and separated by SDS-PAGE. The total amount of EGFP-12xQ/N was assessed by western blot under reducing conditions, using anti-GFP antibody and tubulin as a loading control. Out of the 8 drugs tested, 3 demonstrated an effect in aggregate clearance (**Table 15**).

Figure 48 shows representative western blot assays and the respective quantifications of clearance assay upon drug treatment with the 3 drugs, which resulted to have an effect on EGFP-12xQ/N clearance. The treatment with either thioridazine (TDZ) at 5 µM, nortriptyline (NOR) at 10 µM and chlorpromazine (CPZ) at 10 µM significantly reduced the total level of EGFP-12xQ/N.
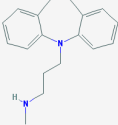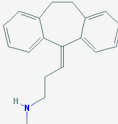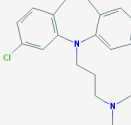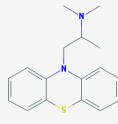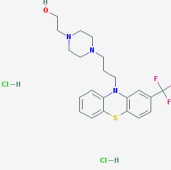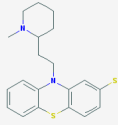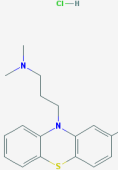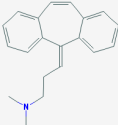
Compound	Drug class	Structure	Effect on aggregate clearance?
Desipramine	Antidepressant		No
Nortriptyline	Antidepressant		Yes
Clomipramine	Antidepressant		No
Promethazine	Antihistaminic		No
Flufenazine	Antihistaminic		No
Thioridazine	Antipsychotic		Yes
Chlorpomazine	Antipsychotic		Yes
Cyclobenzaprine	Muscle relaxant		No

Table 15. Tricyclic compounds and its effect on aggregate clearance.

Drug class, structures and effect on aggregate clearance of tricyclic compounds used in this study. The structures were adapted from NCBI PubChem Data Bank.
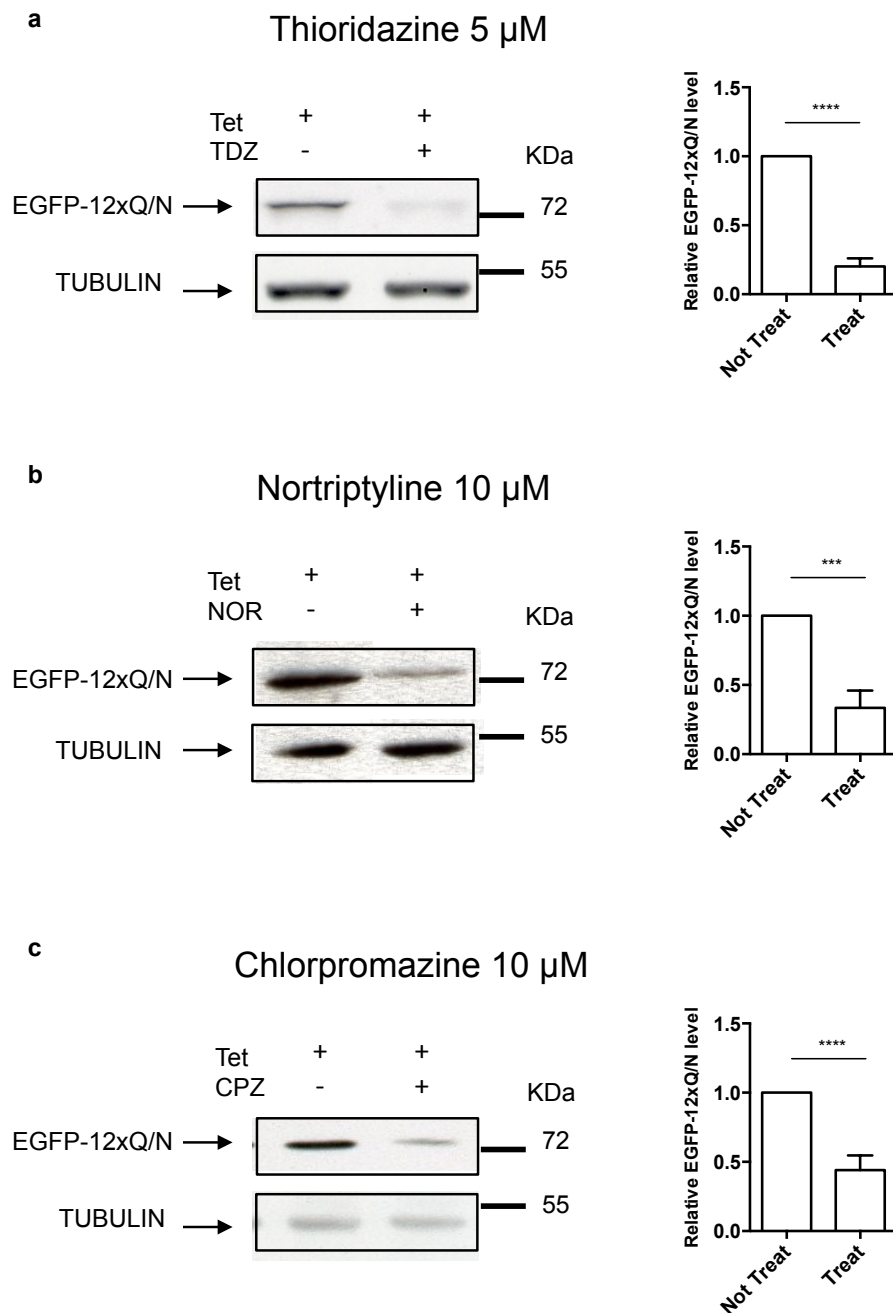
Figure 48. Clearance assay with EGFP-12xQ/N cellular model.

HEK293 EGFP-12xQ/N stable cells were treated with **(a)** thioridazine, **(b)** nortriptyline and **(c)** chlorpromazine, after tetracycline induction. Representative western blots of clearance assay after drug treatment and the respective quantification of 3 independent experiments are shown. The blots were tested with anti-GFP antibody and anti-tubulin as loading control. Unpaired t-test analysis was used to compare measures between 2 groups. *** indicates $p < 0.001$ and **** indicates $p < 0.0001$. Error bars indicate SD.

2.2. TDZ, NOR and CPZ-mediated clearance is not autophagy-dependent

In order to study the proteolytic pathway used for protein clearance upon drug treatment, first we analyzed the involvement of the autophagy pathway by showing the common autophagy markers LC3II and p62. As previously explained (see Introduction section 3.5), the microtubule-associated protein 1A/1B-light chain 3 (LC3) is a soluble protein that, during autophagy, can be converted from its soluble form (LC3-I) to the LC3-phosphatidylethanolamine conjugated form (LC3-II). This process is required for the cargo recruitment into the forming autophagosome. Therefore, the LC3-II levels correlate directly with the amount of autophagosomes present in the cell (Mizushima, 2004). Importantly, due to the lipidation process, LC3 molecular weight changes. LC3-I has an apparent molecular weight of 16 KDa, and after the conversion occurs the LC3-II molecular weight is 18 KDa. However, the lipidation increases also LC3-II hydrophobicity, and even though its molecular weight is higher in comparison to LC3-I, it seems smaller when loaded in SDS-PAGE. In order to analyze the endogenous LC3 pattern and the conversion upon drug treatment, we treated the HEK293 EGFP-12xQ/N cells as for the clearance assay and after treatment with the specific concentration of each compound, the total cellular proteins were extracted and separated by SDS-PAGE followed by western blot with anti-LC3 antibody. **Figure 49** shows that after drug treatment there is an increased LC3II to LC3I ratio.
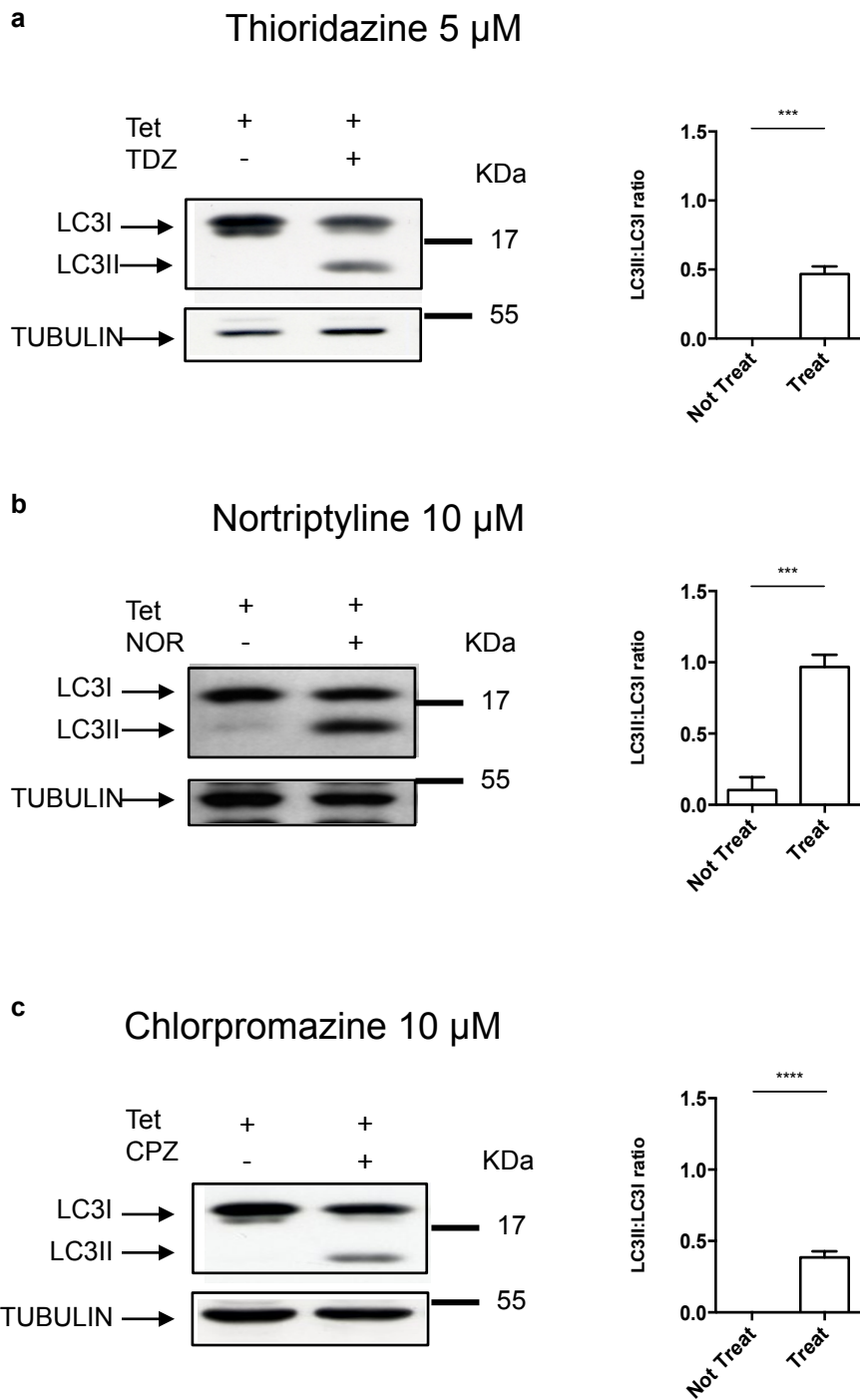
Figure 49. LC3 conversion upon drug treatment.

HEK293 EGFP-12xQ/N stable cells were treated with **(a)** thioridazine, **(b)** nortriptyline and **(c)** chlorpromazine, after tetracycline induction. Representative western blots of LC3 conversion after drug treatment and the respective quantification of 3 independent experiments. The blots were tested with anti-LC3 antibody and anti-tubulin as loading control. Unpaired t-test analysis was used to compare measures between 2 groups. ** indicates p<0,01, *** indicates p<0,001 and **** indicates p<0,0001. Error bars indicate SD.

However, this LC3 conversion from the unconjugated (LC3-I) to the conjugated (LC3-II) form could be a consequence of either, increased autophagosome formation due to an increase in autophagic activity, or reduced turnover of autophagosomes due to an impairment in the degradation pathway. Therefore, the use of autophagy markers such as LC3-II needs to be complemented by other markers that will help understanding the overall autophagic flux. One approach could be to measure p62 level. p62 protein serves as a link between LC3 and ubiquitinated substrates, and becomes incorporated into the completed autophagosome. p62 is itself degraded by autophagy, and therefore, it accumulates when autophagy is inhibited. This makes p62 a good marker to study autophagic flux. Therefore, and to clarify if the LC3-I to LC3-II conversion was a consequence of either autophagic impairment or activation, we analyzed the amount of p62 before and after drug treatment. HEK293 EGFP-12xQ/N cells were treated again as for the clearance assay and after treatment with the specific concentration of each compound, the total cellular proteins were extracted and separated by SDS-PAGE followed by western blot with anti-p62 antibody. As it can be appreciated from **Figure 50** western blot analysis of HEK293 EGFP-12xQ/N cells revealed that p62 accumulates after drug treatment, indicating that all 3 drugs inhibit the autophagic flux. As a consequence, LC3-II accumulates in cells treated with thioridazine, nortriptyline and chlorpromazine.
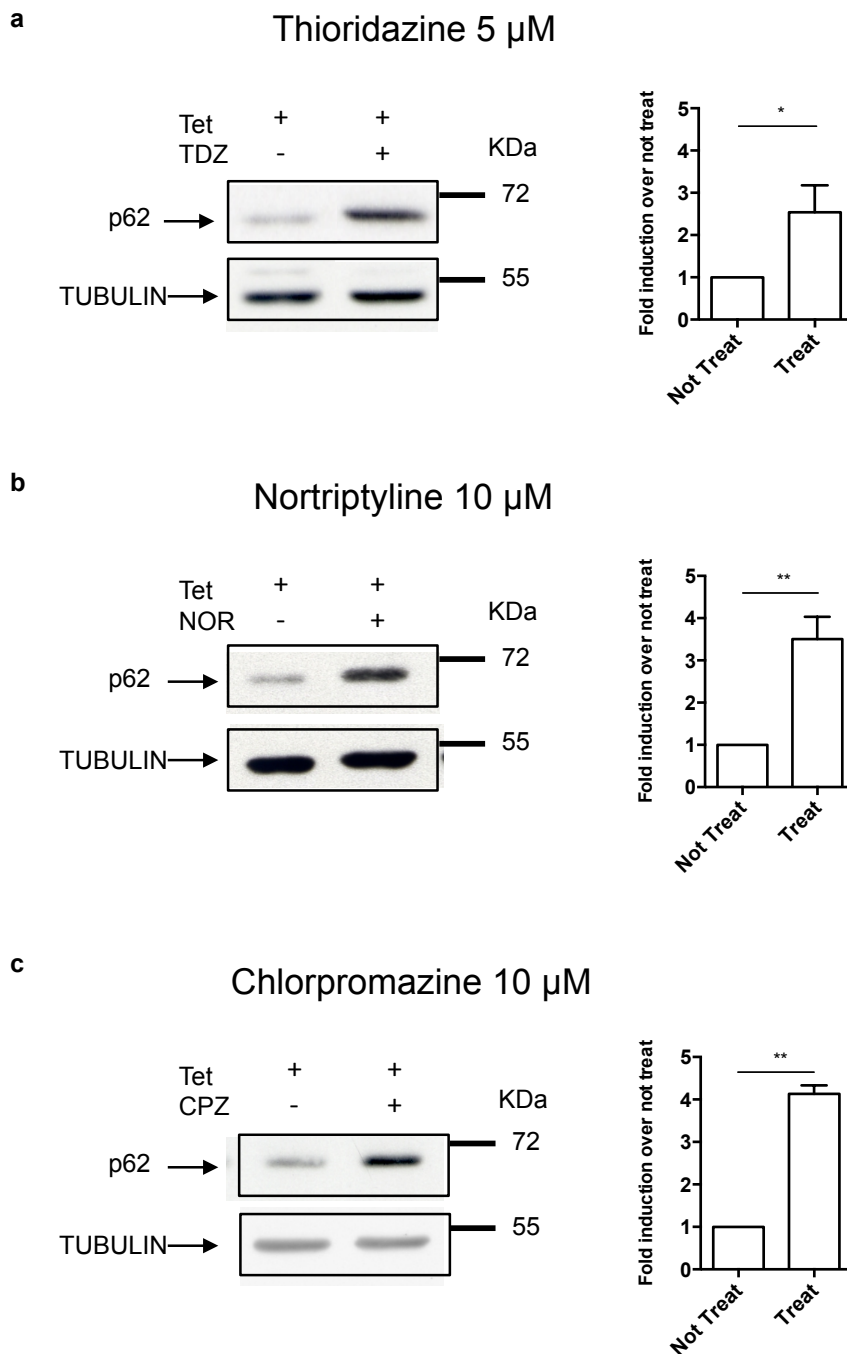
Figure 50. p62 marker accumulates upon drug treatment.

HEK293 EGFP-12xQ/N stable cells were treated with **(a)** thioridazine, **(b)** nortriptyline and **(c)** chlorpromazine, after tetracycline induction. Representative western blots of p62 accumulation after drug treatment and the respective quantification of 3 independent experiments. The blots were tested with anti-p62 antibody and anti-tubulin as loading control. Unpaired t-test analysis was used to compare measures between 2 groups. * indicates p<0,05 and ** indicates p<0,01. Error bars indicate SD.

Altogether these results indicate that all 3 drugs (thioridazine, nortriptyline and chlorpromazine) promote EGFP-12xQ/N aggregate clearance by a mechanism that is independent from autophagy, and moreover, they seem to block this proteolytic pathway. To further confirm this result we examined what happens when cells are treated with the compounds in the presence of the autophagy inhibitor ammonium chloride (NH_4Cl). NH_4Cl changes the pH of the lysosome, inhibiting the fusion of the lysosomes with the forming autophagosome, blocking in this way the autophagic flux.

The first approach was to confirm that NH_4Cl effectively blocks autophagy. For this reason, we controlled LC3 conversion and p62 accumulation upon NH_4Cl treatment. HEK293 EGFP-12xQ/N cells were induced with tetracycline for 24 hours, and after tetracycline removal NH_4Cl was added to the culture media at a concentration of 30 mM for 48 hours. Cells were finally harvested and total proteins were extracted and western blot was performed with anti-LC3 and anti-p62 antibodies. Representative western blots are presented in **Figure 51**, and as it can be seen the NH_4Cl treatment successfully interferes with the autophagy flux, as LC3I is converted into LC3II but p62 is accumulated.
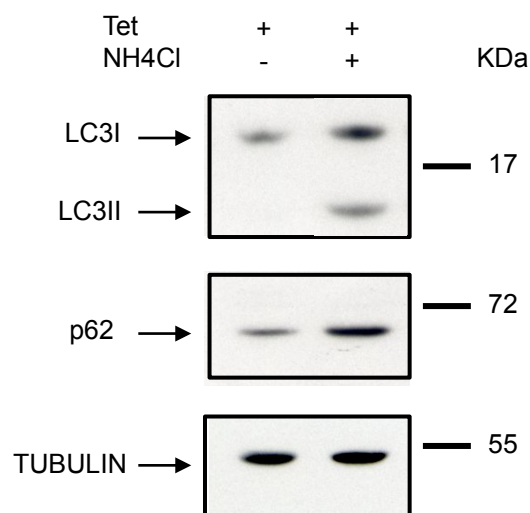
Figure 51. NH_4Cl effectively blocks autophagy.
HEK293 EGFP-12xQ/N stable cells were treated induced with tetracycline for 24 hours and then treated with the autophagy inhibitor NH_4Cl. Representative western of LC3 conversion and p62 accumulation. The blots were tested with anti-LC3 and anti-p62 antibodies and anti-tubulin as loading control.

Once we confirmed that NH$_4$Cl could effectively block autophagy, we treated the cells as for the clearance assay, with the only difference that 1 hour before adding the compounds at each specific concentration, NH$_4$Cl was added to the culture media at a concentration of 30 mM. Then, the total cellular proteins were extracted and a western blot with anti-GFP antibody was performed. As it can be seen in **Figure 52**, even in the presence of the autophagy inhibitor NH$_4$Cl the drugs are still able to degrade EGFP-12xQ/N, further supporting the idea that autophagy is not involved in the clearance mechanism.

a

Thioridazine 5 μM

Tet	+	+	+
TDZ	-	+	+
NH4Cl	-	-	+

KDa

EGFP-12xQ/N →

TUBULIN →

— 72

— 55

Relative EGFP-12xQ/N level (y-axis, 0.0–1.5): Not Treat, TDZ, TDZ+NH4Cl

b

Nortriptyline 10 μM

Tet	+	+	+
NOR	-	+	+
NH4Cl	-	-	+

KDa

EGFP-12xQ/N →

TUBULIN →

— 72

— 55

Relative EGFP-12xQ/N level (y-axis, 0.0–1.5): Not Treat, NOR, NOR+NH4Cl

c

Chlorpromazine 10 μM

Tet	+	+	+
CPZ	-	+	+
NH4Cl	-	-	+

KDa

EGFP-12xQ/N →

TUBULIN →

— 72

— 55

Relative EGFP-12xQ/N level (y-axis, 0.0–1.5): Not Treat, CPZ, CPZ+NH4Cl

Figure 52. Clearance assay with EGFP-12xQ/N cellular model in presence of NH$_4$Cl. HEK293 EGFP-12xQ/N stable cells were induced with tetracycline for 24 hours and then treated with **(a)** thioridazine, **(b)** nortriptyline and **(c)** chlorpromazine in presence or absence of the autophagy inhibitor NH$_4$Cl. Representative western of clearance assay and its respective quantifications under the different conditions. The blots were tested with anti-GFP antibody and anti-tubulin as loading control.

On a more specific approach we treated HEK293 cells with nortriptyline and/or NH$_4$Cl, and analyzed LC3 conversion. As already stated, LC3-II accumulation upon drug treatment simply indicates the accumulation of autophagosomes, but does not guarantee autophagic degradation. If, however, the amount of LC3-II further accumulates in the presence of the drug and the lysosomal inhibitor NH$_4$Cl, this would indicate enhancement of the autophagic flux. However, if the LC3-II level remains unchanged, it is likely that autophagosome accumulation occurred due to the inhibition of the autophagic degradation (Mizushima & Yoshimori, 2007). We could observe that when comparing cells that where treated with nortriptyline or with nortriptyline and the inhibitor, LC3II/I ratio did not increase, further confirming that the drug inhibits the autophagic flux (**Figure 53**). We expect the same would happen with the other two tricyclic compounds.
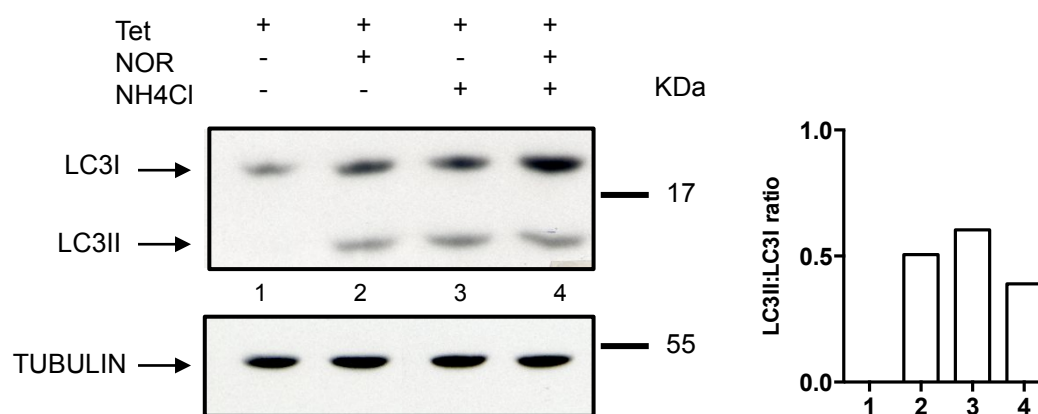
Figure 53. Confirmation that nortriptyline blocks autophagy flux.
HEK293 EGFP-12xQ/N stable cells were induced with tetracycline for 24 hours and then treated with nortriptyline in presence or absence of the autophagy inhibitor NH$_4$Cl. Representative western of clearance assay and its quantification under the different conditions. The blots were tested with anti-LC3 antibody and anti-tubulin as loading control.

2.3. TDZ, NOR and CPZ-mediated clearance is proteasome-dependent

To examine whether EGFP-12xQ/N clearance was happening through the proteasome, we performed the clearance assay with the 3 drugs in the presence of the proteasome inhibitor lactacystin. Lactacystin was added to

the culture media 1 hour before the addition of the drugs treatment. As already stated, this small molecule is currently the only compound known to inhibit the proteasome specifically without inhibiting any other protease (Fenteany and Schreiber, 1998). After the 48 hours of treatment, cells were harvested and proteins were extracted. The lysates were separated by SDS-PAGE and subsequently analyzed by western blot using anti-GFP antibody. Remarkably, the drugs were no longer able to degrade EGFP-12xQ/N in the presence of the proteasome inhibitor (**Figure 54**). Interestingly, not only EGFP-12xQ/N protein was no longer degraded by the drugs when lactacystin was present in the medium, but its levels increased in this case compared to the control (where no drug or inhibitor treatment were performed). It is important to bear in mind that control cells were induced with tetracycline for 24 hours and after induction the tetracycline was washed out, in order to stop aggregate formation, and the cells were further cultured for 48 hours without addition of drugs or inhibitors. During these 48 hours the EGFP-12xQ/N protein was degraded, up to some extent, by the normal cellular response. This clearance is through the proteasomal pathway as, upon lactacystin treatment, we could observe not only that the drug is not capable of degrading EGFP-12xQ/N, but also that it accumulates. To further confirm this, we performed another control were cells were treated, after tetracycline induction, with lactacystin but without drugs. As it can be seen in the last lane of each gel, the protein is accumulated to the same extent.
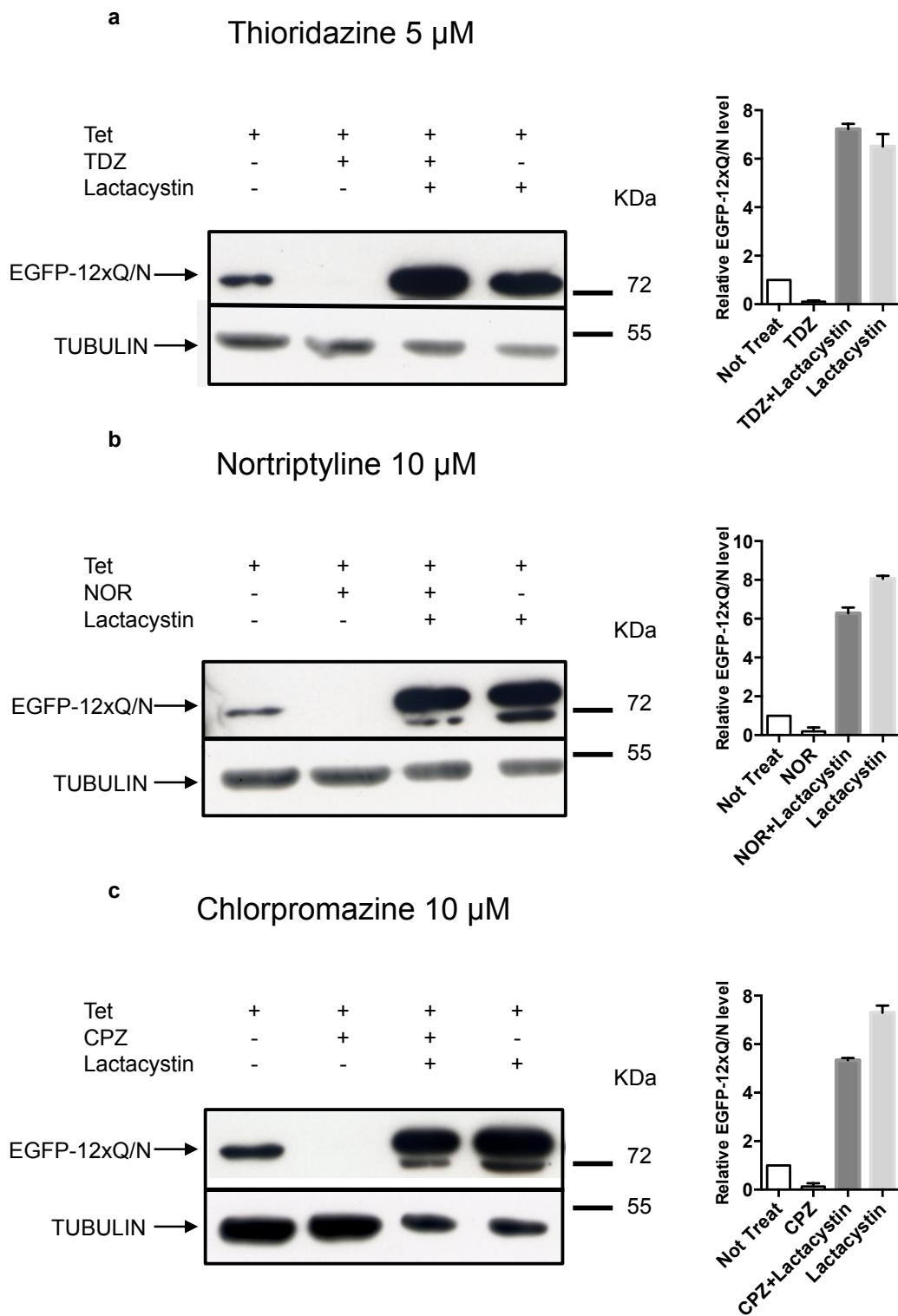
Figure 54. Clearance assay with EGFP-12xQ/N cellular model in presence of lactacystin.

HEK293 EGFP-12xQ/N stable cells were induced with tetracycline for 24 hours and then treated with **(a)** thioridazine, **(b)** nortriptyline and **(c)** chlorpromazine in presence or absence of the proteasome inhibitor lactacystin. Representative western of clearance assay and its respective quantifications under the different conditions. The blots were tested with anti-GFP antibody and anti-tubulin as loading control.

2.4. TDZ, NOR and CPZ also promote aggregate clearance of TDP-12xQ/N

As already explained in the Introduction (see section 3.4.3), EGFP-12xQ/N cellular model failed to accomplish a splicing deterioration, probably due to the ineffective trapping of endogenous TDP-43 into the aggregates. For this reason, TDP-12xQ/N cellular model was generated. This construct includes the 12xQ/N sequence cloned downstream a wild type Flag-TDP-43 protein. The advantage of this model over the previous one is that it induces efficiently aggregate formation that, in this case, produces TDP-43 nuclear depletion, with the consequent *POLDIP3* exon3 splicing loss of function (Budini et al., 2014). A stable cell line under tetracycline regulation was also generated for this new construct. Using this new cellular model the clearance capacity of the 3 drugs was further tested. HEK293 TDP-12xQ/N cells were induced with tetracycline for 72 hours to allow aggregate formation and the corresponding TDP-43 loss of function. Then, tetracycline was washed out and the drugs were added to the culture medium at each specific concentration. After 48 hours of incubation cells were harvested and lysated. The protein extracts were separated by SDS-PAGE and subsequently analyzed by western blot using anti-Flag antibody. **Figure 55** shows that TDZ 5 µM, NOR 10 µM and CPZ 10 µM promote TDP-12xQ/N degradation in the same way they do for the EGFP-12xQ/N.
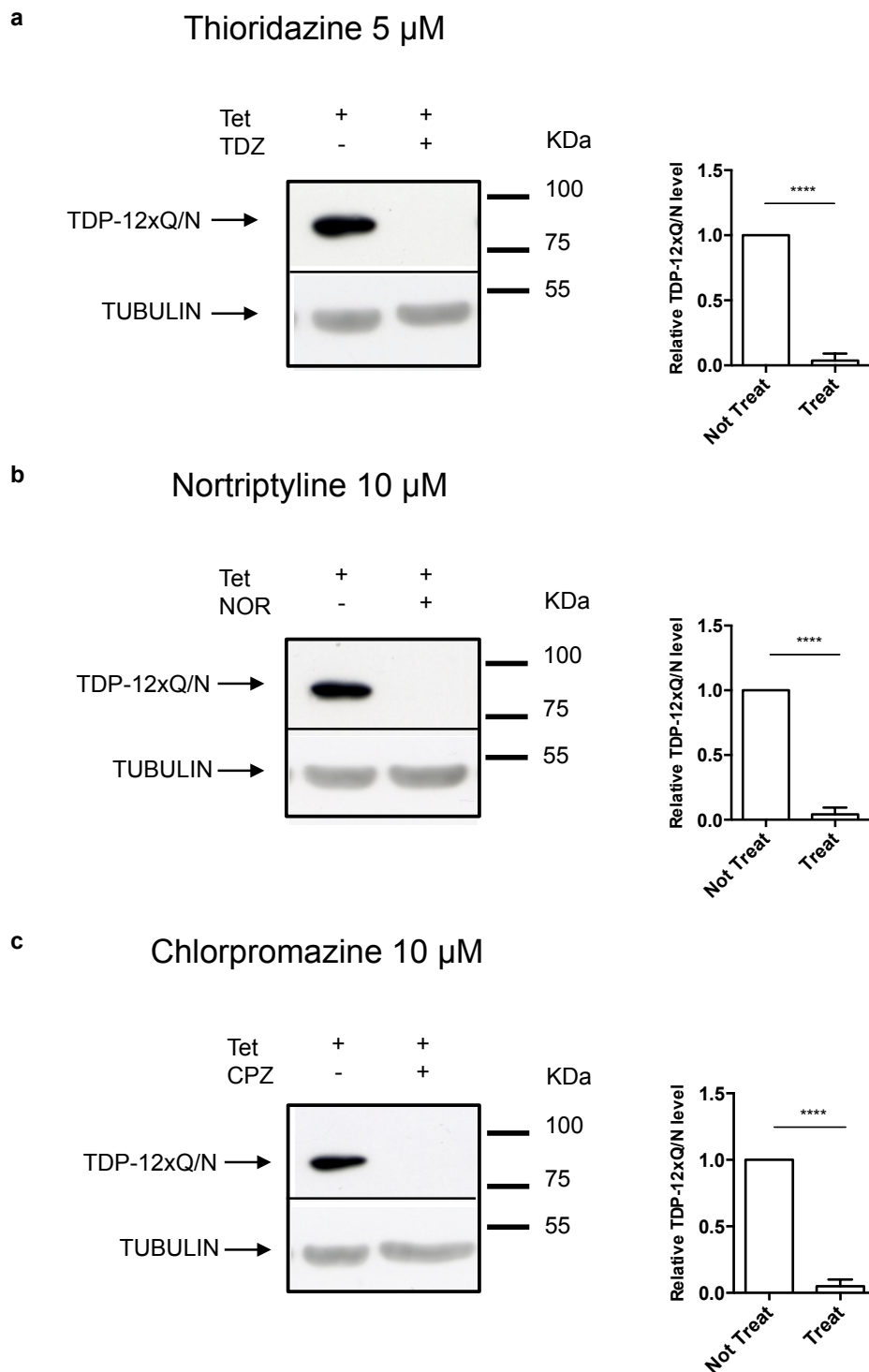
Figure 55. Clearance assay with TDP-12xQ/N cellular model.

HEK293 TDP-12xQ/N stable cells were treated with **(a)** thioridazine, **(b)** nortriptyline and **(c)** chlorpromazine, after tetracycline induction. Representative western blots of clearance assay after drug treatment and the respective quantification of 3 independent experiments. The blots were tested with anti-Flag antibody and anti-tubulin as loading control.

2.5. TDZ, NOR and CPZ are able to recue the loss of function caused by TDP-12xQ/N aggregation

To better understand the functional consequences of degrading the TDP-43 inclusions, we analyzed the splicing pattern of *POLDIP3* before and after drug treatment. As already explained in the Introduction (see section 2.2), *POLDIP3* exon 3 inclusion is highly regulated by the binding of TDP-43 to a conserved sequence downstream exon 3 (Buratti & Baralle, 2012). When TDP-43 is present and available to perform its nuclear functions, it favors the inclusion of exon 3 in the final mRNA of *POLDIP3*, and as a result there is more variant-1 (including exon 3) than variant-2 (without exon 3). On the contrary, when TDP-43 is silenced, *POLDIP3* variant-1 decreases and variant-2 increases (Fiesel et al., 2012; Shiga et al., 2012). Interestingly, upon TDP-43 aggregation *POLDIP3* splicing pattern is similar to the one obtained after TDP-43 silencing. This means that endogenous TDP-43 is no longer able to play its normal role in *POLDIP3* splicing, as it is being sequestered in the cytoplasmic aggregates. In order to evaluate if the clearance of TDP-43 aggregates upon drug treatment correlates with a recovery of the protein functionality, we induced the HEK293 TDP-12xQ/N cell line with tetracycline and analyzed the pattern of *POLDIP3* splicing by RT-PCR before and after drug treatment. As it can be noticed in **Figure 56** tetracycline induction generates a switch in the splicing pattern towards variant-2 (without exon 3), similar to what happens when TDP-43 is silenced. On the contrary, all 3 drugs managed to recover the splicing pattern, which is comparable to the wild type condition (without tetracycline and without drugs, lane 1). We also included a control without tetracycline and with drugs (lane 2) in order to discard the possibility that the drugs have some influence in the splicing pattern *per se*, but as it can be seen this is not the case, as the splicing pattern in this condition is exactly the same as the one observed without tetracycline and without drugs (lane 1).

a Thioridazine 5 µM

	1	2	3	4
Tet	-	-	+	+
TDZ	-	+	-	+

E2 E3 E4 Variant-1
E2 E4 Variant-2

% exon 3 inclusion	75 ± 3.2	76 ± 1.6	56 ± 6.6	68 ± 0.6

b Nortriptyline 10 µM

	1	2	3	4
Tet	-	-	+	+
NOR	-	+	-	+

E2 E3 E4 Variant-1
E2 E4 Variant-2

% exon 3 inclusion	73 ± 2.6	75 ± 1.3	57 ± 4.1	72 ± 2.4

c Chlorpromazine 10 µM

	1	2	3	4
Tet	-	-	+	+
CPZ	-	+	-	+

E2 E3 E4 Variant-1
E2 E4 Variant-2

% exon 3 inclusion	80 ± 3.5	79 ± 2.1	65 ± 1.7	75 ± 2.2
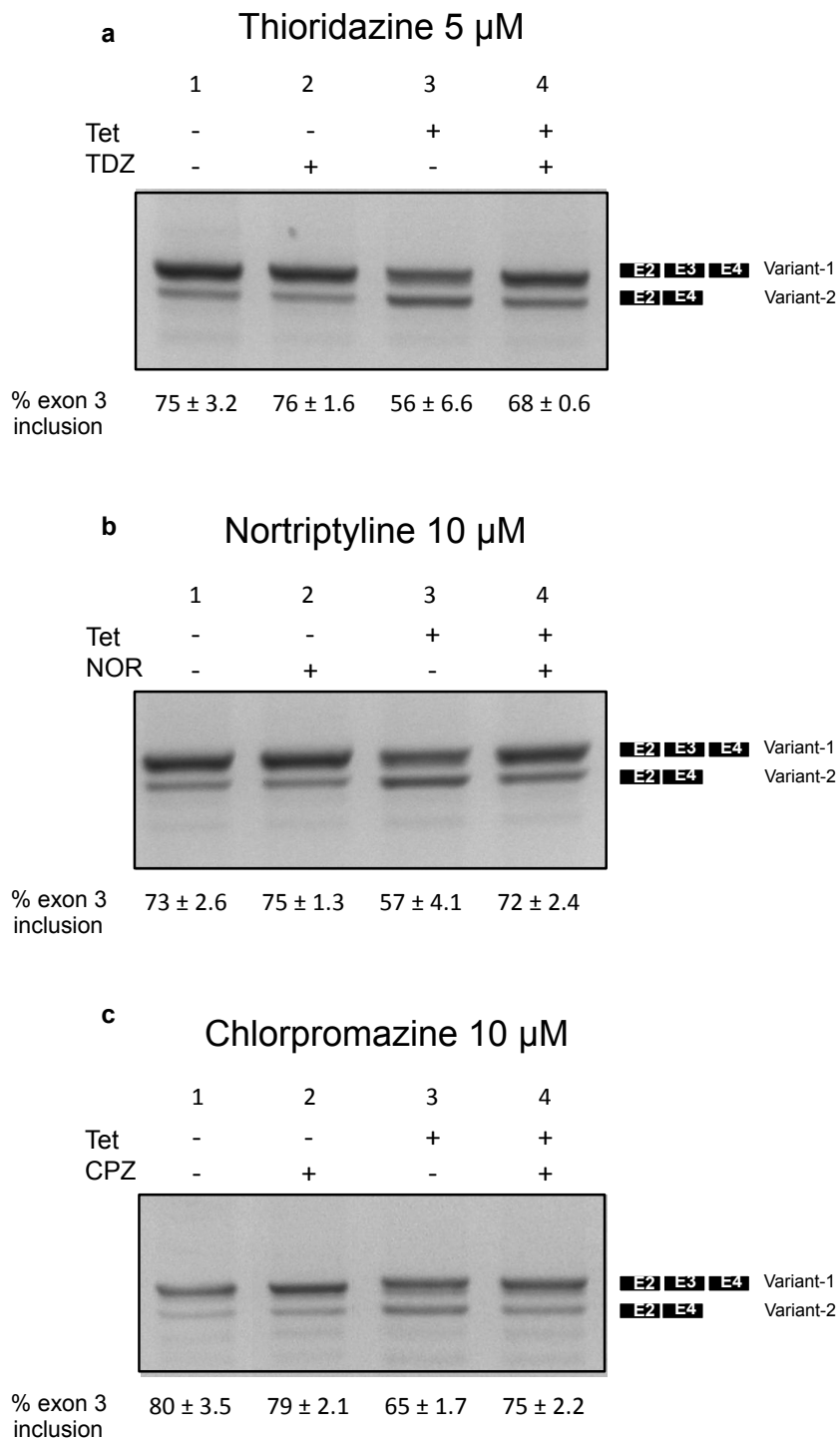
Figure 56. *POLDIP3* alternative splicing in TDP-12xQ/N cells.

HEK293 TDP-12xQ/N stable cells were treated with **(a)** thioridazine, **(b)** nortriptyline and **(c)** chlorpromazine, after tetracycline induction. *POLDIP3* alternative splicing was analyzed by RT-PCR after drug treatment. The respective quantifications of the percentage of exon 3 inclusions are shown at the bottom of each lane. Standard deviations were obtained from three independent experiments.

2.6.   Rescue of climbing deficit in *Drosophila* by feeding NOR

In order to further investigate the functional consequences of the aggregate clearance, we evaluated the effect of nortriptyline treatment in our *Drosophila* EGFP-12xQ/N model. For this reason, we analyzed if nortriptyline feeding could improve the climbing deficit observed in flies upon EGFP-12xQ/N expression. ELAV-Gal4 driver was used for the experiment, and 29°C was the temperature of choice, as the climbing deficit occurs earlier in life in comparison with flies raised at 25°C. Different concentrations of the drug were tested in order to find the one that would not affect the normal survival and climbing abilities of EGFP control flies. No detrimental consequence on the survival rate was observed when flies were fed with 7 mM of nortriptyline, and consequently this concentration was used for the experiment. Flies expressing either EGFP or EGFP-12xQ/N were raised in food containing the drug of interest or in food containing only the vehicle (water). The climbing ability of the flies was tested after 7 days of treatment. As it can be seen in **Figure 57** there is an improvement in the climbing ability of ELAV-Gal4;+/UAS-EGFP-12xQ/N/+ flies upon drug treatment, possible due to a recovery of TDP-43. This is a first indication that the aggregate clearance could be a good therapeutic strategy to treat an ALS-like phenotype. However, further analyses should be made.
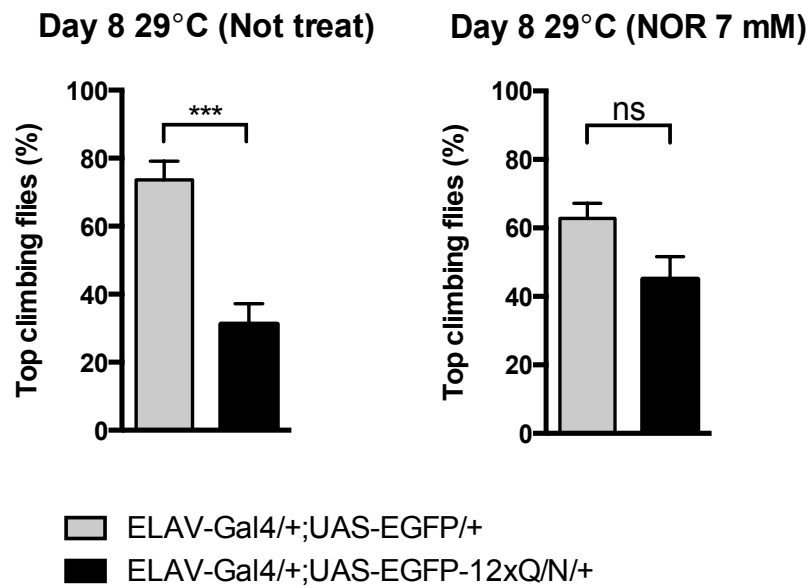
Figure 57. Rescue of climbing deficit in *Drosophila* by feeding nortriptyline.
Climbing assay of ELAV-Gal4/+;UAS-EGFP-12xQ/N/+ flies and ELAV-Gal4/+;UAS-EGFP/+
control flies with and without nortriptyline treatment at 29°C. Unpaired t-test analysis was
used to compare measures between 2 groups. ns indicates p>0,05 (not significant), ***
indicates p<0,001. Error bars indicate SEM.

Discussion

The role of TDP-43 aggregation in the pathogenesis of ALS is still under debate and opinions vary widely, from ascribing to the inclusions the neuronal dysfunction/death to those believing the aggregates are secondary events, possibly even a protective mechanism of the cell to respond to the primary insult that triggered neurodegeneration. Consequently, eliminating the inclusions as a therapeutic strategy is controversial. A better understanding of the connection of the aggregates with the pathogenesis of ALS is thus essential to establish clinical protocols aimed to fight this fatal motor neuron disease that today has no treatment or cure. The main objective of this study was to investigate the impact of TDP-43 aggregation and to better understand if enhancing aggregate clearance could represent an effective therapeutic target for ALS treatment.

In ALS patients' brain the TDP-43 cytoplasmic inclusions are accompanied by the nuclear depletion of the protein that could lead to the loss of TDP-43 normal functions, which in turn may be responsible for the degeneration of motor neurons (Arai et al., 2006; Neumann et al., 2006). However, it has also been suggested that aggregation intermediates or aggregates themselves could display toxic properties, leading to pathogenesis (Blokhuis et al., 2013). In order to distinguish between these two hypothesis (loss versus gain of TDP-43 function) it is useful to create *in vitro* and *in vivo* models that mimic ALS pathology. In general, TDP-43 proteinopathies, such as ALS, present complex etiology that would be even much more obscure without the existence of animal models that reproduce at least some of the hallmarks of each disease (Fernández-Borges et al., 2015). The *in vivo* models, in particular, are of utmost importance as they provide a complete physiological system. In the majority of ALS cases there is no evident genetic cause and in those cases displaying mutations, the role of the variant protein is hard to establish as functionality is mostly preserved as far as splicing process is concerned. This fact makes the animal models an extremely useful tool. We have previously shown that the *Drosophila* and the human TDP-43 are interchangeable as regards their binding activity and their role in splicing (Ayala et al., 2005). Furthermore, the deletion of the TBPH gene results in a

locomotion defective fly, whose climbing activity could be restored by the introduction in motor neurons of both the *Drosophila* and the human TDP-43 (Feiguin et al., 2009), making *Drosophila* an excellent model system for TDP-43 proteinopathies. Hence, in order to provide a fast approach to address the aims mentioned above we created a *Drosophila* model, based on the TDP-43 prion-like region that is situated in its C-terminal domain.

1.   TDP-43 aggregates are not toxic but protective

It has been demonstrated, with the use of both exogenous and endogenous wild type TDP-43 that maintaining normal TDP-43 protein levels in various tissue-types is critical for the proper physiological functioning of the organism (Xu, 2012). The tight regulation of TDP-43 levels is suggestive of its crucial role in the functioning of multiprotein-RNA complexes, where maintaining a certain stoichiometry between TDP-43 and the other components may be crucial.

Several attempts have been carried out to model the disease by overexpression of wild type TDP-43 or one of its familial disease-linked mutants. In all these models overexpression of wild type TDP-43 causes neurodegeneration both *in vivo* and *in vitro*, suggesting that the increased amounts of wild type or mutant TDP-43 function is toxic (Ash et al., 2010; Li et al., 2010; Miguel et al., 2011; Swarup et al., 2011; Voigt et al., 2010). As described in other neurodegenerative diseases, the aggregates formed as a consequence of an excess of TDP-43, might be responsible for this toxicity (Polymenidou & Cleveland, 2011). However, some models have demonstrated that TDP-43 overexpression exerts toxicity even in absence of aggregation (Barmada et al., 2010; Wegorzewska et al., 2009). Furthermore, studies both in flies and worms have reveled that the TDP-43-mediated neurotoxicity strongly depends on its RNA-binding domains (Ash et al., 2010; Ihara et al., 2013; Voigt et al., 2010).

Adult eyes are often used for transgene expression in *Drosophila* models of neurodegenerative diseases to produce easily observable phenotypes. In *Drosophila*, human TDP-43 overexpression within the eye tissue causes degeneration of retinal neurons (photoreceptors), which produces

remarkable phenotypes that can be seen both inside and on the surface of the eye. Furthermore, it was demonstrated previously that while TBPH plays a fundamental structural and functional role in locomotion (i.e.: neuromuscular junction development and maintenance), it is not essential for the development of a normal eye structure, as null-allele TBPH flies do not present any evident external morphology alteration, and the eye structure is completely preserved (Feiguin et al., 2009). This organ is then an ideal testing ground to study the interplay between TBPH overexpression and aggregation. In the case of TDP-43 overexpression in *Drosophila* eye, the phenotypes can range from structural changes to the formation of necrotic patches that sometimes is followed by the concomitant loss of pigmentation. Expression of human TDP-43 in the adult fly eyes causes age and dose-dependent structural degeneration (Estes et al., 2011; Hanson et al., 2010; Li et al., 2010; Miguel et al., 2011; Ritson et al., 2010). This degeneration is associated to the mislocalization of TDP-43 to the cytoplasm, which is sufficient to cause toxicity (Miguel et al., 2011; Ritson et al., 2010).

As reported for the human protein, in this study it was demonstrated, that the overexpression of the TDP-43 *Drosophila* ortholog (TBPH) with GMR-Gal4 driver, also exerts a strong phenotype in the fly eye (**Figure 31b**), confirming previous observations (Diaper et al., 2013; Ritson et al., 2010). By using the eye degeneration as a phenotypic output we addressed the effect of TBPH aggregation when the protein is present in excess. For this purpose, TBPH was co-expressed with the aggregate-inducer EGFP-12xQ/N in the eye tissue. Aggregation of the soluble TBPH in the EGFP12xQ/N aggregates (**Figure 35**), modified the TBPH-associated phenotype to the extent that the eye structure was completely recovered (**Figure 31c**). Furthermore, the suppression of the TBPH-related phenotype by EGFP-12xQ/N was accompanied by a return of the eye functionality, as indicated by the recovery of the normal phototactic behavior of the flies (**Figure 37**). The TBPH entrapment by EGFP-12xQ/N was dependent on TBPH C-terminal tail, as the truncated form (TBPH-ΔC) failed to be trapped within the aggregates, demonstrating that the interaction occurs through this region (**Figure 32**). Moreover, we could determinate that the effect seen with EGFP-12xQ/N is

specific for TBPH-induced neurodegeneration, as its co-expression with Tau, did not prevent Tau-induced neurodegeneration (**Figure 33**).
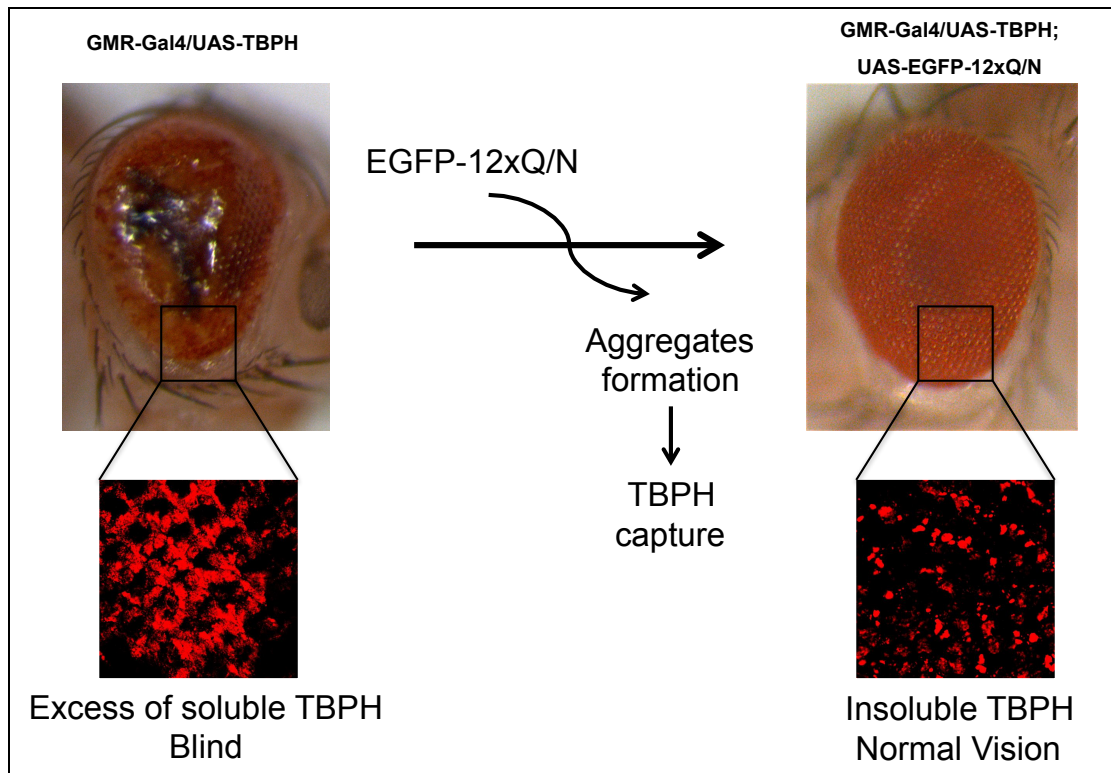
Figure 58. Proposed neuroprotective mechanism of aggregation.
The excess of soluble TBPH in *Drosophila* eye induces remarkable degeneration of the eye surface, which in turn gives rise to loss of phototaxic behavior. Co-expressing TBPH and EGFP-12xQ/N rescues the eye phenotype by aggregating the TBPH in excess. The recovery of the normal eye phenotype correlates with the recue of the normal vision.

Overall these results indicate not only that TBPH aggregation is not toxic by itself. Furthermore, in a context where an excess of TBPH is present, the aggregation may be a neuroprotective mechanism (**Figure 58**).

The toxicity induced by TBPH overexpression could be explained by two possible mechanisms. One explanation could be that when the protein is produced in high amounts, the cellular quality control machinery becomes overwhelmed and the protein starts to become misfolded. The misfolded protein then accumulates, probably because of the malfunctioning of the two main systems of proteolysis, a fact that has been largely documented in ALS (Kabashi et al., 2012; Sasaki, 2011). The misfolded species might be responsible for the toxicity, which is abolished by the complete aggregation

of these species within the EGFP-12xQ/N aggregates. It would be interesting to study which particular molecular species is responsible for the pathogenesis (monomers, oligomers, protofibrils, etc), but this was beyond the scope of this study, for timing reasons.

Another possible explanation could be that the excess of soluble TBPH could exert a toxic effect by sequestering multiple (protein or RNA) binding partners that are essential for neuronal function. As already mentioned, to perform proper biological functions, TDP-43 forms a multi-molecular complex with various target RNAs and interacting proteins (Sephton et al., 2011). For instance, TDP-43 has been shown to be capable of binding directly to several proteins of the heterogeneous nuclear ribonucleoprotein family, in particular hnRNPA1, A2/B1, A3 and C1/C2, which seems to be necessary for the splicing inhibitory activity of TDP-43 (Buratti et al., 2005). However, these identified partners of TDP-43 are not detected in the TDP-43 inclusions present in patients' brains (Neumann et al., 2007a). The same may happen with the RNA binding partners as it has been shown that TDP-43 overexpression toxicity, even in the absence of aggregates, is dependent on its binding capacity, probably because of RNA targets sequestration (Voigt et al., 2010; Xu, 2012).

Although further investigation in needed, we support the idea that in our *Drosophila* model, the excess of soluble TBPH is toxic possibly by sequestration of other hnRNPs or RNA targets, and furthermore, that the TBPH, when trapped in the aggregates, is not able to interact with the protein or RNA partners any more and in this way the toxicity is abolished.

The important conclusion we get from this study is that aggregates are not the primary toxic species leading to neuronal dysfunction, but that they protect cells from the harm caused by TDP-43 overexpression.

2. EGFP-12xQ/N aggregates sequester endogenous TBPH and are able to generate an ALS-like phenotype in *Drosophila*

Several lines of evidence indicate that the loss of TDP-43 function is the main cause of the neuronal degeneration seen in TDP-43-ALS patients' brain. The first important indication that supports this idea is that TDP-43 is found mislocalized and aggregated in the cytoplasm of patients' neurons, and that this phenomenon is accompanied by partial or total nuclear depletion of the protein (Arai et al., 2006; Neumann et al., 2006). Both, the nuclear depletion and the cytoplasmic aggregates are expected to reduce the amount of functional TDP-43 in the nucleus. In fact, the dysfunction of TDP-43 has been demonstrated in patients' samples by two different groups (Shiga et al., 2012; Yang et al., 2014). In both studies, an increment of *POLDIP3* variant-2 mRNA was detected in motor cortex, spinal cord and spinal motor neurons from ALS-patients, confirming that TDP-43 functions are altered in human ALS, and that TDP-43 loss of function may be responsible for the pathogenesis. Furthermore, *in vitro* and *in vivo* studies indicate that knockdown or knockout of TDP-43 may originate morphological and functional defects of the nervous and vascular system, muscle degeneration and, in some cases, even be lethal (Diaper et al., 2013; Feiguin et al., 2009; Fiesel et al., 2010; Lin et al., 2011; Schmid et al., 2013; Wu et al., 2010; Wu et al., 2012). Thus, TDP-43 loss of function can generate cellular malfunction, degeneration and death.

In the second part of this study we wanted to address if the TDP-43 aggregates are able to generate a defect such as a locomotive impairment in *Drosophila*. As ALS is a motor neuron disease it was interesting to see the effect of aggregation in this particular type of cells. Furthermore, TBPH has been shown not to be essential for the development of the normal eye structure, as the TBPH null-allele mutants have completely normal eyes (Feiguin et al., 2009). Consequently, we decided to analyze the effect that EGFP-12xQ/N has in other tissues that do get affected by the absence of TBPH. For this purpose, we expressed the EGFP-12xQ/N construct under ELAV-Gal4 or D42-Gal4 drivers. ELAV-Gal4 is a post-mitotic driver, which

drives the expression of the transgene in *Drosophila* CNS, whereas D42-Gal4 is a more restrictive driver that expresses the transgene mostly in motor neurons. The flies presented EGFP-12xQ/N aggregation in the central brain that co-localized partially with endogenous TBPH (**Figure 44**). Even though the TBPH entrapment by these EGFP-12xQ/N aggregates was not very marked, the flies developed an age-related phenotype that was characterized by deficient locomotive behavior (**Figures 41 and 42**), reduced life span (**Figures 41 and 42**) and reduction of the NMJ (**Figure 45**), analogous to what happens in ALS patients as a consequence of upper and lower motor neuron dysfunction. Intriguingly, the climbing deficit correlated with a physiological reduction in the endogenous TBPH levels (**Figure 46**). Two different groups have previously addressed the physiological reduction of TDP-43 levels in different tissues of wild type mice during aging (Huang et al, 2010; Liu et al., 2015). In this study, this data was corroborated but more interestingly it was also demonstrated that the drop in TDP-43 levels happens also in *Drosophila*, both at protein and RNA level*,* which suggests that it could be an evolutionary conserved mechanism in the aging process. These organisms are able to function normally with low levels of TDP-43. However, we observed that the aggregation, when coupled with the low TDP-43 levels, due to the physiological age drop, generates phenotypical consequences in our *Drosophila* model, probably due to a TDP-43 loss of function.

Therefore, the combination of the reduction of TBPH and the presence of aggregates that act as a sink for the soluble functional TBPH/TDP-43 could be responsible, at least in part, for the pathogenesis of ALS. If this was the case we hypothesized that using a fly model with constitutive reduction of TBPH levels similar to the ones that develop with age (Romano et al., 2014b) crossed with the one expressing the aggregation inducer, the effects of depletion of TBPH should occur at an earlier stage. This was indeed the case (**Figure 47**) reinforcing our conclusion that one of the main contributors to the onset of ALS-like symptoms in *Drosophila,* and maybe in humans, is the age-related physiological decrease in TBPH tissue levels combined with the presence of inefficiently cleared aggregates. It follows that therapeutic approaches aimed either to decrease aggregation or increase functional

147

TDP-43/TBPH levels could be used successfully to recover or delay ALS-like symptoms, indeed preliminary experiments in our model using small molecules capable of reducing the presence of aggregates probably by enhancing their clearance has being carried out (see Discussion section 3).

The fact that TDP-43/TBPH levels are reduced in *Drosophila* and mice make us believe that the same could happen in humans. One observation that supports this hypothesis is that TDP-43 is found aggregated in 30-40% of normal individuals under 65 years old (Uchino et al., 2015). Even in the presence of aggregates, these individuals do not develop the disease. Our results provide a possible explanation for these observations. Only when TDP-43 levels decrease under a certain threshold, maybe as a consequence of further aggregation or because of the physiological drop during aging, does the pathological situation may arise.

Future work directed at how the drop in TDP-43 levels is regulated will shed further light on this argument. From our study we know that it is pre-translational, as RNA levels were also diminished in an age-programmed manner. It will be of interest to study the methylation profile of the TDP-43 promoter region with the aim of analyzing if there are epigenetic changes during aging that could lead to transcriptional repression.

Another interesting observation derived from this part of the study is that when EGFP-12xQ/N was expressed in a more restricted population of neurons with D42-Gal4 driver, notwithstanding the protein levels were lower than with ELAV-Gal4 driver (**Figure 43**), the climbing deficit became evident earlier in life (**compare Figures 41 and 42**). In relation to this, it was demonstrated that hTDP-43 expression by D42-Gal4 driver resulted in a better rescue of TBPH null phenotype in comparison to the expression with the ELAV-Gal4 driver (Feiguin et al., 2009). These data suggest that motor neurons are more sensitive to TDP-43/TBPH dysfunction than other cell types.

Even though the co-localization between endogenous TBPH and EGFP-12xQ/N in *Drosophila* adult brain was observed to a certain extent, we were unable to show TBPH biochemical dysfunction in our *Drosophila* model. The examination of TBPH known targets that undergo changes in absence of TBPH showed no differences in EGFP-12xQ/N flies compared with the

control flies. In fact, HDAC6, whose RNA levels were shown to decrease in cells treated with siRNA for TDP-43 and in a *Drosophila* null-allele model (Fiesel et al., 2010) were unaltered in the EGFP-12xQ/N flies as were Syntaxin levels, whose protein level was shown to be reduced in another *Drosophila* null-allele model (Romano et al., 2014a). One explanation may lie in the fact that entrapment of the protein in our fly model was not efficient enough for a marked change seen by biochemical methods. However, the flies presented an extremely clear locomotion phenotype. Although the reason for this needs further investigation it does imply that a subtle TBPH mis-function is present, probably in the transport of important elements for the maintenance and functioning of the neuromuscular junction. Furthermore, the observed late onset of the paralytic phenotype, again a feature present in ALS patients, allowed us to search for the trigger of this phenomenon. It is well established by epidemiological studies that the age of onset of ALS does not change significantly in the presence of TDP-43 mutations and is fixed at around 50-60 years of age. It may be possible that metabolic changes occurring during aging in that period, combined with other factors may be responsible of this rather uniform age of onset. In this work, we have identified one such a change that is the drop of TDP-43 levels found both in *Drosophila* and mice.

Recent work by our group has determined TDP-43 additional structural elements present in the N-terminus of the protein, which are responsible for efficient aggregation and the consequent loss of function (Budini et al., 2014). For this purpose a new cellular model TDP-12xQ/N was developed (for more detailed explanation see Discussion section 3). Furthermore, deletions of both the C-terminal and N-terminal within the TDP-12xQ/N construct were done. Compared with full-length Flag-TDP-12xQ/N, the deletion of the C-terminal region (Flag-TDP-12xQ/N ΔRRM1/2, ΔC) had little impact on aggregation induction and consequent loss-of-function effect. Moreover, the protein maintained the ability to form insoluble aggregates. On the contrary, by deleting the N-terminal domain of TDP-43 within the TDP-12xQ/N construct (Flag-TDP-12xQ/N ΔRRM1/2,ΔN), aggregation was still occurring, but the interaction between endogenous TDP-43 and the inclusions was abolished, recovering the normal functions and splicing

activity of the protein. This observation demonstrates that the TDP-43 N-terminal domain is needed, in addition to the Q/N region, for efficient TDP-43 entrapment and loss of function effect (Budini et al., 2014).

The above observations are the basis to construct another model of transgenic *Drosophila* line that may have a more acute loss of function effect than the one described in this thesis. This could be achieved by the expression in *Drosophila* of TDP-12xQ/N construct that already showed misregulation of TDP-43 targets in the cellular model. However, which of these two models will be closer to the human ALS pathogenesis is debatable as ALS has a long silent period of development.

Furthermore, it would be interesting to map the contribution of different amino acid residues within the Q/N rich region to the aggregation process. It is possible that the aggregation effect and splicing function could be dissected and separated, yielding molecules useful to restore function in the presence of aggregates.

3. The clearance of the TDP-43 aggregates recovers TDP-43 normal function. Could this be a novel therapeutic approach for ALS?

As stated, the toxicity caused by an excess of soluble TDP-43 is possibly due to misfolding or unproductive binding to the partners. This constitutes a gain of function that can be abrogated by TDP-43 aggregation. However, there is still no convincing evidence that TDP-43 levels are elevated in human patients with TDP-43 proteinopathies. So far, no copy number variation of the *TARDBP* gene has been found, and brain mRNA levels of TDP-43 were also found unchanged in patients (Bäumer et al., 2009), with the exception of a single patient with 3'UTR variant of TDP-43, which showed a 2-fold increase in TDP-43 expression levels compared to controls (Gitcho et al., 2009). Nevertheless, an important finding reported here is that TDP-43 needs to be maintained within certain levels to prevent toxicity, and that the aggregates are not toxic by themselves. However, continued addition of TDP-43 to the inclusions results in eventually capture of the majority of the

TDP-43 produced by the cell. This situation will lead to a lack of soluble TDP-43, leading to a loss of function. In conclusion, large aggregates are not toxic species, however they are detrimental as they sequester so much endogenous protein, which leads to loss of function. By restoring the proper TDP-43 folding and/or clearing TDP-43 inclusions, we predicted that the loss of function could be reverted. Consequently, in this last part of the study we were interested to understand if the clearance of TDP-43 aggregates could be an effective strategy to treat ALS, by recovering TDP-43 function.

There are several intrinsic cellular mechanisms that can act to either prevent or resolve protein misfolding and aggregation, such as the autophagy and the proteasomal pathways. Autophagy and proteasomal activation have been indeed previously proposed as possible therapeutic approaches to treat ALS. Regarding autophagy, proof of concept studies have shown that autophagy activators such as rapamycin, spermidine, carbamazepine and tamoxifen rescue or partially reduce the phenotype in a mouse model of TDP-43 proteinopathy (Wang et al., 2012). Furthermore, it was shown by Caccamo et al. that aggregate clearance through autophagy induction with rapamycin, rescues TDP-43 mislocalization in a cellular model of TDP-43 proteinopathy (Caccamo et al., 2009). Recently this topic was also approached by Barmada et al. who showed that autophagy induction enhances TDP-43 turnover and survival in a human stem cell-derived neurons (Barmada et al., 2014). On the other hand, proteasome up regulation has shown to be beneficial in a Huntington's disease neuronal model (Seo et al., 2007), indicating that the induction of the cellular proteolysis mechanisms may be a valid therapeutic target also for TDP-43 proteinopathies.

For this part of the study, we took advantage of the two previously developed cellular models, EGFP-12xQ/N and TDP-12xQ/N. As already explained, the expression of EGFP-12xQ/N in cultured cells promotes the formation of aggregated complexes that are able to sequester wild type TDP-43. Notwithstanding that EGFP-12xQ/N aggregates were shown to co-localize with the endogenous TDP-43, EGFP-12xQ/N cellular system did not display any detectable deterioration of the splicing function, suggesting that the aggregates were not capable of trapping enough endogenous TDP-43 to

cause a loss of function in the short interval measured in a cell system. Consequently, an improved version of the previous aggregation model was developed. This model was generated by attaching the 12xQ/N region downstream a wild type Flag-TDP-43. The introduction of this construct in cultured cells triggers aggregation, which traps endogenous TDP-43 in an efficient manner. Importantly, a complete nuclear clearance of TDP-43 can be observed in some cells upon induction of the transgene, same as what happens in the neurons of ALS patients. As a consequence of the absence of nuclear TDP-43 the splicing patterns of the two best-characterized TDP-43 RNA targets (*CFTR9* and *POLDIP3*) were shown to be mis-regulated, similar to what happens upon depletion of TDP-43 using RNAi.

By using these two cellular models we performed a screening to find drugs that can trigger aggregate clearance, in order to understand if, by clearing the aggregates, TDP-43 loss of function can be recovered. The compounds we chose belong to the tricyclic family, and they were shown to be neuroprotective in several proteinopathies. As part of the neuroprotective effect, there is evidence that these drugs could trigger aggregate clearance through the autophagy pathway (Barmada et al., 2014; Tsvetkov et al., 2010). Furthermore, it was demonstrated by Prusiner's group that tricyclic compounds (including chlorpromazine and thioridazine) with an aliphatic side chain constitute a new class of antiprion reagents (Korth et al., 2001), and we thought that the same could be applied to ALS taking into account the recently identification of the prion-like domain present in TDP-43 (Polymenidou & Cleveland, 2011).

We were able to show that among the eight drugs that we chose, three (thioridazine, nortriptyline and chlorpromazine) were able to degrade EGFP-12xQ/N (**Figure 48**) and TDP-12xQ/N aggregates (**Figure 55**), and, more important, that upon aggregate clearance, TDP-43 function was recovered (**Figure 56**). However, contrary to the publication by Finkbeiner's group (Tsvetkov et al., 2010) we have seen that the drugs instead of activating autophagy are blocking this pathway (**Figures 49 and 50**). Furthermore, the clearance of the aggregates seems to be happening through the proteasome system, as the clearance upon drug treatment is abolished in presence of the proteasomal inhibitor lactacystin (**Figure 54**). One possible explanation for

this contradiction could be that in the study conducted by Tsvetkov, the authors analyzed only LC3II/I ratio upon drug treatment, and as already explained throughout this study, the increased LC3II/I ratio indicates the accumulation of autophagosomes, but does not guarantee autophagic degradation.

The tricyclic drugs used in this study were previously shown to accumulate in lysosomes (Nadanaciva et al., 2011). Compounds that accumulate in lysosomes are called lysosomotropic agents (de Duve et al., 1974). These compounds are able to penetrate membranes including those of lysosomes, but once inside the acidic environment of the lysosomes, they become protonated and are unable to exit the lysosome to re-enter the cytoplasm (Kaufmann & Krise, 2007). There is evidence that lysosomotropic compounds behave as autophagy inhibitors, by increasing the pH of lysosomes and thereby impairing lysosomal acid hydrolases. This process most probably results in the inhibition of the degradation of autophagolysosomes (Ashoor et al., 2013). This is in line with our results in which we see increased LC3II/I ration upon drug treatment but accumulation of p62 (**Figures 49 and 50**). Furthermore, treatment with nortriptyline together with the autophagy inhibitor NH_4Cl did not enhance further the LC3II/I ratio, verifying autophagy blockage (**Figure 53**). However, there is still an open question that arises from these experiments that is whether the inhibition of the autophagy flux is related to the activation of the proteasomal pathway. It has been previously demonstrated that impairment of the proteasome system leads to increased autophagic function (Pandey et al., 2007), but the opposite has not yet been demonstrated. However, under conditions in which one degradation system is compromised, enhance degradation by an alternate pathway may become critical to maintaining pools of amino acids for protein synthesis and may protect against the accumulation of toxic species (Nedelsky et al., 2008).

Regarding the proteasomal degradation of the aggregates, Petrucelli's lab has previously demonstrated that TDP-43 inclusions can be degraded by the proteasome system (Zhang et al., 2010). They created a cellular model by expression of GFP-tagged caspase-cleaved C-terminal TDP-43 fragment. The expression of the GFP-CTF was performed for 5 days and once the

inclusions were formed the cells were treated with the proteasome inhibitor MG-132. Interestingly, the aggregates in MG-132 treated cells were larger compared to those in control cells. In conclusion, the authors showed that inclusions are reversible and can be cleared preferentially through the ubiquitin proteasome system, an observation consistent with our results.

Finally, it will be interesting to investigate if the drug treatment could be used as a protective mechanism. For this purpose, a good approach could be to induce TDP-12xQ/N aggregate formation with tetracycline, in the presence or absence of the active compound (thioridazine, nortriptyline or chlorpromazine). By evaluation of *POLDIP3* alternative splicing pattern, we could determine if in presence if the drug, the occurrence of TDP-43 loss of function is retarded or avoided.

As a preliminary approach we treated ELAV-Gal4/+;UAS-EGFP-12xQ/N/+ flies with nortriptyline in order to test its effect *in vivo*. Although partially harmful to the control flies, administration of 7 mM nortriptyline partially rescued the climbing ability of the flies (Figure 57). Further work has to be done in order to evaluate the effective aggregate clearance upon drug treatment, and to identify the efficacious dosages and appropriate timing for administration of the drugs. Furthermore, a *Drosophila* model that achieves earlier TDP-43 loss of function, with consequent TDP-43 function deterioration evaluated by biochemical parameters, is crucial for drug validation and screening.

All the three tricyclic drugs that were effective in recovering TDP-43 function by degradation of the aggregates have been used as anti-psychotics or anti-depressives for more than 50 years. The preclinical investigation of the impact of psychotropic drugs on molecular processes pertinent to neuroprotection varies considerable (Lauterbach & Mendez, 2011). This variation is due to the degree of investigation, cell lines studied, methodological approaches, varying use of neural tissues and neuronal cell types, among other issues. As a consequence, it is not easy to draw definitive conclusions. However, some studies have shown a tendency of these drugs to neuroprotection (Tang et al., 2005; Wang et al., 2007).

Furthermore, these drugs are able to cross the blood brain barrier, and they were shown to be safe for long-term use, having only minor side effects,

making them promising therapeutic agents to treat TDP-43 proteinopathies in humans (Stavrovskaya et al., 2004).

The fact that it is possible to reverse the damage caused by TBPH/TDP 43 depletion has been elegantly shown in a *Drosophila* model by Romano et al (Romano et al., 2014a). They created a TBPH null-allele fly model and after the disease onset in the adult fly, characterized by deficit in climbing ability, reduced life span, and misregulation of presynaptic markers, they were able to recover all these parameters by inducing the late expression of TBPH. This is an important finding as it reveals late-stage functional and structural neuronal plasticity.

Recently the reversibility of the phenotype was also confirmed in a new mouse model that was generated with doxycycline (Dox)-suppressible expression of human TDP-43 harboring a defective nuclear localization signal (ΔNLS) under the control of the *neurofilament heavy chain* promoter (Walker et al., 2015). Expression of hTDP-43 ΔNLS in these mice resulted in the formation of TDP-43 aggregates in brain and spinal cord, with the concomitant loss of nuclear mouse TDP-43. Furthermore, these mice presented a severe phenotype characterized by brain atrophy, muscle denervation, dramatic motor neuron loss and progressive motor impairments leading to death. Interestingly, the suppression of hTDP-43 ΔNLS in presence of Dox after disease onset caused a dramatic reduction in TDP-43 aggregation, and more importantly an increase in nuclear mTDP-43 in comparison to control levels. This is an important indication that even after the disease onset, functional recovery can be achieved by the removal of TDP-43 aggregates.

The findings reported here may have profound clinical implications, as by enhancing the degradation of TDP-43 aggregates, TDP-43 functionality can be recovered, making the aggregate clearance a possible therapeutic strategy for ALS, even when disease is advanced.

4. Proposed mechanism of TDP-43 proteinopathies

It is well known that ALS is an age-dependent disorder, and even the familial forms manifest in an age-dependent manner. This indicates that one

or more age-related changes in brain function might act as a co-trigger and induce TDP-43 accumulation. A new factor that we have discussed in this thesis is the important change in TDP-43 metabolism that occurs physiologically during aging, in particular the decrease in cellular TDP-43 levels. Furthermore, it has also been suggested that during aging, the cells lose their ability to efficiently deal with misfolded proteins as the capacity of the proteasome and autophagy pathways declines. Moreover, reduced activity of these two pathways is known to be associated with neurodegenerative diseases and this may lead to accumulation of TDP-43.

In addition, the initiation of the aggregation process may be due to an environmental insult such as oxidative stress. Whatever promotes or accelerates the misfolding processes is facilitated by the fact that TDP-43 is itself an aggregation-prone protein and contains a prion-like domain. TDP-43 may self-promote its aggregation that will be possibly followed by propagation and spread. Ultimately, all the cellular TDP-43 will be trapped within the aggregates and subsequently, the nucleus will remain empty and the genes that are controlled by TDP-43 will become deregulated. This pathological situation could be reverted by triggering the clearance of TDP-43 inclusions that act as sink for the newly produced TDP-43. **Figure 59** shows a simplified scheme of the proposed mechanism of TDP-43 proteinopathies.
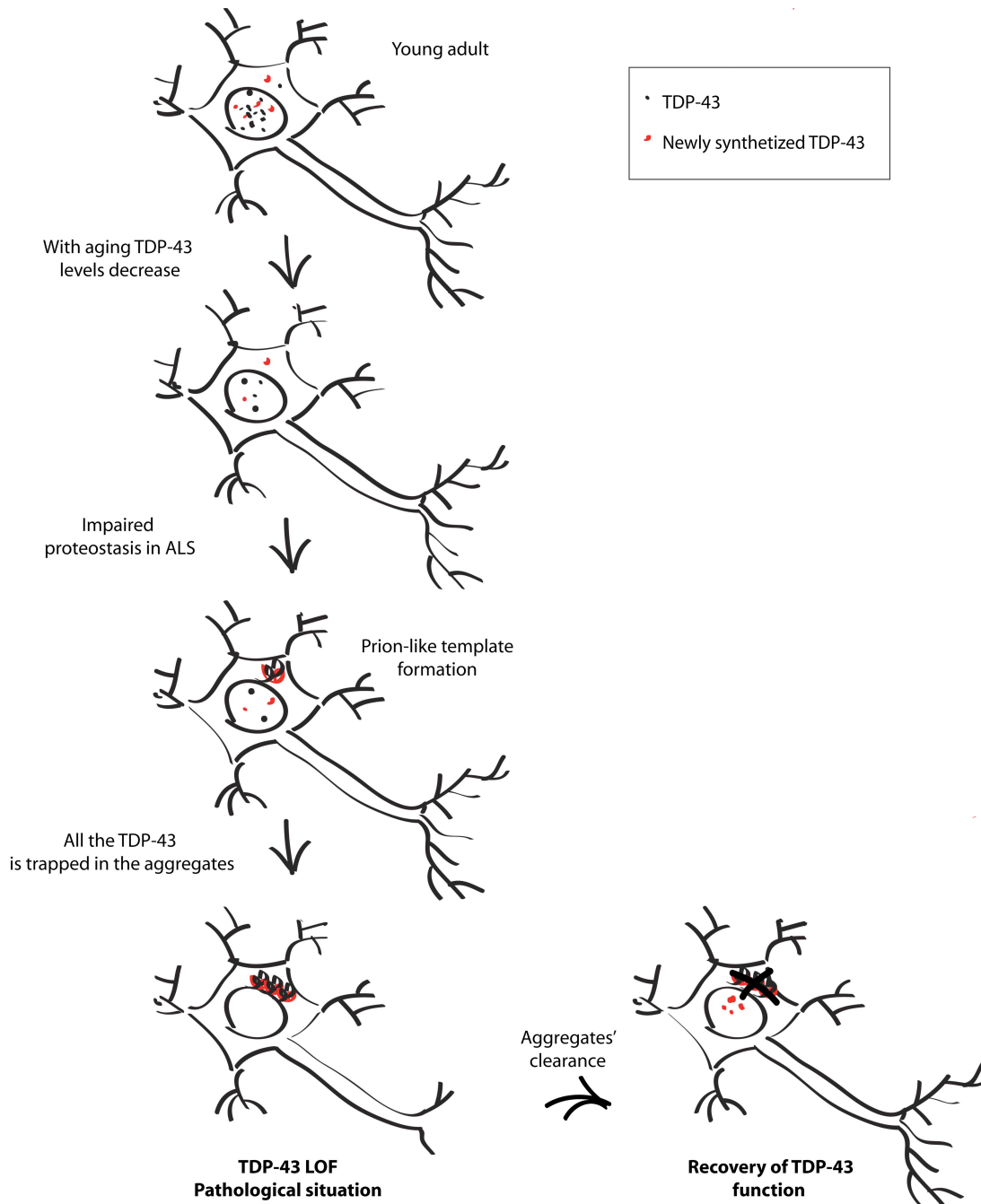
Figure 59. Proposed mechanism for TDP-43 proteinopathies.

During normal aging many physiological mechanisms become deregulated, for instance the capacity of producing TDP-43 decreases. Furthermore, decline proteostasis is common in ALS, which may lead to accumulation of TDP-43, which provokes prion-like template that act as a sink for the remaining TDP-43. Eventually all the TDP-43 will be trapped in the aggregates, causing loss of nuclear TDP-43 and degeneration of the NMJ. By clearing the aggregates, this pathological situation may de recovered, as the newly synthetized TDP-43 will be less trapped, and free to carry out its normal function.

Concluding remarks

The main conclusions of this thesis can be summarized as follows:

1. EGFP-12xQ/N model of TDP-43 aggregation is a valuable tool to investigate the prion-like properties of TDP-43.

2. TDP-43 aggregates are not intrinsically toxic. On the contrary, in a context where an excess of TBPH is present, aggregation seems to be a protective mechanism.

3. TDP-43 levels physiologically decrease with aging, and this phenomenon when coupled with aggregation triggers an ALS-like phenotype, possibly due to a TDP-43 loss of function.

4. Tricyclic compounds thioridazine, nortriptyline and chlorpromazine promote the clearance of EGFP-12xQ/N and TDP-12xQ/N aggregates, possibly via proteasome stimulation.

5. The clearance of TDP-43 inclusions, allows the return of the normal TDP-43 function, and this could be a valuable therapeutic strategy for ALS.

Bibliography

Alexander, M. D., Traynor, B. J., Miller, N., Corr, B., Frost, E., McQuaid, S., … Hardiman, O. (2002). "True" sporadic ALS associated with a novel SOD-1 mutation. *Annals of Neurology*, *52*(5), 680–3. doi:10.1002/ana.10369

Aman, P., Panagopoulos, I., Lassen, C., Fioretos, T., Mencinger, M., Toresson, H., … Mitelman, F. (1996). Expression patterns of the human sarcoma-associated genes FUS and EWS and the genomic structure of FUS. *Genomics*, *37*(1), 1–8. doi:10.1006/geno.1996.0513

Andersen, P. M. (2006). Amyotrophic lateral sclerosis associated with mutations in the CuZn superoxide dismutase gene. *Current Neurology and Neuroscience Reports*, *6*(1), 37–46.

Andersson, M. K., Ståhlberg, A., Arvidsson, Y., Olofsson, A., Semb, H., Stenman, G., … Aman, P. (2008). The multifunctional FUS, EWS and TAF15 proto-oncoproteins show cell type-specific expression patterns and involvement in cell spreading and stress response. *BMC Cell Biology*, *9*, 37. doi:10.1186/1471-2121-9-37

Anglade, P., Vyas, S., Herrero, M. T., Michel, P. P., Marquez, J., Ruberg, M., … Agid, Y. (1997). Apoptosis and autophagy in nigral neurons of patients with Parkinson ' s disease. *Histology and Hystopathology*, *12*, 25–31.

Arai, T., Hasegawa, M., Akiyama, H., Ikeda, K., Nonaka, T., Mori, H., … Oda, T. (2006). TDP-43 is a component of ubiquitin-positive tau-negative inclusions in frontotemporal lobar degeneration and amyotrophic lateral sclerosis. *Biochemical and Biophysical Research Communications*, *351*(3), 602–11. doi:10.1016/j.bbrc.2006.10.093

Ash, P. E. a, Zhang, Y.-J., Roberts, C. M., Saldi, T., Hutter, H., Buratti, E., … Link, C. D. (2010). Neurotoxic effects of TDP-43 overexpression in C. elegans. *Human Molecular Genetics*, *19*(16), 3206–18. doi:10.1093/hmg/ddq230

Ashoor, R., Yafawi, R., Jessen, B., & Lu, S. (2013). The contribution of lysosomotropism to autophagy perturbation. *PloS One, 8*(11), e82481. doi:10.1371/journal.pone.0082481

Avendaño-Vázquez, S. E., Dhir, A., Bembich, S., Buratti, E., Proudfoot, N., & Baralle, F. E. (2012). Autoregulation of TDP-43 mRNA levels involves interplay between transcription, splicing, and alternative polyA site selection. *Genes & Development*, *26*(15), 1679–84. doi:10.1101/gad.194829.112.

Ayala, Y. M., De Conti, L., Avendaño-Vázquez, S. E., Dhir, A., Romano, M., D'Ambrogio, A., … Baralle, F. E. (2011). TDP-43 regulates its mRNA levels through a negative feedback loop. *The EMBO Journal*, *30*(2), 277–88. doi:10.1038/emboj.2010.310.

Ayala, Y. M., Pantano, S., D'Ambrogio, A., Buratti, E., Brindisi, A., Marchetti, C., … Baralle, F. E. (2005). Human, Drosophila, and C.elegans TDP43: nucleic acid binding properties and splicing regulatory function. *Journal of Molecular Biology*, *348*(3), 575–88. doi:10.1016/j.jmb.2005.02.038

Ayala, Y. M., Zago, P., D'Ambrogio, A., Xu, Y.-F., Petrucelli, L., Buratti, E., & Baralle, F. E. (2008). Structural determinants of the cellular localization and shuttling of TDP-43. *Journal of Cell Science*, *121*(Pt 22), 3778–85. doi:10.1242/jcs.038950

Baloh, R. (2011). TDP-43: The relationship between between protein aggregation and neurodegeneration in ALS and FTLD. *FEBS*, *278*(19), 3539–3549. doi:10.1111/j.1742-4658.2011.08256.x.

Barmada, S. J., Serio, A., Arjun, A., Bilican, B., Daub, A., Ando, D. M., … Finkbeiner, S. (2014). Autophagy induction enhances TDP43 turnover and survival in neuronal ALS models. *Nature Chemical Biology*, *10*(8), 677–85. doi:10.1038/nchembio.1563

Barmada, S. J., Skibinski, G., Korb, E., Rao, E. J., Wu, J. Y., & Finkbeiner, S. (2010). Cytoplasmic mislocalization of TDP-43 is toxic to neurons and enhanced by a mutation associated with familial amyotrophic lateral sclerosis. *The Journal of Neuroscience*, *30*(2), 639–49. doi:10.1523/JNEUROSCI.4988-09.2010

Bäumer, D., Parkinson, N., & Talbot, K. (2009). TARDBP in amyotrophic lateral sclerosis: identification of a novel variant but absence of copy number variation. *Journal of Neurology, Neurosurgery, and Psychiatry*, *80*(11), 1283–5. doi:10.1136/jnnp.2008.166512

Bedford, L., Hay, D., Devoy, A., Paine, S., Powe, D. G., Seth, R., … Mayer, R. J. (2008). Depletion of 26S proteasomes in mouse brain neurons causes neurodegeneration and Lewy-like inclusions resembling human pale bodies. *The Journal of Neuroscience : The Official Journal of the Society for Neuroscience*, *28*(33), 8189–98. doi:10.1523/JNEUROSCI.2218-08.2008

Bembich, S., Herzog, J. S., De Conti, L., Stuani, C., Avendaño-Vázquez, S. E., Buratti, E., … Baralle, F. E. (2013). Predominance of spliceosomal complex formation over polyadenylation site selection in TDP-43 autoregulation. *Nucleic Acids Research*, *42*(5), 3362–71. doi:10.1093/nar/gkt1343

Bensimon G., Lacomblez L., Meininger V., A. S. G. (1994). A controlled trial of riluzole in amyotrophic lateral sclerosis. *The New England Journal of Medicine*, *330*(9), 585–591.

Benzer, S. (1967). BEHAVIORAL MUTANTS OF Drosophila ISOLATED BY COUNTERCURRENT DISTRIBUTION. *Proceedings of the National Academy of Sciences of the United States of America*, *58*(3), 1112–1119. doi:10.1073/pnas.58.3.1112

Berger, Z., Ravikumar, B., Menzies, F. M., Oroz, L. G., Underwood, B. R., Pangalos, M. N., … Rubinsztein, D. C. (2006). Rapamycin alleviates toxicity of different aggregate-prone proteins. *Human Molecular Genetics*, *15*(3), 433–42. doi:10.1093/hmg/ddi458

Bhardwaj, A., Myers, M. P., Buratti, E., & Baralle, F. E. (2013). Characterizing TDP-43 interaction with its RNA targets. *Nucleic Acids Research*, *41*(9), 5062–5074. doi:10.1093/nar/gkt189

Bigio, E. H., Wu, J. Y., Deng, H. X., Bit-Ivan, E. N., Mao, Q., Ganti, R., … Mesulam, M. (2013). Inclusions in frontotemporal lobar degeneration with TDP-43 proteinopathy (FTLD-TDP) and amyotrophic lateral sclerosis (ALS), but not FTLD with FUS proteinopathy (FTLD-FUS), have properties of amyloid. *Acta Neuropathologica*, *125*(3), 463–465. doi:10.1007/s00401-013-1089-6

Bischof, J., Maeda, R. K., Hediger, M., Karch, F., & Basler, K. (2007). An optimized transgenesis system for Drosophila using germ-line-specific phiC31 integrases. *Proceedings of the National Academy of Sciences of the United States of America*, *104*(9), 3312–7. doi:doi/10.1073/pnas.0611511104.

Bjørkøy, G., Lamark, T., Brech, A., Outzen, H., Perander, M., Overvatn, A., … Johansen, T. (2005). p62/SQSTM1 forms protein aggregates degraded by autophagy and has a protective effect on huntingtin-induced cell death. *The Journal of Cell Biology*, *171*(4), 603–14. doi:10.1083/jcb.200507002

Blokhuis, A. M., Groen, E. J. N., Koppers, M., van den Berg, L. H., & Pasterkamp, R. J. (2013). Protein aggregation in amyotrophic lateral sclerosis. *Acta Neuropathologica*, *125*(6), 777–94. doi:10.1007/s00401-013-1125-6

Boillée, S., Vande Velde, C., & Cleveland, D. W. (2006). ALS: a disease of motor neurons and their nonneuronal neighbors. *Neuron*, *52*(1), 39–59. doi:10.1016/j.neuron.2006.09.018

Braak, H., Brettschneider, J., Ludolph, A. C., Lee, V. M., John, Q., & Tredici,

K. Del. (2014). Amytrophic lateral sclerosis-a model of corticofugal axonal spread. *Nat. Rev. Neurol.*, *9*(12), 708–714. doi:10.1038/nrneurol.2013.221.Amyotrophic

Brand, A. H., & Perrimon, N. (1993). Targeted gene expression as a means of altering cell fates and generating dominant phenotypes. *Development*, *118*(2), 401–15.

Brooks, B. R. (1994). El Escorial World Federation of Neurology criteria for the diagnosis of amyotrophic lateral sclerosis. Subcommittee on Motor Neuron Diseases/Amyotrophic Lateral Sclerosis of the World Federation of Neurology Research Group on Neuromuscular Diseases and th. *Journal of the Neurological Sciences*, *124 Suppl*, 96–107.

Brooks, B. R., Miller, R. G., Swash, M., & Munsat, T. L. (2000). El Escorial revisited: revised criteria for the diagnosis of amyotrophic lateral sclerosis. *Amyotrophic Lateral Sclerosis and Other Motor Neuron Disorders : Official Publication of the World Federation of Neurology, Research Group on Motor Neuron Diseases*, *1*(5), 293–9.

Brown, I. R. (2007). Heat shock proteins and protection of the nervous system. *Annals of the New York Academy of Sciences*, *1113*, 147–58. doi:10.1196/annals.1391.032

Bruijn, L. I., Miller, T. M., & Cleveland, D. W. (2004). Unraveling the mechanisms involved in motor neuron degeneration in ALS. *Annual Review of Neuroscience*, *27*, 723–49. doi:10.1146/annurev.neuro.27.070203.144244

Bruijn, L. I., Houseweart M. K., Kato, S., Anderson, K. L., Anderson, S. D., Ohama, E., Reaume, A. G., Scott, R. W., Cleveland, D. W. (1998). Aggregation and Motor Neuron Toxicity of an ALS-Linked SOD1 Mutant Independent from Wild-Type SOD1. *Science*, *281*(5384), 1851–1854. doi:10.1126/science.281.5384.1851

Budini, M., Buratti, E., Stuani, C., Guarnaccia, C., Romano, V., De Conti, L., & Baralle, F. E. (2012a). Cellular model of TAR DNA-binding protein 43 (TDP-43) aggregation based on its C-terminal Gln/Asn-rich region. *The Journal of Biological Chemistry*, *287*(10), 7512–25. doi:10.1074/jbc.M111.288720

Budini, M., Romano, V., Avendaño-Vázquez, S. E., Bembich, S., Buratti, E., & Baralle, F. E. (2012b). Role of selected mutations in the Q/N rich region of TDP-43 in EGFP-12xQ/N-induced aggregate formation. *Brain Research*, *1462*, 139–50. doi:10.1016/j.brainres.2012.02.031

Budini, M., Romano, V., Quadri, Z., Buratti, E., & Baralle, F. E. (2014). TDP-43 loss of cellular function through aggregation requires additional structural determinants beyond its C-terminal Q/N prion-like domain. *Human Molecular Genetics*, 1–12. doi:10.1093/hmg/ddu415

Buratti, E., & Baralle, F. E. (2001). Characterization and functional implications of the RNA binding properties of nuclear factor TDP-43, a novel splicing regulator of CFTR exon 9. *The Journal of Biological Chemistry*, *276*(39), 36337–43. doi:10.1074/jbc.M104236200

Buratti, E., & Baralle, F. E. (2012). TDP-43: gumming up neurons through protein-protein and protein-RNA interactions. *Trends in Biochemical Sciences*, *37*(6), 237–47. doi:10.1016/j.tibs.2012.03.003

Buratti, E., Brindisi, A., Giombi, M., Tisminetzky, S., Ayala, Y. M., & Baralle, F. E. (2005). TDP-43 binds heterogeneous nuclear ribonucleoprotein A/B through its C-terminal tail: An important region for the inhibition of cystic fibrosis transmembrane conductance regulator exon 9 splicing. *Journal of Biological Chemistry*, *280*(45), 37572–37584. doi:10.1074/jbc.M505557200

Buratti, E., Dörk, T., Zuccato, E., Pagani, F., Romano, M., & Baralle, F. E. (2001). Nuclear factor TDP-43 and SR proteins promote in vitro and in vivo CFTR exon 9 skipping. *The EMBO Journal*, *20*(7), 1774–84. doi:10.1093/emboj/20.7.1774

Bursch, W., & Ellinger, A. (2005). Autophagy-a basic mechanism and a potential role for neurodegeneration. *Folia Neuropathologica*, *43*(4), 297–310.

Caccamo, A., Majumder, S., Deng, J. J., Bai, Y., Thornton, F. B., & Oddo, S. (2009). Rapamycin rescues TDP-43 mislocalization and the associated low molecular mass neurofilament instability. *The Journal of Biological Chemistry*, *284*(40), 27416–24. doi:10.1074/jbc.M109.031278

Cataldo, A. M., Hamilton, D. J., Barnett, J. L., Paskevich, P. A., & Nixon, R. A. (1996). Abnormalities of the endosomal-lysosomal system in Alzheimer's disease: relationship to disease pathogenesis. *Advances in Experimental Medicine and Biology*, *389*, 271–80.

Charcot, J.-M. (1869). Deux cas d'atrophie musculaire progressive avec lésions de la substance grise et des faisceaux antérolatéraux de la moelle épinière. *Arch. Physiol. Neurol. Path. 2*, 744–754.

Chen, S., Sayana, P., Zhang, X., & Le, W. (2013). Genetics of amyotrophic lateral sclerosis: an update. *Molecular Neurodegeneration*, *8*(1), 28. doi:10.1186/1750-1326-8-28

Cherra, S. J., & Chu, C. T. (2008). Autophagy in neuroprotection and neurodegeneration: A question of balance. *Future Neurol.*, *3*(3), 309–323. doi:10.2217/14796708.3.3.309.

Chuang, D.-M. (2004). Neuroprotective and neurotrophic actions of the mood stabilizer lithium: can it be used to treat neurodegenerative diseases? *Critical Reviews in Neurobiology*, *16*(1-2), 83–90. doi:10.1615/CritRevNeurobiol.v16.i12.90

Coux, O., Tanaka, K., & Goldberg, A. L. (1996). STRUCTURE AND FUNCTIONS OF THE 20s AND 26s. *Annu. Rev. Biochem.*, *65*, 801–47.

Cozzolino, M., & Carrì, M. T. (2012). Mitochondrial dysfunction in ALS. *Progress in Neurobiology*, *97*(2), 54–66. doi:10.1016/j.pneurobio.2011.06.003

Crozat, A., Aman, P., Mandahl, N., & Ron, D. (1993). Fusion of CHOP to a novel RNA-binding protein in human myxoid liposarcoma. *Nature*, *363*(6430), 640–4. doi:10.1038/363640a0

Cushman, M., Johnson, B. S., King, O. D., Gitler, A. D., & Shorter, J. (2010). Prion-like disorders: blurring the divide between transmissibility and infectivity. *Journal of Cell Science*, *123*(Pt 8), 1191–1201. doi:10.1242/jcs.051672

D'Ambrogio, A., Buratti, E., Stuani, C., Guarnaccia, C., Romano, M., Ayala, Y. M., & Baralle, F. E. (2009). Functional mapping of the interaction between TDP-43 and hnRNP A2 in vivo. *Nucleic Acids Research*, *37*(12), 4116–26. doi:10.1093/nar/gkp342

de Duve, C., de Barsy, T., Poole, B., Trouet, A., Tulkens, P., & Van Hoof, F. (1974). Commentary. Lysosomotropic agents. *Biochemical Pharmacology*, *23*(18), 2495–531.

Dejesus-Hernandez, M., Mackenzie, I. R., Boeve, B. F., Boxer, A. L., Baker, M., Rutherford, N. J., … Boylan, K. (2012). Expanded GGGGCC hexanucleotide repeat in non-coding region of C9ORF72 causes chromoseme 9p-linked frontotemporal dementia and amyotrophic lateral sclerosis, *72*(2), 245–256. doi:10.1016/j.neuron.2011.09.011.

Diaper, D. C., Adachi, Y., Sutcliffe, B., Humphrey, D. M., Elliott, C. J. H., Stepto, A., … Hirth, F. (2013). Loss and gain of Drosophila TDP-43 impair synaptic efficacy and motor control leading to age-related neurodegeneration by loss-of-function phenotypes. *Human Molecular Genetics*, *22*(8), 1539–57. doi:10.1093/hmg/ddt005

Dobson, C. M. (2003). Protein folding and misfolding. *Nature*, *426*(6968), 884–90. doi:10.1038/nature02261

Dormann, D., & Haass, C. (2011). TDP-43 and FUS: a nuclear affair. *Trends in Neurosciences*, *34*(7), 339–48. doi:10.1016/j.tins.2011.05.002

Estes, P. S., Boehringer, A., Zwick, R., Tang, J. E., Grigsby, B., & Zarnescu, D. C. (2011). Wild-type and A315T mutant TDP-43 exert differential neurotoxicity in a Drosophila model of ALS. *Human Molecular Genetics*, *20*(12), 2308–21. doi:10.1093/hmg/ddr124

Feiguin, F., Godena, V. K., Romano, G., D'Ambrogio, A., Klima, R., & Baralle, F. E. (2009). Depletion of TDP-43 affects Drosophila motoneurons terminal synapsis and locomotive behavior. *FEBS Letters*, *583*(10), 1586–92. doi:10.1016/j.febslet.2009.04.019

Fenteany, G. (1998). Lactacystin, Proteasome Function, and Cell Fate. *Journal of Biological Chemistry*, *273*(15), 8545–8548. doi:10.1074/jbc.273.15.8545

Fernández-Borges, N., Eraña, H., Venegas, V., Elezgarai, S. R., Harrathi, C., & Castilla, J. (2015). Animal models for prion-like diseases. *Virus Research*, *207*, 5–24. doi:10.1016/j.virusres.2015.04.014

Fiesel, F. C., Voigt, A., Weber, S. S., Van den Haute, C., Waldenmaier, A., Görner, K., … Kahle, P. J. (2010). Knockdown of transactive response DNA-binding protein (TDP-43) downregulates histone deacetylase 6. *The EMBO Journal*, *29*(1), 209–21. doi:10.1038/emboj.2009.324

Fiesel, F. C., Weber, S. S., Supper, J., Zell, A., & Kahle, P. J. (2012). TDP-43 regulates global translational yield by splicing of exon junction complex component SKAR. *Nucleic Acids Research*, *40*(6), 2668–2682. doi:10.1093/nar/gkr1082

Forman, M. S., Trojanowski, J. Q., & Lee, V. M. (2004). Neurodegenerative diseases : a decade of discoveries paves the way for therapeutic breakthroughs, *10*(10), 1055–1063. doi:10.1038/1113

Fornai, F., Longone, P., Cafaro, L., Kastsiuchenka, O., Ferrucci, M., Manca, M. L., … Paparelli, A. (2008a). Lithium delays progression of amyotrophic lateral sclerosis. *Proceedings of the National Academy of Sciences of the United States of America*, *105*(6), 2052–7. doi:10.1073/pnas.0708022105

Fornai, F., Longone, P., Ferrucci, M., Lenzi, P., Isidoro, C., Ruggieri, S., & Paparelli. (2008b). Autophagy and amyotrophic lateral sclerosis: The multiple roles of lithium. *Autophagy*, *4*(4), 527–530. doi:http://dx.doi.org/10.4161/auto.5923

165

Franco, M. C., Dennys, C. N., Rossi, F. H., & Estévez, A. G. (2013). Superoxide Dismutase and Oxidative Stress in Amyotrophic Lateral Sclerosis. In *Current Advances in Amyotophic Lateral Sclerosis*. doi:10.5772/56488

Fuentealba, R. a, Udan, M., Bell, S., Wegorzewska, I., Shao, J., Diamond, M. I., … Baloh, R. H. (2010). Interaction with polyglutamine aggregates reveals a Q/N-rich domain in TDP-43. *The Journal of Biological Chemistry*, *285*(34), 26304–14. doi:10.1074/jbc.M110.125039

Furukawa, Y., Kaneko, K., Watanabe, S., Yamanaka, K., & Nukina, N. (2011). A seeding reaction recapitulates intracellular formation of Sarkosyl-insoluble transactivation response element (TAR) DNA-binding protein-43 inclusions. *The Journal of Biological Chemistry*, *286*(21), 18664–72. doi:10.1074/jbc.M111.231209

Geser, F., Martinez-Lage, M., Kwong, L. K., Lee, V. M.-Y., & Trojanowski, J. Q. (2009). Amyotrophic lateral sclerosis, frontotemporal dementia and beyond: the TDP-43 diseases. *Journal of Neurology*, *256*(8), 1205–14. doi:10.1007/s00415-009-5069-7

Geser, F., Robinson, J. L., Malunda, J. a, Xie, S. X., Clark, C. M., Kwong, L. K., … Trojanowski, J. Q. (2010). Pathological 43-kDa transactivation response DNA-binding protein in older adults with and without severe mental illness. *Archives of Neurology*, *67*(10), 1238–50. doi:10.1001/archneurol.2010.254

Gill, A., Kidd, J., Vieira, F., Thompson, K., & Perrin, S. (2009). No benefit from chronic lithium dosing in a sibling-matched, gender balanced, investigator-blinded trial using a standard mouse model of familial ALS. *PloS One*, *4*(8), e6489. doi:10.1371/journal.pone.0006489

Gitcho, M. A., Bigio, E., Mishra, M., Johnson, N., Weintraub, S., Mesulam, M., … Cairns, N. J. (2009). TARDBP 3′-UTR variant in autopsy-confirmed frontotemporal lobar degeneration with TDP-43 proteinopathy. *Acta Neuropathologica*, *118*(5), 633–645. doi:10.1007/s00401-009-0571-7.TARDBP

Glover, J. R., & Lindquist, S. (1998). Hsp104, Hsp70, and Hsp40: a novel chaperone system that rescues previously aggregated proteins. *Cell*, *94*(1), 73–82.

Gomez-Deza, J., Lee, Y., Troakes, C., Nolan, M., Al-Sarraj, S., Gallo, J.-M., & Shaw, C. E. (2015). Dipeptide repeat protein inclusions are rare in the spinal cord and almost absent from motor neurons in C9ORF72 mutant amyotrophic lateral sclerosis and are unlikely to cause their degeneration. *Acta Neuropathologica Communications*, *3*(1), 38. doi:10.1186/s40478-015-0218-y

Gong, Z. F. (2012). Innate preference in Drosophila melanogaster. *Science China Life Sciences*, *55*(1), 8–14. doi:10.1007/s11427-012-4271-5

Groll, M., Ditzel, L., Löwe, J., Stock, D., Bochtler, M., Bartunik, H. D., & Huber, R. (1997). Structure of 20S proteasome from yeast at 2.4 A resolution. *Nature*, *386*(6624), 463–71. doi:10.1038/386463a0

Haigis, M. C., & Yankner, B. A. (2010). The aging stress response. *Mol. Cell.*, *40*(2), 333–344. doi:10.1016/j.molcel.2010.10.002.The

Hanson, K. a, Kim, S. H., Wassarman, D. a, & Tibbetts, R. S. (2010). Ubiquilin modifies TDP-43 toxicity in a Drosophila model of amyotrophic lateral sclerosis (ALS). *The Journal of Biological Chemistry*, *285*(15), 11068–72. doi:10.1074/jbc.C109.078527

Hartl, F. U., Bracher, A., & Hayer-Hartl, M. (2011). Molecular chaperones in protein folding and proteostasis. *Nature*, *475*(7356), 324–32. doi:10.1038/nature10317

Hasegawa, M., Arai, T., Nonaka, T., Kametani, F., Yoshida, M., Hashizume, Y., … Akiyama, H. (2008). Phosphorylated TDP-43 in frontotemporal lobar degeneration and amyotrophic lateral sclerosis. *Annals of Neurology*, *64*(1), 60–70. doi:10.1002/ana.21425

Haverkamp, L. J., Appel, V., & Appel, S. H. (1995). Natural history of amyotrophic lateral sclerosis in a database population. Validation of a scoring system and a model for survival prediction. *Brain : A Journal of Neurology*, *118*(3), 707–19. doi:10.1093/brain/118.3.707

Hayward, L. J., Rodriguez, J. a, Kim, J. W., Tiwari, A., Goto, J. J., Cabelli, D. E., … Brown, R. H. (2002). Decreased metallation and activity in subsets of mutant superoxide dismutases associated with familial amyotrophic lateral sclerosis. *The Journal of Biological Chemistry*, *277*(18), 15923–31. doi:10.1074/jbc.M112087200

He, C., & Klionsky, D. J. (2010). Regulation mechanisms and signaling pathways of autophagy. *Annu. Rev. Gent.*, *218*(2), 333–346. doi:10.1146/annurev-genet-102808-114910

Hebbar, S., Hall, R. E., Demski, S. A., Subramanian, A., & Fernandes, J. J. (2006). The Adult Abdominal Neuromuscular Junction of Drosophila : A Model for Synaptic Plasticity. *Wiley InterScience*, *66*, 1140–1155. doi:10.1002/neu

Hebron, M. L., Lonskaya, I., Sharpe, K., Weerasinghe, P. P. K., Algarzae, N. K., Shekoyan, A. R., & Moussa, C. E.-H. (2013). Parkin ubiquitinates Tar-DNA binding protein-43 (TDP-43) and promotes its cytosolic accumulation via interaction with histone deacetylase 6 (HDAC6). *The Journal of Biological Chemistry*, *288*(6), 4103–15. doi:10.1074/jbc.M112.419945

Hewamadduma, C. a a, Grierson, A. J., Ma, T. P., Pan, L., Moens, C. B., Ingham, P. W., … Shaw, P. J. (2013). Tardbpl splicing rescues motor neuron and axonal development in a mutant tardbp zebrafish. *Human Molecular Genetics*, *22*(12), 2376–86. doi:10.1093/hmg/ddt082

Huang, C., Xia, P. Y., & Zhou, H. (2010). Sustained Expression of TDP-43 and FUS in Motor Neurons in Rodent's Lifetime. *International Journal of Biological Sciences*, *6*(4), 396–406. doi:10.7150/ijbs.6.396

Igaz, L. M., Kwong, L. K., Chen-Plotkin, A., Winton, M. J., Unger, T. L., Xu, Y., … Lee, V. M.-Y. (2009). Expression of TDP-43 C-terminal Fragments in Vitro Recapitulates Pathological Features of TDP-43 Proteinopathies. *The Journal of Biological Chemistry*, *284*(13), 8516–24. doi:10.1074/jbc.M809462200

Ihara, R., Matsukawa, K., Nagata, Y., Kunugi, H., Tsuji, S., Chihara, T., … Iwatsubo, T. (2013). RNA binding mediates neurotoxicity in the transgenic Drosophila model of TDP-43 proteinopathy. *Human Molecular Genetics*, *22*(22), 4474–4484. doi:10.1093/hmg/ddt296

Ince, P. G., Shaw, P. J., Slade, J. Y., Jones, C., & Hudgson, P. (1996). Familial amyotrophic lateral sclerosis with a mutation in exon 4 of the Cu/Zn superoxide dismutase gene: pathological and immunocytochemical changes. *Acta Neuropathologica*, *92*(4), 395–403.

Inukai, Y., Nonaka, T., Arai, T., Yoshida, M., Hashizume, Y., Beach, T. G., … Hasegawa, M. (2008). Abnormal phosphorylation of Ser409/410 of TDP-43 in FTLD-U and ALS. *FEBS Letters*, *582*(19), 2899–904. doi:10.1016/j.febslet.2008.07.027

Jan, L. Y., & Jan, Y. N. (1982). Antibodies to horseradish peroxidase as specific neuronal markers in Drosophila and in grasshopper embryos. *Proceedings of the National Academy of Sciences of the United States of America*, *79*(8), 2700–2704. doi:10.1073/pnas.79.8.2700

Jariel-Encontre, I., Bossis, G., & Piechaczyk, M. (2008). Ubiquitin-independent degradation of proteins by the proteasome. *Biochimica et Biophysica Acta, 1786*(2), 153–77. doi:10.1016/j.bbcan.2008.05.004

Johansen, T., & Lamark, T. (2011). Selective autophagy mediated by autophagic adapter proteins. *Autophagy, 7*(3), 279–296. doi:10.4161/auto.7.3.14487

Johnson, B. S., Snead, D., Lee, J. J., McCaffery, J. M., Shorter, J., & Gitler, A. D. (2009). TDP-43 is intrinsically aggregation-prone, and amyotrophic lateral sclerosis-linked mutations accelerate aggregation and increase toxicity. *The Journal of Biological Chemistry, 284*(30), 20329–39. doi:10.1074/jbc.M109.010264

Jucker, M., & Walker, L. C. (2013). Self-propagation of pathogenic protein aggregates in neurodegenerative diseases. *Nature, 501*(7465), 45–51. doi:10.1038/nature12481

Kabashi, E., Agar, J. N., Hong, Y., Taylor, D. M., Minotti, S., Figlewicz, D. a, & Durham, H. D. (2008a). Proteasomes remain intact, but show early focal alteration in their composition in a mouse model of amyotrophic lateral sclerosis. *Journal of Neurochemistry, 105*(6), 2353–66. doi:10.1111/j.1471-4159.2008.05317.x

Kabashi, E., Agar, J. N., Strong, M. J., & Durham, H. D. (2012). Impaired proteasome function in sporadic amyotrophic lateral sclerosis. *Amyotrophic Lateral Sclerosis, 13*(4), 367–71. doi:10.3109/17482968.2012.686511

Kabashi, E., Agar, J. N., Taylor, D. M., Minotti, S., & Durham, H. D. (2004). Focal dysfunction of the proteasome: a pathogenic factor in a mouse model of amyotrophic lateral sclerosis. *Journal of Neurochemistry, 89*(6), 1325–35. doi:10.1111/j.1471-4159.2004.02453.x

Kabashi, E., Lin, L., Tradewell, M. L., Dion, P. a, Bercier, V., Bourgouin, P., … Drapeau, P. (2010). Gain and loss of function of ALS-related mutations of TARDBP (TDP-43) cause motor deficits in vivo. *Human Molecular Genetics, 19*(4), 671–83. doi:10.1093/hmg/ddp534

Kabashi, E., Valdmanis, P. N., Dion, P., Spiegelman, D., McConkey, B. J., Vande Velde, C., … Rouleau, G. a. (2008b). TARDBP mutations in individuals with sporadic and familial amyotrophic lateral sclerosis. *Nature Genetics, 40*(5), 572–4. doi:10.1038/ng.132

Kalmar, B., Lu, C.-H., & Greensmith, L. (2013). The role of heat shock proteins in Amyotrophic Lateral Sclerosis: The therapeutic potential of Arimoclomol. *Pharmacology & Therapeutics*, *141*(1), 40–54. doi:10.1016/j.pharmthera.2013.08.003

Kasai, T., Tokuda, T., Ishigami, N., Sasayama, H., Foulds, P., Mitchell, D. J., … Nakagawa, M. (2009). Increased TDP-43 protein in cerebrospinal fluid of patients with amyotrophic lateral sclerosis. *Acta Neuropathologica*, *117*(1), 55–62. doi:10.1007/s00401-008-0456-1

Kaufmann, A. M., & Krise, J. P. (2007). Lysosomal sequestration of amine-containing drugs: analysis and therapeutic implications. *Journal of Pharmaceutical Sciences*, *96*(4), 729–46. doi:10.1002/jps.20792

Kegel, K. B., Kim, M., Sapp, E., McIntyre, C., Castaño, J. G., Aronin, N., & DiFiglia, M. (2000). Huntingtin expression stimulates endosomal-lysosomal activity, endosome tubulation, and autophagy. *The Journal of Neuroscience : The Official Journal of the Society for Neuroscience*, *20*(19), 7268–78.

Keller, J. N., Hanni, K. B., & Markesbery, W. R. (2000). Possible involvement of proteasome inhibition in aging: implications for oxidative stress. *Mechanisms of Ageing and Development*, *113*(1), 61–70. doi:10.1016/S0047-6374(99)00101-3

Keller, J. N., Hanni, K. B., & Markesbery, W. R. (2001). Impaired Proteasome Function in Alzheimer's Disease. *Journal of Neurochemistry*, *75*(1), 436–439. doi:10.1046/j.1471-4159.2000.0750436.x

Kieran, D., Kalmar, B., Dick, J. R. T., Riddoch-Contreras, J., Burnstock, G., & Greensmith, L. (2004). Treatment with arimoclomol, a coinducer of heat shock proteins, delays disease progression in ALS mice. *Nature Medicine*, *10*(4), 402–5. doi:10.1038/nm1021

King, O. D., Gitler, A. D., & Shorter, J. (2013). The tip of the iceberg: RNA-binding proteins with prion-like domains in neurodegenerative diseases. *Brain Res.*, *14*(62), 61–80. doi:10.1016/j.brainres.2012.01.016.The

Komatsu, M., Waguri, S., Chiba, T., Murata, S., Iwata, J., Tanida, I., … Tanaka, K. (2006). Loss of autophagy in the central nervous system causes neurodegeneration in mice. *Nature*, *441*(7095), 880–4. doi:10.1038/nature04723

Korth, C., May, B. C., Cohen, F. E., & Prusiner, S. B. (2001). Acridine and phenothiazine derivatives as pharmacotherapeutics for prion disease. *Proceedings of the National Academy of Sciences of the United States of America*, *98*(17), 9836–9841. doi:10.1073/pnas.161274798

Kraft, C., Peter, M., & Hofmann, K. (2010). Selective autophagy: ubiquitin-mediated recognition and beyond. *Nature Cell Biology*, *12*(9), 836–41. doi:10.1038/ncb0910-836

Krecic, A. M., & Swanson, M. S. (1999). hnRNP complexes : composition, structure, and function. *Current Opinion in Cell Biology*, *11*, 363–371.

Kwiatkowski, T. J., Bosco, D. a, Leclerc, a L., Tamrazian, E., Vanderburg, C. R., Russ, C., … Brown, R. H. (2009). Mutations in the FUS/TLS gene on chromosome 16 cause familial amyotrophic lateral sclerosis. *Science (New York, N.Y.)*, *323*(5918), 1205–8. doi:10.1126/science.1166066

Kwong, L. K., Uryu, K., Trojanowski, J. Q., & Lee, V. M.-Y. (2007). TDP-43 proteinopathies: neurodegenerative protein misfolding diseases without amyloidosis. *Neuro-Signals*, *16*(1), 41–51. doi:10.1159/000109758

Lagier-Tourenne, C., & Cleveland, D. W. (2009). Rethinking ALS: the FUS about TDP-43. *Cell*, *136*(6), 1001–4. doi:10.1016/j.cell.2009.03.006

Lagier-Tourenne, C., Polymenidou, M., & Cleveland, D. W. (2010). TDP-43 and FUS/TLS: emerging roles in RNA processing and neurodegeneration. *Human Molecular Genetics*, *19*(R1), R46–64. doi:10.1093/hmg/ddq137

Lauterbach, E. C., & Mendez, M. F. (2011). Psychopharmacological Neuroprotection in Neurodegenerative Diseases, Part III: Criteria-Based Assessment: A Report of the ANPA Committee on Research. *Journal of Neuropsychiatry*, *23*(3), 242–260. doi:10.1176/appi.neuropsych.23.3.242

Lee, J.-Y., Koga, H., Kawaguchi, Y., Tang, W., Wong, E., Gao, Y.-S., … Yao, T.-P. (2010). HDAC6 controls autophagosome maturation essential for ubiquitin-selective quality-control autophagy. *The EMBO Journal*, *29*(5), 969–80. doi:10.1038/emboj.2009.405

Leigh, P. N., Whitwell, H., Garofalo, O., Buller, J., Swash, M., Martin, J. E., … Anderton, B. H. (1991). Ubiquitin-immunoreactive intraneuronal inclusions in amyotrophic lateral sclerosis. Morphology, distribution, and specificity. *Brain : A Journal of Neurology*, *114*(2), 775–88.

Li, H.-Y., Yeh, P.-A., Chiu, H.-C., Tang, C.-Y., & Tu, B. P. (2011). Hyperphosphorylation as a defense mechanism to reduce TDP-43 aggregation. *PloS One*, *6*(8), e23075. doi:10.1371/journal.pone.0023075

Li, Q., Yokoshi, M., Okada, H., & Kawahara, Y. (2015). The cleavage pattern of TDP-43 determines its rate of clearance and cytotoxicity. *Nature Communications*, *6*, 1–12. doi:10.1038/ncomms7183

Li, W. Z., Li, S. L., Zheng, H. Y., Zhang, S. P., & Xue, L. (2012). A broad expression profile of the GMR-GAL4 driver in Drosophila melanogaster. *Genetics and Molecular Research : GMR*, *11*(3), 1997–2002. doi:10.4238/2012.August.6.4

Li, Y., Ray, P., Rao, E. J., Shi, C., Guo, W., Chen, X., … Wu, J. Y. (2010). A Drosophila model for TDP-43 proteinopathy. *Proceedings of the National Academy of Sciences of the United States of America*, *107*(7), 3169–74. doi:10.1073/pnas.0913602107.

Liachko, N. F., Guthrie, C. R., Kraemer, B. C. (2011). Phosphorylation promotes neurotoxicity in a C. elegans model of TDP-43 proteinopathy. *J. Neurosci.*, *30*(48), 16208–16219. doi:10.1523/JNEUROSCI.2911-10.2010

Lin, M.-J., Cheng, C.-W., & Shen, C.-K. J. (2011). Neuronal function and dysfunction of Drosophila dTDP. *PloS One*, *6*(6), e20371. doi:10.1371/journal.pone.0020371

Ling, S.-C., Polymenidou, M., & Cleveland, D. W. (2013). Converging mechanisms in ALS and FTD: disrupted RNA and protein homeostasis. *Neuron*, *79*(3), 416–38. doi:10.1016/j.neuron.2013.07.033

Liu, J., Lillo, C., Jonsson, P. A., Vande Velde, C., Ward, C. M., Miller, T. M., … Cleveland, D. W. (2004). Toxicity of familial ALS-linked SOD1 mutants from selective recruitment to spinal mitochondria. *Neuron*, *43*(1), 5–17. doi:10.1016/j.neuron.2004.06.016

Liu, Y., Atkinson, R. a. K., Fernandez-Martos, C. M., Kirkcaldie, M. T. K., Cui, H., Vickers, J. C., & King, A. E. (2015). Changes in TDP-43 expression in development, aging, and in the neurofilament light protein knockout mouse. *Neurobiology of Aging*, *36*, 1151–1159. doi:10.1016/j.neurobiolaging.2014.10.001

Lowe, J. (1994). New pathological findings in amyotrophic lateral sclerosis. *Journal of the Neurological Sciences*, *124 Suppl*, 38–51.

Ludolph, a. C., & Brettschneider, J. (2015). TDP-43 in amyotrophic lateral sclerosis - is it a prion disease? *European Journal of Neurology*, *22*(5), 753–761. doi:10.1111/ene.12706

Ma, X. M., Yoon, S. O., Richardson, C. J., Jülich, K., & Blenis, J. (2008). SKAR Links Pre-mRNA Splicing to mTOR/S6K1-Mediated Enhanced Translation Efficiency of Spliced mRNAs. *Cell*, *133*(2), 303–313. doi:10.1016/j.cell.2008.02.031

Mackenzie, I. R. a, Bigio, E. H., Ince, P. G., Geser, F., Neumann, M., Cairns, N. J., … Trojanowski, J. Q. (2007). Pathological TDP-43 distinguishes sporadic amyotrophic lateral sclerosis from amyotrophic lateral sclerosis with SOD1 mutations. *Annals of Neurology*, *61*(5), 427–34. doi:10.1002/ana.21147

Mccord, J. M., & Fridovich, I. (1969). Superoxide Dismutase: AN ENZYMIC FUNCTION FOR ERYTHROCUPREIN (HEMOCUPREIN). *J. Biol. Chem.*, *244*, 6049–6055.

McNaught, K. S. ., & Jenner, P. (2001). Proteasomal function is impaired in substantia nigra in Parkinson's disease. *Neuroscience Letters*, *297*(3), 191–194. doi:10.1016/S0304-3940(00)01701-8

Miguel, L., Frébourg, T., Campion, D., & Lecourtois, M. (2011). Both cytoplasmic and nuclear accumulations of the protein are neurotoxic in Drosophila models of TDP-43 proteinopathies. *Neurobiology of Disease*, *41*(2), 398–406. doi:10.1016/j.nbd.2010.10.007

Miller, R. G., Mitchell, J. D., Lyon, M., & Moore, D. H. (2007). Riluzole for amyotrophic lateral sclerosis (ALS)/motor neuron disease (MND). *The Cochrane Database of Systematic Reviews*, (1), CD001447. doi:10.1002/14651858.CD001447.pub2

Miller, T. M., Pestronk, A., David, W., Rothstein, J., Simpson, E., Appel, S. H., … Cudkowicz, M. E. (2013). An antisense oligonucleotide against SOD1 delivered intrathecally for patients with SOD1 familial amyotrophic lateral sclerosis: a phase 1, randomised, first-in-man study. *Lancet Neurology*, *12*(5), 435–42. doi:10.1016/S1474-4422(13)70061-9

Mizushima, N. (2004). Methods for monitoring autophagy. *The International Journal of Biochemistry & Cell Biology*, *36*(12), 2491–502. doi:10.1016/j.biocel.2004.02.005

Mizushima, N., & Yoshimori, T. (2007). How to interpret LC3 immunoblotting. *Autophagy*, *3*(6), 542–545.

Mompeán, M., Buratti, E., Guarnaccia, C., Brito, R. M. M., Chakrabartty, A., Baralle, F. E., & Laurents, D. V. (2014). Structural characterization of the minimal segment of TDP-43 competent for aggregation. *Archives of Biochemistry and Biophysics*, *545*, 53–62. doi:10.1016/j.abb.2014.01.007

Mori, K., Weng, S.-M., Arzberger, T., May, S., Rentzsch, K., Kremmer, E., … Edbauer, D. (2013). The C9orf72 GGGGCC repeat is translated into aggregating dipeptide-repeat proteins in FTLD/ALS. *Science (New York, N.Y.)*, *339*(6125), 1335–8. doi:10.1126/science.1232927

Nadanaciva, S., Lu, S., Gebhard, D. F., Jessen, B. A., Pennie, W. D., & Will, Y. (2011). A high content screening assay for identifying lysosomotropic compounds. *Toxicology in Vitro*, *25*(3), 715–723. doi:10.1016/j.tiv.2010.12.010

Nakatogawa, H., Suzuki, K., Kamada, Y., & Ohsumi, Y. (2009). Dynamics and diversity in autophagy mechanisms: lessons from yeast. *Nature Reviews. Molecular Cell Biology*, *10*(7), 458–67. doi:10.1038/nrm2708

Nedelsky, N., Todd, P. K., & Taylor, P. J. (2008). Autophagy and the ubiquitin-proteasome system: collaborators in neuroprotection. *Biochim Biophys Acta*, *1782*(12), 691–699. doi:10.1016/j.bbadis.2008.10.002.Autophagy

Nehls, J., Koppensteiner, H., Brack-Werner, R., Floss, T., & Schindler, M. (2014). HIV-1 Replication in Human Immune Cells Is Independent of TAR DNA Binding Protein 43 (TDP-43) Expression. *PLoS ONE, 9*(8), e105478. doi:10.1371/journal.pone.0105478

Neumann, M., Igaz, L. M., Kwong, L. K., Nakashima-Yasuda, H., Kolb, S. J., Dreyfuss, G., … Lee, V. M. Y. (2007a). Absence of heterogeneous nuclear ribonucleoproteins and survival motor neuron protein in TDP-43 positive inclusions in frontotemporal lobar degeneration. *Acta Neuropathologica*, *113*(5), 543–548. doi:10.1007/s00401-007-0221-x

Neumann, M., Kwong, L. K., Sampathu, D. M., Trojanowski, J. Q., & Lee, V. M.-Y. (2007b). TDP-43 proteinopathy in frontotemporal lobar degeneration and amyotrophic lateral sclerosis: protein misfolding diseases without amyloidosis. *Archives of Neurology*, *64*(10), 1388–94. doi:10.1001/archneur.64.10.1388

Neumann, M., Sampathu, D. M., Kwong, L. K., Truax, A. C., Micsenyi, M. C., Chou, T. T., … Lee, V. M.-Y. (2006). Ubiquitinated TDP-43 in frontotemporal lobar degeneration and amyotrophic lateral sclerosis. *Science (New York, N.Y.)*, *314*(5796), 130–3. doi:10.1126/science.1134108

Nonaka, T., Kametani, F., Arai, T., Akiyama, H., & Hasegawa, M. (2009). Truncation and pathogenic mutations facilitate the formation of intracellular aggregates of TDP-43. *Human Molecular Genetics*, *18*(18), 3353–3364. doi:10.1093/hmg/ddp275

Nonaka, T., Masuda-Suzukake, M., Arai, T., Hasegawa, Y., Akatsu, H., Obi, T., … Hasegawa, M. (2013). Prion-like Properties of Pathological TDP-43 Aggregates from Diseased Brains. *Cell Reports*, *4*(1), 124–134. doi:10.1016/j.celrep.2013.06.007

Otomo, A., Pan, L., & Hadano, S. (2012). Dysregulation of the autophagy-endolysosomal system in amyotrophic lateral sclerosis and related motor neuron diseases. *Neurology Research International*, *2012*, 498428. doi:10.1155/2012/498428

Ou, S. H., Wu, F., Harrich, D., Gaynor, R. B., & Gaynor, R. B. (1995). Cloning and characterization of a novel cellular protein, TDP-43, that binds to human immunodeficiency virus type 1 TAR DNA sequence motifs. *Journal of Virology*, *69*(6), 3584–3596.

Pandey, U. B., Nie, Z., Batlevi, Y., McCray, B. a, Ritson, G. P., Nedelsky, N. B., … Taylor, J. P. (2007). HDAC6 rescues neurodegeneration and provides an essential link between autophagy and the UPS. *Nature*, *447*(7146), 859–63. doi:10.1038/nature05853

Parsell, D. A., Kowal, A. S., Singer, M. A., & Lindquist, S. (1994). Protein disaggregation mediated by heat-shock protein Hsp104. *Nature*, *372*(6505), 475–8. doi:10.1038/372475a0

Pasinelli, P., & Brown, R. H. (2006). Molecular biology of amyotrophic lateral sclerosis: insights from genetics. *Nature Reviews. Neuroscience*, *7*(9), 710–23. doi:10.1038/nrn1971

Phase II/III Randomized, Placebo-controlled Trial of Arimoclomol in SOD1 Positive Familial Amyotrophic Lateral Sclerosis - ClinicalTrials.gov. (n.d.). Retrieved November 17, 2015, from https://clinicaltrials.gov/ct2/show/NCT00706147

Pilkington, G. J., Akinwunmi, J., & Amar, S. (2006). The role of tricyclic drugs in selective triggering of mitochondrially-mediated apoptosis in neoplastic glia : a therapeutic option in malignant glioma ? *Radiol Oncol*, *40*(2), 73–85.

Polymenidou, M., & Cleveland, D. W. (2011). The seeds of neurodegeneration: Prion-like spreading in ALS. *Cell*, *147*(3), 498–508. doi:10.1016/j.cell.2011.10.011

Prusiner, S. B. (2001). Special Article. *New England Journal of Medicine*, *344*(20), 1516–1526.

Rabbitts, T. H., Forster, A., Larson, R., & Nathan, P. (1993). Fusion of the dominant negative transcription regulator CHOP with a novel gene FUS by translocation t(12;16) in malignant liposarcoma. *Nature Genetics*, *4*(2), 175–80. doi:10.1038/ng0693-175

Rahman, M., Ham, H., Liu, X., Sugiura, Y., Orth, K., & Krämer, H. (2012). Visual neurotransmission in Drosophila requires expression of Fic in glial capitate projections. *Nature Neuroscience*, *15*(6), 871–875. doi:10.1038/nn.3102

Ravikumar, B., Vacher, C., Berger, Z., Davies, J. E., Luo, S., Oroz, L. G., … Rubinsztein, D. C. (2004). Inhibition of mTOR induces autophagy and reduces toxicity of polyglutamine expansions in fly and mouse models of Huntington disease. *Nature Genetics*, *36*(6), 585–95. doi:10.1038/ng1362

Reaume, A. G., Elliott, J. L., Hoffman, E. K., Kowall, N. W., Ferrante, R. J., Siwek, D. F., … Snider, W. D. (1996). Motor neurons in Cu/Zn superoxide dismutase-deficient mice develop normally but exhibit enhanced cell death after axonal injury. *Nature Genetics*, *13*(1), 43–7. doi:10.1038/ng0596-43

Reiter, L. T., Potocki, L., Chien, S., Gribskov, M., & Bier, E. (2001). A systematic analysis of human disease-associated gene sequences in Drosophila melanogaster. *Genome Research*, *11*(6), 1114–25. doi:10.1101/gr.169101

Renton, A. E., Chiò, A., & Traynor, B. J. (2014). State of play in amyotrophic lateral sclerosis genetics. *Nature Neuroscience*, *17*(1), 17–23. doi:10.1038/nn.3584

Renton, A. E., Majounie, E., Waite, A., Simón-sánchez, J., Rollinson, S., Gibbs, J. R., … Taynor, B. (2012). A hexanucleotide repeat expansion in C9ORF72 is the cause of chromosome 9p21-linked ALS-FTD, *72*(2), 257–268. doi:10.1016/j.neuron.2011.09.010.A

Ritson, G. P., Custer, S. K., Freibaum, B. D., Guinto, J. B., Geffel, D., Moore, J., … Taylor, J. P. (2010). TDP-43 mediates degeneration in a novel Drosophila model of disease caused by mutations in VCP/p97. *J. Neurosci.*, *30*(22), 7729–7739. doi:10.1523/JNEUROSCI.5894-09.2010.TDP-43

Robinson, J. L., Geser, F., Stieber, A., Umoh, M., Kwong, L. K., Van Deerlin, V. M., … Trojanowski, J. Q. (2012). TDP-43 skeins show properties of amyloid in a subset of ALS cases. *Acta Neuropathologica*, *29*(1), 997–1003. doi:10.1016/j.biotechadv.2011.08.021.Secreted

Rodriguez Moncalvo, V. G., & Campos, A. R. (2009). Role of serotonergic neurons in the Drosophila larval response to light. *BMC Neuroscience*, *10*, 66. doi:10.1186/1471-2202-10-66

Romano, G., Klima, R., Buratti, E., Verstreken, P., Baralle, F. E., & Feiguin, F. (2014a). Chronological requirements of TDP-43 function in synaptic organization and locomotive control. *Neurobiology of Disease*, *71*, 95–109. doi:10.1016/j.nbd.2014.07.007

Romano, M., Buratti, E., Romano, G., Klima, R., Del Bel Belluz, L., Stuani, C., … Feiguin, F. (2014b). Evolutionarily conserved heterogeneous nuclear ribonucleoprotein (hnRNP) A/B proteins functionally interact with human and Drosophila TAR DNA-binding protein 43 (TDP-43). *The Journal of Biological Chemistry*, *289*(10), 7121–30. doi:10.1074/jbc.M114.548859

Rosen, D. R., Siddique, T., Patterson, D., Figlewicz, D. A., Sapp, P., Hentati, A., … Deng, H. X. (1993). Mutations in Cu/Zn superoxide dismutase gene are associated with familial amyotrophic lateral sclerosis. *Nature*, *362*(6415), 59–62. doi:10.1038/362059a0

Ross, C. a, & Poirier, M. a. (2005). Opinion: What is the role of protein aggregation in neurodegeneration? *Nature Reviews. Molecular Cell Biology*, *6*(11), 891–8. doi:10.1038/nrm1742

Rowe, M. K., & Chuang, D.-M. (2004). Lithium neuroprotection: molecular mechanisms and clinical implications. *Expert Reviews in Molecular Medicine*, *6*(21), 1–18. doi:10.1017/S1462399404008385

Rowland, L. P. (1998). Diagnosis of amyotrophic lateral sclerosis. *Journal of the Neurological Sciences*, *160 Suppl*, S6–24.

Rowland, L. P., & Shneider, N. A. (2001). Amyotrophic lateral sclerosis. *The New England Journal of Medicine*, *344*(22), 1688–700. doi:10.1056/NEJM200105313442207

Rubinsztein, D. C. (2006). The roles of intracellular protein-degradation pathways in neurodegeneration. *Nature*, *443*(7113), 780–6. doi:10.1038/nature05291

Sanyal, S. (2009). Genomic mapping and expression patterns of C380, OK6 and D42 enhancer trap lines in the larval nervous system of Drosophila. *Gene Expression Patterns*, *9*(5), 371–380. doi:10.1016/j.gep.2009.01.002

Sarkar, S., Floto, R. A., Berger, Z., Imarisio, S., Cordenier, A., Pasco, M., … Rubinsztein, D. C. (2005). Lithium induces autophagy by inhibiting inositol monophosphatase. *The Journal of Cell Biology*, *170*(7), 1101–11. doi:10.1083/jcb.200504035

Sarkar, S., Krishna, G., Imarisio, S., Saiki, S., O'Kane, C. J., & Rubinsztein, D. C. (2008). A rational mechanism for combination treatment of Huntington's disease using lithium and rapamycin. *Human Molecular Genetics*, *17*(2), 170–8. doi:10.1093/hmg/ddm294

Sasaki, S. (2011). Autophagy in spinal cord motor neurons in sporadic amyotrophic lateral sclerosis. *Journal of Neuropathology and Experimental Neurology*, *70*(5), 349–59. doi:10.1097/NEN.0b013e3182160690

Schmid, B., Hruscha, A., Hogl, S., Banzhaf-Strathmann, J., Strecker, K., van der Zee, J., … Haass, C. (2013). Loss of ALS-associated TDP-43 in zebrafish causes muscle degeneration, vascular dysfunction, and reduced motor neuron axon outgrowth. *Proceedings of the National Academy of Sciences of the United States of America*, *110*(13), 4986–91. doi:10.1073/pnas.1218311110

Schmitten, T., & Livak, K. (2008). Analyzing real-time PCR data by the comparative C(T) method. - PubMed - NCBI. *Nat. Protoc.*, *3*(6), 1101–8.

Schneider, I. (1972). Cell lines derived from late embryonic stages of Drosophila melanogaster. *Journal of Embryology and Experimental Morphology*, *27*(2), 353–365. doi:VL - 27

Schubert, U., Antón, L. C., Gibbs, J., Norbury, C. C., Yewdell, J. W., & Bennink, J. R. (2000). Rapid degradation of a large fraction of newly synthesized proteins by proteasomes. *Nature*, *404*(6779), 770–4. doi:10.1038/35008096

Schymick, J. C., Scholz, S. W., Fung, H.-C., Britton, A., Arepalli, S., Gibbs, J. R., … Traynor, B. J. (2007). Genome-wide genotyping in amyotrophic lateral sclerosis and neurologically normal controls: first stage analysis and public release of data. *Lancet Neurology*, *6*(4), 322–8. doi:10.1016/S1474-4422(07)70037-6

Scotter, E. L., Vance, C., Nishimura, A. L., Lee, Y.-B., Chen, H.-J., Urwin, H., … Shaw, C. E. (2014). Differential roles of the ubiquitin proteasome system and autophagy in the clearance of soluble and aggregated TDP-43 species. *Journal of Cell Science*, *127*(Pt 6), 1263–78. doi:10.1242/jcs.140087

Seo, H., Sonntag, K.-C., Kim, W., Cattaneo, E., & Isacson, O. (2007). Proteasome activator enhances survival of Huntington's disease neuronal model cells. *PloS One*, *2*(2), e238. doi:10.1371/journal.pone.0000238

Sephton, C. F., Cenik, C., Kucukural, A., Dammer, E. B., Cenik, B., Han, Y., … Yu, G. (2011). Identification of neuronal RNA targets of TDP-43-containing ribonucleoprotein complexes. *Journal of Biological Chemistry*, *286*(2), 1204–1215. doi:10.1074/jbc.M110.190884

Shaw, C. E., Al-Chalabi, A., & Leigh, N. (2001). Progress in the pathogenesis of amyotrophic lateral sclerosis. *Current Neurology and Neuroscience Reports*, *1*(1), 69–76. doi:10.1007/s11910-001-0078-7

Shaw, P. J. (2005). Molecular and cellular pathways of neurodegeneration in motor neurone disease. *Journal of Neurology, Neurosurgery, and Psychiatry*, *76*(8), 1046–57. doi:10.1136/jnnp.2004.048652

Shiga, A., Ishihara, T., Miyashita, A., Kuwabara, M., Kato, T., Watanabe, N., … Onodera, O. (2012). Alteration of POLDIP3 splicing associated with loss of function of TDP-43 in tissues affected with ALS. *PLoS ONE*, *7*(8), 1–11. doi:10.1371/journal.pone.0043120

Sikorska, B., & Liberski, P. P. (2012). Human prion diseases: from Kuru to variant Creutzfeldt-Jakob disease. *Sub-Cellular Biochemistry*, *65*, 457–96. doi:10.1007/978-94-007-5416-4_17

Silani, V., Messina, S., Poletti, B., Morelli, C., Doretti, A., Ticozzi, N., & Maderna, L. (2011). The diagnosis of Amyotrophic lateral sclerosis. *Archives Italiennes de Biologie*, *149*(1), 5–27.

Skovronsky, D. M., Lee, V. M.-Y., & Trojanowski, J. Q. (2006). Neurodegenerative diseases: new concepts of pathogenesis and their therapeutic implications. *Annual Review of Pathology*, *1*, 151–70. doi:10.1146/annurev.pathol.1.110304.100113

Slow, E. J., Graham, R. K., Osmand, A. P., Devon, R. S., Lu, G., Deng, Y., … Hayden, M. R. (2005). Absence of behavioral abnormalities and neurodegeneration in vivo despite widespread neuronal huntingtin inclusions. *Proceedings of the National Academy of Sciences of the United States of America*, *102*(32), 11402–7. doi:10.1073/pnas.0503634102

Smethurst, P., Sidle, K. C. L., & Hardy, J. (2015). Review: Prion-like mechanisms of transactive response DNA binding protein of 43 kDa (TDP-43) in amyotrophic lateral sclerosis (ALS). *Neuropathology and Applied Neurobiology*, *41*(5), 578–97. doi:10.1111/nan.12206

Soto, C. (2003). Unfolding the role of protein misfolding in neurodegenerative diseases. *Nature Reviews. Neuroscience*, *4*(1), 49–60. doi:10.1038/nrn1007

Sreedharan, J., Blair, I. P., Tripathi, V. B., Hu, X., Vance, C., Rogelj, B., … Shaw, C. E. (2008). TDP-43 mutations in familial and sporadic amyotrophic lateral sclerosis. *Science (New York, N.Y.)*, *319*(5870), 1668–72. doi:10.1126/science.1154584

St. Pierre, SE, Ponting, L, Stefanscik, R, McQuilton P, and the F. C. (2014). FlyBase 102 - advance approaches to interrogating FlyBase. *Nucleic Acid Res.*, *42*(D1), D780–D788. doi:10.1093/nar/gkt1092

Stavrovskaya, I. G., Narayanan, M. V, Zhang, W., Krasnikov, B. F., Heemskerk, J., Young, S. S., … Kristal, B. S. (2004). Clinically Approved Heterocyclics Act on a Mitochondrial Target and Reduce Stroke-induced Pathology. *J. Exp. Med.*, *200*(2), 211–222. doi:10.1084/jem.20032053

Swarup, V., Phaneuf, D., Bareil, C., Robertson, J., Rouleau, G. a, Kriz, J., & Julien, J.-P. (2011). Pathological hallmarks of amyotrophic lateral sclerosis/frontotemporal lobar degeneration in transgenic mice produced with TDP-43 genomic fragments. *Brain : A Journal of Neurology*, *134*(Pt 9), 2610–26. doi:10.1093/brain/awr159

Tanaka, K., & Matsuda, N. (2014). Proteostasis and neurodegeneration: the roles of proteasomal degradation and autophagy. *Biochimica et Biophysica Acta*, *1843*(1), 197–204. doi:10.1016/j.bbamcr.2013.03.012

Tanaka, K., Mizushima, T., & Saeki, Y. (2012). The proteasome : molecular machinery and pathophysiological roles. *Biol. Chem.*, *393*, 217–234. doi:10.1515/hsz-2011-0285

Tang, T.-S., Slow, E., Lupu, V., Stavrovskaya, I. G., Sugimori, M., Llinás, R., … Bezprozvanny, I. (2005). Disturbed Ca2+ signaling and apoptosis of medium spiny neurons in Huntington's disease. *Proceedings of the National Academy of Sciences of the United States of America*, *102*(7), 2602–7. doi:10.1073/pnas.0409402102

Tanida, I., Ueno, T., & Kominami, E. (2008). LC3 and Autophagy. *Methods in Molecular Biology (Clifton, N.J.)*, *445*, 77–88. doi:10.1007/978-1-59745-157-4_4

Tsvetkov, A. S., Miller, J., Wong, J. S., Pleiss, M. A., & Finkbeiner, S. (2010). A small-molecule scaffold induces autophagy in primary neurons and protects against toxicity in a Huntington disease model. *PNAS*, *107*(39), 16982–16987. doi:10.1073/pnas.1004498107

Tyedmers, J., Mogk, A., & Bukau, B. (2010). Cellular strategies for controlling protein aggregation. *Nature Reviews. Molecular Cell Biology*, *11*(11), 777–88. doi:10.1038/nrm2993

Uchino, A., Takao, M., Hatsuta, H., Sumikura, H., Nakano, Y., Nogami, A., … Murayama, S. (2015). Incidence and extent of TDP-43 accumulation in aging human brain. *Acta Neuropathologica Communications*, *3*(1), 35. doi:10.1186/s40478-015-0215-1

Vaccaro, A., Tauffenberger, A., Ash, P. E. a, Carlomagno, Y., Petrucelli, L., & Parker, J. A. (2012). TDP-1/TDP-43 regulates stress signaling and age-dependent proteotoxicity in Caenorhabditis elegans. *PLoS Genetics*, *8*(7), e1002806. doi:10.1371/journal.pgen.1002806

Van Damme, P., Dewil, M., Robberecht, W., & Van Den Bosch, L. (2005). Excitotoxicity and amyotrophic lateral sclerosis. *Neuro-Degenerative Diseases*, *2*(3-4), 147–59. doi:10.1159/000089620

Vance, C., Rogelj, B., Hortobagyi, T., De Vos, K., Nishimura, A. L., Sreedharan, J., … Shaw, C. E. (2009). Mutations in FUS, an RNA Processing Protein, Cause Familial Amyotrophic Lateral Sclerosis Type 6. *Science*, *323*, 1208–1211. doi:10.1126/science.1165942

Voigt, A., Herholz, D., Fiesel, F. C., Kaur, K., Müller, D., Karsten, P., … Schulz, J. B. (2010). TDP-43-mediated neuron loss in vivo requires RNA-binding activity. *PloS One*, *5*(8), e12247. doi:10.1371/journal.pone.0012247

Walker, A. K., Spiller, K. J., Ge, G., Zheng, A., Xu, Y., Zhou, M., … Lee, V. M.-Y. (2015). Functional recovery in new mouse models of ALS/FTLD after clearance of pathological cytoplasmic TDP-43. *Acta Neuropathologica*. doi:10.1007/s00401-015-1460-x

Wang, H., Guan, Y., Wang, X., Smith, K., Cormier, K., Zhu, S., … Friedlander, R. M. (2007). Nortriptyline delays disease onset in models of chronic neurodegeneration. *The European Journal of Neuroscience*, *26*(3), 633–41. doi:10.1111/j.1460-9568.2007.05663.x

Wang, I.-F., Guo, B.-S., Liu, Y.-C., Wu, C.-C., Yang, C.-H., Tsai, K.-J., & Shen, C.-K. J. (2012). Autophagy activators rescue and alleviate pathogenesis of a mouse model with proteinopathies of the TAR DNA-binding protein 43. *Proceedings of the National Academy of Sciences of the United States of America*, *109*(37), 15024–9. doi:10.1073/pnas.1206362109

Wang, X., Fan, H., Ying, Z., Li, B., Wang, H., & Wang, G. (2010). Degradation of TDP-43 and its pathogenic form by autophagy and the ubiquitin-proteasome system. *Neuroscience Letters*, *469*(1), 112–6. doi:10.1016/j.neulet.2009.11.055

Watanabe, M., Dykes-Hoberg, M., Culotta, V. C., Price, D. L., Wong, P. C., & Rothstein, J. D. (2001). Histological evidence of protein aggregation in mutant SOD1 transgenic mice and in amyotrophic lateral sclerosis neural tissues. *Neurobiology of Disease*, *8*(6), 933–41. doi:10.1006/nbdi.2001.0443

Webb, J. L., Ravikumar, B., Atkins, J., Skepper, J. N., & Rubinsztein, D. C. (2003). Alpha-Synuclein is degraded by both autophagy and the proteasome. *The Journal of Biological Chemistry*, *278*(27), 25009–13. doi:10.1074/jbc.M300227200

Wegorzewska, I., Bell, S., Cairns, N. J., Miller, T. M., & Baloh, R. H. (2009). TDP-43 mutant transgenic mice develop features of ALS and frontotemporal lobar degeneration. *Proceedings of the National Academy of Sciences of the United States of America*, *106*(44), 18809–14. doi:10.1073/pnas.0908767106

Westermark, G. T., Johnson, K. H., & Westermark, P. (1999). Staining methods for identification of amyloid in tissue. *Methods in Enzymology*, *309*, 3–25. doi:10.1016/S0076-6879(99)09003-5

Wickelgren, I. (1996). For the Cortex , Neuron Loss May Be Less Than Thought. *Science*, *273*(5271), 48–50.

Williams, A., Sarkar, S., Cuddon, P., Ttofi, E. K., Saiki, S., Kane, J. O., … Rubinsztein, D. C. (2008). Novel targets for Huntington ' s disease in an mTOR-independent autophagy pathway. *Nat. Chem. Biol.*, *4*(5), 295–305. doi:10.1038/nchembio.79.

Wilson, S. M., & Standley, C. J. (2011). Treatment of protein aggregation diseases. United States Patent Application Publication.

Winton, M. J., Igaz, L. M., Wong, M. M., Kwong, L. K., Trojanowski, J. Q., & Lee, V. M.-Y. (2008). Disturbance of nuclear and cytoplasmic TAR DNA-binding protein (TDP-43) induces disease-like redistribution, sequestration, and aggregate formation. *The Journal of Biological Chemistry*, *283*(19), 13302–9. doi:10.1074/jbc.M800342200

Wu, J. S., & Luo, L. (2006). A protocol for dissecting Drosophila melanogaster brains for live imaging or immunostaining. *Nature Protocols*, *1*(4), 2110–5.

Wu, L.-S., Cheng, W.-C., Hou, S.-C., Yan, Y.-T., Jiang, S.-T., & Shen, C.-K. J. (2010). TDP-43, a neuro-pathosignature factor, is essential for early mouse embryogenesis. *Genesis (New York, N.Y. 2000)*, *48*(1), 56–62. doi:10.1002/dvg.20584.

Wu, L.-S., Cheng, W.-C., & Shen, C.-K. J. (2012). Targeted depletion of TDP-43 expression in the spinal cord motor neurons leads to the development of amyotrophic lateral sclerosis-like phenotypes in mice. *The Journal of Biological Chemistry*, *287*(33), 27335–44. doi:10.1074/jbc.M112.359000

Xu, Z.-S. (2012). Does a loss of TDP-43 function cause neurodegeneration? *Molecular Neurodegeneration*, *7*(1), 27. doi:10.1186/1750-1326-7-27

Yang, C., Wang, H., Qiao, T., Yang, B., Aliaga, L., Qiu, L., … Xu, Z. (2014). Partial loss of TDP-43 function causes phenotypes of amyotrophic lateral sclerosis. *Proceedings of the National Academy of Sciences of the United States of America*, *111*(12), E1121–9. doi:10.1073/pnas.1322641111

Yannoni, Y. M., & White, K. (1999). Domain necessary for Drosophila ELAV nuclear localization: function requires nuclear ELAV. *Journal of Cell Science*, *112 (Pt 2*, 4501–4512.

Yao, T. (2010). The role of ubiquitin in autophagy-dependent protein aggregate processing. *Genes & Cancer*, *1*(7), 779–786. doi:10.1177/1947601910383277

Yim, M. B. I. N., Kangt, J., Yim, H., Kwakt, H., Chock, P. B., & Stadtman, E. R. (1996). Cu, Zn-superoxide dismutase mutant: An enhancement of free radical formation due to a decrease in Km for hydrogen peroxide, *93*, 5709–5714.

Yoo, Y.-E., & Ko, C.-P. (2012). Dihydrotestosterone ameliorates degeneration in muscle, axons and motoneurons and improves motor function in amyotrophic lateral sclerosis model mice. *PloS One*, *7*(5), e37258. doi:10.1371/journal.pone.0037258

Zhang, T., Hwang, H.-Y., Hao, H., Talbot, C., & Wang, J. (2012). Caenorhabditis elegans RNA-processing protein TDP-1 regulates protein homeostasis and life span. *The Journal of Biological Chemistry*, *287*(11), 8371–82. doi:10.1074/jbc.M111.311977

Zhang, Y.-J., Gendron, T. F., Xu, Y.-F., Ko, L.-W., Yen, S.-H., & Petrucelli, L. (2010). Phosphorylation regulates proteasomal-mediated degradation and solubility of TAR DNA binding protein-43 C-terminal fragments. *Molecular Neurodegeneration*, *5*(1), 33. doi:10.1186/1750-1326-5-33

Zhang, Y.-J., Xu, Y.-F., Cook, C., Gendron, T. F., Roettges, P., Link, C. D., … Petrucelli, L. (2009). Aberrant cleavage of TDP-43 enhances aggregation and cellular toxicity. *Proceedings of the National Academy of Sciences of the United States of America*, *106*(18), 7607–12. doi:10.1073/pnas.0900688106

Zu, T., Gibbens, B., Doty, N. S., Gomes-pereira, M., Huguet, A., & Stone, M. D. (2010). Non-ATG – initiated translation directed by microsatellite expansions. *PNAS*, *108*(1), 260–265. doi:10.1073/pnas.1013343108

Acknowledgments

First, I want to thank Sergio that allowed me to be part of BTU since the beginning. Thanks for the immediate trust you had on me. Thanks for all the conversations and advices.

Thanks to Marco for giving me the opportunity to do this PhD, and for the consistent supervision of my thesis.

My deep gratitude is express to Tito for providing me with great guidance. I learnt a lot from your experience, and it was a pleasure for me to be able to discuss with you.

A special thank goes to Natasa. Thanks for being always there for me, both professionally and personally. I admire the passion you have for what you do, which inspired me many times during my PhD.

Thanks to Fabian for allowing me to collaborate with the Neurobiology Group. It was a great pleasure for me to be part of the group. Thanks for the support and the guidance.

I would also like to express a special thank to Raffa. It was great to have the opportunity to work with you. Thanks for your time, professionalism and patience. You started this work, and without you it wouldn´t have been possible.

Thanks to Giulia. Thank you for your silences, I learnt a lot from them. Sometimes keeping quite is a good way of saying many things.

Thanks to Simona. Thanks for being part of this project and for all the discussion. Thanks a lot for your friendship and conversations during these years.

More thanks go to my dear friend Chiara. I feel really fortunate to have met you. Thanks for having been part of all this experience. Thanks for having shared your knowledge with me and for all the conversations we had during these years.

A really special thank is reserved to Eli. You came in the moment in which I most needed you. Thanks for making me realized that even during the adulthood it is possible to make long-lasting friends. You were the perfect partner of this journey. Thanks for helping me in the bench and especially in the writing of my thesis.

The most important acknowledgment is for my family. Without your unconditional love and support nothing of this would have been possible.

List of publications

The candidate has published during the PhD period the following articles, on which most of the thesis work is based:

Cragnaz, L., Klima, R., Skoko, N., Budini, M., Feiguin, F., & Baralle, F. E. (2014). Aggregate formation prevents dTDP-43 neurotoxicity in the Drosophila melanogaster eye. Neurobiology of Disease, 71, 74–80. doi:10.1016/j.nbd.2014.07.009

Cragnaz, L., Klima, R., De Conti, L., Romano, G., Feiguin, F., Buratti, E., … Baralle, F. E. (2015). An age-related reduction of brain TBPH/TDP-43 levels precedes the onset of locomotion defects in a Drosophila ALS model. Neuroscience, 311, 415–421. doi:10.1016/j.neuroscience.2015.10.037
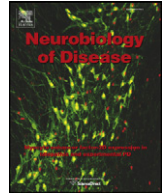
Aggregate formation prevents dTDP-43 neurotoxicity in the *Drosophila melanogaster* eye

Lucia Cragnaz [1], Raffaela Klima [1], Natasa Skoko, Mauricio Budini, Fabian Feiguin, Francisco E. Baralle *

ICGEB — International Centre for Genetic Engineering and Biotechnology, Padriciano 99, 34149 Trieste, Italy

ABSTRACT

TDP-43 inclusions are an important histopathological feature in various neurodegenerative disorders, including Amyotrophic Lateral Sclerosis and Fronto-Temporal Lobar Degeneration. However, the relation of these inclusions with the pathogenesis of the disease is still unclear. In fact, the inclusions could be toxic themselves, induce loss of function by sequestering TDP-43 or a combination of both. Previously, we have developed a cellular model of aggregation using the TDP-43 Q/N rich amino acid sequence 331–369 repeated 12 times (12xQ/N) and have shown that these cellular inclusions are capable of sequestering the endogenous TDP-43 both in non-neuronal and neuronal cells. We have tested this model *in vivo* in the *Drosophila melanogaster* eye. The eye structure develops normally in the absence of dTDP-43, a fact previously seen in knock out fly strains. We show here that expression of EGFP 12xQ/N does not alter the structure of the eye. In contrast, TBPH overexpression is neurotoxic and causes necrosis and loss of function of the eye. More important, the neurotoxicity of TBPH can be abolished by its incorporation to the insoluble aggregates induced by EGFP 12xQ/N. This data indicates that aggregation is not toxic *per se* and instead has a protective role, modulating the functional TBPH available in the tissue. This is an important indication for the possible pathological mechanism in action on ALS patients.

Introduction

The human hnRNP TDP-43 has shifted from a modest player in obscure splicing mechanisms (Buratti and Baralle, 2001) to the main protagonist in the pathogenesis of neurodegenerative diseases, such as Amyotrophic Lateral Sclerosis and Fronto-Temporal Lobar Degeneration. TDP-43 is mislocalized to the cytoplasm in the affected neurons of ALS patients, forming inclusions that contain ubiquitinated, hyperphosphorylated and cleaved TDP-43 (Neumann et al., 2006; Arai et al., 2006). This observation was followed by the identification in 2008 of mutations in the TARDBP gene in ALS patients (Sreedharan et al., 2008; Kabashi et al., 2008). However, it is important to notice that TARDBP gene mutations represent 1% of sALS cases and 4% of fALS cases, but TDP-43 is found aggregated in the 97% of all ALS cases (Ling et al., 2013). This means that TDP-43 aggregates in patients mostly

in the absence of TARDBP mutations, making the understanding of the aggregation process more difficult. TDP-43 inclusions are the main histopathological feature of the disease, but their relation with the pathogenesis of ALS is still unclear. The possibilities that the inclusions could be toxic themselves induce loss of function by sequestering TDP-43 and hence depleting the nucleus of this essential factor or a combination of both these possibilities has been considered.

It is well known that lack of TDP-43 is deleterious for the cells and for the organisms in general (Ayala et al., 2008; Feiguin et al., 2009; L.-S. Wu et al., 2010). On the other hand, excessive production of TDP-43 is harmful for the cells and the whole organism, even when there is no detectable aggregation (Barmada et al., 2010; Hanson et al., 2010; Wegorzewska et al., 2009). Not surprisingly, a very tight self-regulation mechanism is in place to ensure the right level of TDP-43 in cells, whereby TDP-43 controls its mRNA production at post-transcriptional RNA processing level by binding to its own transcript and triggering a series of events that lead to degradation of the RNA (Ayala et al., 2011; Avendaño-Vázquez et al., 2012; Bembich et al., 2013).

The mechanisms that trigger aggregation and how the aggregates increase in size are unknown. Several attempts were done to mimic the TDP-43 aggregation in cells. It was early observed that the TDP-43 C-terminal tail contains a Q/N rich region that is involved in protein–protein interaction (D'Ambrogio et al., 2009). Moreover, it was shown that expression of C-terminal fragments of TDP-43 is sufficient to generate cytoplasmic aggregates (Igaz et al., 2009). The importance

---

of the Q/N rich region within the C-terminal tail of TDP-43 in the self-aggregation process was also confirmed by Fuentealba et al. (Fuentealba et al., 2010). Based on this information and with the aim of looking for methodologies that could model the disease, we have developed a cellular model of aggregation using a 30 amino acid TDP-43 C-terminal peptide to promote TDP-43 aggregation (Budini et al., 2012a; Budini et al., 2012b). The inclusion bodies formed are predominantly cytoplasmic, ubiquitinated and phosphorylated like the ones found in patients. An animal model to extend these studies looking at *in vivo* phenotypes was needed and, in the first place, it was essential to test the aggregation profile in neurons and the effect it has on TDP-43 concentration in the target tissues.

TDP-43 is a highly conserved protein, which has a very close ortholog in *Drosophila melanogaster*, coded by the TBPH gene. As regards their binding activity and their role in splicing, the human and *Drosophila* proteins were shown to be interchangeable (Ayala et al., 2005). Furthermore, the deletion of the TBPH gene results in a locomotion defective fly (D23 and D142 strains), whose climbing ability could be restored with the expression in motor neurons of both *Drosophila* and human TDP-43 (Feiguin et al., 2009). The D23 and D142 flies do not present any evident external morphology alteration, and the eye structure is completely conserved (Feiguin et al., 2009). It follows that while TBPH plays a fundamental structural and functional role in locomotion (*i.e.*: neuromuscular junction development and maintenance), it is not essential for the development of a normal eye structure. This organ is then an ideal testing ground to study the interplay between TBPH overexpression and aggregation.

The results described here analyze the effect of TBPH overexpression in the eye, its toxic effects and their reduction by the formation of TBPH aggregates. Our results show that aggregation is not toxic *per se*. Furthermore, in the retinal tissue we demonstrated that the aggregates have a protective role, as they capture and insolubilize the excess of TBPH, blocking its toxic effect.

Materials and methods

Transgenic flies

Endogenous TBPH, its truncated form TBPHΔC (1–332) and human Tau cDNA (4N2R isoform) were Flag tagged and cloned in pKS69. EGFP-12xQ/N (12 repetitions of the TDP-43 331–369 sequence) and EGFP constructs were cloned in the pUASTattB vector (Bischof et al., 2007). All the constructs have been sequenced and subsequently used to create transgenic flies by standard embryo injections (Best Gene Inc.). While random insertions in yellow-white stain have been chosen for TBPH, TBPHΔC and human Tau, a specific insertion using strain 24486 was chosen for EGFP-12xQ/N and EGFP. All transgenic flies have been subsequently balanced on the required chromosome.

W1118, Oregon-R and GMR-Gal4 were obtained from Bloomington Drosophila Stock Center at Indiana University. Flies were fed on standard cornmeal (2.9%), sugar (4.2%), yeast (6.3%) fly food, maintained and crossed in a humidified incubator at 25 °C with a 12 hour–12 hour light–dark cycle.

Light microscopy of fly eyes

Eye phenotypes of 1 day-old flies were analyzed with a stereomicroscope (Leica MZ75) and photographed with a camera (Leica DFC420C).

For the quantitative analysis of the induced eye phenotypes we defined arbitrarily 3 categories: (1) normal eye, (2) loss of pigmentation and small regions of necrosis and (3) loss of pigmentation and massive regions of necrosis. At least 50 1 day-old flies were analyzed for each genotype.

Immunoblot

Drosophila heads were homogenized in lysis buffer (10 mM Tris–HCl, pH 7.4, 150 mM NaCl, 5 mM EDTA, 5 mM EGTA, 10% glycerol, 50 mM NaF, 5 mM DTT, 4 M urea, and protease inhibitors (Roche Diagnostic # 11836170001)). Proteins were separated by 8% SDS-PAGE, transferred to nitrocellulose membranes (Whatman # NBA083C) and probed with primary antibodies: rabbit anti-TBPH (1:3000, homemade) and mouse anti-tubulin (1:4000, Calbiochem # CP06). The membranes were incubated with the secondary antibodies: HRP-labeled anti-mouse (1:1000, Thermo Scientific # 32430) or HRP-labeled anti-rabbit (1:1000, Thermo Scientific # 32460). Finally, protein detection was assessed with Femto Super Signal substrate (Thermo Scientific # 34095).

Immunostaining

Immunostaining was performed according to standard protocols (J. S. Wu and Luo, 2006). Briefly, wandering third instar larvae were dissected in phosphate buffer and fixed in ice-cold 4% paraformaldehyde (Alfa Aesar # 30525-89-4) for 20 min, washed in Phosphate Buffer with 0.1% Tween 20 (PBT) and blocked with Normal Goat Serum (NGS, Chemicon # S26-100 ML) 30 min at room temperature. The samples were incubated with primary antibodies mouse anti-FlagM5 (1:200, Sigma # F4042), rabbit anti-GFP (1:250, Life technologies # A11122) and rat anti-ELAV (1:300, Hydridoma bank # 7E8A10) over night at 4 °C with agitation, and treated with fluorescent conjugated secondary antibodies Alexa 555 anti-mouse (1:500, Invitrogen # A21422), Alexa 488 anti-rabbit (1:500, Invitrogen # A11008) and Alexa 647 anti-rat (1:500, Invitrogen # A21472) for 2 h at room temperature. All primary and secondary antibodies were diluted in PBT-5% NGS. SlowFade Gold Antifade reagent (Life technologies # S36936) was used as a mounting medium. The samples were imaged under a confocal laser-scanning microscope (LSM 510 META; Carl Zeiss, Inc.). Images were acquired by using 63× oil immersion objective and 2× zoom. Image processing was done with ImageJ software. All images were displayed as a single section of 0.5 μm.

Solubility test

24 adult fly heads were dissected and homogenized in 192 ul of RIPA buffer (50 mM Tris–HCl, pH 8, 150 mM NaCl, 2 mM EDTA, 1% Nonidet-P40 (v/v), 0.1% SDS, 1% Na-deoxycholate and a cocktail of protease inhibitors (Roche Diagnostic # 11836170001)). The samples were incubated under agitation for 1 h at 4 °C and then centrifuged at 1000 g for 10 min at 4 °C. An aliquot was taken at this point as the input, and after a further centrifugation step at 100,000 g for 30 min at 4 °C, the supernatant was collected as the soluble fraction. The remaining pellet was re-extracted in 60 ul of urea buffer (9 M urea, 50 mM Tris–HCl, pH 8, 1% CHAPS and a cocktail of protease inhibitors (Roche # 04693159001)) and spun down to remove any precipitate, while the 9 M urea soluble material was collected as the insoluble fraction. Proteins were separated by 8% SDS-PAGE. The different samples were loaded in a proportion 1:1:1 for the input, soluble and insoluble fractions. Proteins were electro-blotted to a nitrocellulose membrane (Whatman # NBA083C) and probed with the following primary antibodies: rabbit anti-TBPH (1:3000, home-made), mouse anti-GFP (1:2000, Roche # 11814460001) and mouse anti-tubulin (1:4000, Calbiochem # CP06). The membranes were incubated with the secondary antibodies: HRP-labeled anti-mouse (1:1000, Thermo Scientific # 32430) or HRP-labeled anti-rabbit (1:1000, Thermo Scientific # 32460). Finally, protein detection was assessed with Femto Super Signal substrate (Thermo Scientific # 34095).

Climbing assay

1 day-old flies were transferred without anesthesia to a 15 ml conical tube, tapped to the bottom of the tube, and their subsequent climbing activity was quantified as number of flies that reach the top of the tube in 15 s. At least 100 flies of each genotype were tested. In each set of experiments 20 flies were introduced in the cylinder and tested three times. The number of top climbing flies was converted into % value, and the mean % value (±SEM) was calculated for at least 5 experiments.

Phototaxis assay

Phototaxis assay was performed in a Y-maze with one arm exposed to violet light (peak wavelength 400 nm) and the other arm completely in the dark. Flies from each genotype were independently introduced into the stem of the Y-maze, and had the choice between violet light and the dark. After 30 s the number of flies that moved towards the illuminated chamber was determined. In each test 50 flies were analyzed. At least 100 flies of each genotype were tested. The number of phototactic flies was converted into % value, and the mean % value (±SEM) was calculated.

Statistics

One-way ANOVA followed by Bonferroni's multiple comparison was used to compare measures among 4 groups. Unpaired t-test analysis was used to compare measures between 2 groups. The significance between the variables was shown based on the p-value obtained (ns indicates $p > 0.05$, * indicates $p < 0.05$, ** indicates $p < 0.01$, *** indicates $p < 0.001$ and **** indicates $p < 0.0001$). Values are presented as a mean and error bars indicate standard error of the mean (SEM).

Results and discussion

EGFP-12xQ/N expression forms insoluble aggregates in retinal cells with no consequence for the eye structure

Our previously developed cellular model of TDP-43 aggregation showed that repeated TDP-43 amino acid sequence 331–369 (12xQ/N)

is capable of interacting with TDP-43 inducing its aggregation both in non-neuronal and neuronal cells (Budini et al., 2012a).

To determinate whether similar interactions occur *in vivo*, we created transgenic *D. melanogaster* lines encoding either the *Drosophila* TDP-43 ortholog, TBPH, or the 12 repetitions of the 331–369 sequence of TDP-43 tagged with EGFP (EGFP-12xQ/N), under the control of the upstream activating sequence (UAS) (Brand and Perrimon, 1993).

After crossing the transgenic line EGFP-12xQ/N with the eye-specific GMR-Gal4 driver, we analyzed biochemically the solubility of the expressed protein and observed that EGFP-12xQ/N is mainly in the insoluble fraction, while EGFP alone is a soluble protein (Fig. 1a). Moreover, we found that neither the expression of the EGFP-12xQ/N, nor the expression of EGFP alone affect the external structure of the eye (Fig. 1b), meaning that EGFP-12xQ/N aggregates, *per se*, are not neurotoxic.

EGFP-12xQ/N expression rescues TBPH-induced neurodegeneration

As reported for the human protein (Li et al., 2010; Miguel et al., 2011), the overexpression of TBPH with the GMR-Gal4 driver induced a remarkable degeneration of the external surface of the eye, with the formation of necrotic patches, followed by the consistent loss of eye pigmentation (*compare* Figs. 2a and b). Surprisingly, such a strong neurodegeneration was completely reverted by the co-expression of TBPH together with EGFP-12xQ/N (Fig. 2c). We assumed that this improvement was due to the modulation of the TBPH cellular levels by sequestration of the protein in the EGFP-12xQ/N aggregates.

Such recovery of the degenerated phenotype is 12xQ/N related and cannot be due to a non-specific effect since the co-expression of EGFP, without the 12xQ/N tail, and TBPH did not prevent the retinal degeneration induced by TBPH expression (Fig. 2d). A quantitative analysis of the phenotypes was performed examining at least 50 flies per genotype (Fig. 2e).

The TBPH C-terminal amino acids are essential for the interaction with the EGFP-12xQ/N aggregates

In previously published results (Budini et al., 2012a) we demonstrated that the C-terminal tail of human TDP-43 is the part of the protein required for the protein–protein interaction. The expression of TBPH lacking the C-terminal tail under GMR-Gal4 driver induced also a strong
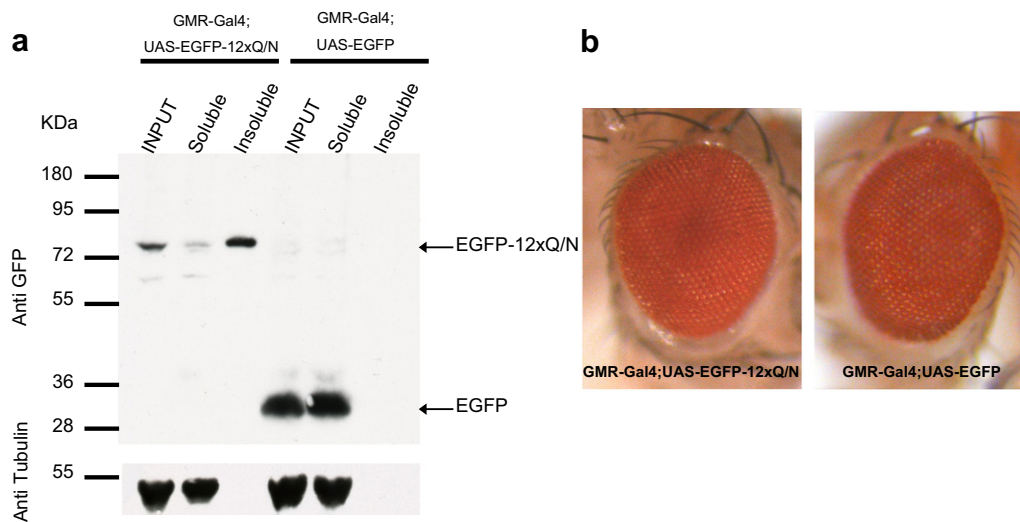

Fig. 1. (a) Western blot of fractionated proteins obtained from GMR-Gal4;UAS-EGFP-12xQ/N and GMR-Gal4;UAS-EGFP adult fly heads. Total proteins were fractionated into soluble and insoluble fractions. The proteins were detected using an anti-GFP antibody. EGFP-12xQ/N is mainly an insoluble protein, whereas EGFP alone is found only in the soluble fraction. Tubulin served as loading control. (b) External eye phenotype of flies GMR-Gal4;UAS-EGFP-12xQ/N and GMR-Gal4;UAS-EGFP, the external eye phenotype of both flies is completely normal.
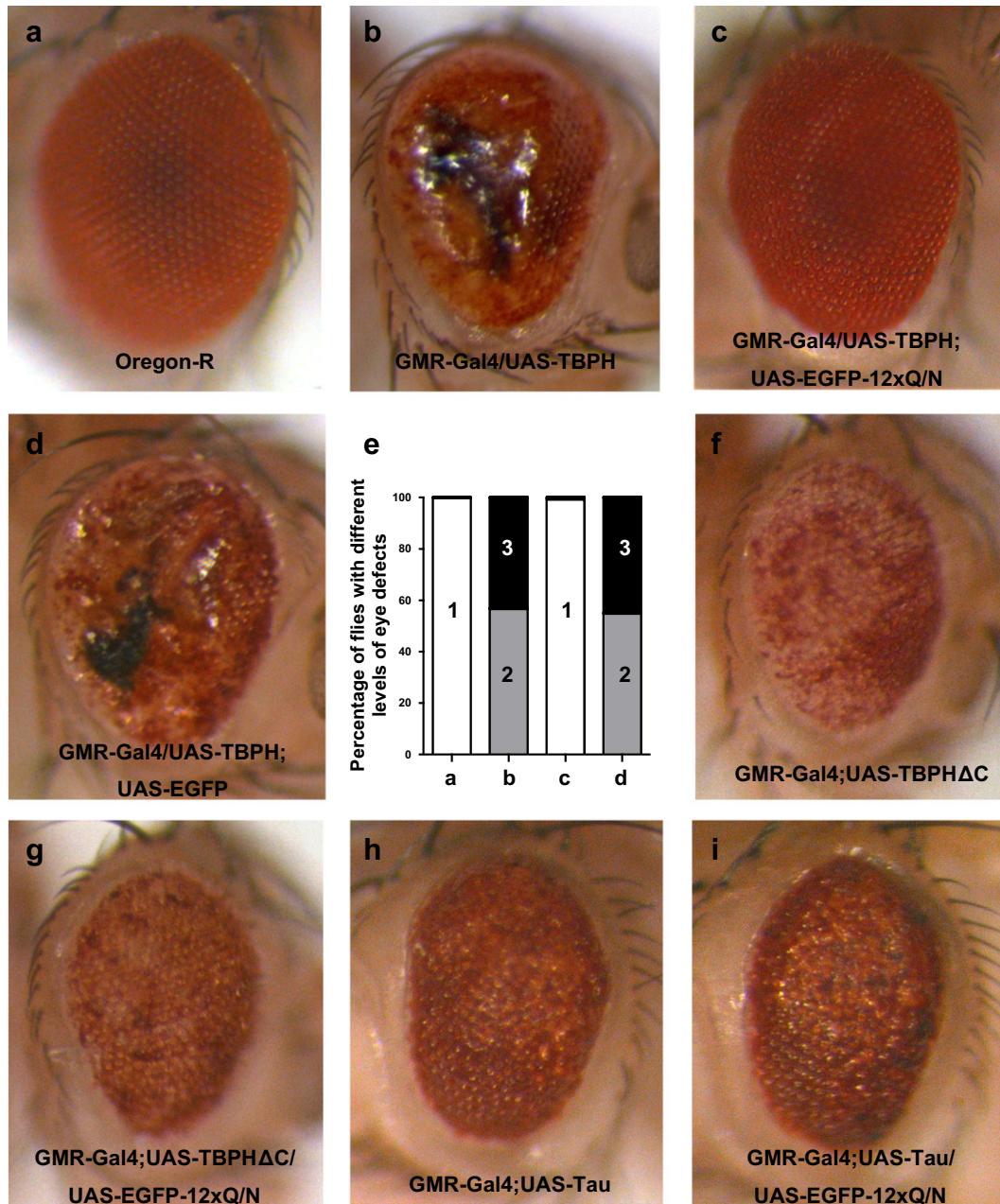
Fig. 2. External eye phenotype of flies: (a) Oregon-R, (b) GMR-Gal4/UAS-TBPH, (c) GMR-Gal4/UAS-TBPH;UAS-EGFP-12xQ/N, (d) GMR-Gal4/UAS-TBPH;UAS-EGFP, (f) GMR-Gal4;UAS-TBPHΔC, (g) GMR-Gal4;UAS-TBPHΔC/UAS-EGFP-12xQ/N, (h) GMR-Gal4;UAS-Tau, (i) GMR-Gal4;UAS-Tau/UAS-EGFP-12xQ/N. (e) Quantification of eye defects for Oregon-R, GMR-Gal4/UAS-TBPH, GMR-Gal4/UAS-TBPH;UAS-EGFP-12xQ/N, GMR-Gal4/UAS-TBPH;UAS-EGFP flies. We defined arbitrarily 3 categories: (1) normal eye, (2) loss of pigmentation and small regions of necrosis and (3) loss of pigmentation and massive regions of necrosis. Expression of TBPH induces degeneration in Drosophila eye (b). The co-expression of EGFP-12xQ/N rescues the eye degeneration (c), whereas the co-expression of EGFP alone does not change the phenotype induced by TBPH expression (d). On the other hand, expression of TBPHΔC also induces degeneration in *Drosophila* eye (f). The co-expression of EGFP-12xQ/N does not rescue this degeneration (g). The expression of Tau also induces degeneration in *Drosophila* eye (h), and the co-expression of EGFP-12xQ/N does not rescue this degeneration (i).

phenotype in the eye that includes rough degeneration of the eye surface and extensive depigmentation of the retina (Fig. 2f). Although this phenotype was milder compared to the expression of the TBPH full-length protein, we did not observe any modification of the phenotype upon co-expression of TBPHΔC and EGFP-12xQ/N (*compare* Figs. 2f and g). This result suggests that the direct interaction between these proteins is required to prevent TBPH-mediated neurodegeneration.

Moreover, we investigated if the effect seen with EGFP-12xQ/N was specific for the neurodegeneration induced by TBPH overexpression. For this purpose, we focused on Tau protein, which is involved in other proteinopathies. Tau expression in *Drosophila* eye caused degeneration

of the retinal tissue, which could not be rescue by the co-expression of EGFP-12xQ/N (*compare* Figs. 2h and i).

EGFP-12xQ/N expression promotes TBPH aggregation in retinal cells

Importantly, EGFP-12xQ/N expression does not suppress the TBPH-induced eye phenotype simple through down-regulation of transgene expression, as reveled by western blot analysis (Fig. 3). Co-expression of TBPH and EGFP-12xQ/N or EGFP did not change the total TBPH level, pointing to a different functionality of the protein, most probably due to its physical status.
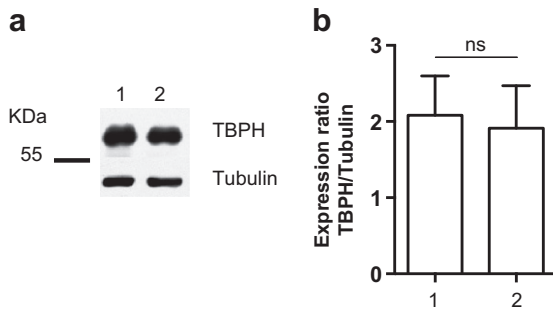
a

b

Fig. 3. (a) Quantification of TBPH level on total protein extracts prepared from adult fly heads GMR-Gal4/UAS-TBPH;UAS-EGFP-12xQ/N (1) and GMR-Gal4/UAS-TBPH;UAS-EGFP (2). A representative western blot is shown. Tubulin was used as a loading control. (b) Image J quantification of TBPH was performed from three independent experiments. ns indicates p > 0.05 (not significant) calculated by unpaired t-test. Error bars indicate SEM.

In order to further explore the mechanism behind the recovery of the TBPH-induced eye phenotype by EGFP-12xQ/N expression, we looked for potential modifications in the intracellular pattern of TBPH by performing a biochemical fractionation of the *Drosophila* adult head proteins extracted from GMR-Gal4/UAS-TBPH;UAS-EGFP and GMR-Gal4/UAS-TBPH;UAS-EGFP-12xQ/N expressing flies. Fig. 4 shows a clear shift in the TBPH solubility pattern when it is co-expressed with EGFP-12xQ/N compared with EGFP control. In the case of GMR-Gal4/UAS-TBPH;UAS-EGFP flies, TBPH appears mainly in the soluble fraction, whereas in GMR-Gal4/UAS-TBPH;UAS-EGFP-12xQ/N flies, the majority of the TBPH is present in the insoluble fraction.

EGFP-12xQ/N and TBPH co-localize in the Drosophila eye discs

The fact that the TBPH-induced degeneration was completely rescued when EGFP-12xQ/N was co-expressed with TBPH (Fig. 2c), taken together with the solubility data reported above (Fig. 4), implied that
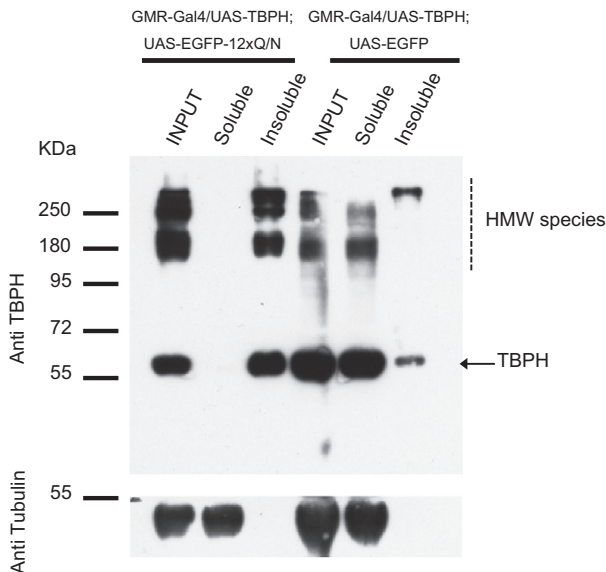

Fig. 4. Western blot of fractionated proteins obtained from GMR-Gal4/UAS-TBPH;UAS-EGFP-12xQ/N and GMR-Gal4/UAS-TBPH;UAS-EGFP adult fly heads. Total proteins were separated into soluble and insoluble fractions. Proteins were detected with anti-TBPH antibody (arrow and high molecular weight (HMW) species). Tubulin served as a loading control. Co-expression of EGFP-12xQ/N and TBPH leads to formation of insoluble protein aggregates. In contrast, TBPH remains mainly soluble when it is co-express with EGFP.

TBPH may be sequestered in the EGFP-12xQ/N aggregates, allowing a reduction in TBPH availability and avoiding the relative degeneration induced by its high level. To test this hypothesis we analyzed the localization of both proteins in the retinal cells. Immunohistochemistry of the third instar larvae eye discs was performed in order to examine the cellular distribution of the proteins, in GMR-Gal4/UAS-TBPH;UAS-EGFP and GMR-Gal4/UAS-TBPH;UAS-EGFP-12xQ/N transgenic lines. In the case of the larvae expressing TBPH and EGFP, both proteins were homogeneously distributed (Fig. 5a), while TBPH was found aggregated and co-localizing with the EGFP-12xQ/N aggregates when both proteins were co-expressed (Fig. 5b). Moreover, we confirmed that the observed co-localization of TBPH and EGFP-12xQ/N in the aggregates was abrogated when the C-terminal tail of TBPH was not present (Fig. 5c).

It can be concluded that the neurotoxicity caused by increased level of TBPH *in vivo* is modulated by its aggregation. In fact, the co-expression of EGFP-12xQ/N in *Drosophila* eye is protective by titrating the excess of the active TBPH.

This effect differs from the protective role postulated for Lewy bodies (present in Parkinson's disease and composed mainly by mutant α-synuclein), hyperphosphorylated Tau aggregates (Alzheimer's disease) and huntingtin inclusions that result from polyglutamine expansions (Huntington's disease). In all these cases, it has been proposed that the toxicity is a consequence of a mutation or abnormal modification of the protein, and that the aggregation is able to reduce this toxicity (Arrasate et al., 2004; Cowan and Mudher, 2013; Tanaka et al., 2004). However, in our case, the aggregates have a protective effect as just remove the wild type TBPH in excess.

EGFP-12xQ/N expression restores eye functionality in TBPH expressing flies

To determinate whether the suppression of TBPH toxicity by EGFP-12xQ/N is correlated with eye functionality, phototaxis assay was performed with 1 day-old flies of the different genotypes (Fig. 6a). TBPH overexpressing flies were not attracted to the light source, meaning that they were blind, consistent with the defective morphology of the eye structure. In flies co-expressing TBPH and EGFP-12xQ/N the vision was restored to normal levels, as there was not significant difference compared to the wild type flies, consistent with the recovery of the eye morphology. Moreover, the visual deficit was still present in flies co-expressing EGFP and TBPH.

Fig. 6b shows that the climbing ability of the flies of all the genotypes analyzed was comparable to the wild type flies, meaning that the negative phototaxis result is not due to a motor impairment.

Conclusions

We have shown here that the neurotoxicity caused by increased level of TBPH *in vivo* can be modulated by its aggregation. The co-expression of EGFP-12xQ/N, an inducer of TBPH aggregation, in *Drosophila* eye is protective, because the excess TBPH becomes a non-functional insoluble protein as part of the induced inclusions.

TDP-43 has a natural tendency to aggregate and in normal circumstances a small fraction of the protein is insoluble in the tissues. During aging, the clearance of TDP-43 aggregates by, for example, the autophagy pathway or by the proteasomes may become more difficult. The increasing capture of TDP-43 by growing cytoplasmic aggregates may lower the amount of TDP-43 returning to the nucleus. This drop in levels will be sensed by the self-regulation mechanism, and may in turn increase the TDP-43 mRNA levels and hence the protein levels. This over-expression of TDP-43 could be initially modulated by the aggregates that capture the protein in excess, maintaining acceptable levels of active protein in the cell. However, continued addition to the inclusions will make them grow to a point in which they will capture so much protein that the nuclear capacity to produce TDP-43 mRNA will be overcome. This situation will lead to a lack of TDP-43, and its nuclear function will be lost, leading to neuronal loss.
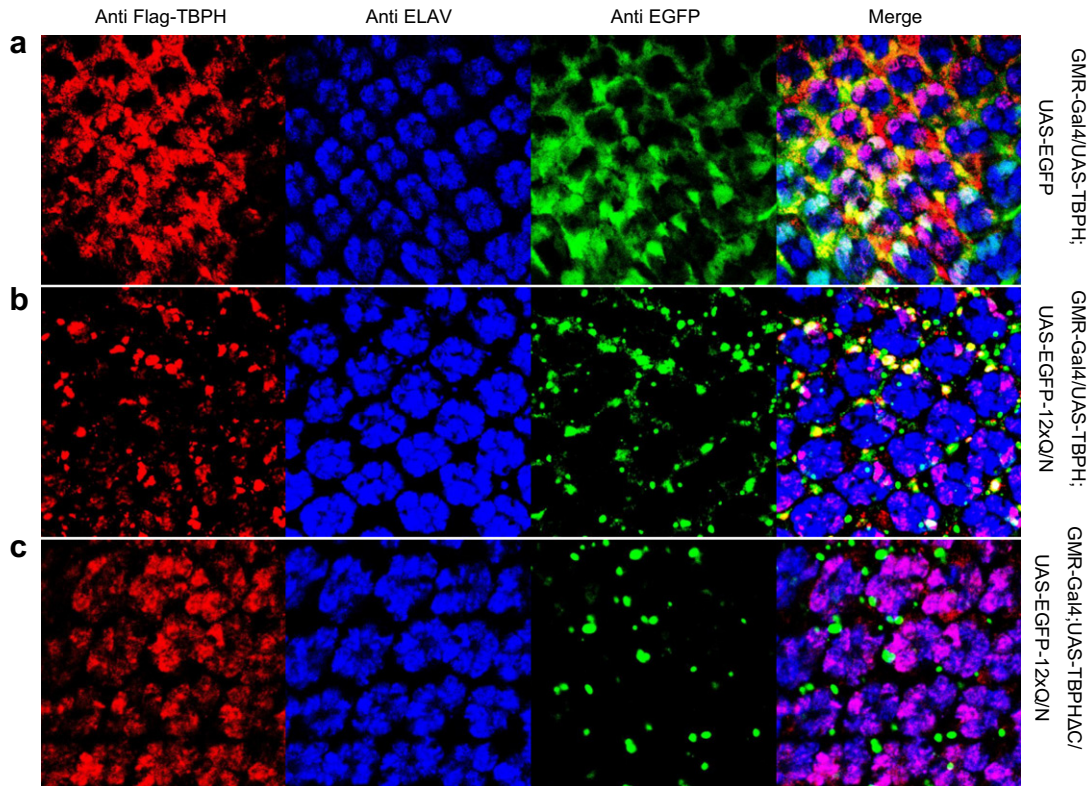
Fig. 5. Confocal images of third instar larvae eye disc co-expressing TBPH and EGFP (a), TBPH and EGFP-12xQ/N (b), TBPHΔC and EGFP-12xQ/N (c). Samples were stained for ELAV, Flag-TBPH, and EGFP. All the figures correspond to a single confocal section.
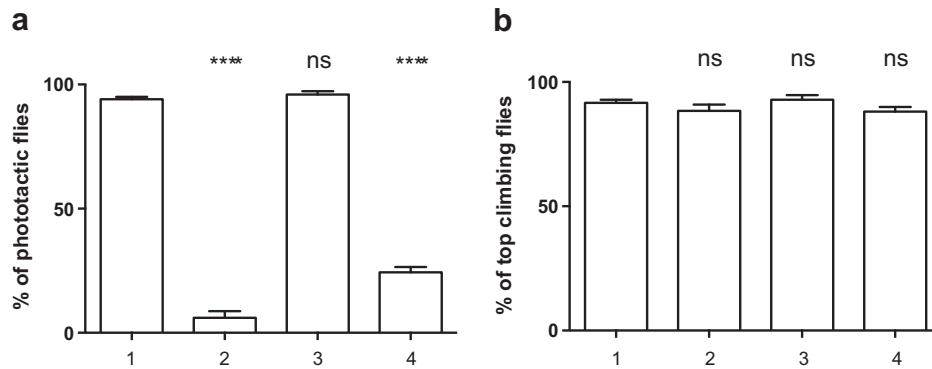

Fig. 6. Phototaxis assay of 1-day-old flies of different genotypes indicated as follows: (1) Oregon-R, (2) GMR-Gal4/UAS-TBPH, (3) GMR-Gal4/UAS-TBPH;UAS-EGFP-12xQ/N, (4) GMR-Gal4/UAS-TBPH;UAS-EGFP. Flies expressing TBPH are not attracted to the light, whereas flies co-expressing TBPH and EGFP-12xQ/N are attracted in the same proportion as wild type flies. On the contrary, the co-expression of TBPH and EGFP does not restore the vision. **** indicates $p < 0.0001$ and ns indicates $p > 0.05$ (not significant) calculated by one-way ANOVA followed by Bonferroni's multiple comparison. Error bars indicate SEM. (b) Climbing assay of 1-day-old flies of different genotypes. The climbing ability of all the genotypes was comparable to the wild type. ns indicates $p > 0.05$ (not significant) calculated by one-way ANOVA followed by Bonferroni's multiple comparison. Error bars indicate SEM.

References

Arai, T., Hasegawa, M., Akiyama, H., Ikeda, K., Nonaka, T., Mori, H., Oda, T., 2006. TDP-43 is a component of ubiquitin-positive tau-negative inclusions in frontotemporal lobar degeneration and amyotrophic lateral sclerosis. Biochem. Biophys. Res. Commun. 351 (3), 602–611. http://dx.doi.org/10.1016/j.bbrc.2006.10.093.

Arrasate, M., Mitra, S., Schweitzer, E.S., Segal, M.R., Finkbeiner, S., 2004. Inclusion body formation reduces levels of mutant huntingtin and the risk of neuronal death. Nature 431 (7010), 805–810. http://dx.doi.org/10.1038/nature02998.

Avendaño-Vázquez, S.E., Dhir, A., Bembich, S., Buratti, E., Proudfoot, N., Baralle, F.E., 2012. Autoregulation of TDP-43 mRNA levels involves interplay between transcription, splicing, and alternative polyA site selection. Genes Dev. 26 (15), 1679–1684. http://dx.doi.org/10.1101/gad.194829.112.

Ayala, Y.M., Pantano, S., D'Ambrogio, A., Buratti, E., Brindisi, A., Marchetti, C., Baralle, F.E., 2005. Human, *Drosophila*, and *C. elegans* TDP43: nucleic acid binding properties and splicing regulatory function. J. Mol. Biol. 348 (3), 575–588. http://dx.doi.org/10.1016/j.jmb.2005.02.038.

Ayala, Y.M., Misteli, T., Baralle, F.E., 2008. TDP-43 regulates retinoblastoma protein phosphorylation through the repression of cyclin-dependent kinase 6 expression. Proc. Natl. Acad. Sci. U. S. A. 105 (10), 3785–3789. http://dx.doi.org/10.1073/pnas.0800546105.

Ayala, Y.M., De Conti, L., Avendaño-Vázquez, S.E., Dhir, A., Romano, M., D'Ambrogio, A., Baralle, F.E., 2011. TDP-43 regulates its mRNA levels through a negative

feedback loop. EMBO J. 30 (2), 277–288. http://dx.doi.org/10.1038/emboj.2010.310.

Barmada, S.J., Skibinski, G., Korb, E., Rao, E.J., Wu, J.Y., Finkbeiner, S., 2010. Cytoplasmic mislocalization of TDP-43 is toxic to neurons and enhanced by a mutation associated with familial amyotrophic lateral sclerosis. J. Neurosci. Off. J. Soc. Neurosci. 30 (2), 639–649. http://dx.doi.org/10.1523/JNEUROSCI.4988-09.2010.

Bembich, S., Herzog, J.S., De Conti, L., Stuani, C., Avendaño-Vázquez, S.E., Buratti, E., Baralle, F. E., 2013. Predominance of spliceosomal complex formation over polyadenylation site selection in TDP-43 autoregulation. Nucleic Acids Res. 42 (5), 3362–3371. http://dx.doi.org/10.1093/nar/gkt1343.

Bischof, J., Maeda, R.K., Hediger, M., Karch, F., Basler, K., 2007. An optimized transgenesis system for *Drosophila* using germ-line-specific phiC31 integrases. Proc. Natl. Acad. Sci. U. S. A. 104 (9), 3312–3317. http://dx.doi.org/10.1073/pnas.0611511104.

Brand, a H., Perrimon, N., 1993. Targeted gene expression as a means of altering cell fates and generating dominant phenotypes. Dev. Suppl. 118 (2), 401–415.

Budini, M., Buratti, E., Stuani, C., Guarnaccia, C., Romano, V., De Conti, L., Baralle, F.E., 2012a. Cellular model of TAR DNA-binding protein 43 (TDP-43) aggregation based on its C-terminal Gln/Asn-rich region. J. Biol. Chem. 287 (10), 7512–7525. http://dx.doi.org/10.1074/jbc.M111.288720.

Budini, M., Romano, V., Avendaño-Vázquez, S.E., Bembich, S., Buratti, E., Baralle, F.E., 2012b. Role of selected mutations in the Q/N rich region of TDP-43 in EGFP-12xQ/N-induced aggregate formation. Brain Res. 1462, 139–150. http://dx.doi.org/10.1016/j.brainres.2012.02.031.

Buratti, E., Baralle, F.E., 2001. Characterization and functional implications of the RNA binding properties of nuclear factor TDP-43, a novel splicing regulator of CFTR exon 9. J. Biol. Chem. 276 (39), 36337–36343. http://dx.doi.org/10.1074/jbc.M104236200.

Cowan, C.M., Mudher, A., 2013. Are tau aggregates toxic or protective in tauopathies? Front. Neurol. 4 (August), 114. http://dx.doi.org/10.3389/fneur.2013.00114.

D'Ambrogio, A., Buratti, E., Stuani, C., Guarnaccia, C., Romano, M., Ayala, Y.M., Baralle, F.E., 2009. Functional mapping of the interaction between TDP-43 and hnRNP A2 *in vivo*. Nucleic Acids Res. 37 (12), 4116–4126. http://dx.doi.org/10.1093/nar/gkp342.

Feiguin, F., Godena, V.K., Romano, G., D'Ambrogio, A., Klima, R., Baralle, F.E., 2009. Depletion of TDP-43 affects *Drosophila* motoneurons terminal synapsis and locomotive behavior. FEBS Lett. 583 (10), 1586–1592. http://dx.doi.org/10.1016/j.febslet.2009.04.019.

Fuentealba, R. a, Udan, M., Bell, S., Wegorzewska, I., Shao, J., Diamond, M.I., Baloh, R.H., 2010. Interaction with polyglutamine aggregates reveals a Q/N-rich domain in TDP-43. J. Biol. Chem. 285 (34), 26304–26314. http://dx.doi.org/10.1074/jbc.M110.125039.

Hanson, K. a, Kim, S.H., Wassarman, D. a, Tibbetts, R.S., 2010. Ubiquilin modifies TDP-43 toxicity in a *Drosophila* model of amyotrophic lateral sclerosis (ALS). J. Biol. Chem. 285 (15), 11068–11072. http://dx.doi.org/10.1074/jbc.C109.078527.

Igaz, L.M., Kwong, L.K., Chen-Plotkin, A., Winton, M.J., Unger, T.L., Xu, Y., Lee, V.M.-Y., 2009. Expression of TDP-43 C-terminal fragments in vitro recapitulates pathological features of TDP-43 proteinopathies. J. Biol. Chem. 284 (13), 8516–8524. http://dx.doi.org/10.1074/jbc.M809462200.

Kabashi, E., Valdmanis, P.N., Dion, P., Spiegelman, D., McConkey, B.J., Vande Velde, C., Rouleau, G.a., 2008. TARDBP mutations in individuals with sporadic and familial amyotrophic lateral sclerosis. Nat. Genet. 40 (5), 572–574. http://dx.doi.org/10.1038/ng.132.

Li, Y., Ray, P., Rao, E.J., Shi, C., Guo, W., Chen, X., Wu, J.Y., 2010. A *Drosophila* model for TDP-43 proteinopathy. Proc. Natl. Acad. Sci. U. S. A. 107 (7), 3169–3174. http://dx.doi.org/10.1073/pnas.0913602107.

Ling, S.-C., Polymenidou, M., Cleveland, D.W., 2013. Converging mechanisms in ALS and FTD: disrupted RNA and protein homeostasis. Neuron 79 (3), 416–438. http://dx.doi.org/10.1016/j.neuron.2013.07.033.

Miguel, L., Frébourg, T., Campion, D., Lecourtois, M., 2011. Both cytoplasmic and nuclear accumulations of the protein are neurotoxic in *Drosophila* models of TDP-43 proteinopathies. Neurobiol. Dis. 41 (2), 398–406. http://dx.doi.org/10.1016/j.nbd.2010.10.007.

Neumann, M., Sampathu, D.M., Kwong, L.K., Truax, A.C., Micsenyi, M.C., Chou, T.T., Lee, V.M.-Y., 2006. Ubiquitinated TDP-43 in frontotemporal lobar degeneration and amyotrophic lateral sclerosis. Science (New York, N.Y.) 314 (5796), 130–133. http://dx.doi.org/10.1126/science.1134108.

Sreedharan, J., Blair, I.P., Tripathi, V.B., Hu, X., Vance, C., Rogelj, B., Shaw, C.E., 2008. TDP-43 mutations in familial and sporadic amyotrophic lateral sclerosis. Science (New York, N.Y.) 319 (5870), 1668–1672. http://dx.doi.org/10.1126/science.1154584.

Tanaka, M., Kim, Y.M., Lee, G., Junn, E., Iwatsubo, T., Mouradian, M.M., 2004. Aggresomes formed by alpha-synuclein and synphilin-1 are cytoprotective. J. Biol. Chem. 279 (6), 4625–4631. http://dx.doi.org/10.1074/jbc.M310994200.

Wegorzewska, I., Bell, S., Cairns, N.J., Miller, T.M., Baloh, R.H., 2009. TDP-43 mutant transgenic mice develop features of ALS and frontotemporal lobar degeneration. Proc. Natl. Acad. Sci. U. S. A. 106 (44), 18809–18814. http://dx.doi.org/10.1073/pnas.0908767106.

Wu, J.S., Luo, L., 2006. A protocol for dissecting *Drosophila melanogaster* brains for live imaging or immunostaining. Nat. Protoc. 1 (4), 2110–2115.

Wu, L.-S., Cheng, W.-C., Hou, S.-C., Yan, Y.-T., Jiang, S.-T., Shen, C.-K.J., 2010. TDP-43, a neuro-pathosignature factor, is essential for early mouse embryogenesis. Genesis 48 (1), 56–62. http://dx.doi.org/10.1002/dvg.20584.

AN AGE-RELATED REDUCTION OF BRAIN TBPH/TDP-43 LEVELS PRECEDES THE ONSET OF LOCOMOTION DEFECTS IN A *DROSOPHILA* ALS MODEL

L. CRAGNAZ, R. KLIMA, L. DE CONTI, G. ROMANO,
F. FEIGUIN, E. BURATTI, M. BARALLE AND
F. E. BARALLE *

ICGEB – International Centre for Genetic Engineering and Biotechnology, Padriciano 99, 34149 Trieste, Italy

Abstract—Amyotrophic lateral sclerosis (ALS) is a fatal neurodegenerative disease. The average age of onset of both sporadic and familial cases is 50–60 years of age. The presence of cytoplasmic inclusions of the RNA-binding protein TAR DNA-binding protein-43 (TDP-43) in the affected neurons is seen in 95% of the ALS cases, which results in TDP-43 nuclear clearance and loss of function. The *Drosophila melanogaster* ortholog of TDP-43 (TBPH) shares many characteristics with the human protein. Using a TDP-43 aggregation inducer previously developed in human cells, we created a transgenic fly that shows an adult locomotive defect. Phenotype onset correlates with a physiologically age-related drop of TDP-43/TBPH mRNA and protein levels, seen both in mice and flies. Artificial reduction of mRNA levels, *in vivo*, anticipates the locomotion defect to the larval stage. Our study links, for the first time, aggregation and the age-related, evolutionary conserved reduction of TDP-43/TBPH levels with the onset of an ALS-like locomotion defect in a *Drosophila* model. A similar process might trigger the human disease. © 2015 The Authors. Published by Elsevier Ltd. on behalf of IBRO. This is an open access article under the CC BY-NC-ND license (http://creativecommons.org/licenses/by-nc-nd/4.0/).

Key words: TDP-43/TBPH levels, aggregation, *Drosophila*, ALS.

INTRODUCTION

The major histopathological feature, seen in around 95% of amyotrophic lateral sclerosis (ALS) patients, is the presence of cytoplasmic TAR DNA-binding protein-43 (TDP-43) inclusions in the affected neurons (Ling et al., 2013; Gomez-Deza et al., 2015), resulting in TDP-43 nuclear clearance and loss of TDP-43 nuclear function, which in turn may lead to cellular dysfunctions (Neumann et al., 2006; Arai et al., 2006).

TDP-43 is a protein that has a marked tendency to unfold and become insoluble both *in vitro* and *in vivo*. In particular, its C-terminal end has a so-called "prion-like domain" between amino acids 331–369 (Udan and Baloh 2011; Nonaka et al., 2013). This sequence is rich in Glutamine (Q) and Asparagine (N), and is involved both in the interactions with other proteins and the self-aggregation process (D'Ambrogio et al., 2009; Igaz et al., 2009; Budini et al., 2012; Budini et al., 2014). We have previously developed a cellular model of aggregation using the TDP-43 Q/N rich amino acid sequence repeated 12 times linked to the EGFP sequence. These cellular inclusions were shown to be capable of sequestering the endogenous TDP-43 both in non-neuronal and neuronal cells (Budini et al., 2012).

The link between aggregate formation and loss of function, to date is still not fully understood. It has been suggested that the late onset of ALS in humans may be due to mitochondrial dysfunction, ineffective unfolded protein response and defects in the autophagy or proteasome systems (Ling et al., 2013; Cozzolino and Carrì, 2012). Indeed, if the clearance system is defective there will be persistence of aggregates in the cell. However, this does not provide an explanation for why the aggregates may persist for many years with no ALS-related symptoms. In fact, 29% of normal individuals over 65 years old present TDP-43 inclusions in the brain (Geser et al., 2010). Furthermore, there is still no answer to the question of why mutations in TDP-43 or other TDP-43-ALS related genes do not anticipate the onset of the symptoms in human patients.

In this work, we have used the EGFP-12xQ/N aggregation model to explore the connection between the aggregate formation and the onset of the disease. We present here data indicating that the combination of physiological age-related reduction of TAR DNA-binding protein-43 *Drosophila melanogaster* ortholog (TBPH)/TDP-43 levels with the presence of aggregates, that sequester this protein in the cytoplasm, leads to a locomotion defect due to the depletion of functional TDP-43 in a *Drosophila* ALS model.

EXPERIMENTAL PROCEDURES

Fly stocks

EGFP-12xQ/N (12 repetitions of the TDP-43 amino acids stretch 331–369 sequence tagged with EGFP) and EGFP constructs were cloned in the pUASTattB vector. All the

---

*Corresponding author.
E-mail address: baralle@icgeb.org (F. E. Baralle).
Abbreviations: 12xQ/N, repeated TDP-43 amino acid sequence 331–369; ALS, amyotrophic lateral sclerosis; CNS, central nervous system; TDP-43, TAR DNA-binding protein-43; TBPH, TAR DNA-binding protein-43 *Drosophila melanogaster* ortholog.

constructs have been sequenced and subsequently used to create transgenic flies by standard embryo injections (Best Gene Inc.). Specific insertion of the transgene was performed using strain 24486. Transgenic flies have been subsequently balanced on the required chromosome.

RNA interference flies for TBPH (ID 38377) were obtained from VDRC Vienna. W1118 and ELAV-Gal4 were obtained from Bloomington *Drosophila* Stock Center at Indiana University. Flies were fed on standard cornmeal (2.9%), sugar (4.2%), yeast (6.3%) fly food, maintained and crossed in a humidified incubator at 25 °C (unless stated otherwise) with a 12 h–12 h light–dark cycle.

Climbing assay

Flies were transferred without anesthesia to a 50 ml glass-cylinder, taped to the bottom of the tube, and their subsequent climbing activity was quantified as the number of flies that reach the top of the tube in 15 s. At least 100 flies of each genotype were tested. In each set of experiments 20 flies (1:1 male:female ratio) were introduced in the cylinder and tested in triplicate. The number of top climbing flies was converted into % value, and the mean % value (±SEM) was calculated for at least five experiments.

Life span

Adult flies were collected for 2 days and transferred to tubes with food. Each tube contained 20 flies in a proportion 1:1 male:female ratio. Every third day, flies were transferred to a fresh tube and deaths were scored. Survival rate was plotted as percentage of survival flies against day. Approximately 100 flies were tested of each genotype.

Larval movement

Wandering third instar larvae were selected, washed and transferred to a Petri dish with a layer of 0.7% agarose. After a period of adaptation, the peristaltic waves were counted within 2 min. At least 20 larvae from each genotype were counted, and the mean was calculated.

Drosophila immunoblotting

Drosophila heads were homogenized in lysis buffer (10 mM Tris–HCl, pH 7.4, 150 mM NaCl, 5 mM EDTA, 5 mM EGTA, 10% Glycerol, 50 mM NaF, 5 mM DTT, 4 M Urea, and protease inhibitors (Roche Diagnostic # 11836170001, Mannheim, Germany)).

Larval brains were dissected in Phosphate Buffer with 0.1% Tween 20 (PBT) and collected in Loading Buffer (30 mM Tris, pH 6.8, 9% Glycerol, 2.4% SDS, 3% 2-mercaptoethanol, 0.03% bromophenol blue) and homogenized.

Proteins were separated by 8% SDS–PAGE, transferred to nitrocellulose membranes (Whatman # NBA083C, Clifton, USA) and probed with primary antibodies: rabbit anti-TBPH (1:1500, home-made), mouse anti-synapsin (1:4000, Hybridoma Bank # 3C11,

Iowa, USA) and mouse anti-tubulin (1:4000, Calbiochem # CP06, Billerica, USA). The membranes were incubated with the secondary antibodies: HRP-labeled anti-mouse (1:1000, Thermo Scientific # 32430, Rockford, USA) or HRP-labeled anti-rabbit (1:1000, Thermo Scientific # 32460). Finally, protein detection was assessed with Femto Super Signal substrate (Thermo Scientific # 34095).

Protein bands were quantified using NIH ImageJ. The intensity of the band of interest was normalized with tubulin. The respective histogram for each western blot shows the relative expression of at least two independent experiments.

Mouse immunoblotting

Whole brains were homogenized with mechanical agitator (ForLab, Bergamo, Italy) in RIPA buffer (150 mM NaCl, 1% NP-40, 0.5% DOC, 0.1% SDS, 50 mM Tris HCl, pH8, 2× protease inhibitors (Roche Diagnostic # 11836170001)). Total protein extracts were separated by 10% SDS–PAGE, transferred to nitrocellulose membranes (Whatman # NBA083C) and probed with primary antibodies: rabbit anti-TDP43 (1:1000, Proteintech # 10782-2-AP), rabbit anti-synapsin I (1:1000, abcam # ab18814), rabbit anti GAPDH (1:1000, Santa Cruz # sc-25778). The membranes were incubated with the secondary antibodies: HRP-labeled anti-rabbit (1:1000, Thermo Scientific # 32460). Finally, protein detection was assessed with ECL Western Blotting Substrate (Thermo Scientific # 32106). Protein bands were quantified using NIH ImageJ. The intensity of the band of interest was normalized with GAPDH. The histogram for the western blot shows the relative expression of at least three independent experiments.

RNA extraction and real-time PCR

Total RNA was extracted from *Drosophila* heads (25 °C) with TRIzol reagent (Invitrogen # 15596-026) according to manufacturer's instructions. Regarding mouse brain total RNA, the same protocol was performed with the exception that the whole brain was homogenized using a mechanical agitator (ForLab, Bergamo, Italy) in TRIzol prior to RNA extraction. cDNA was synthesized starting from 1 μg of total RNA by using Superscript III (Invitrogen # 18080-044) reverse transcriptase and OligodT primers. Specific primers were designed to amplify TBPH (forward: 5′-CGGCAAGCCGAGCACGAT GAG-3′, reverse: 5′-CGCGGAGTTCGCTCCAACGAG-3′) and mouse TDP-43 (forward: 5′-GCAGTCCA GAAAACA-3′, reverse: 5′-CACCATCGCCCATCTA-3′). The expression levels were assessed by real-time PCR using Rpl-11 as fly housekeeping gene (forward: 5′-CCA TCGGTATCTATGGTCTGGA-3′, reverse: 5′-CATCG TATTTCTGCTGGAACCA-3′) and GAPDH as mouse housekeeping gene (forward: 5′-AGGTCGGTGT GAACGG-3′, reverse: 5′-AGTCATACTGGAACAT-3′). All amplifications were done on CFX96 real-time PCR detection system (Biorad) using SYBR Green technology (Biorad # 720000601). The relative expression levels were calculated according to the Livak

method (Schmitten and Livak 2008), using the equation $\Delta C_T = C_{T(target)} - C_{T(normalizer)}$ for Ct normalization; and the difference between $\Delta C_{T(test)}$ and $\Delta C_{T(calibrator)}$ to calculate the expression ratio and compare the expression levels. Statistical significance was calculated using student's *t*-test (indicated as * for $P \leqslant 0.05$ and ns for not statistically significant).

Mouse brain RNA Northern Blotting

Total RNA from mouse brains was isolated as already described in the real-time PCR section. RNA samples (20 μg) were loaded on 1% formaldehyde agarose gels, transferred to Hybond N^+ nylon membranes (Amersham Biosciences # RPN119B) and probed with internally ^{32}P-labeled sequences following pre-hybridization in ULTRAhyb® Ultrasensitive Hybridization Buffer (Ambion # AM8670). Pre-hybridization and hybridization were carried out at 40 °C. The probes were generated by PCR using primers Mus TDP-43 ex2 Fw 5′-atgggacggtgttgctgt-3′ and Mus TDP-43 ex3 Rv 5′-agtctttcagatcctgct-3′ and labeled with Rediprime II DNA Labeling System (GE Healthcare # RPN1633). The probe to detect GAPDH was generated using the same primers as for the mouse brain real-time PCR. Visualization of transcripts was carried out with a Cyclone Plus Storage Phosphor Scanner and the included OptiQuant Software (Perkin Elmer).

Statistics

Statistics were performed using GraphPad Prism. One-way ANOVA followed by Bonferroni's multiple comparison was used to compare measures among three groups. Unpaired *t*-test analysis was used to compare measures between two groups. Long rank test was performed to compare survival distribution between genotypes. The significance between the variables was shown based on the *p*-value obtained (ns indicates $p > 0.05$,* indicates $p < 0.05$, ** indicates $p < 0.01$, *** indicates $p < 0.001$ and **** indicates $p < 0.0001$). Values are presented as a mean and error bars indicate standard error means (SEM), unless otherwise stated.

RESULTS AND DISCUSSION

The expression of the TBPH aggregate inducer in *Drosophila* CNS does not hamper normal development

In this study we have exploited our previous work on *Drosophila* models for TDP-ALS (Feiguin et al., 2009; Romano et al., 2014; Cragnaz et al., 2014), and created a fly TDP-43/TBPH aggregation model centered on the cellular inclusions of EGFP-12xQ/N. This aggregation model was previously shown (Budini et al., 2012; Budini et al., 2014) to be capable of sequestering TDP-43 in cell lines. To construct the transgenic fly expressing EGFP-12xQ/N, the construct coding for the protein was placed under the control of the upstream activating sequence (UAS). After crossing the transgenic line EGFP-12xQ/N with the pan-neuronal ELAV-Gal4 (Brand and Perrimon, 1993), brain neurons showed co-localization of *Droso-*

phila TDP-43 (TBPH) with EGFP-12xQ/N aggregates, as previously reported in the eye tissue (Cragnaz et al., 2014). The flies developed normally, and no early neurological toxicity caused by these aggregates was observed. This is shown by the identical larval peristaltic waves count both at 25 °C and 29 °C (the higher temperature accelerates aging in the flies), in larvae expressing EGFP-12xQ/N or EGFP alone (Fig. 1).

EGFP-12xQ/N expression triggers an age-related locomotion defect in *Drosophila*

After the pupae stage, the adult flies were kept either at 25 °C or 29 °C. Also in the adult fly brain, TBPH co-localized with EGFP-12xQ/N aggregates (data not shown). The locomotion phenotype was measured by climbing assay at regular intervals. As shown in Fig. 2, the climbing ability at 25 °C of the transgenic flies constitutively producing aggregates starts to be significantly lower than the control at 14 days. The flies kept at 29 °C display a climbing deficit already at day 3. The survival curves follow a similar tendency, with the 25 °C and 29 °C flies having, respectively, a half-life 20% and 40% shorter than the EGFP control.

The locomotion defect follows an age-related decrease in TBPH levels

A peculiarity of the flies was that notwithstanding the constitutive production of EGFP-12xQ/N, the resulting aggregates do not result in a phenotypic consequence until adulthood. Previous reports have shown that TDP-43 levels decrease with age in different regions of the mouse brain such as cerebellum, forebrain and brainstem (Huang et al., 2010; Liu et al., 2015). It was then decided to investigate whether this programed reduction of TDP-43 levels arose early in evolution and can be observed also in non-mammalian species, specifically in *Drosophila* TBPH expression levels. As it can be seen in Fig. 3a, the relative TBPH levels decrease during aging in wild-type fly heads at 25 °C and 29 °C. It should
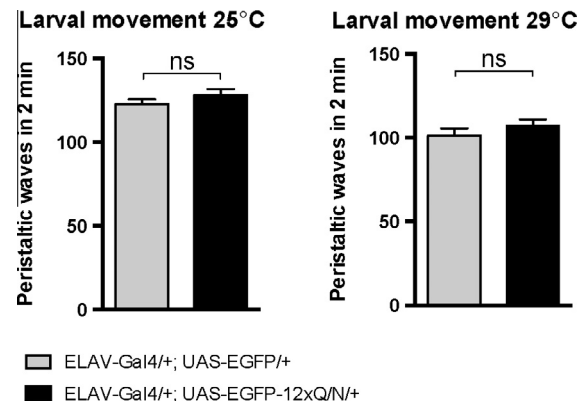

Fig. 1. EGFP-12xQ/N expression generates no early neurological toxicity. Quantification of peristaltic waves of third instar larvae, expressing EGFP-12xQ/N or EGFP alone under ELAV-Gal4 driver. More than 20 larvae from each genotype were counted, and the mean was calculated. ns indicates $p > 0.05$ (not significant) calculated by unpaired *t*-test. Error bars indicate SEM.
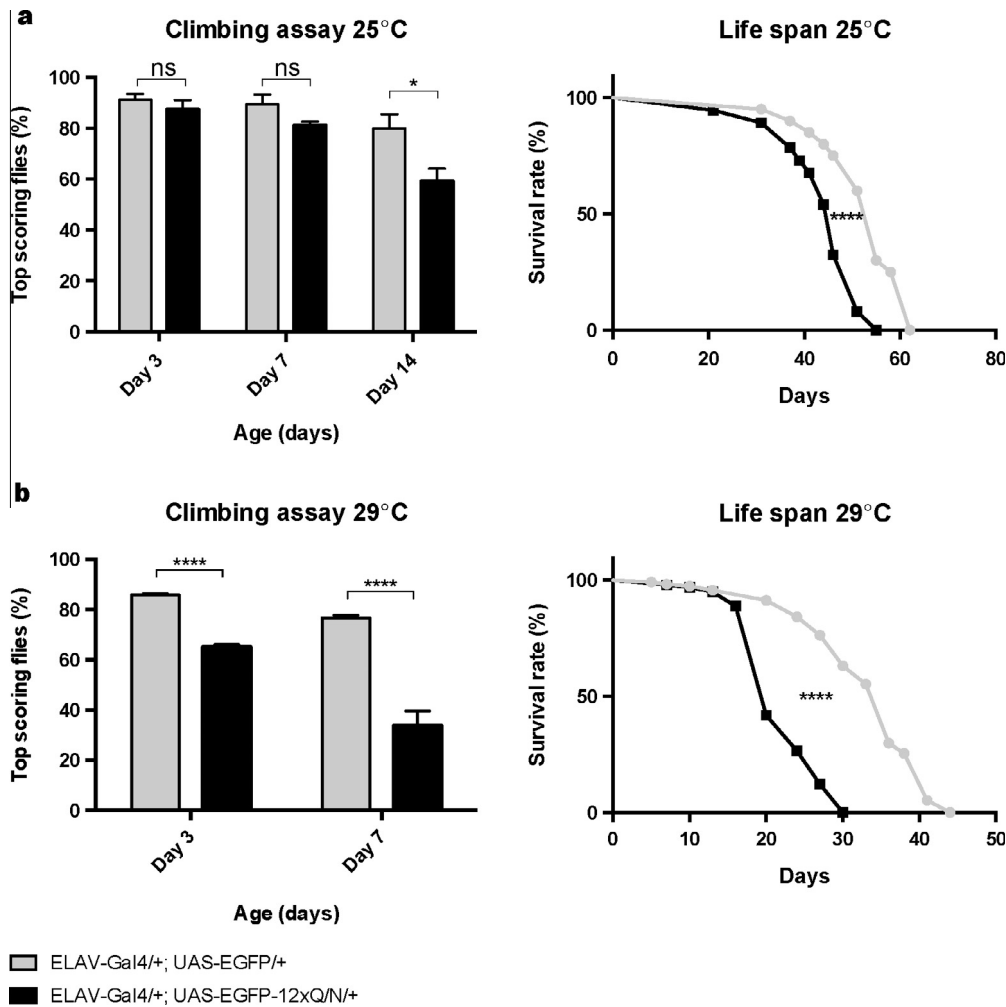
Fig. 2. The climbing ability and percentage of survival of EGFP-12xQ/N flies are compromised during aging. (a) Climbing assay and life span analyses at 25 °C (b) and 29 °C. Unpaired t-test analysis was used to compare measures between two groups. Long rank test was performed to compare survival distribution between genotypes. ns indicates $p > 0.05$ (not significant), * indicates $p < 0.05$, **** indicates $p < 0.0001$. Error bars indicate SEM.

be noted that the TBPH levels decrease faster in the case of accelerated aging (29 °C). Interestingly, the final drop (4-fold lower than in the immediate after pupa stage) coincides with the time point where the locomotive defect starts to be visible in the transgenic EGFP-12xQ/N fly (indicated by an arrow). Furthermore, the same trend in the levels of endogenous TBPH during aging was also confirmed in EGFP-12xQ/N- and EGFP-expressing flies (Fig. 3b). Fig. 3c confirms previous reports of an age-related decrease of TDP-43 protein levels in mouse brain samples following a pattern similar to the fly.

To discard an age-related neuronal loss we compared in fly and mouse the variations of TBPH/TDP-43 levels during aging with the fluctuation in levels of synapsin, a strictly neuronal protein (Figs. 3a, c). Data clearly indicate that the reduction of brain TBPH/TDP-43 levels is not due to significant neuronal loss as in that case a similar decrease in synapsin would have been observed. Furthermore, synapsin levels were previously shown to increase during mouse development between days 5 and 20 (Bogen et al., 2009). In addition, we are analyzing relatively young age groups not expected to

have any significant neuronal loss. This observation is also consistent with what has been reported to occur in humans (Wickelgren 1996).

The lower protein levels correspond to lower mRNA levels measured by real-time PCR both in flies (Fig. 3d) and mouse (Fig. 3e, left panel), indicating that there is a pre-translational mechanism for age-programed reduction of TDP-43/TBPH levels. The drop in TDP-43 levels in mouse brain was further confirmed by Northern Blot analyses (Fig. 3e, right panel).

Our data strengthen the hypothesis that the decrease of TBPH/TDP-43 levels represents an evolutionary conserved feature characteristic of aging of the organisms.

Constitutive reduction of TBPH levels from birth anticipates the locomotive defect in EGFP-12xQ/N expressing flies

If low TBPH levels seen with aging predispose to the locomotion defects observed upon expression of EGFP-12xQ/N, it follows that the sensitivity to the presence of
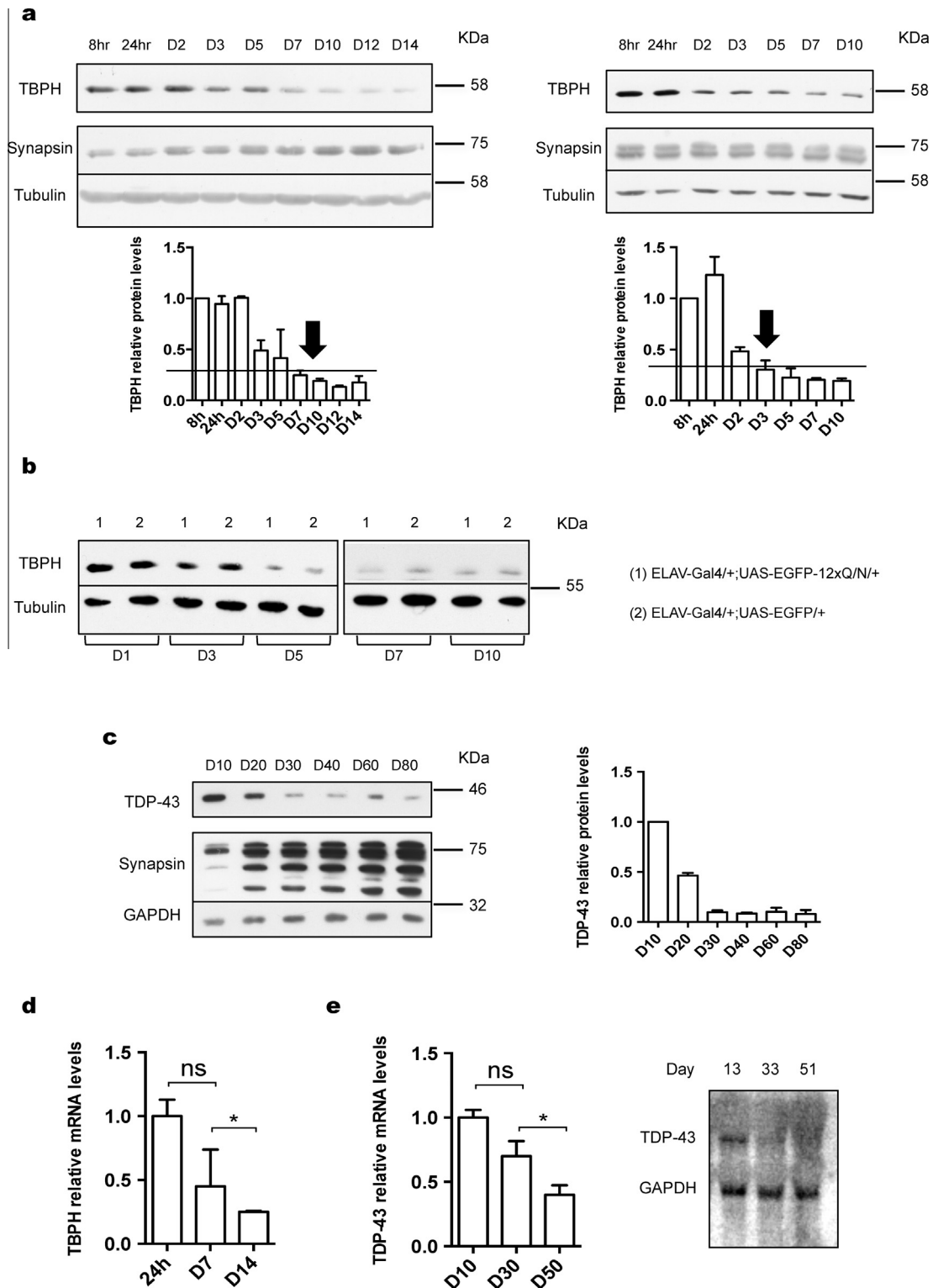
Fig. 3. *Drosophila* and mouse TDP-43 levels drop during normal aging. (a) Western blot analyses showing endogenous TBPH and synapsin levels from adult wild-type fly heads aged at 25 °C (left panel) and 29 °C (right panel). The histograms show the TBPH expression levels normalized with tubulin. D stands for day. The arrow indicates the point where the climbing ability of the flies is significantly reduced (see Fig. 2). Error bars indicate SD. (b) Western blot analyses showing endogenous TBPH levels from adult (1) ELAV-Gal4/+; UAS-EGFP-12xQ/N/+ and (2) ELAV-Gal4/+; UAS-EGFP/+ fly heads aged at 25 °C. Tubulin was used as loading control. (c) Western blot analyses showing endogenous TDP-43 and synapsin levels from wild-type mice during aging. The corresponding histogram shows the relative expression levels of TDP-43 normalized with GADPH. Error bars indicate SD. (d) Real-time PCR quantification of fly TBPH at different time points. The RNA levels were normalized with Rpl-11. ns indicates $p > 0.05$ (not significant) and * indicates $p < 0.05$. Error bars indicate SD. (e) Real-time PCR quantification of mouse TDP-43 at different time points (left panel). RNA levels were normalized with GADPH. ns indicates $p > 0.05$ (not significant) and * indicates $p < 0.05$. Error bars indicate SD. Northern Blot of mouse TDP-43 at different time points (right panel). GADPH was used as loading control.
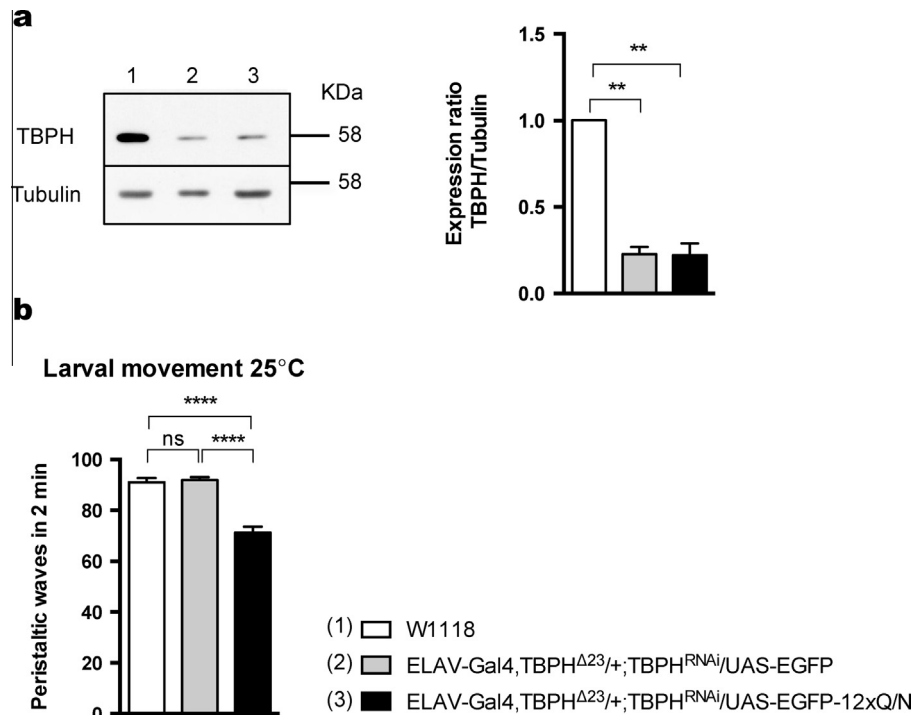
Fig. 4. EGFP-12xQ/N expression induces a defect in larval motility when TBPH levels are down regulated by silencing. (a) Quantification of TBPH level in wild-type (W1118) larval brains and larvae expressing TBPH siRNA. The different genotypes are indicated and defined by the color and number code at the bottom of the figure. The histogram shows the TBPH expression levels normalized with tubulin. One-way ANOVA followed by Bonferroni's multiple comparison was used to compare measures among three groups. ** indicates $p < 0.01$. Error bars indicate SD. (b) Quantification of peristaltic waves of third instar larvae. A one-way ANOVA followed by Bonferroni's multiple comparison was used to compare measures among three groups. ns indicates $p > 0.05$ (not significant) and **** indicates $p < 0.0001$. Error bars indicate SEM.

aggregates will be higher in a fly with low TBPH levels from birth and hence the phenotype should arise earlier than day 14 of the adult life. To test this hypothesis we created a fly expressing constitutively a siRNA against TBPH in neurons. Fig. 4a shows that this fly has from birth reduced TBPH levels, comparable to 14 day-old flies, but that this level is sufficient for their development. However, when EGFP-12xQ/N aggregates are present, the locomotion phenotype can be already observed at the third instar larval stage at 25 °C (Fig. 4b), indicating that the phenotypic consequence of the EGFP-12xQ/N aggregates is also dependent on endogenous TDP-43 levels.

Our data demonstrate the existence of a physiological decrease of TDP-43/TBPH levels with aging in brain tissue both in wild-type mice and flies, showing that it is an evolutionary conserved phenomenon. The maintenance of most functions sustained by TBPH/TDP-43 depends on the cell capacity of producing this protein and its availability in a functional form and in the proper cellular location. Available TDP-43 levels lower than a certain threshold would lead to abnormal function of TDP-43 on targets critical for neuronal structure and function, which might be responsible for the ALS pathologies.

CONCLUSIONS

Our observations suggest that sequestering of TBPH by the aggregates in young animals can be overcome by the higher production of this protein. However, during

aging the lower cellular capacity for TDP-43 production becomes critical, and the continuous capture of endogenous TDP-43 by the aggregates will likely produce a loss of its nuclear function, impossible to be compensated. Furthermore, the profile of the decline suggests an evolutionary conserved, programed reduction during the life span of the organism.

Based on this evidence, we suggest that a critical event for the onset of the human disease could be an age-related, physiological drop in TDP-43 expression. At this point, the continuous capture of endogenous TBPH/TDP-43 by the aggregates will likely produce a loss of its nuclear function. We are currently following up these observations to definitively prove this point. It should be noted that, according to this model, aggregates could exist from a very early stage without causing symptoms.

REFERENCES

Arai T, Hasegawa M, Akiyama H, Ikeda K, Nonaka T, Mori H, Mann D, et al. (2006) TDP-43 is a component of ubiquitin-positive tau-negative inclusions in frontotemporal lobar degeneration and amyotrophic lateral sclerosis. Biochem Biophys Res Commun 351(3):602–611. http://dx.doi.org/10.1016/j.bbrc.2006.10.093.

Bogen IL, Jensen V, Hvalby O, Walaas SI (2009) Synapsin-dependent development of glutamatergic synaptic vesicles and

presynaptic plasticity in postnatal mouse brain. Neuroscience 158 (1):231–241. http://dx.doi.org/10.1016/j.neuroscience.2008.05.055.

Brand AH, Perrimon N (1993) Targeted gene expression as a means of altering cell fates and generating dominant phenotypes. Development 118(2):401–415.

Budini M, Buratti E, Stuani C, Guarnaccia C, Romano V, DeConti L, Baralle FE (2012) Cellular model of TAR DNA-binding protein 43 (TDP-43) aggregation based on its C-terminal Gln/Asn-rich region. J Biol Chem 287(10):7512–7525. http://dx.doi.org/10.1074/jbc.M111.288720.

Budini M, Romano V, Quadri Z, Buratti E, Baralle FE (2014) TDP-43 loss of cellular function through aggregation requires additional structural determinants beyond its C-terminal Q/N prion-like domain. Human Mol Genet:1–12. http://dx.doi.org/10.1093/hmg/ddu415.

Cozzolino M, Carrì MT (2012) Mitochondrial dysfunction in ALS. Progr Neurobiol 97(2):54–66. http://dx.doi.org/10.1016/j.pneurobio.2011.06.003.

Cragnaz L, Klima R, Skoko N, Budini M, Feiguin F, Baralle FE (2014) Aggregate formation prevents dTDP-43 neurotoxicity in the *Drosophila melanogaster* eye. Neurobiol Dis 71:74–80. http://dx.doi.org/10.1016/j.nbd.2014.07.009.

D'Ambrogio A, Buratti E, Stuani C, Guarnaccia C, Romano M, Ayala YM, Baralle FE (2009) Functional mapping of the interaction between TDP-43 and hnRNP A2 in vivo. Nucleic Acids Res 37 (12):4116–4126. http://dx.doi.org/10.1093/nar/gkp342.

Feiguin F, Godena VK, Romano G, D'Ambrogio A, Klima R, Baralle FE (2009) Depletion of TDP-43 affects *Drosophila motoneurons* terminal synapsis and locomotive behavior. FEBS Lett 583 (10):1586–1592. http://dx.doi.org/10.1016/j.febslet.2009.04.019.

Geser F, Robinson JL, Malunda JA, Xie SX, Clark CM, Kwong LK, Moberg PJ, et al. (2010) Pathological 43-kDa transactivation response DNA-binding protein in older adults with and without severe mental illness. Arch Neurol 67(10):1238–1250. http://dx.doi.org/10.1001/archneurol.2010.254.

Gomez-Deza J, Lee Y-B, Troakes C, Nolan M, Al-Sarraj S, Gallo J-M, Shaw CE (2015) Dipeptide repeat protein inclusions are rare in the spinal cord and almost absent from motor neurons in C9ORF72 mutant amyotrophic lateral sclerosis and are unlikely to cause their degeneration. Acta Neuropathologica

Communications 3(1):38. http://dx.doi.org/10.1186/s40478-015-0218-y.

Huang C, Xia PY, Zhou H (2010) Sustained expression of TDP-43 and FUS in motor neurons in rodent's lifetime. Int J Biol Sci 6 (4):396–406. http://dx.doi.org/10.7150/ijbs.6.396.

Igaz LM, Kwong LK, Chen-Plotkin A, Winton MJ, Unger TL, Xu Y, Neumann M, Trojanowski JQ, Lee VM-Y (2009) Expression of TDP-43 C-terminal fragments in vitro recapitulates pathological features of TDP-43 proteinopathies. J Biol Chem 284 (13):8516–8524. http://dx.doi.org/10.1074/jbc.M809462200.

Ling S-C, Polymenidou M, Cleveland DW (2013) Converging mechanisms in ALS and FTD: disrupted RNA and protein homeostasis. Neuron 79(3):416–438. http://dx.doi.org/10.1016/j.neuron.2013.07.033.

Liu Y, Atkinson RAK, Fernandez-Martos CM, Kirkcaldie MTK, Cui H, Vickers JC, King AE (2015) Changes in TDP-43 expression in development, aging, and in the neurofilament light protein knockout mouse. Neurobiol Aging 36:1151–1159. http://dx.doi.org/10.1016/j.neurobiolaging.2014.10.001.

Neumann M, Sampathu DM, Kwong LK, Truax AC, Micsenyi MC, Chou TT, Bruce J, et al. (2006) Ubiquitinated TDP-43 in frontotemporal lobar degeneration and amyotrophic lateral sclerosis. Science (New York, NY) 314(5796):130–133. http://dx.doi.org/10.1126/science.1134108.

Nonaka T, Masuda-Suzukake M, Arai T, Hasegawa Y, Akatsu H, Obi T, Yoshida M, et al. (2013) Prion-like properties of pathological TDP-43 aggregates from diseased brains. Cell Rep 4(1):124–134. http://dx.doi.org/10.1016/j.celrep.2013.06.007.

Romano G, Klima R, Buratti E, Verstreken P, Baralle FE, Feiguin F (2014) Chronological requirements of TDP-43 function in synaptic organization and locomotive control. Neurobiol Dis 71 (November):95–109. http://dx.doi.org/10.1016/j.nbd.2014.07.007.

Schmitten TD, Livak KJ (2008) Analyzing real-time PCR data by the comparative C(T) method – PubMed – NCBI. Nat Protoc 3 (6):1101–1108.

Udan M, Baloh RH (2011) Implications of the prion-related Q/N domains in TDP-43 and FUS. Prion 5(1):1–5. http://dx.doi.org/10.4161/pri.5.1.14265.

Wickelgren I (1996) For the cortex, neuron loss may be less than thought. Science 273(5271):48–50.